TECHNOLOGY OF REPAIR FOR CORRODED REINFORCED CONCRETE

ROGER GEORGE HARDON

Doctor of Philosophy

THE UNIVERSITY OF ASTON IN BIRMINGHAM

January 1989

SUMMARY

THE UNIVERSITY OF ASTON IN BIRMINGHAM

TECHNOLOGY OF REPAIR FOR CORRODED REINFORCED CONCRETE

Roger George Hardon Doctor of Philosophy 1989

A number of factors relating to various methods of repair for chloride initiated corrosion damage of reinforced concrete have been studied.

A novel methodology has been developed to facilitate the measurement of macro and micro-cell corrosion rates for steel electrodes embedded in mortar prisms containing a chloride gradient. The galvanic bar specimen comprised electrically isolatable segmental mild steel electrodes and was constructed such that macro-cell corrosion currents were determinable for a number of electrode combinations. From this, the conditions giving rise to an incipient anode were established.

The influence of several reinforcement and substrate primer systems upon macro-cell corrosion, arising from an incipient anode, within a patch repair have been investigated.

Measurements of electrochemical noise were made in order to investigate the suitability of the technique as an on-site means of assessing corrosion activity within chloride contaminated reinforced concrete. For this purpose the standard deviation of potential noise was compared to macro-cell galvanic current data and micro-cell corrosion intensity determined by linear polarisation.

Hydroxyl ion pore solution analyses were carried out on mortar taken from cathodically protected specimens. These specimens, containing sodium chloride, were cathodically protected over a range of polarisation potentials. Measurement of the hydroxyl ion concentrations were made in order to examine the possibility of alkali-silica reactions initiated by cathodic protection of reinforced concrete.

A range of mortars containing a variety of generic type additives were examined in order to establish their resistances to chloride ion diffusion. The effect of surfactant addition rate was investigated within a cement paste containing various dosages of naphthalene sulphonate.

Key words : corrosion, chlorides, galvanic bar, primers, cathodic protection

THIS WORK IS DEDICATED TO MY PARENTS,

IRENE AND GERALD

ACKNOWLEDGEMENTS

The author would like to thank Dr. C.L. Page for the help and supervision given during the course of this work, additionally, Fosroc International for their support.

Thanks are also due to a number of individuals who have given their help throughout the duration of this work. In particular, the author would like to mention his selfless typist, Pamela Lambert, Dr. Rob Lambe of Fosroc, Colin Thompson, for his fine technical assistance, Roger Quemby for help in preparing figures, Cal Geens, for direction in the workshop, Paul Lambert for his assistance in areas, too various to mention. Thanks must also be given to Henry Rawlinson and Maxine Leech for proof reading and finally, Technotrade Limited, my current employer, for their consideration shown during the write up of this work.

LIST OF CONTENTS

	Page Number
TITLE PAGE	1
THESIS SUMMARY	2
DEDICATION	3
ACKNOWLEDGEMENTS	4
LIST OF CONTENTS	5
LIST OF FIGURES AND TABLES	9
CHAPTER 1 INTRODUCTION	17
1.1 Background	17
1.2 Purpose of Investigation	22
1.3 Plan of Presentation	24
CHAPTER 2 MATERIALS AND EXPERIMENTAL TECHNIQUES	26
2.1 Introduction	26
2.2 Materials	26
2.3 Determination of Flow	28
2.4 Compressive Strength Measurements	29
2.5 Pore Solution Expression	29
2.6 Hydroxyl ion (pH) Analysis	30
2.7 Chloride ion Analysis	30
2.8 Electron Microscopy	31
2.9 Porosimetry Measurements	32
2.10 Electrode Potentials	33
2.11 Polarisation Resistance measurements	34
2.12 Resistivity Measurements	35
2.13 Galvanic Current	36
CHAPTER 3 DEVELOPMENT OF A METHODOLOGY FOR THE STUDY OF ELECTROCHEMICAL PROCESSES ASSOCIATED WITH PATCH REPAIRS IN REINFORCED CONCRETE	54
3.1 Introduction	54
3.2 Previous Work	56

		Page Number
3.3	Experimental	60
3.4	Results and Discussion	68
3.5	Conclusions	76
CHAPTER 4	PATCH REPAIRS AND PRIMERS - MICRO AND MACRO-CELL EFFECTS	96
4.1	Introduction	96
4.2	Previous Work	98
4.3	Experimental	100
4.4	Results and Discussion	103
4.5	Conclusions	111
CHAPTER 5	A STUDY OF ELECTROCHEMICAL NOISE GENERATED BY STEEL EMBEDDED IN A CHLORIDE CONTAMINATED ENVIRONMENT	169
5.1	Introduction	169
5.2	Previous Work	170
5.3	Experimental	172
5.4	Results and Discussion	176
5.5	Conclusions	178
CHAPTER 6	THE INFLUENCE OF CATHODIC PROTECTION ON HYDROXYL ION CONCENTRATIONS IN CONCRETE PORE SOLUTIONS	189
6.1	Introduction	189
6.2	Previous Work	195
6.3	Experimental	198
6.4	Results and Discussion	201
6.5	Conclusions	206
CHAPTER 7	CHLORIDE DIFFUSION THROUGH HARDENED MODIFIED BASED SYSTEMS	214
7.1	Introduction	214
7.2	Previous Work	216
7.3	Experimental	221
7.4	Results and Discussion	225

		Page Number
7.5	Conclusions	232
CHAPTER 8	GENERAL CONCLUSIONS AND RECOMMENDATIONS FOR FURTHER WORK	242
8.1	General Conclusions	242
8.2	Recommendations for Further Work	246
REFERENCES		249
APPENDIX 1	Details of certain mix additives and surface treatments used in the production of diffusion specimens described in Chapter 7	271
APPENDIX 2	Details of reinforcement and mortar primers used in Chapter 4	272
APPENDIX 3	Details of the proprietary repair mortar used in Chapter 4	273
APPENDIX 4	Twenty eight day compressive strength determination used for the specimens in Chapter 7	274
APPENDIX 5	Example of the calculation of hydroxyl ion concentration	275
APPENDIX 6	Example of pore size distribution calculation	276
APPENDIX 7	Traces of macro-cell galvanic current against time	277
7.1	Wet Conditions	278
7.2	Dry Conditions	280
APPENDIX 8	Traces of galvanic current (cathodic) against time	282
8.1	Wet Conditions	283
8.2	Dry Conditions	285
APPENDIX 9	Traces of corrosion potential against time	287
9.1	5.0% wet	288
9.2	5.0% dry	290
9.3	1.0% wet	292
9.4	1.0% dry	294
9.5	0.1% wet	296

Page Number

9.6 0.1% dry 298

9.7 0.0% wet 300

9.8 0.0% dry 305

APPENDIX 10 Details of the grout, described in Chapter 4, used to seal cracks 310

APPENDIX 11 Example of calculated and actual weight loss previously obtained 311

APPENDIX 12 Details of the diffusion specimens described in Chapter 7 312

PUBLISHED WORK 328

LIST OF FIGURES AND TABLES

FIGURE 1.1 An example of the type of diagram used by Galileo to illustrate Discorsi Dimostrazioni Matematiche

TABLE 2.1 Chemical analyses of cements

TABLE 2.2 Mix details for various specimens

TABLE 2.3 Chemical analyses of metals

FIGURE 2.1 Flow table

FIGURE 2.2 Pore press diagram

FIGURE 2.3 Pore press

FIGURE 2.4 Spectrophotometer

FIGURE 2.5 Scanning Electron Microscope

FIGURE 2.6 Link analysis system

FIGURE 2.7 Porosimeter

FIGURE 2.8 Porosimeter glass cell

FIGURE 2.9 Half cell potential measurement system

FIGURE 2.10 Multistat system

FIGURE 2.11 Polarisation curve

FIGURE 2.12 Multistat system schematic diagram

FIGURE 2.13 Wenner Four Probe Unit

FIGURE 2.14 Resistance measurement experimental arrangement

FIGURE 2.15 Resistance meter

FIGURE 2.16 Digital ammeter

FIGURE 3.1 Shouldered washer

FIGURE 3.2 Sealing of connection wires

FIGURE 3.3 End treatment used on galvanic bar specimens

FIGURE 3.4 Galvanic bar

FIGURE 3.5 Galvanic bar embedded within mortar prism

FIGURE 3.6 Segment configurations used for galvanic current measurements

FIGURE 3.7 Galvanic current/time traces for wet conditions

FIGURE 3.8 Galvanic current/time traces for dry conditions

FIGURE 3.9 Galvanic current (cathodic)/time trace wet conditions

FIGURE 3.10 Galvanic current (cathodic)/time trace dry conditions

FIGURE 3.11 Micro-cell corrosion values

FIGURE 3.12 Corrosion potential/time trace 5% chloride segment wet conditions

FIGURE 3.13 Corrosion potential/time trace 5% chloride segment dry conditions

FIGURE 3.14 Corrosion potential/time trace for 1% chloride segment in wet conditions

FIGURE 3.15 Corrosion potential/time trace for 1% chloride segment in dry conditions

FIGURE 3.16 Corrosion potential/time trace for 0.1% chloride segment in wet conditions

FIGURE 3.17 Corrosion potential/time trace for 0.1% chloride segment in dry conditions

FIGURE 3.18 Corrosion potential/time trace for chloride free segment in wet conditions

FIGURE 3.19 Corrosion potential/time trace for chloride free segment in dry conditions

FIGURE 3.20 Calculated vs actual weight loss

FIGURE 3.21 Resistance profile

FIGURE 3.22 Proportion of long itudinal cracking

FIGURE 3.23 Cracking within mortar prism

FIGURE 3.24 Corrosion products upon 5% chloride segment

FIGURE 3.25 Galvanic bar at end of exposure period

FIGURE 3.26 Galvanic bar at end of exposure period (chloride free segments)

FIGURE 3.27 Condition of chloride free segments

FIGURE 3.28 End segment (chloride free)

TABLE 4.1 Comparison of micro-cell intensities

TABLE 4.2 Comparison of macro-cell intensities

FIGURE 4.1 Repair system 1

FIGURE 4.2 Repair system 2

FIGURE 4.3 Repair system 3

FIGURE 4.4 Repair system 4

FIGURE 4.5 Repair system 5

FIGURE 4.6 Repaired segment, repair system 1

FIGURE 4.7 Repaired segment, repair system 3

FIGURE 4.8 Repaired segment, repair system 5

FIGURE 4.9 Friable layer

FIGURE 4.10 Macro showing black regions (magnetite)

FIGURE 4.11 Repair system 1 galvanic current/time traces for wet and dry conditions

FIGURE 4.12 Repair system 2 galvanic current/time traces for wet and dry conditions

FIGURE 4.13 Repair system 3 galvanic current/time traces for wet and dry conditions

FIGURE 4.14 Repair system 4 galvanic current/time traces for wet and dry conditions

FIGURE 4.15 Repair system 5 galvanic current/time traces for wet and dry conditions

FIGURE 4.16 Repair system 1 galvanic current (cathodic)/time traces for wet and dry conditions

FIGURE 4.17 Repair system 2 galvanic current (cathodic)/time traces for wet and dry conditions

FIGURE 4.18 Repair system 3 galvanic current (cathodic)/time traces for wet and dry conditions

FIGURE 4.19 Repair system 4 galvanic current (cathodic)/time traces for wet and dry conditions

FIGURE 4.20 Repair system 5 galvanic current (cathodic)/time traces for wet and dry conditions

FIGURE 4.21 Repair system 1 corrosion potential/time traces for repaired segment wet and dry conditions

FIGURE 4.22 Repair system 2 corrosion potential/time traces for repaired segment wet and dry conditions

FIGURE 4.23 Repair system 3 corrosion potential/time traces for repaired segment wet and dry conditions

FIGURE 4.24 Repair system 4 corrosion potential/time traces for repaired segment wet and dry conditions

FIGURE 4.25 Repair system 5 corrosion potential/time traces for repaired segment wet and dry conditions

FIGURE 4.26 Repair system 1 corrosion potential/time traces for 1% chloride segment wet and dry conditions

FIGURE 4.27 Repair system 2 corrosion potential/time traces for 1% chloride segment wet and dry conditions

FIGURE 4.28 Repair system 3 corrosion potential/time traces for 1% chloride segment wet and dry conditions

FIGURE 4.29 Repair system 4 corrosion potential/time traces for 1% chloride segment wet and dry conditions

FIGURE 4.30 Repair system 5 corrosion potential/time traces for 1% chloride segment wet and dry conditions

FIGURE 4.31 Repair system 1 corrosion potential/time traces for 0.1% chloride segment wet and dry conditions

FIGURE 4.32 Repair system 2 corrosion potential/time traces for 0.1% chloride segment wet and dry conditions

FIGURE 4.33 Repair system 3 corrosion potential/time traces for 0.1% chloride segment wet and dry conditions

FIGURE 4.34 Repair system 4 corrosion potential/time traces for 0.1% chloride segment wet and dry conditions

FIGURE 4.35 Repair system 5 corrosion potential/time traces for 0.1% chloride segment wet and dry conditions

FIGURE 4.36 Repair system 1 corrosion potential/time traces for chloride free segment wet and dry conditions

FIGURE 4.37 Repair system 2 corrosion potential/time traces for chloride free segment wet and dry conditions

FIGURE 4.38 Repair system 3 corrosion potential/time traces for chloride free segment wet and dry conditions

FIGURE 4.39 Repair system 4 corrosion potential/time traces for chloride free segment wet and dry conditions

FIGURE 4.40 Repair system 5 corrosion potential/time traces for chloride free segment wet and dry conditions

FIGURE 4.41 OPC slurry and acrylic bonding agent repair

FIGURE 4.42 OPC slurry repair

FIGURE 4.43 Macro of zinc rich primer showing corrosion product

FIGURE 4.44 Macro of zinc rich primer typical surface

FIGURE 4.45 Zinc rich primer and acrylic bonding agent

FIGURE 4.46 Comparison of zinc coating and adjacent segment

FIGURE 4.47 Macro of pitted region

FIGURE 4.48 Macro of pitting site

FIGURE 4.49 Influence of pH upon dissolution of zinc

FIGURE 4.50 Electron photomicrograph of zinc rich primer and acrylic bonding agent

FIGURE 4.51 Electron photomicrograph of cratered zinc rich surface

FIGURE 4.52 Electron photomicrograph showing typical zinc surface

FIGURE 4.53 Electron photomicrograph showing collapsed spheroid and empty crater

FIGURE 4.54 E.D.X.A. traces for collapsed sphere and empty crater

FIGURE 4.55 Electron photomicrograph showing . Intact spheroid

FIGURE 4.56 Electron photomicrograph showing broken sphere smooth lining

FIGURE 4.57 E.D.X.A. traces for Intact and broken spheres

FIGURE 4.58 Electron photomicrograph of rough textured surface

FIGURE 4.59 E.D.X.A. for zinc primer surface

FIGURE 4.60 Electron photomicrograph showing fracture through zinc rich primer coating

FIGURE 4.61 Electron photomicrograph showing zinc/substrate region

FIGURE 4.62 Electron photomicrograph showing thick zinc layer

FIGURE 4.63 Electron photomicrograph showing spheroidal nature of zinc primer layer

FIGURE 4.64 E.D.X.A. traces for the interior of the zinc rich layer

FIGURE 4.65 Electron photomicrograph showing structure of zinc layer

FIGURE 4.66 Electron photomicrograph showing tightly packed spheroids

FIGURE 4.67 Electron photomicrograph showing cross linking within the spheroidal layer

FIGURE 4.68 1%, 0.1% and chloride free segments corresponding to a zinc rich primer and acrylic bonding agent repair

TABLE 5.1 Values of micro-cell corrosion rate and predicted corrosion rate

TABLE 5.2 Values of macro-cell galvanic current corrosion rate and predicted corrosion rate

FIGURE 5.1 Schematic diagram showing the experimental arrangement used for potential noise measurement

FIGURE 5.2 General arrangement for potential noise measurement for system 1

FIGURE 5.3 The arrangement for potential noise measurement for system 2

FIGURE 5.4 The general arrangement for potential noise measurement for system 3

FIGURE 5.5 Arrangement of counter electrodes used for linear polarisation measurement

FIGURE 5.6 Results of potential noise micro-cell study corrosion rate using carbon rod counter electrode

FIGURE 5.7 Results of potential noise micro-cell study corrosion rate using adjacent segment as counter electrode

FIGURE 5.8 Results of potential noise macro-cell study system 2

FIGURE 5.9 Results of potential noise macro-cell study system 3

TABLE 6.1 Results of hydroxyl ion pore solution analysis

TABLE 6.2 Hydroxyl ion concentrations of various cements

FIGURE 6.1 Theoretical basis for cathodic protection shown graphically

FIGURE 6.2 Plot of influence of chloride upon the passivation and corrosion of iron

FIGURE 6.3 Isometric showing the cathodically protected mortar prism

FIGURE 6.4 Isometric showing the cathodic protection system experimental arrangement

FIGURE 6.5 Pore solution hydroxyl ion concentrations for various cements

FIGURE 6.6 Plot of variation in oxygen diffusion with humidity

TABLE 7.1 Details of the specimens produced for diffusion studies

TABLE 7.2 Average diffusion coefficients for mortar and cement paste systems

TABLE 7.3 28 day compressive strengths and flow measurements for various mixes

FIGURE 7.1 Mould assembly used for casting diffusion specimens

FIGURE 7.2 Glass diffusion cell

FIGURE 7.3 Plot of increase in chloride concentration with time within the diffusion cell

FIGURE 7.4 Pore size distributions for 0.6 W/C mortar and 0.4 W/C mortar

FIGURE 7.5 Pore size distributions for naphthalene sulphonate mortars at 0.6 W/C

FIGURE 7.6 Pore size distributions for 0.28 W/C cement paste and 0.28 W/C cement pastes with naphthalene sulphonate

FIGURE 7.7 Pore size distributions for 0.6 W/C and 0.4 W/C with polyvinyl acetate or styrene butadiene additions

FIGURE 7.8 Pore size distributions for 0.6 W/C mortar coated with alkoxy silane or methyl methacrylate

CHAPTER 1

INTRODUCTION

1.1 BACKGROUND

An engineer's art would appear to be advanced when some part of the science of that art is usefully applied to his practice. Within the sphere of early modern civil engineering, grand feats of construction were achieved with nothing more than a rule-of-thumb approach to design, this approach being based upon past experience. Thomas Telford (1757-1834), the 'Colossus of Roads', probably built more bridges than anyone else in history. Typically, he used masonry or cast iron arches in compression for short spans. For greater spans he pioneered the suspension bridge using wrought iron chain in tension. Telford's most notable achievement being the Menai road bridge (1819), here the shape of the chain catenaries were determined not by calculation, but from a large scale model erected over a dry valley. Wrought iron chains, as opposed to large beams were used owing to Telford's lack of confidence in beam theory and the availability of suitable wrought iron plates.

Perhaps the most notable example of an early structure whose mechanical integrity was reliant upon theoretical calculation, rather than convention and experience, was the Menai rail bridge. The structure was opened in 1850, the novel feature of the design being the use of wrought iron hollow box sections, weighing 1500 tonnes, forming the main spans. Robert Stephenson and his designer, William Fairbairn, were responsible for this grand engineering achievement. The theories upon which Stephenson and Fairbairn based

their stress analysis calculations had been in existence for at least two centuries. Galileo Galilei (1564-1642) published Discorsi Dimostrazioni Matematiche (1.1) in 1638, the work, more commonly known as Two new Sciences, represents the first published treatise on the theory and analysis of bending stresses in inanimate solids. Galileo's work on mechanics consists of a series of propositions which systematically expound a theory using illustrations of the type shown in figure 1.1.

Galileo's theories remained beyond the grasp of sceptical practical engineers for over two hundred years. After disasters such as the Tay bridge, proper calculations were gradually adopted by practicing engineers. Subsequently it was found that by building structures whose design relied on calculation rather than rule-of-thumb, economy of material was possible without compromising safety.

Whilst the use of reliable theory has enabled economy of scale in construction, the development of new engineering materials has, amongst other things, provided a means for engineers to solve problems in a more elegant fashion.

Today, the most widely used constructional material is reinforced concrete. Lime and pozzolan concretes were used in various forms for two millennia before the significant development of Joseph Aspdin's cement in 1824. In this year Aspdin took out a patent for the manufacture of Portland cement, so named owing to its resemblance to Portland stone. Used in the manufacture of concrete, Portland cement constitutes the binding component of a mixture of crushed stone and water. Hardened concrete exhibits fine compressive characteristics but poor tensile properties, so the invention of a concrete reinforced with a strong tensile component

was necessary to extend its range of possible applications.

The Frenchmen, Louis Lambot and Joseph Monier are popularly credited with the invention of reinforced concrete, Monier with reinforced cement flower pots and Lambot with a reinforced cement boat patented in 1855 (1.2). In both cases iron rods provided the enhanced tensile characteristics. However, these examples were preceded by one year by the flooring system patented by William Boutland Wilkinson of Newcastle (1.3). Wilkinson's flooring material comprised a cementitious type of concrete matrix reinforced with wire ropes "or iron in other forms in a state of tension" (1.4). Thus the principle of tensile reinforcement to concrete was firmly established and the combination of concrete and steel allowed long unsupported slender members to be produced. The design of such components was largely empirical (1.5).

The combination of steel and concrete is mutually beneficial in ways other than those purely related to physical strength. For example, unprotected steel exposed to the atmosphere will tend to corrode. Embedding steel within concrete provides a physical barrier through which corrosive agents must pass. Concrete also comprises a chemical environment of a highly alkaline nature, imparting passivity to embedded steel.

A complex series of reactions is initiated when water is mixed with Portland cement. The hydration of calcium silicates produces a calcium silicate hydrate gel (C-S-H gel) which gives rise to physical strength of the matrix. The cement matrix is a porous medium and held within the pores is an alkaline pore solution. This solution contains high concentrations of sodium and potassium hydroxides responsible for the high pH. It is not uncommon after a few weeks hydration to record pH values greater than 13 for

Portland cement pastes of water/cement ratios typically used in practice (1.6, 1.7). With reference to the Pourbaix diagram (1.8) for iron in an aerated alkaline environment, it is likely that steel embedded within concrete will remain passive, over a range of potentials, owing to the maintenance of a protective thin oxide film.

Degradation processes likely to impair passivity are carbonation and/or the presence of chloride ions. Carbonation reduces the pH of the pore solution to values at which the oxide film becomes unstable resulting in general corrosion; chloride ions initiate local pitting corrosion at sites of weaknesses in the passive film (1.9). Steel exposed to these conditions in a moist environment is likely to corrode with differences in electrical potential on the steel's surface, giving rise to anodic and cathodic sites. Metal is dissolved at the anode according to the oxidation process

$$Fe\ (metal) = Fe^{2+}(aq.) + 2e^{-}$$

Simultaneously, reduction occurs at the cathodic site, typically

$$\tfrac{1}{2}\ O_2 + H_2O + 2e^{-}\ (metal) = 2OH^{-}\ (aq.)$$

The ions involved in the reduction process are transported via the electrolyte whilst the electrons produced at the anodic sites are conducted through the metal.

The result of the above processes is to convert the iron, present in the reinforcing steel, into several forms of iron oxide. These forms of oxide, collectively known as corrosion products, occupy a greater volume than the parent metal, and so exert tensile stresses within the concrete matrix. Such forces are able to exceed the low tensile capacity of the concrete, consequently cracking and

spalling the concrete (1.10).

Considering the above degradation processes and consequential impaired serviceability of structures so affected, the importance of the depth and quality of concrete cover to embedded reinforcements becomes apparent. This concrete cover can be of prime importance in governing time to corrosion, for a given environment. It is therefore perhaps surprising that design cover depths, stipulated in relevant design codes (1.11-1.13), are largely based upon rule-of-thumb principles.

Research has identified processes and rate limiting steps giving rise to loss of passivity of steel reinforcements in concrete (1.14). Studies of a similar nature may be suitable as a basis, upon which theoretical models for service-life prediction may be developed.

Owing to the many variables involved in the construction process, not least on-site practices, the application of such service-life modelling to practical problems must be done cautiously. It is indeed true to say that the production, placing and curing of site concrete is far from an exact science. These inherent limitations accepted, it is still evident that more consideration must be given to durability, at least at the design stage of construction. It is becoming increasingly important that designers and specifiers look more thoughtfully at aspects of design, other than mechanical integrity, which are likely to influence durability. The duty cycle of a structure must be given more careful consideration if reinforced concrete is to retain its essentially sound record as a most durable and reliable constructional material.

The maladies of certain nationally important infrastructure

are now becoming apparent, new works are commencing on the internationally important channel tunnel link. It is, therefore, pertinent to make the analogy between 'sceptical practical engineers' who ultimately adopted Galileo's theories of bending and the current need for national bodies to establish better founded design guidelines, within their codes of practice and standards, in order that more durable reinforced concrete may be designed and produced.

Whilst improvements in design practice and on-site procedures (particularly curing) will combine to produce structures of enhanced serviceability, there is an existing need to repair structures suffering corrosion related damage.

Those repair systems available range from making good spalled and cracked concrete, by using traditional methods and materials, to those involving cathodic protection of a structure. Whilst a considerable body of work exists relating to corrosion of steel in concrete (1.15), the same is not true of repair. Consequently, there has been a call for better understanding of the science and practice of concrete repair (1.14, 1.16).

1.2 PURPOSE OF INVESTIGATION

The general aims of this work have been to study certain chemical and electro-chemical factors relating the corrosion and repair of reinforced concrete. These aims may be more specifically defined as follows:

1. To devise a methodology that facilitates the measurement of micro and macro-cell corrosion currents, generated by differential

chloride ion concentrations, as may be found in actual chloride contaminated structures. Such a methodology would provide a basis for the study, under laboratory conditions, of the measurement of changes in corrosion activity resulting from the repair of an isolated region of the specimen.

2. To apply the previously devised methodology in order to study the effect of reinforcement primer systems, as used in patch repair, upon incipient anode macro-cell corrosion currents. At present there is little work on the influence of patch repair and subsequent corrosion processes, particularly the role that may be played by primers in the control of such processes.

3. To establish a relationship between both macro and micro-cell corrosion and potential electrochemical noise, in order to assess the merits of using electrochemical noise as an on-site monitoring technique. Conventional on-site non-destructive testing techniques (e.g. potential mapping) will not yield data related to corrosion rates.

4. To establish the effects of polarisation potential, using a laboratory cathodic protection system, upon hydroxyl ion concentrations within the concrete. Under certain conditions, such as concrete containing marginal aggregates, an increase in the hydroxyl ion concentration may initiate an alkali-silica reaction.

5. To determine the effects of certain mix additives upon the rates of chloride ion diffusion in well hydrated mortars and cement pastes of fixed water/cement ratio. Whilst published data is

available regarding chloride ion diffusion in cementitious materials, such studies largely relate to materials most suited to new construction works. Presently, a considerable number of pre-batched cementitious mortars, containing additives, are produced specifically for concrete repair applications. Little work is available regarding the ability of these additives to limit chloride ion diffusion.

1.3 PLAN OF PRESENTATION

The introduction given in Chapter 1 covers a general background to the use of reliable theories in civil engineering, and a brief history of the development of reinforced concrete. Following this is a synopsis of the scope of the individual experimental chapters contained within the thesis. Chapter 2 details the methods and materials used within the experimental sections of the research. The following five experimental chapters have a common format of an introduction in which a particular investigation is related to the general sphere of study; previous work and experimental procedure follow. Each experimental chapter ends with a discussion of results and conclusions drawn. General conclusions and recommendations for further work are given in Chapter 8.

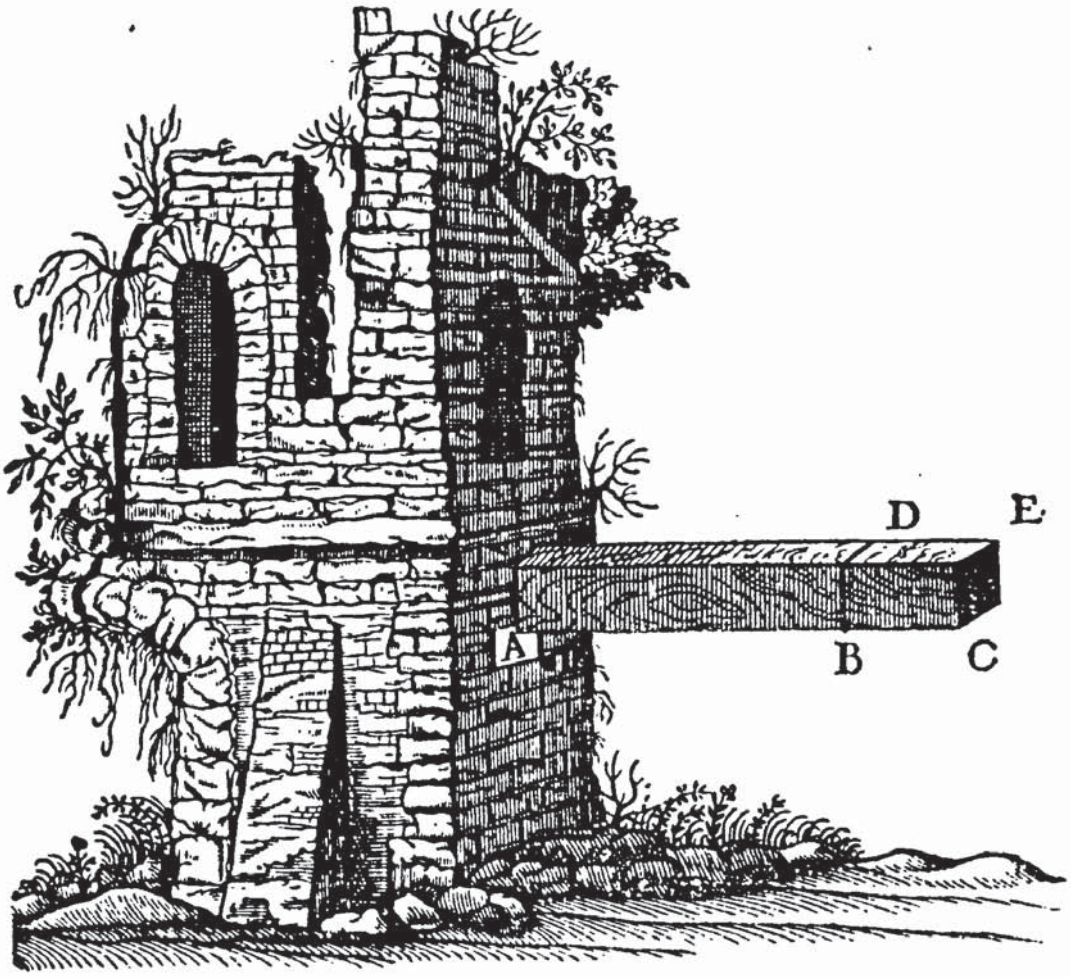

FIGURE 1.1 An example of the type of diagram used by Galileo to illustrate Discorsi Dimostrazioni Matematiche (1.1)

CHAPTER 2

MATERIALS AND EXPERIMENTAL TECHNIQUES

2.1 INTRODUCTION

This chapter is concerned with a description of the majority of experimental procedures used within the subsequent experimental chapters. Additionally, details of a number of the materials used in the preparation of specimens are given. In a number of instances, however, where more appropriate, certain experimental techniques are described within specific experimental chapters (i.e. where development of a technique has taken place), or, in the case of materials, within the Appendices.

2.2 MATERIALS

CEMENTS

The majority of specimens described within the experimental chapters were prepared from research grade ordinary Portland cement. The cement was supplied as a single batch by the Ketton cement company. The cement, used solely in the manufacture of specimens described in Chapter 6, was a research grade ordinary Portland cement supplied by the Blue Circle cement company. Both types of cement were kept in polythene sacks and stored within airtight drums, each drum containing approximately 25 kilograms of cement. Chemical analyses of each cement are given in table 2.1. In both cases the cements complied with British Standard BS 12 : 1978

(2.1) and BS 4550 : 1970 (2.2).

AGGREGATE

Unless otherwise indicated, the aggregate used in the work was a Leighton Buzzard sand, washed and dried, of 300-600μm and 500-1000μm particle size.

ADDITIVES

The additives used in Chapter 7, in the preparation of specimens for diffusion studies, were frequently a proprietary formulation. It is for reasons of commercial secrecy that precise details of formulation etc, cannot be given. Physical and chemical data is given within the Appendices, wherever possible.

PRIMERS

The reinforcement, and concrete priming systems used in Chapter 4 were proprietary compounds. The manufacturer's specification for the individual materials used are given in the Appendices. Owing to commercial considerations, exact details of formulation etc, cannot be given.

CEMENT MORTARS AND PASTES

With the exception of the mortar used in Chapter 6, the mortar used throughout this work was prepared in accordance with the procedures given in BS 4551 : 1980 (2.3). In view of the mass of

material involved in the preparation of the specimens : described in Chapter 6, a 0.5 m^3 forced action 'Creteangle' pan mixer was used, otherwise the method was similar to that described above. In the case of cement paste preparation, care was necessary in order to avoid balling of the dry material. Curing and compaction procedures are given within the appropriate experimental chapters.

The proprietary repair mortar, used in the repair of specimens in Chapter 4, was mixed at the design water/powder ratio and the specification for the material is given within the Appendices. The proportions of the various mixes, together with their water/cement ratios, are given in table 2.2.

METALS

Mild steel and stainless steel used in this work were commercially available grades of material. Their analyses are given in table 2.3. The cleaning and surface preparation procedures are given within the appropriate experimental chapters.

2.3 DETERMINATION OF FLOW

In order to establish a measure of the rheological properties of mortars - described in Chapter 7 - flow measurements were made on mortar whilst still in a fresh, plastic state. For this purpose the procedure given in British Standard BS 4551 : 1980 (2.3) was followed. The method followed involves forming a truncated cone of mortar upon a platen of fixed mass. The platen, together with mortar, is raised and dropped a given distance 25 times, over a 15 second period. This resulted in a spreading of the mortar over the

surface of the platen . The apparatus used is shown in figure 2.1. Results are reported as the percentage increase in diameter of the spread mortar.

2.4 COMPRESSIVE STRENGTH MEASUREMENTS

In order to quantify a frequently defined physical property of the materials described in Chapter 7, the British Standard compressive strength test was carried out (2.4). For each batch of diffusion specimens cast, three 100mm standard test cubes were cast. Cubes were demoulded at 24 hours and cured under water until 28 days old. Cubes were weighed and then tested in a compression machine compliant with the requirement of the British Standard grade A machines (2.5).

Cubes were loaded until failure. The compressive strength of each cube was calculated, by dividing the maximum load sustained, by the cross-sectional area across which the stress was applied. An example of the calculation is given within the Appendices.

2.5 PORE SOLUTION EXPRESSION

The study of pore solution extracted at high pressure from hardened cementitious matrices has furthered the investigation of cement chemistry (2.6-2.9). A pressure vessel of a design based on that originally devised by Longuet, et al (2.10) has been employed in this investigation (2.2 - 2.3). The procedure involved loading the constrained sample via the piston assembly to a maximum stress of approximately 375 MPa. A small volume of solution was forced from the sample and was collected within a plastic

syringe via the fluid drain. The extracted pore solution, thought to closely resemble the aqueous phase of the hardened cementitious matrix, was temporarily stored within airtight plastic vials prior to analysis.

2.6 HYDROXYL ION (pH) ANALYSIS

In order to establish changes of hydroxyl ion concentration in pore solutions taken from specimens used in the cathodic protection investigation in Chapter 6, a standard acid/base titration with 10 milli-molar nitric acid was carried out using a phenolphthalein indicator. Titrations were performed manually by dispensing the nitric acid titrant from a graduated microburette (0.01 millilitre increments). Upon reaching the end-point of the titration, the volume of titrant dispensed was recorded, and the pH of the solution was calculated from the hydroxyl ion concentration. An example of the calculation is given in the Appendices.

2.7 CHLORIDE ION ANALYSIS

A considerable number of chloride ion concentration determinations were made in order to establish diffusion coefficients. The most reliable and convenient technique available was a spectrophotometric method. Each 0.1 millilitre of diffusant taken from the diffusion cell was made up to 10 millilitres with deionised water. To this solution was added 2 millilitres of 0.25 molar ferric ammonium sulphate in 9 molar nitric acid and 2 millilitres of saturated mercuric thiocyanate in ethanol. The thiocyanate ion was complexed with the ferric ion, in the presence

of chloride ;

$$2Cl^- + Hg(SCN)_2 + 2Fe^{3+} \rightarrow HgCl_2 + 2(Fe(SCN))^{2+} \quad (2.11)$$

The result of the thiocyanate complexation produced a coloured solution, the intensity of colouration being proportional to the concentration of chloride ion present. This may be measured with a spectrophotometer (figure 2.4). The spectrophotometer measures the absorption of light at specific wavelengths. The characteristic wavelength used here was 460nm.

Absorption was measured by filling a precision glass optical cell with the coloured solution, a second matched cell was filled with deionised water in order to establish a blank reference. With both cells positioned within the spectrophotometer, a beam of light was passed through each cell in turn. The difference in absorption between the solutions was subsequently interpreted in terms of molarity, by making reference to a calibration curve constructed from chloride standards.

2.8 ELECTRON MICROSCOPY

A Cambridge Steroscan 150 scanning electron microscope fitted with a "Link" energy dispersive x-ray analysis spectrometer (EDXA) was used for the microscopy study (figures 2.5 and 2.6). The EDXA facility permits rapid element analysis of particular surfaces selected. Analysis was performed by detecting characteristic x-rays, associated with certain elements, produced by bombarding a surface with an electron beam. This results in an excitation of the electron structure of the sample, resulting in the emission of characteristic x-rays.

A silicon detector, held at liquid nitrogen temperature,

measures the energies of the x-rays and transmits signals to a micro-computer, from which an elemental analysis was obtained.

2.9 POROSIMETRY MEASUREMENTS

In order to establish measurements of pore size distribution (psd), the mercury intrusion porosimetry technique was used. The technique has previously been successfully employed in the study of hydrated cementitious systems (2.12, 2.13). All measurements were carried out using a Micromeritics Instrument Corporation model 900/910 porosimeter, as shown in figure 2.7.

The technique involved forcing a non-wetting liquid (mercury) into the pores of a specimen and was carried out as follows : A small mass of sample material was dried to constant weight by heating to 105° C. The sample was then placed within a calibrated glass cell (figure 2.8) which was fixed within the pressure vessel of the porosimeter. The system was then evacuated in order to remove absorbed gases and vapours. Once evacuated, mercury was introduced to the cell, and hydraulic fluid introduced to the vessel; pressure was then applied in incremental stages. From the Washburn equation (2.14) the pressure at which mercury enters a cylindrical pore of given size may be calculated :

$$P = \frac{-4\gamma \cos\Theta}{d}$$

where

P = the applied pressure (Pascals Nm^{-2})

d = the pore diameter (microns/μm)

γ = the surface tension of mercury (N/mm)

Θ = the contact angle between mercury and the material (degrees)

From this equation the volume of pores of a particular size may be calculated knowing the pressure and volume of mercury intruded at the particular pressure. An example of the calculation is given within the Appendices.

Owing to a number of assumptions and limitations attendant to mercury intrusion porosimetry, as applied to cementitious systems, a number of workers have been critical of the method. Such criticism is discussed in Chapter 7, where the technique has been employed.

2.10 ELECTRODE POTENTIALS

The corrosion of a metal when in contact with an electrolyte involves a flow of current between anodic and cathodic sites. The flow of electrons implies that a potential difference must exist between the two sites. The potential difference developed between a point on the metal surface and a close position within the electrolyte is known as the electrode potential.

Absolute values of electrode potential are indeterminate, but, relative values may be established when measured on an arbitarily defined scale. The scale adopted is determined by the type of reference half-cell used. In the case of steel in concrete, the copper sulphate electrode is most frequently used for site investigations. The reference electrode is connected to the reinforcement, via a voltmeter, and moved over the concrete surface (figure 2.9). Readings are usually taken in millivolts and may indicate net anodic and cathodic regions within the concrete.

Within this work the copper sulphate electrode (CSE) was used most frequently, although the saturated calomel electrode (SCE) was

used in Chapters 5 and 6.

2.11 POLARISATION RESISTANCE MEASUREMENT

Polarisation resistance or linear polarisation has been used in order to measure corrosion rates. Measurements were carried out using a Thompson Electrochem Multistat system comprising ; d.c. potentiostat, master control unit, micro-computer and ancillary equipment (figure 2.10).

The technique is based upon the theoretical background established by Stern and Geary (2.15, 2.16), and developed by Stern (2.17) for the measurement of corrosion rate from polarisation data.

Essentially the technique involves polarising an electrode several millivolts (ΔE) either side of the corrosion potential (E_{corr}). The resulting current passed per unit area (Δi) is plotted against potential and the polarisation resistance (R_p) is obtained from the curve :

$$R_p = \left(\frac{\Delta E}{\Delta i}\right) \quad \Delta E \longrightarrow 0$$

The corrosion rate (i_{corr}) is calculated from the Stern Geary equation (2.15).

$$i_{corr} = \frac{\beta a \, \beta c}{2.3(\beta a + \beta c)} \cdot \frac{1}{R_p}$$

where

βa and βc = the anodic and cathodic Tafel coefficients for the system.

Ideally Tafel coefficients should be determined experimentally for each specimen, but unfortunately this involves a several hundred millivolt scan either side of E_{corr}. The large shifts in potential may alter the electrochemical state of the electrode. For practical purposes, therefore, it is usual to assume βa and βc = 0.12 (volts/decade) and so simplify the equation :

$$i_{corr} = \frac{0.026}{R_p}$$

The method as described applies if; ΔE is small, the ohmic potential drop (iR) between working and reference electrode is small (or, alternatively, is compensated for), and the area of the working electrode is accurately known.

For this work it was found practicable to use a scan rate of 10mV/min, scanning ±20mV for low corrosion rates and ± 10mV for greater corrosion rates. An example of the polarisation resistance curve so obtained is shown in figure 2.11, and the components comprising the measurement system in figure 2.12.

The technique was originally shown to be applicable to steel/concrete systems by Andrade et al (2.18), and has subsequently been employed by other workers (2.19-2.21).

2.12 RESISTIVITY MEASUREMENTS

The method most commonly used for the on-site measurement of concrete resistivity is based on a soil resistance technique devised by Wenner (2.22). The instrument used for this study was the Norma D3950 Digital Grounding Meter (figure 2.15), measuring to 199.9 KΩ, with a 4 probe unit.

Having first drilled a series of shallow holes along the

length of each test specimen, the centres being compatible with the electrode spacing on the 4 probe unit, measurements were taken sequentially along the length of each specimen. A 40 milliamp current (108 Hz) was induced through the outer probes C_1 and C_2 (figure 2.13, and the potential difference was measured across the inner probes P_1 and P_2. The voltage drop between P_1 and P_2 was compared to inner reference resistors and a value obtained in ohms. This value was subsequently converted to apparent resistivity by using the following equation (2.23).

$$\rho = 2 a R \pi$$

where

ρ = resistivity (ohm cm)

a = distance between electrodes

R = resistance (ohms)

A potassium chloride electrode gel was used to improve probe to mortar conductivity. Figure 2.14 shows the experimental arrangement.

2.13 GALVANIC CURRENT

The specimens described in Chapter 3 involve an electrode comprising several electrically isolated segments. In order to measure the flow of current between assumed net anodic and cathodic segments a digital ammeter was used. A Thurlby 190SA digital meter (figure 2.16), resolving to one μA was employed. The instrument was employed on account of its' high input resistance ($>1000M\Omega$) and low capacitance (100 pF); both desirable features when measuring current of low charge, and voltage where high circuit resistance is involved.

Analyses	Blue Circle Cement Company	Ketton Cement Company
Insoluble residue	0.65	0.60
Loss on ignition at 0-925°C	1.10	1.14
Sulphate as SO_3	2.6	2.7
Silica as SiO_2	19.8	20.5
Iron as Fe_2O_3	3.1	3.0
Calcium as CaO	61.9	64.6
Magnesium as MgO	1.4	< 0.01
Potassium as K_2O	0.6	0.6
Sodium as Na_2O	0.3	0.2
Aluminium as Al_2O_3	4.4	4.4
Titanium as TiO_2	-	0.4
Manganese as Mn_2O_3	-	0.04

TABLE 2.1 Chemical analyses of cement by % weight on weight; Blue Circle cement used in Chapter 6 and Ketton cement used elsewhere

Specimen	Aggregate proportions	Aggregate/ cement ratio	Water/ cement ratio
Mortar comprising the prism for the galvanic bar	2:1 (300>600 μm: 500>1000 μm particle size)	3:1	0.5
Mortar comprising the cathodic protection prisms	zone 2 concreting sand	2:1	0.5
Mortar comprising the diffusion specimens	2:1 (300>600 μm: 500>1000 μm particle size)	3:1	0.4
Mortar comprising the diffusion specimens	2:1 (300>600 μm: 500>1000 μm)	3:1	0.6
Cement paste comprising the diffusion specimen	-	-	0.28

TABLE 2.2 Mix details for various specimens

Element	Mild steel A	Mild steel B	Stainless steel
Carbon	0.14	0.11	0.04
Silicon	0.20	0.23	0.62
Manganese	0.87	0.40	1.14
Phosphorous	0.018	0.013	0.040
Sulphur	0.028	0.002	0.012
Chromium	0.20	0.05	18.00
Molybdenum	0.05	0.01	0.39
Nickel	0.18	0.03	9.00
Titanium	-	-	0.33
Niobium	-	-	0.02
Iron	BALANCE		

TABLE 2.3 Chemical analyses of metal by % weight on weight; mild steel A and stainless steel used in Chapter 6, mild steel B used for galvanic bar

FIGURE 2.1 Flow table and cone mould; the apparatus used for the determination of flow during the preparation of mortar diffusion specimens

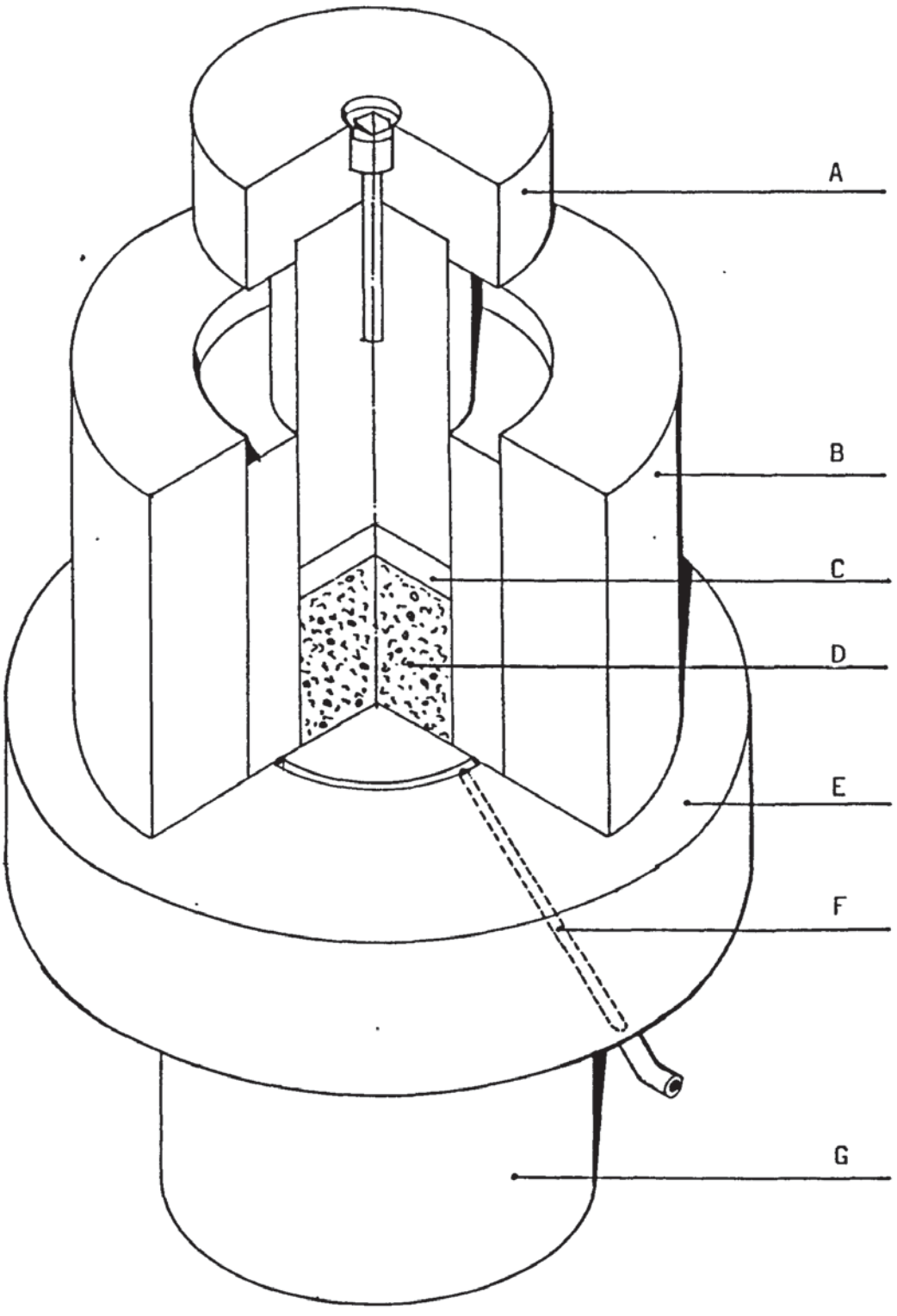

FIGURE 2.2 Cut-away isometric of pore press showing the following components; A = piston, B = die body, C = P.T.F.E. disc, D = specimen, E = platen, F = fluid drain, G = base

FIGURE 2.3 Pore press assembly used for the extraction of pore fluid

FIGURE 2.4 The Beckman spectrophotometer used during the determination of chloride concentration

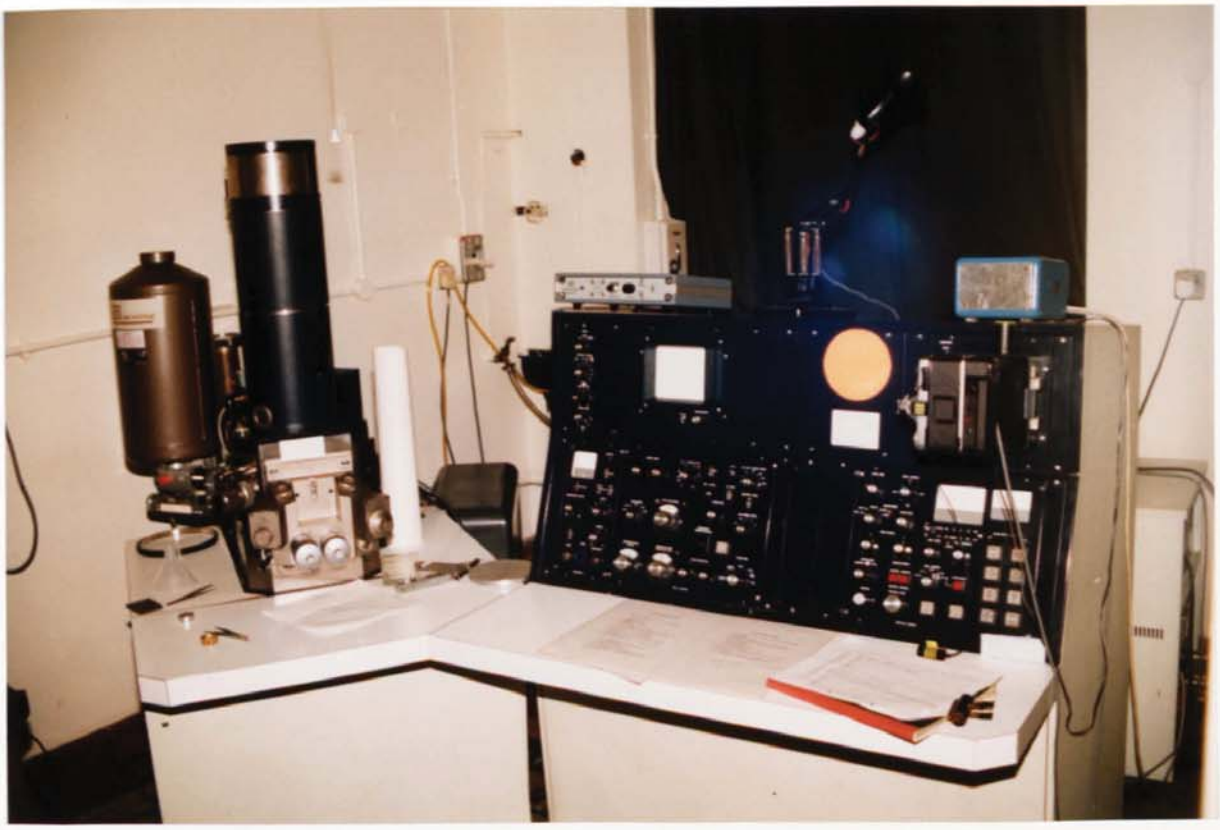

FIGURE 2.5 Scanning electron microscope, Cambridge Stereoscan 150

FIGURE 2.6 The Link E.D.X.A. analysis system used in conjunction with the SEM

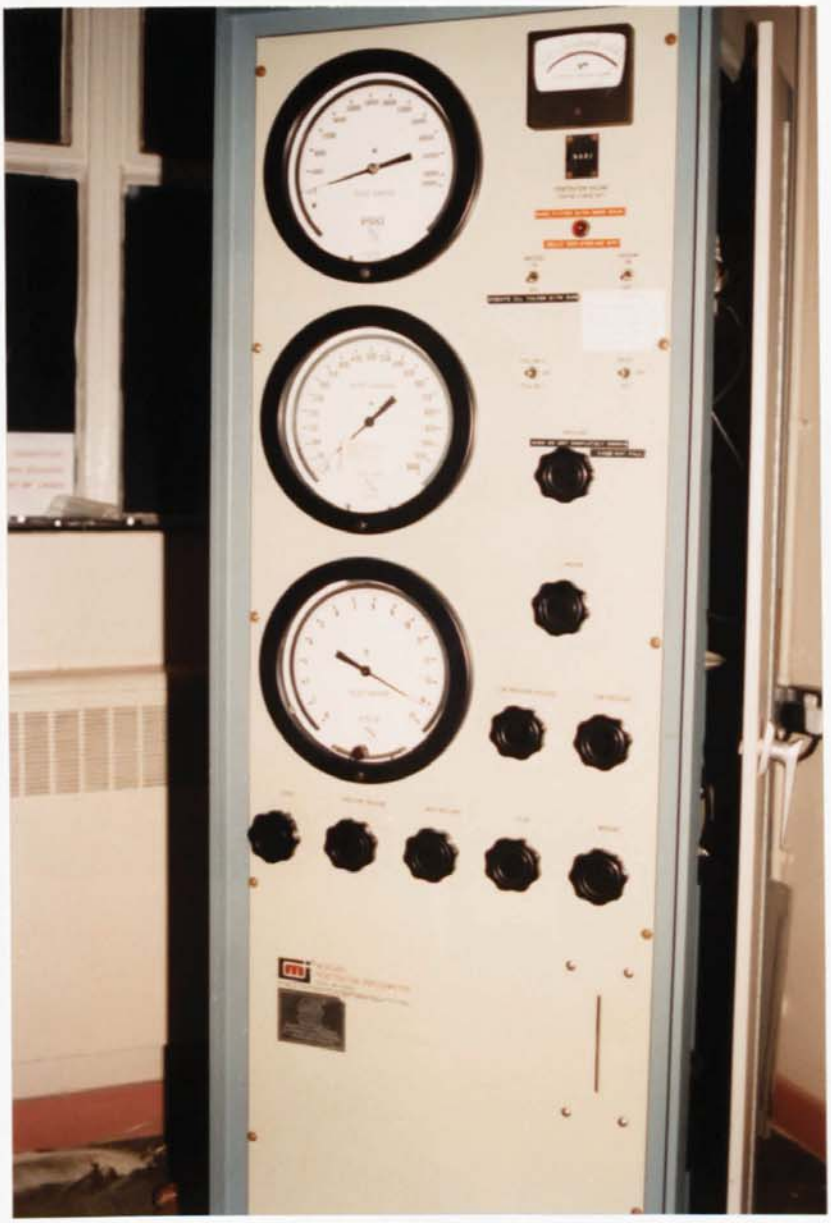

FIGURE 2.7 Porosimeter used for the determination of pore size by mercury intrusion

FIGURE 2.8 Precision ground glass specimen cell (held within the fluid containing pressure vessel) into which mercury was introduced

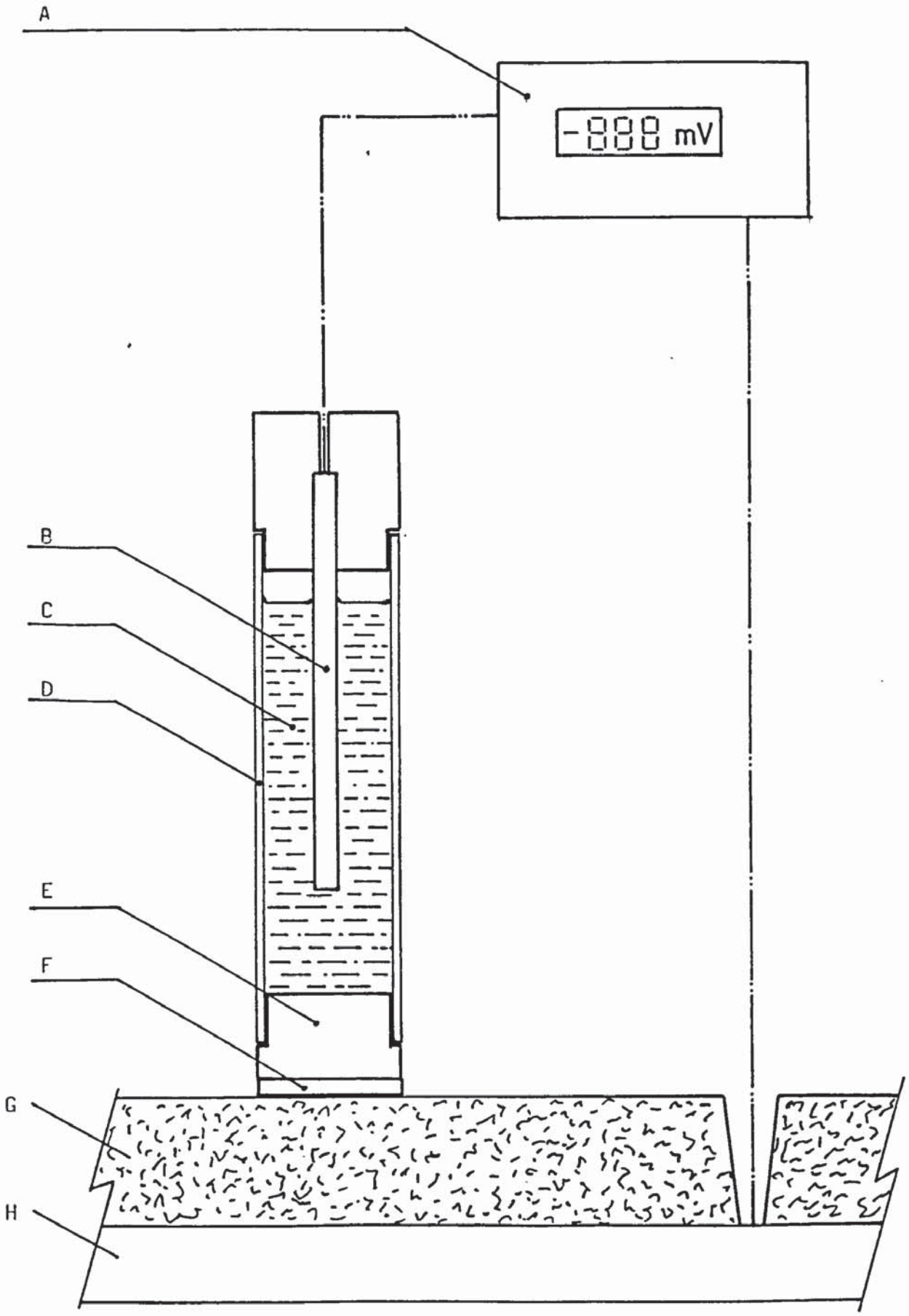

FIGURE 2.9 Half cell potential measurement system comprising; A = high impedence digital voltmeter, B = copper rod, C = saturated copper sulphate solution, D = acrylic body, E = porous plug, F = sponge, G = concrete, H = steel reinforcement

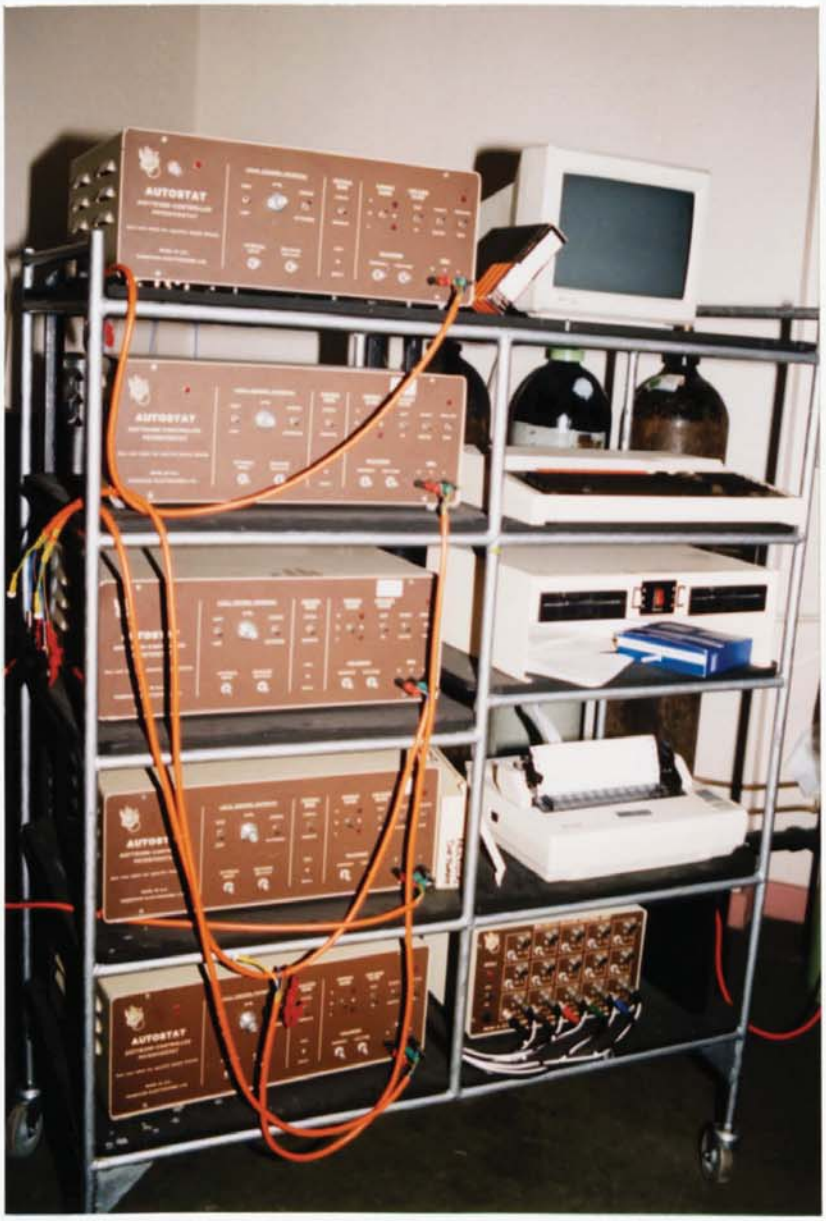

FIGURE 2.10 The equipment comprising the Multistat system; potentiostats (LHS), micro processor (RHS) and control unit (bottom RHS)

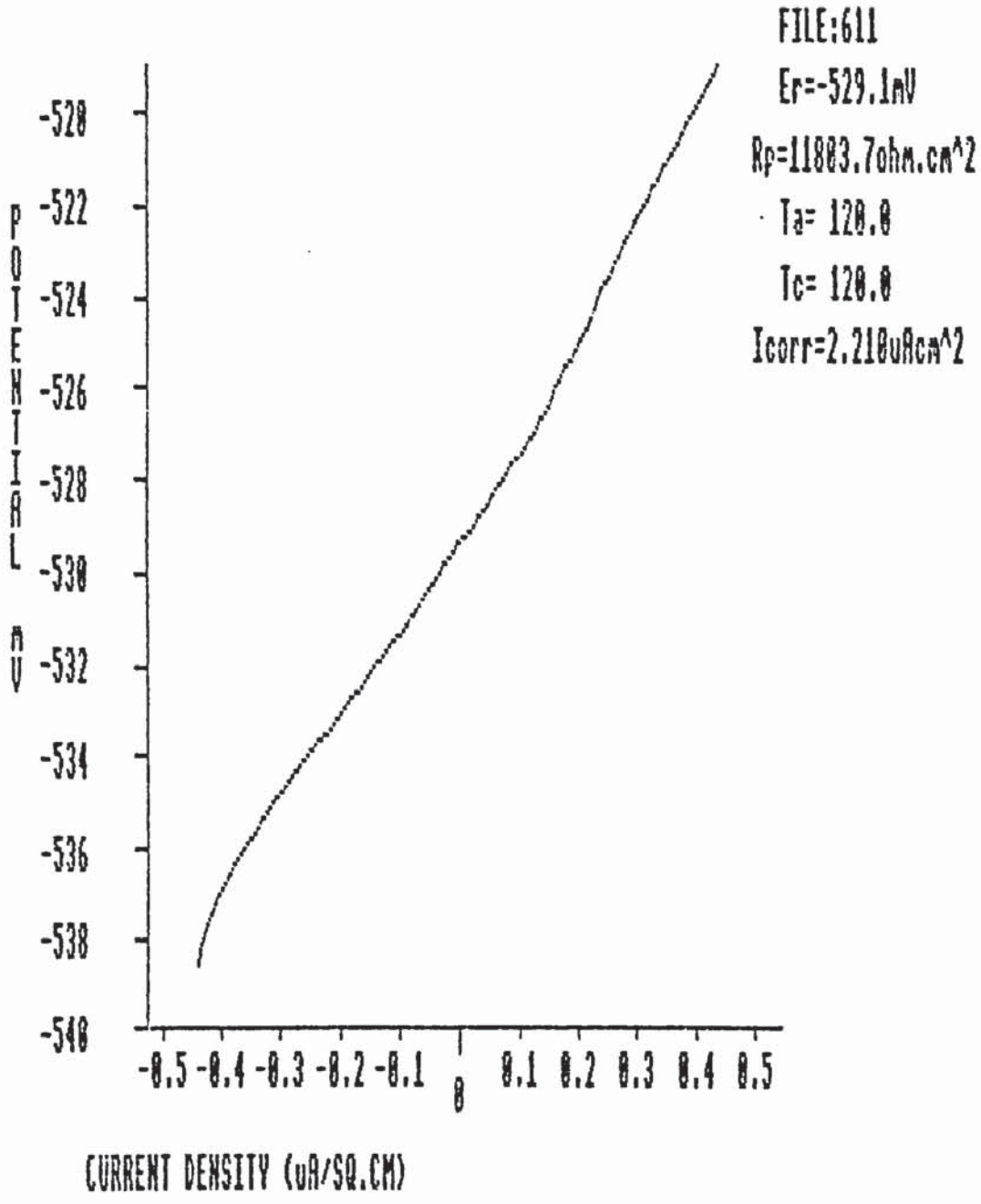

FIGURE 2.11 Polarisation curve from the Multistat system, in this instance for an active segment within a 5% chloride (by weight of cement) environment

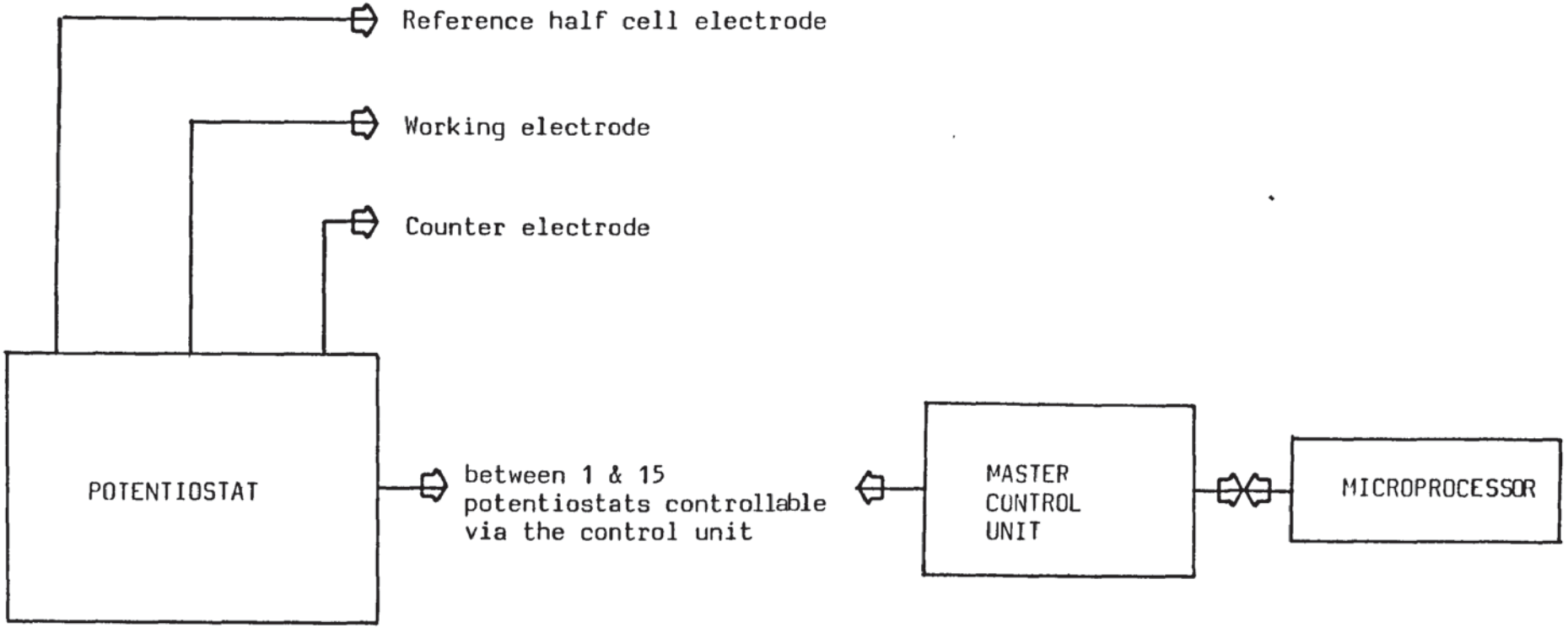

FIGURE 2.12 Schematic showing the components comprising the Multistat system

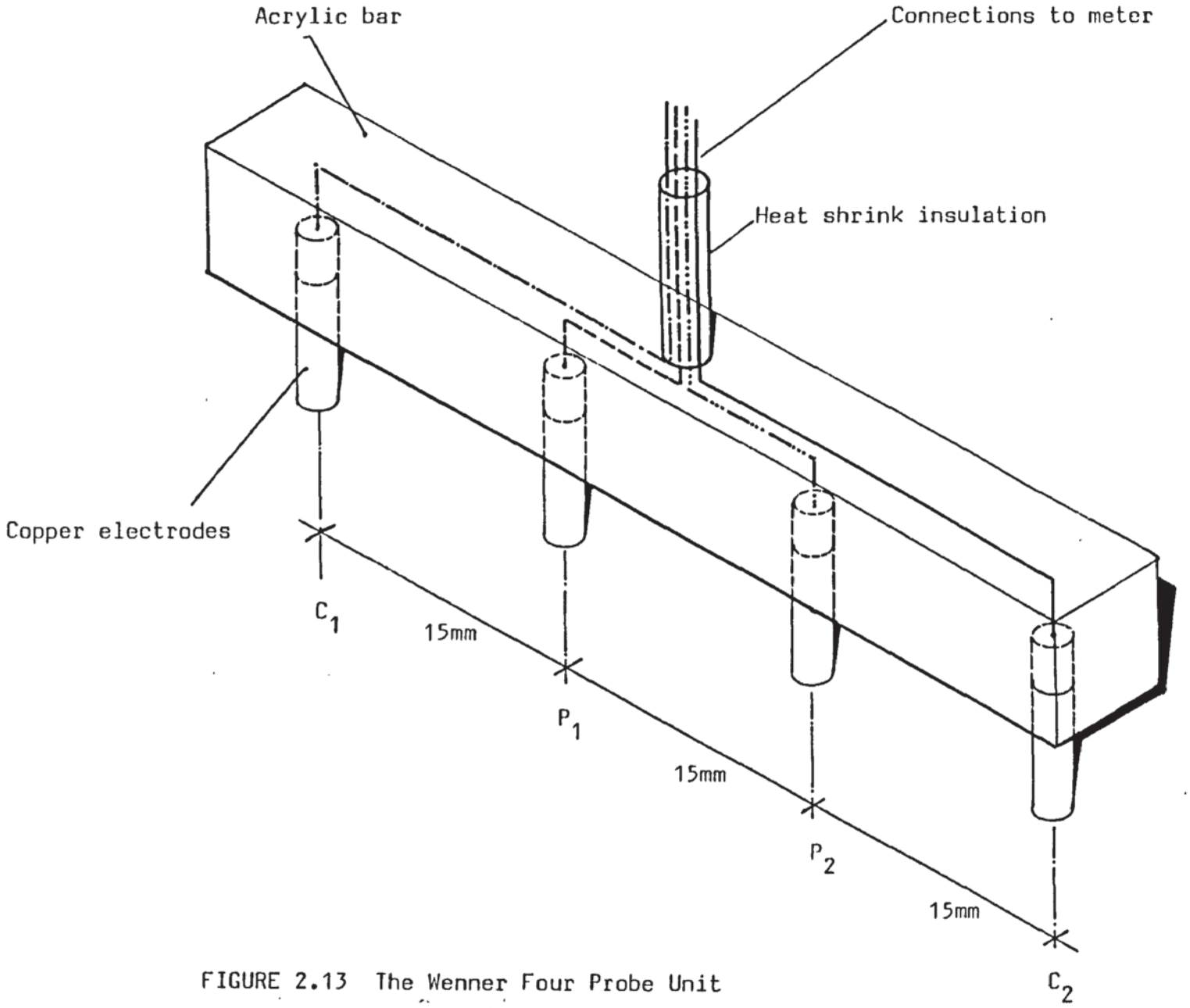

FIGURE 2.13 The Wenner Four Probe Unit

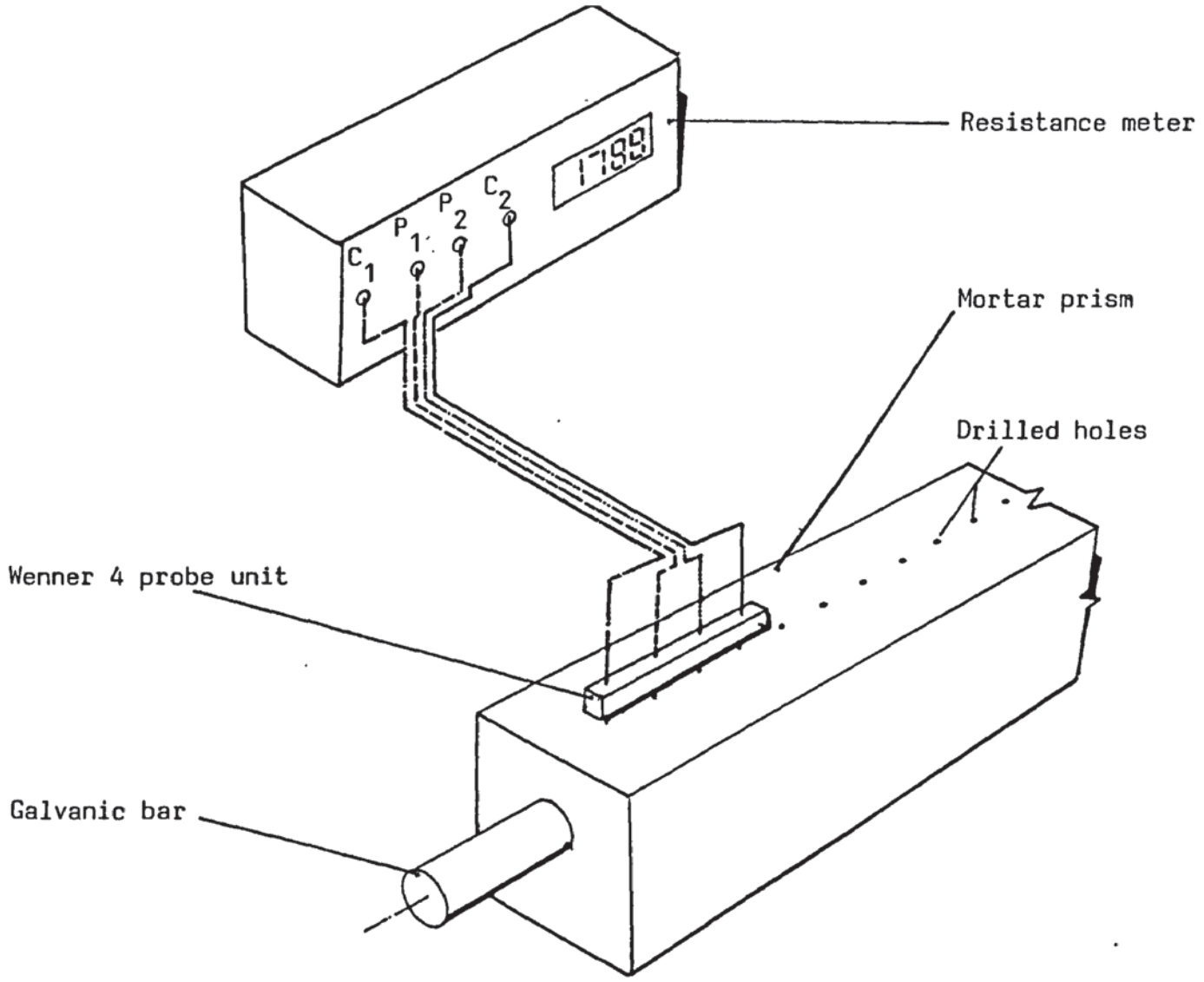

Figure 2.14 The experimental arrangement for resistance measurements

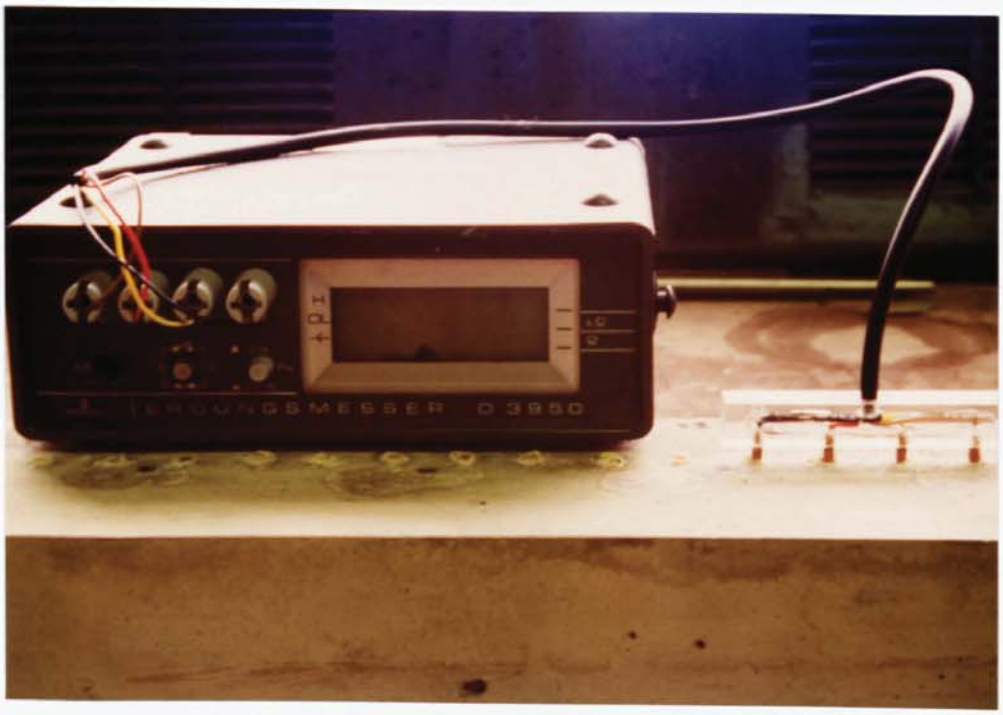

Figure 2.15 The resistance meter and Wenner four probe unit

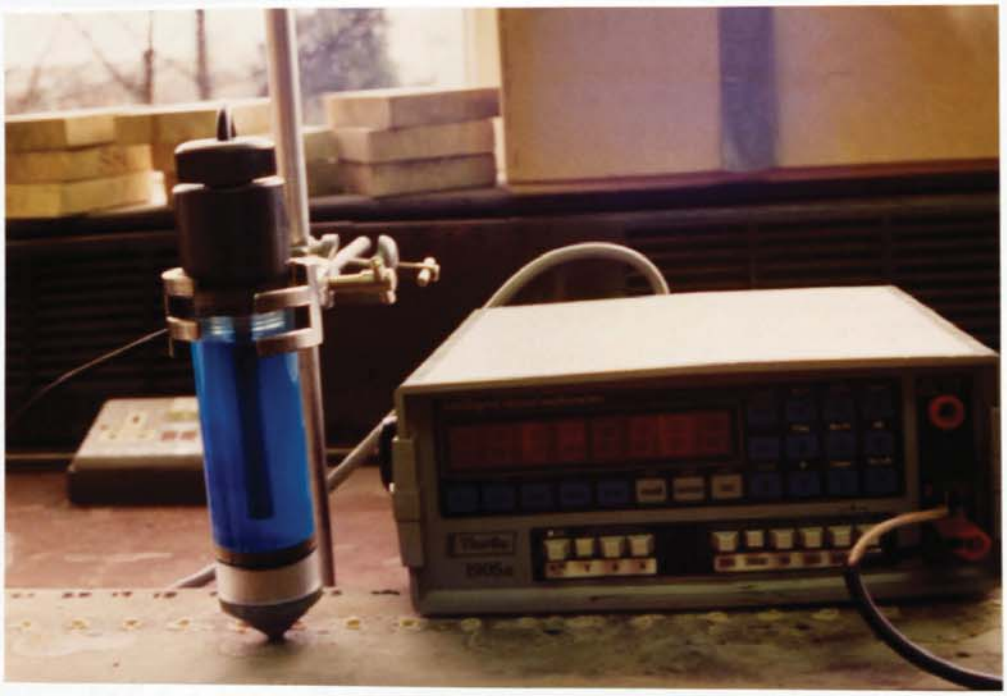

Figure 2.16 The Thurlby digital ammeter

CHAPTER 3

DEVELOPMENT OF A METHODOLOGY FOR THE STUDY OF ELECTROCHEMICAL PROCESSES ASSOCIATED WITH PATCH REPAIRS IN REINFORCED CONCRETE

3.1 INTRODUCTION

Whilst enhanced durability arising from new and improved materials will benefit future construction projects, the immediate problem of deteriorated existing structures requires attention. There is a need to repair and maintain the serviceability of such structures, restoring structural integrity and halting deterioration.

The necessity to repair has given rise to a number of rehabilitation practices, these frequently being developments of systems used originally on bridge decks in the United States, where chloride corrosion has been recognised for some time. The most widely used technique is patching, involving the removal of isolated spalled areas of concrete and reinstating usually with a modified concrete or mortar. Whilst this approach to maintaining serviceability is the most obvious mode of repair, the rationale for the approach is simplistic. It has been found that some time subsequent to the repair, corrosion can be exacerbated in non-repaired areas of the structure (3.1, 3.2). A possible explanation for this phenomenon is that patching leaves areas of the structure containing chlorides, which within the pre-repair condition were unable to stimulate significant corrosion. However, in the post-repair condition, these chloride levels are able to stimulate more significant rates of reinforcement corrosion. This may be due to

nearby cathodic sites (the chloride free patch areas) now being available to stimulate conditions conducive to activating incipient anodes.

There is an increasing body of opinion that suggests patch repairs can be responsible for accelerating corrosion of reinforcements (activating incipient anodes), within non-repaired areas of chloride contaminated structures. However, as there would appear to be little quantitative evidence to support this notion, it was considered to be of some interest to investigate the phenomenon.

It would be possible to evaluate the incipient anode hypothesis by the potential mapping of a structure both before and after repair. Equally, a similar type of investigation would be possible under controlled laboratory conditions. Such investigations would not provide any information on actual rates of corrosion, only on its likelihood. Whilst a number of laboratory based techniques are available for the non-destructive determination of corrosion rate of embedded steel electrodes, they will not provide data relating to specific portions of a single electrode experiencing several rates of corrosion at different sites along its length. This is likely to be the condition of an embedded rebar within a structure containing several levels of chloride contamination. Consequently, if a laboratory specimen were to be designed comprising an electrically continuous single electrode cast within a concrete containing a range of chloride concentrations, measurements of corrosion rate relating to specific regions of the electrode, experiencing a local chloride level, would not be practicable.

It was, therefore, the purpose of the investigation described

in this chapter to design and develop a test methodology for measuring local corrosion rates of portions of a single electrode embedded in mortar containing a range of chloride levels.

3.2 PREVIOUS WORK

For laboratory-based study of the corrosion behaviour of steel in concrete, several types of monitoring technique may be employed. The forms of metal/electrolyte system utilised in such studies may be described as being of two types. First, there are systems involving electrodes, usually mild steel, physically embedded within a cementitious matrix. Secondly, there are systems using electrodes, immersed within an aqueous medium, the composition of which is designed to resemble the pore electrolyte phase of the particular concrete matrix under consideration.

Investigations into cathodic reactions in cathodic protection systems have employed solutions of various composition in order to determine the protection potential associated with hydrogen bubble evolution (3.3). Saturated calcium hydroxide solutions containing different levels of sodium chloride were used to determine pitting potentials for steel exposed to several oxygen levels and temperatures (3.4). Protection criteria for cathodically protected steel in concrete were investigated by means of steel rods in saturated lime solution. The experimental arrangement used electrodes surrounded by packed limestone, the intention being for the aggregate packing to entrap air bubbles against the steel surface when adding the electrolyte (3.5). Lime solutions containing chloride additions were used to establish threshold concentrations giving rise to corrosion of steel rods (3.6).

Boundary conditions for inhibition of pitting of steel rods in aerated alkaline solution containing chlorides were defined (3.7). Using alkaline solutions a relationship was found between hydroxyl ion concentration and the threshold chloride ion concentration giving rise to corrosion or inhibition (3.8).

Studies of these types involving artificial pore electrolyte solutions suffer from certain limitations, particularly when trying to match such studies with field exposure trials. The principal soluble components of hydrated Portland cement produce a pH at least as high as a saturated lime solution (pH 12.5). It is not uncommon to find Portland cements producing alkalinities in excess of pH 13.5 (3.9). The ability of individual Portland cements to remove free chloride from the pore solution will vary according to the aluminate and ferrite constituents (3.10, 3.11). It is thought that the tricalcium aluminate content of a Portland cement will influence the extent to which chloride ions, present at the mixing stage, are complexed to form chloroaluminate hydrate (3.10, 3.12). There is also some speculation as to the complexing ability of the calcium silicate hydrate gel (3.13, 3.14).

The most apparent limitation of studies involving immersed electrodes is that the electrolytic medium cannot provide diffusion kinetics of reactants and products, involved in the corrosion processes, that would be typical for a concrete matrix. The diffusion rates of reactants are related to the nature of the pore structure of the hydrated cement matrix. Diffusion rates for species such as chloride (3.15, 3.16) and oxygen (3.17, 3.18) within cementitious matrices have been found to vary. Certain specific aspects of the cement matrix will serve to modify diffusional characteristics, for example, the interaction between

the embedded steel and the cement giving rise to a lime rich layer at the steel/cement interface (3.19).

From the foregoing it is apparent that investigations involving immersed electrodes are subject to several limitations. The alternative approach to studying the corrosion of steel in concrete involves electrodes embedded within a hydrated cementitious matrix. Studies of this type are not without difficulties and a circumspect approach must be adopted in the design and preparation of specimens. A failure to do so is liable to yield results containing significant artefacts. The most common problem associated with the design and preparation of specimens using embedded electrodes concerns the method of masking external connections in the embedded electrode so that crevice corrosion at the electrode/masking interface is avoided (3.20). Masking materials commonly used for this purpose are prone to degradation when subjected to a highly alkaline environment, therefore, Portland cement exacerbates the problem. A successful masking technique involving a duplex coating of ordinary Portland cement and epoxy has, however, been devised to avoid crevice corrosion (3.21).

Investigations employing embedded electrodes may involve chlorides introduced at the mixing stage of specimen preparation or, alternatively, hydrated specimens exposed to an external source of chloride.

Subjecting specimens to a source of chloride at the post hydration stage has the desirable feature of introducing a depassivating ion as a diffusion controlled process. This arrangement may tend to more closely resemble conditions often found in practice. However, investigations of this form are inconvenient since long specimen exposure periods may be required

to initiate significant corrosion. It is apparent also that in subjecting an embedded electrode to a solution of known ionic concentration, it is not possible to control the range of chloride concentrations at several sites along the electrode.

Introduction of the depassivating ion at the mixing stage of specimen preparation, usually dissolved within the mix water, avoids the time delay. However, a specimen containing a relatively uniform chloride ion concentration does not represent the variations in contamination present throughout a real structure. The effect of such variations in chloride concentrations found in practice is to generate macro-cell corrosion causing galvanic currents to flow.

Whilst it is practical to embed a single electrode within a range of chloride levels, by casting in several stages, the problem arises in monitoring the corrosion rate of the portion of electrode subject to a specific level of chloride. It would be possible to measure corrosion potentials, in the form of a potential map, relating specific corrosion potentials to portions of electrode subject to a specific chloride level. Such measurements do not yield data on the rate of corrosion. As indicated previously, a problem encountered in applying conventional methods for determination of corrosion rate is that the area of steel polarised during the investigation is unknown. Theoretical treatments have sought to model the areas of steel under investigation, but no account for the effect of macro-cell interactions is made (3.22). In order to determine galvanic macro-cell corrosion currents a further problem is evident; measurement of galvanic current requires the electrical isolation of the net anode and cathode.

A specimen facilitating the measurement of macro-cell corrosion currents, associated with a range of chloride levels, is likely to be of considerable use in the laboratory modelling of pre and post repair corrosion processes. Several parameters may be considered; including, chloride concentrations, anode and cathode areas, and moisture condition of the concrete. By monitoring the corrosion processes by several methods an evaluation may be made of various forms of monitoring. Several applications are possible (monitoring cathodic protection etc), but of interest here, is the application of the method to concrete patch repair and reinforcement priming systems. At present, no comparative means is available for the assessment of a repair systems' ability to limit the corrosion rate of any incipient anode stimulated.

The work to be described in this chapter was aimed at developing a methodology capable of meeting these requirements.

3.3 EXPERIMENTAL

The primary goal of the experimental work in this chapter was to devise a specimen of such a type that macro galvanic corrosion currents might be determined. To achieve this end, it was important that the following features should be incorporated within the design.

The electrode representing a reinforcing bar should be segmented so that effects of :

1. Coupling and decoupling of various portions of the steel could be examined.

2. Each portion of the electrode should be subjected to a specific level of chloride contamination.

3. A portion of the specimen should be repairable, as in a patch repair, at some point during the exposure period.

4. The completed specimen should be subject to a regime of environmental cycling.

5. The specimen should be reasonably robust and free from features which may generate spurious data (crevices).

The above requirements were thought to be best achieved by the construction of a specimen of the following design :

The overall dimensions of the electrode fitted conveniently within a British Standard 500 x 100 x 100mm prism. The electrode itself, employed seven segments of mild steel thick wall tube of 25.4mm outside diameter; an analysis of the composition of the material is given in Chapter 2. Individual segments of bar were cut to an oversize approximate length and subsequently machined and faced to the design length of 80mm. Each segment was drilled through its wall, a few millimetres from the face end, then again mid way across the wall thickness such that the two holes were consistent. The latter blind hole was tapped and fitted with a counter sunk grub screw. The purpose of providing coincident holes was to afford a means, at a latter stage, of securely attaching an external wire to the inside of the tube. This wire served as a means of connecting/disconnecting segments via a junction switching

box. Segments were degreased with a trichlorothane type commercial solvent (inhibisol) and then lightly surface abraided using a 600 grade silicon carbide paper to produce a consistent surface finish. Segments with significant surface flaws were rejected.

In order to provide a means of physically joining adjacent segments, and also to provide a means of electrically isolating segments, insulating washers were fabricated. Having initially experimented with acrylic, Bakelite and various types of Tuffnol, a fine weave alkali-resistant Tuffnol material was adopted. This material was found to be particularly suited to accurate cutting; machining thin sections without excessive deformation or fracture. Bakelite and acrylic materials were found to be unsuitable due to their relatively brittle nature when machined to slender thickness. Other types of Tuffnol, whilst being suitable for machining requirements, were found to degrade in completed mortar specimens due to the highly alkaline environment.

In order to construct seven mild steel segments and six Tuffnol washers in a single rigid assembly, a central tie rod was employed. This mild steel rod passed through the central axis of the assembly locating all six insulating washers. The washers, in turn, which were machined with a double shoulder, supported the respective steel segment (figure 3.1). Each end of the tie rod was fitted with a shouldered end nut.

The sequence of assembly of the components involved first attaching lengths of insulated wire to each segmental electrode, secure location of the wire being provided by the grub screw. Where wire had been stripped of its insulation and bare conductors were exposed, an insulating epoxy was used to reinsulate, so avoiding the risk of a mixed metal corrosion couple. Wired segments were

then fed onto the central tie rod, locating with a partial interference fit, onto the washer shoulder with the steel/Tuffnol interface having first been coated with an adhesive. The purpose of the adhesive was to prevent ingress of pore water/moisture from the mortar matrix of the completed specimen, into the hollow section of the segmental electrode. Prototype specimens used a silicon rubber preparation at the steel/Tuffnol interface but this was found to be unsuitable, owing to the promotion of crevice corrosion, probably as a result of the acetic acid present in the formulation. After a short period had elapsed following application of the adhesive, the hollow section of the segment was filled with a proprietory inhibitive anti-corrosion grease (Duckham's D7). The object of this was to avoid any 'hollow leg' corrosion artefacts appearing in the corrosion rate measurements. Prototype specimens employed segments internally coated with a bituminous paint, but this was found to be prone to undercutting. The wire from each segment was fed through one of the radially drilled holes in the insulating washer, the washer then being seated upon the segment so providing isolated location at either end of the segment. Again, steel/Tuffnol interfaces were coated with adhesive. This procedure was repeated until six segmental electrodes and six insulating washers had been assembled.

The seventh and final segment, which was to be out of circuit and only partially embedded within the mortar prism, was drilled and tapped with a tapered hole through which the six external connection wires were passed. The use of a tapered gas thread was found to be necessary to ensure a water-tight seal when a tubular upstand (containing all six wires) was later fitted to the segment. The second end nut was then fitted and tightened sufficiently to

stress the components as a rigid structure. The assembly was then tested for the electrical continuity of all external connections, and for electrical discontinuity between individual segments, this being achieved simply by establishing resistance.

When it had been checked that the segmental electrodes were free from surface defects and all electrical connections were sound, the completed electrodes were supported within modified British Standard prism moulds. In this position masking of the end segments was effected. As described in the previous section, this end treatment was necessary in order to minimise the risk of crevice corrosion at these exposed positions. A previously developed anti-crevice masking technique, comprising a duplex coating ordinary Portland cement slurry with styrene butadiene rubber, and an epoxy topcoat was utilised (3.21). The tapered wire feed hole was temporarily masked with waterproof tape in order to prevent inadvertent contamination of the hollow-section with fluid mix material during casting, albeit the section filled with grease.

The need for modification of the prism mould arose due to the requirement for casting a specimen containing a range of chloride concentrations. It was thought that this gradient could be best achieved by casting the prism in several layers, in an end-on manner as a tall column may be cast. By using several mixes (four in total, containing different chloride additions), a gradient was produced along the length of the entire electrode. Individual layers within the gradient corresponded to single electrode segments, with the interfaces between mixes occurring at the washer portion of the electrode.

The mortar mix was a 1:3 ordinary Portland cement, and Leighton Buzzard aggregate, of water/cement ratio 0.5, with 5%, 1%,

0.1% and 0% chloride ion (by weight of cement) introduced as sodium chloride. Mixes containing 5%, 1% and 0.1% chloride ion corresponded to single segmental electrodes whilst the chloride-free mix corresponded to three electrodes. The purpose of this was to ensure that a large cathodic area was provided. The range of chloride contamination levels were selected on the basis that a strongly anodic site would be provided by 5% chloride addition, whilst a less active site would result from the 1% addition. The primary purpose of the 1% addition was to provide a zone which could then become an incipient anode adjacent to a region that was to be patched. The 0.1% addition was provided as a marginal level of contamination.

With the masked galvanic bar electrode temporarily held securely within the modified mould, the front blanking plate of marine plywood could be bolted to the long itudinal opening of the mould, which normally represents the finished/struck surface of a cast prism. The mould was securely held in plumb alignment within a frame, by an arrangement of clamps and folding wedges, and the frame, in turn, was clamped to a vibrating table.

The constituents of each mix are described in Chapter 2, compaction of each layer being achieved by a combination of vibrating poker, and vibrating the entire casting rig via the vibrating table. The additional careful use of the vibrating poker was found to be necessary due to the large mass of the casting rig rendering the use of the vibrating table alone ineffective for attaining adequate compaction. In placing the individual layers of each mix, it was found that a certain amount of foreign fluid mortar was prone to contaminate electrodes other than the specific electrode for which the material was intended. To avoid this (eg 5%

chloride mix contaminating a segment subsequently to be embedded within 0.1% chloride mortar) a retractable sleeve was employed. This sleeve masked electrodes which were to be subsequently cast and was lifted in a sequential manner as each mortar layer was completed. A period of approximately thirty minutes was allowed to elapse before placing a consecutive layer of mortar, in order to permit an initial stiffening of the mortar already placed.

Cast specimens were initially cured within their moulds under normal curing conditions for twenty four hours. After demoulding, specimens were cured for twenty one days, and during this period the acrylic tubular upstand was fitted to the tapered thread within the end segment of the bar. Also, during this curing period, all the necessary wiring from the individual segments to the junction switching box was connected. As the acrylic upstand presented a possible source of entry for potentially corrosive reactants within the galvanic bar (despite the hollow section being packed with grease), considerable care was exercised in sealing the space between wires and the inside of the upstand. First, all void space was packed with the anti-corrosion grease used earlier, this grease having first been warmed in order to reduce the viscosity and improve its flow around the wires within the tube. The top of the tube was finally built up and sealed with several layers of heat shrink sleeve (figure 3.2)

During the curing period, the end portions of the galvanic bar not embedded within the prism, were masked. The masking treatment involved coating the end portions with three coats of an ordinary Portland cement and styrene butadiene rubber slurry. After the final coat of slurry had set, an overcoat of air curing epoxy was applied. The purpose of this treatment was to reduce the influence

of differential diffusion of oxygen and water to the electrode segments nearest the end surface of the prism. Both treated ends were finally painted with three coats of bituminous paint in order to further improve the effect of the end treatment (figure 3.3).

The wiring arrangement involved all wires from segments being soldered to sockets within the junction switching box. The most convenient and effective means of coupling and decoupling segments into the required combination for monitoring purposes employed stacking 4mm banana plugs. By interconnecting the banana plugs, electrical continuity between all segments was provided, with the segments in this interconnected format a single electrically continuous length of reinforcement was represented. Only during periods of monitoring was the electrically continuous format disturbed. The completed specimen is shown in figures 3.4 and 3.5. Measurement of galvanic current was carried out with the segments in four configurations, as shown in figure 3.6.

In order to vary the moisture condition, and so the resistivity of the mortar matrix, the specimens were subjected to alternate periods of wetting and drying. Wetting was achieved by placing specimens in a water tank, the water level being kept approximately 10-15mm from the top surface of the specimen. Complete submersion of the specimen was avoided in order to minimise any possibility of restricting oxygen access to the electrodes. Drying of the specimen was achieved by exposing specimens to the ambient laboratory atmosphere.

During the exposure period galvanic current and corrosion potential were monitored. Galvanic currents and corrosion potentials were determined at the end of every wetting or drying cycle. The initiation and propagation of cracks in the mortar

prisms were recorded periodically. Near the end of the exposure period, when the corrosion data was stable, the corrosion rate of individual segmental electrodes was determined. This was done by the linear polarisation technique, with the segment under investigation in electrical isolation from the remainder of the galvanic bar and having settled for at least 30 minutes. Changes in resistivity were measured first as a function of change in moisture content and secondly as a function of the chloride gradient. In order to give an indication of the validity of the non-destructive electrochemical corrosion data, weight loss determinations were made on a small sample of segmental electrodes. This was done by first carefully cutting and then breaking open the mortar prism in order to remove the galvanic bar. The individual segments were then separated and gravimetric determinations were made having removed corrosion products with Clark's solution.

3.4 RESULTS AND DISCUSSION

Within this section, plots of current or potential against time are shown. Average values taken from several specimens have been used. In all cases the results obtained for individual specimens are given in the Appendices.

The results obtained from the galvanic current ($\dot{\iota}_{galv}$) measurements are shown in figures 3.7 to 3.10. In all instances where percentage values are quoted, these refer to the weight of chloride ion by weight of ordinary Portland cement (OPC). Figures 3.7 and 3.8 show the anodic $\dot{\iota}_{galv}$ /time traces for both wet and dry conditions. The figures show three traces :

System 1. $\dot{\iota}_{galv}$ measured between 5% segments and all other segments

System 2. $\dot{\iota}_{galv}$ measured between 1% segments and all other segments in a lower chloride environment

System 3. $\dot{\iota}_{galv}$ measured between 0.1% segments and chloride free segments

The cathodic currents (system 4) measured between 1% segments and all others, including the 5% segment, for both wet and dry conditions, are shown in the $\dot{\iota}_{galv}$ (cathodic)/time traces given in figures 3.9 and 3.10.

Values of corrosion intensity ($\dot{\iota}_{corr}$) have been determined for the micro-cell conditions by linear polarisation. This was carried out for individual isolated segments in a wet condition. The values obtained for $\dot{\iota}_{corr}$ have been plotted against the particular level of chloride to which the segment was exposed and are shown in figure 3.11.

Corrosion potential/time traces for 5%, 1%, 0.1% and 0% segments, in wet and dry conditions, are given in figures 3.12 to 3.19.

Values of actual weight loss, due to corrosion, of selected specimens have been plotted against calculated weight loss, and are given in figure 3.20. Change in resistance of the mortar matrix has been measured at equidistant increments along the length of two specimens. This was done for wet and dry conditions and a resistance profile has been constructed for each condition, as shown in figure 3.21.

Crack propagation has been monitored over the exposure period for each specimen. Longditudinal cracking, expressed as a

percentage of overall specimen length, has been plotted against time and the results are given in figure 3.22.

The anodic galvanic current plots, given in figures 3.7 and 3.8 show the 5% chloride region as a strongly anodic macro-cell.

In the case of traces referring to 5% segments in a wet condition, the magnitude of i_{galv} appears to remain relatively constant over the duration of the exposure period. The traces representing segments in a dry condition, show values of i_{galv} to be smaller and also a tendency for i_{galv} to decrease with time. This trend is pronounced for several specimens and may, in part, be due to the availability of nearby cathodic sites becoming diminished with time. The formation of corrosion products which may restrain i_{galv} in dry conditions, owing to resistance control within the electrolyte, would tend to have an increasing effect with time due to the continued formation of corrosion products on the 5% segment itself. The effect would be less pronounced in wet conditions as the resistivity of the electrolyte phase would be reduced so making more distant cathodic sites available.

The traces of anodic i_{galv} for 1% and 0.1% segments are well defined for specimens in a wet state, the 1% segment being clearly identified as anodic. There is no significant long term trend for 1% or 0.1% i_{galv} values, in wet or dry conditions, to decrease with time as was found in the case of the 5% segments. This overall lack of change in i_{galv} with time may support the explanation offered for the decreasing values of i_{galv} found in the 5% case. The cathodes coupled to either 1% or 0.1% segments have undergone only low levels of anodic activity and consequently no significant reduction in the cathodic site would occur due to the formation of corrosion products.

The cathodic current time traces for specimens in both wet and dry conditions, figures 3.9 and 3.10, clearly demonstrate the influence of the adjacent strongly anodic segment. Referring to figures 3.7 and 3.8, the 1% segment is coupled to 0.1% and chloride free segments and acts as a net anode. In figures 3.9 and 3.10, the 1% segment is coupled to the 5%, 0.1% and chloride free segments and results in net cathodic behaviour. The traces of i_{galv}(cathodic) represent the electrochemical condition of the 1% segment when the entire specimen is in its normal exposure condition with all segments interconnected and acting as a single electrically continuous electrode. Thus, one would not expect to find significant corrosion products visible on the surface of a 1% electrode. Figure 3.24 shows a 5% electrode exhibiting a significant volume of corrosion product with the adjacent 1% segment largely free of corrosion product.

A comparison of the two conditions investigated for the 1% segment shows the effect of the macro corrosion cell; the 5% segment suppresses anodic activity at the 1% segment, the net effect being that of partial cathodic protection.

In order to establish the micro-cell corrosion intensity of individual segments, decoupled from all other segments, values of i_{corr} were determined by linear polarisation. The results are shown in figure 3.11, the plot of corrosion intensity against chloride concentration. The plot shows values of i_{corr} increasing as a function of increased chloride level. The percentage values of chloride ion are quoted as those introduced at the time of specimen preparation. It is, however, likely that the levels of chloride actually pertaining at the time of obtaining i_{corr} values, will have differed slightly from those quoted. This would be due to some

interdiffusion throughout the chloride gradient. Linear polarisation was only used with the specimens in a wet condition, owing to difficulties in applying a polarisation potential - via an external counter electrode - with specimens in a dry state. Figure 3.11 indicates several reasonably well defined bands of i_{corr} for the steel segments embedded within mortar matrices containing a number of chloride levels. In a small number of cases certain end segments, originally within a chloride free environment, have suffered crevice corrosion. Thus, exceptionally high values of i_{corr} have been determined for these end segments.

The corrosion potential/time traces for 5% segments in wet and dry conditions are given in figures 3.12 and 3.13. In all cases the corrosion potentials are on the copper/copper sulphate scale. In the great majority of cases the initial potential recorded, for all 5% regions, was more negative than -400mV. There is a trend for potentials of wet specimens to become more negative with time, the final values being approximately -600mV in most cases. This trend may be due to the passive film becoming increasingly less resistant to rupture and subsequent pit initiation. It may also be possible that after pit initiation, pit growth occurs more easily due to the more aggressive electrolyte formed within the pits, resulting from the hydrolysis of anodic products. In the case of 5% segments in a dry condition, the initial corrosion potentials recorded fall between -400mV and -500mV. These relatively negative initial values, subsequently tended to move in a positive direction. This is consistent with the values of i_{galv} for dry 5% segments, which become smaller with time, possibly due to a rate limiting resistance control.

Traces of corrosion potential/time for 1% segments are given

in figure 3.14 for wet conditions, and figure 3.15 for dry conditions. The traces representing wet conditions are approximately as negative, and of the same form, as those traces of the 5% segments (figure 3.12). It is likely that these quite negative potentials are due to a significant degree of cathodic polarisation induced by cathodic protection, provided to the 1% segments by the adjacent and strongly anodic 5% segments.

Corrosion potential against time traces are given for 0.1% segments in figures 3.16 and 3.17. The potential traces for dry conditions indicate relatively inactive potentials throughout the exposure period, the majority of points falling within a range of -300mV to -400mV. The potential traces for wet conditions exhibit a trend of becoming more negative with time, with a significant number of final potentials more negative than -500mV. Such negative corrosion potentials would suggest an active electrode; however, the typical values of i_{galv} and i_{corr} are not supportive of this possibility.

Corrosion potential against time traces are given for all chloride free segments in figures 3.18 and 3.19. Traces representing wet conditions range between -300mV and -400mV which corresponds to relatively passive values, as may be expected for steel electrodes in a cementitious chloride free environment. The potentials obtained for dry conditions show a shift in the positive direction, with the majority of values falling within a band of -250mV to -350mV. In a smaller number of cases, abnormally negative potentials have been recorded, these instances corresponding to end segments which have suffered some crevice corrosion.

Gravimetric weight loss determinations have been made on a limited number of electrodes. Calculated weight losses were

determined from the macro (i_{galv}) and micro (i_{corr}) cells. As no values of i_{corr} were determined for the micro-cell in dry conditions, a percentage (33 and 41%) of the i_{corr} wet value, based upon the reduction in i_{galv} due to drying, was used in the calculations. From figure 3.20 reasonable agreement has been found between actual and calculated weight losses. The magnitude of the variation in chloride ion levels, which influences corrosion rate, has contributed to producing a plot showing bunching of data points. The degree of scatter of the data is unremarkable; an example of a similar plot of actual and calculated weight losses for steel in chloride contaiminated concretes is given within the Appendices.

The weight losses calculated from the corrosion currents i_{corr} and i_{galv} show the macro-cell currents to predominate at 5% and 1% chloride levels, whereas at 0.1% chloride levels the micro-cell currents are the stronger. Where the macro-cell currents are the greater, (5% and 1% segments), it is likely to be due to the availability of nearby cathodic segments and the throwing power associated with these high chloride concentrations. The 0.1% chloride level is not normally associated with significant corrosion rates of steel in concrete. The rate of metal dissolution of the 0.1% segment is most likely to be rate limited by anodic control, the availability of further cathodes not inducing a significant macro-cell effect.

The resistivity of the cement mortar matrix for specimens in wet and dry conditions has been determined. The resistivity profile, given in figure 3.21 was determined by taking a series of resistance measurements along the length of the chloride gradient. In wet (saturated surface dry conditions) there is little

significant variation in conductivity, due to the presence of moisture throughout the pore structure. A small increase in conductivity, corresponding to the chloride regions can be observed. The influence of drying is to exaggerate the form of the wet profile. The influence of the chloride regions is to maintain a residual conductivity within the electrolytic phase. There would not appear to be any significant differences in resistivity identifiable for 1% and 0.1% chloride levels. Values of resistivity increase significantly within the chloride free regions from approximately 10-15 ohm meters (wet) to 75-100 ohm meters (dry).

The results of the monitoring of crack growth are given in figure 3.22. Crack initiation takes place at the free end of the 5% region, and propagates in the chloride free direction. The results of the study, which for reasons of speed and simplicity only considered cracks greater than 0.1mm wide, show a relatively high degree of scatter. A crack width measuring device, incorporating an optical graticule, was used for the measurements. There is some conjecture as to the influence of cracks upon corrosion (3.24-3.27); it is thought that corrosion products seal narrow cracks (3.28) so rendering their influence negligible. Figure 3.23 shows the cracking evident at the end of the exposure period, the maximum crack width being 1.85mm, this decreasing to 0.70mm at 90mm (from the 5% end) and to 0.1mm at 190mm. Figure 3.24 shows extensive corrosion products upon the 5% segment but also corrosion product adhering to the mortar substrate. Clear evidence of corrosion product away from the location of the electrode is shown.

The general condition of the entire galvanic bar at the end of the exposure period is shown in figures 3.25 and 3.26. Significant corrosion product is evident on the electrode corresponding to the

5% chloride region, whilst only a comparatively small amount of product is apparent on adjacent 1% segments. The 0.1% segments were free from visual signs of corrosion. The chloride free segments showed no evidence of corrosion, (figure 3.27), including the end segment which was thought to be susceptible to crevice corrosion (figure 3.28).

3.5 CONCLUSIONS

A methodology has been devised enabling the study of macro and micro-cell corrosion activity using a segmented model reinforcing bar. The galvanic bar electrode utilised several electrically isolated segmental mild steel electrodes of hollow section. By using an arrangement of external electrical connection a variety of electrode combinations were studied. The galvanic bars were cast within mortar prisms containing a chloride gradient in order to stimulate corrosion activity at individual electrodes and the gradient ranged between 0 and 5% chloride ion by weight of cement.

Galvanic macro-cell corrosion currents, $\dot{\iota}_{galv}$, were established for several conditions over a fixed exposure period. It was found that anodic activity was suppressed within regions in close proximity to other strongly anodic electrodes. This effect was attributed to the intensely anodic region cathodically protecting the adjacent segmental electrode.

Corrosion intensity, $\dot{\iota}_{corr}$, of the micro-cells operating within segments were found to increase with increasing chloride levels. Reasonable agreement was found between calculated weight losses - $\dot{\iota}_{corr}$ (micro-cell) plus $\dot{\iota}_{galv}$ (macro-cell) and actual weight loss measurements. Comparison of weight losses calculated

for the macro and micro-cells showed the macro-cell to predominate at 5% and 1% chloride levels due to the throwing power associated with these high chloride contents.

Throughout the exposure period, specimens were subjected to wetting and drying cycles. It was found that the corrosion rates, with specimens in a drying condition, were resistance controlled.

The visual inspection of the specimens revealed substantial corrosion products associated with the 5% segments. A limited volume of corrosion product was visible upon 1% chloride segments, which supported the macro-cell current data. The 0.1% and chloride free segments were generally free from corrosion products.

From this work it is clear that the assessment of corrosion risk within real structures, based soley upon half cell potential measurements, may not be entirely reliable. Half cell potentials sufficiently negative as to be suggestive of corrosion, may in fact correspond to an insignificant corrosion current. Additionally, apparently anomalous situations where high chloride concentrations and large negative potentials are found to correspond to reinforcement showing no significant signs of corrosion, may be explained by the partial cathodic potection phenomenon.

Clearly there is a requirement for a more quantitative method for the on-site investigations of corrosion of steel in concrete. This is an area where further work is required.

FIGURE 3.1 Shouldered washer containing radially drilled holes

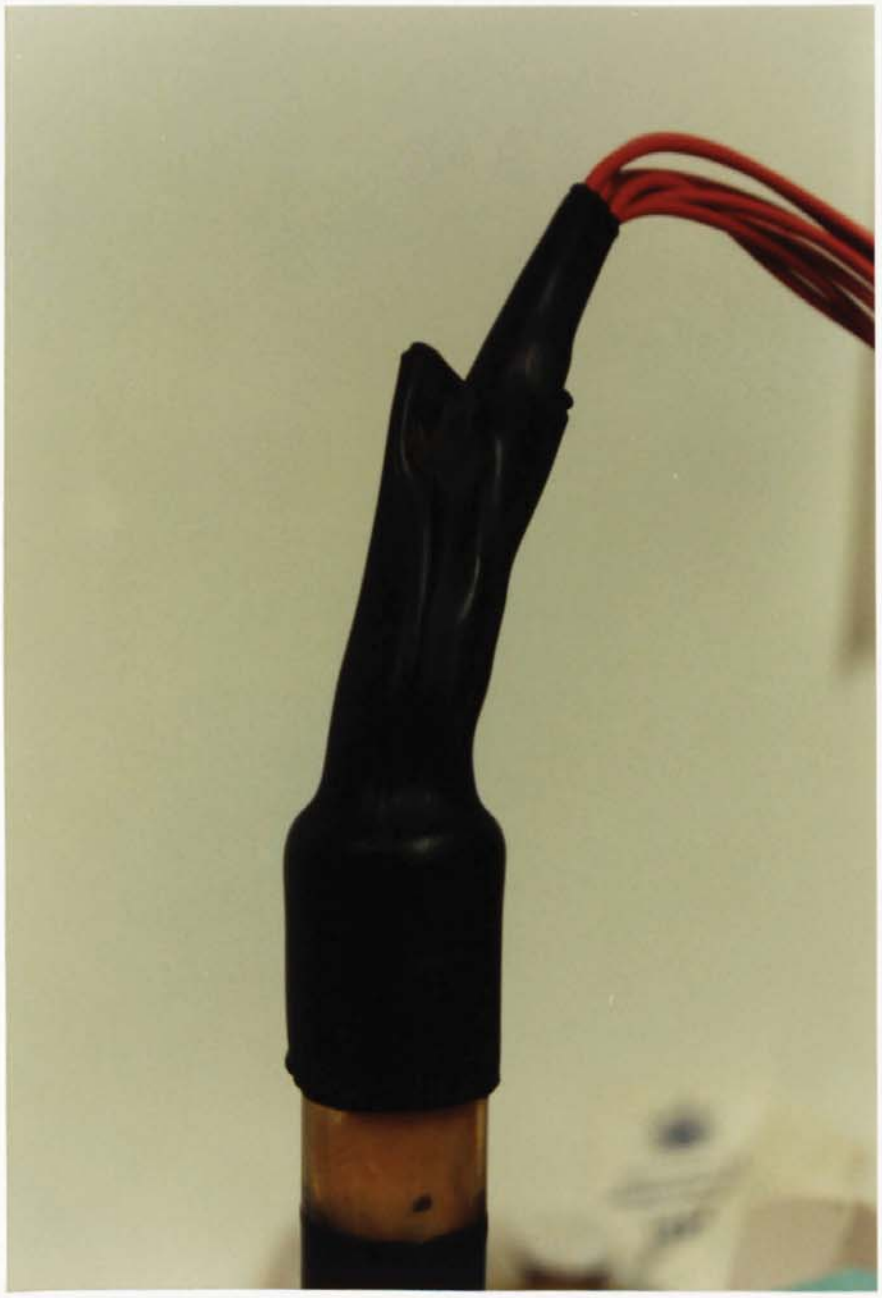

FIGURE 3.2 Heat shrink sleeve used to seal the acrylic tube containing the segment connection wire and grease packing

FIGURE 3.3 Bituminous paint end treatment used on all specimens

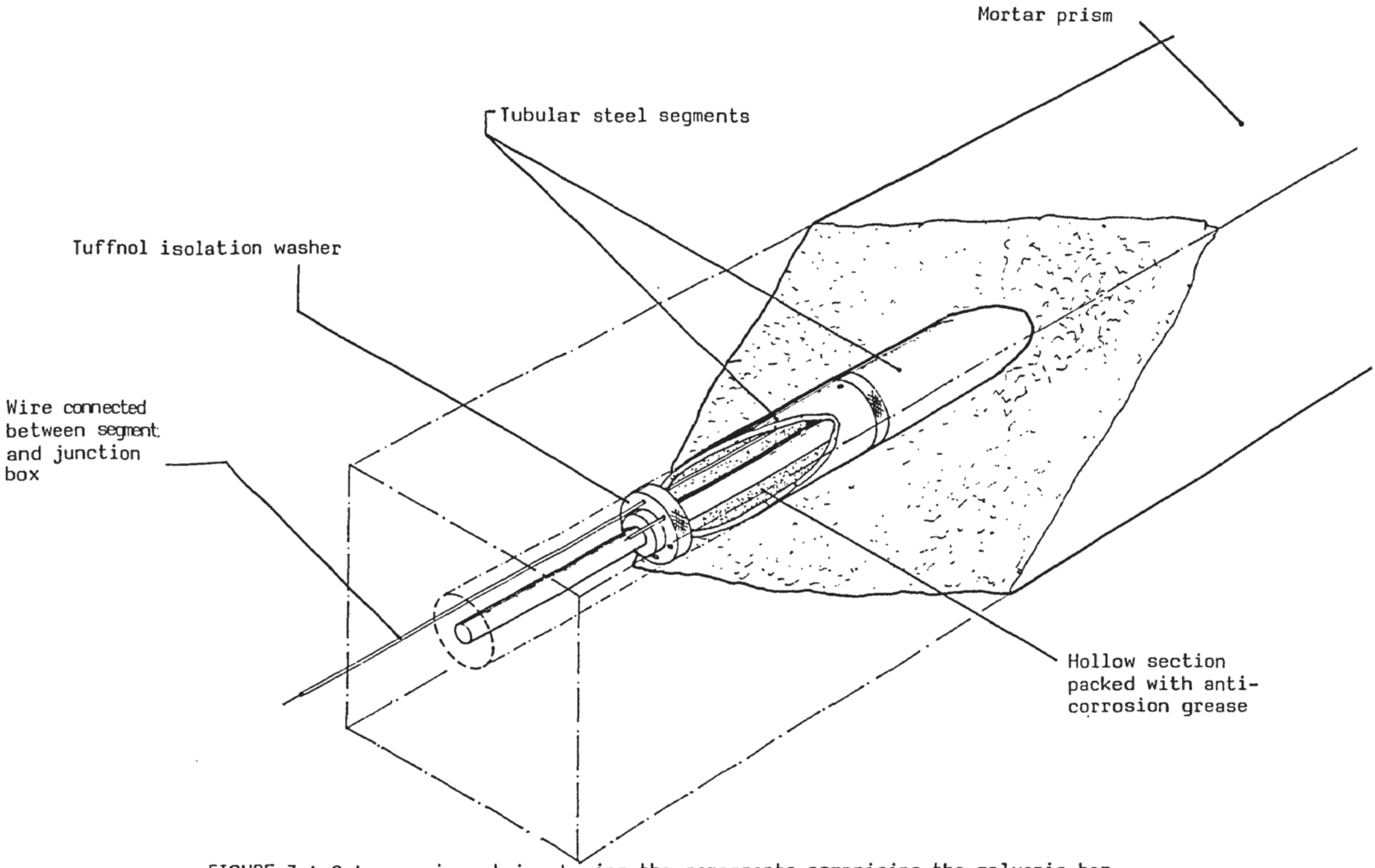

FIGURE 3.4 Cut-away isometric showing the components comprising the galvanic bar

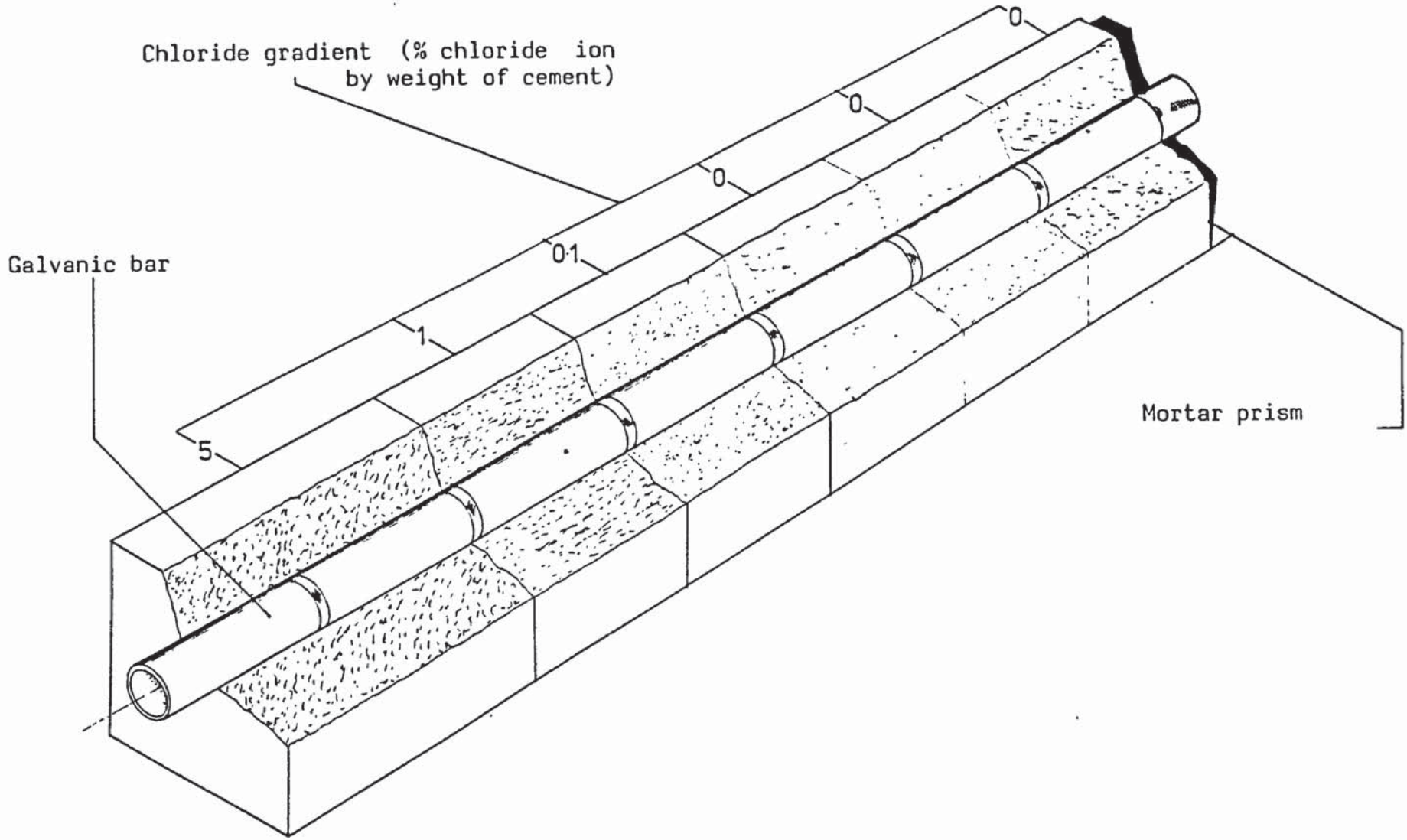

FIGURE 3.5 Cut-away isometric showing the position of the galvanic bar in relation to the chloride gradient contained in the completed mortar prism

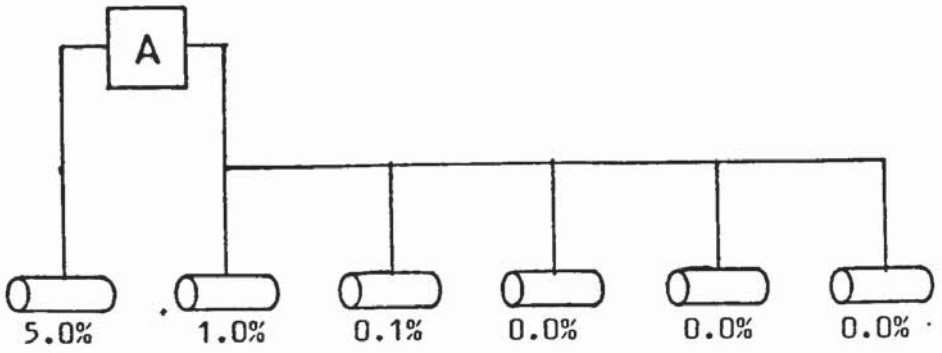

SYSTEM ONE

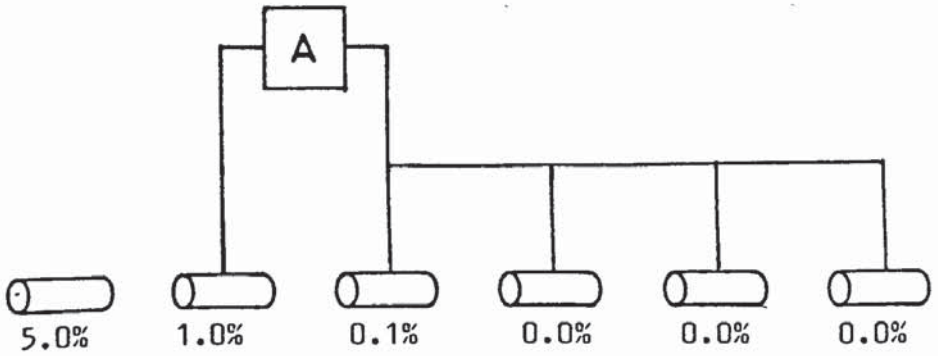

SYSTEM TWO

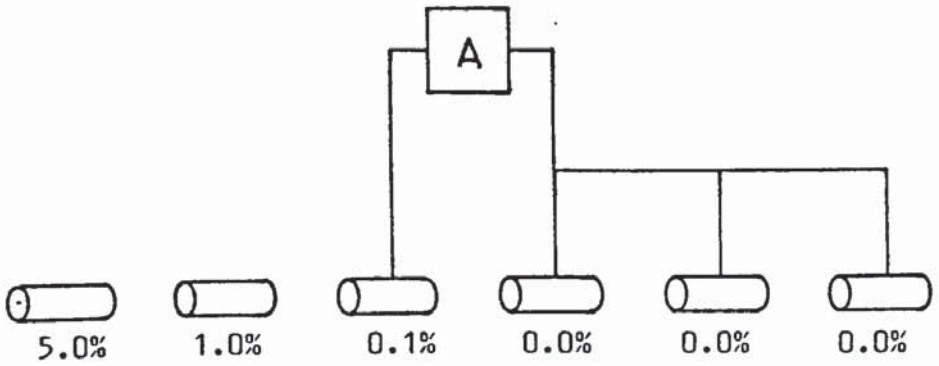

SYSTEM THREE

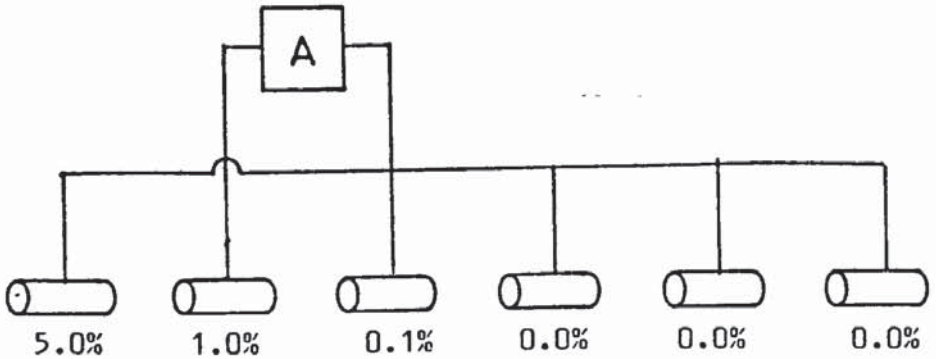

CATHODIC CURRENT SYSTEM FOUR

FIGURE 3.6 Schematic diagrams showing the segment configurations used for the galvanic current measurements
A = ammeter

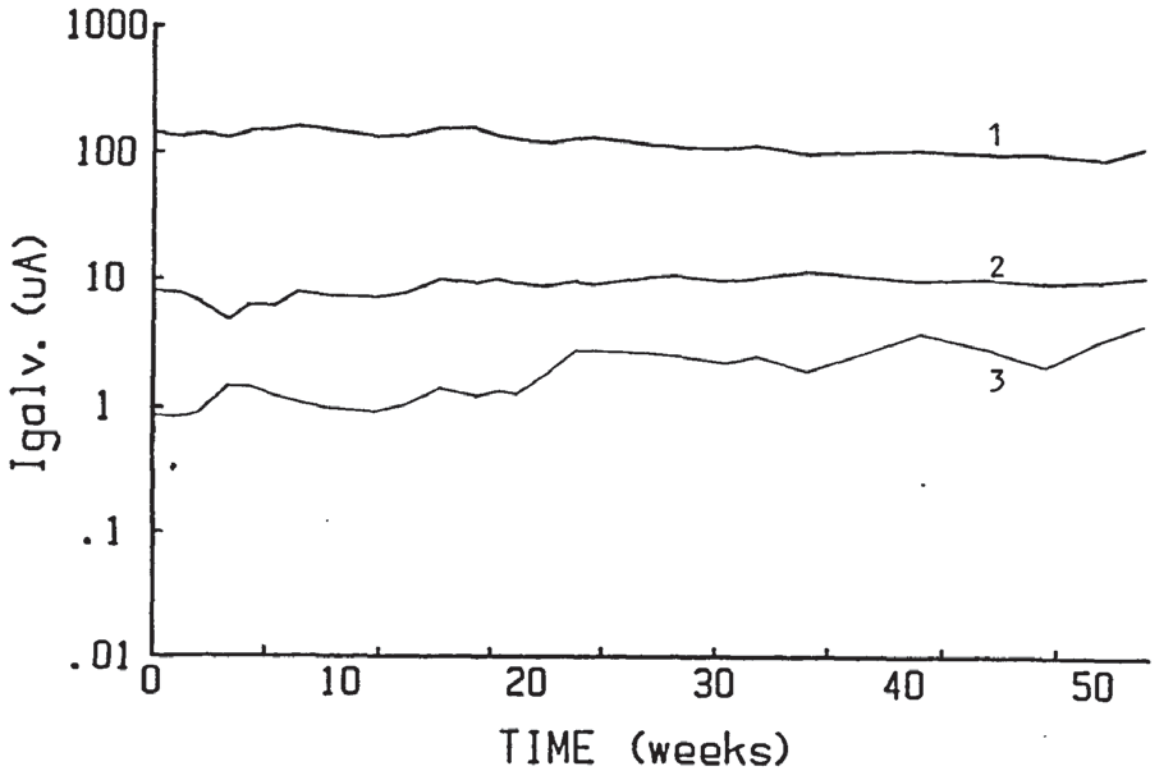

FIGURE 3.7 i_{galv}/time traces for wet condition, for the following segment combinations (% chloride ion by weight of cement);1=5% vs 1% + 0.1% + 0.0%, 2 = 1% vs 0.1% + 0.0%, 3 = 0.1% vs 0.0%

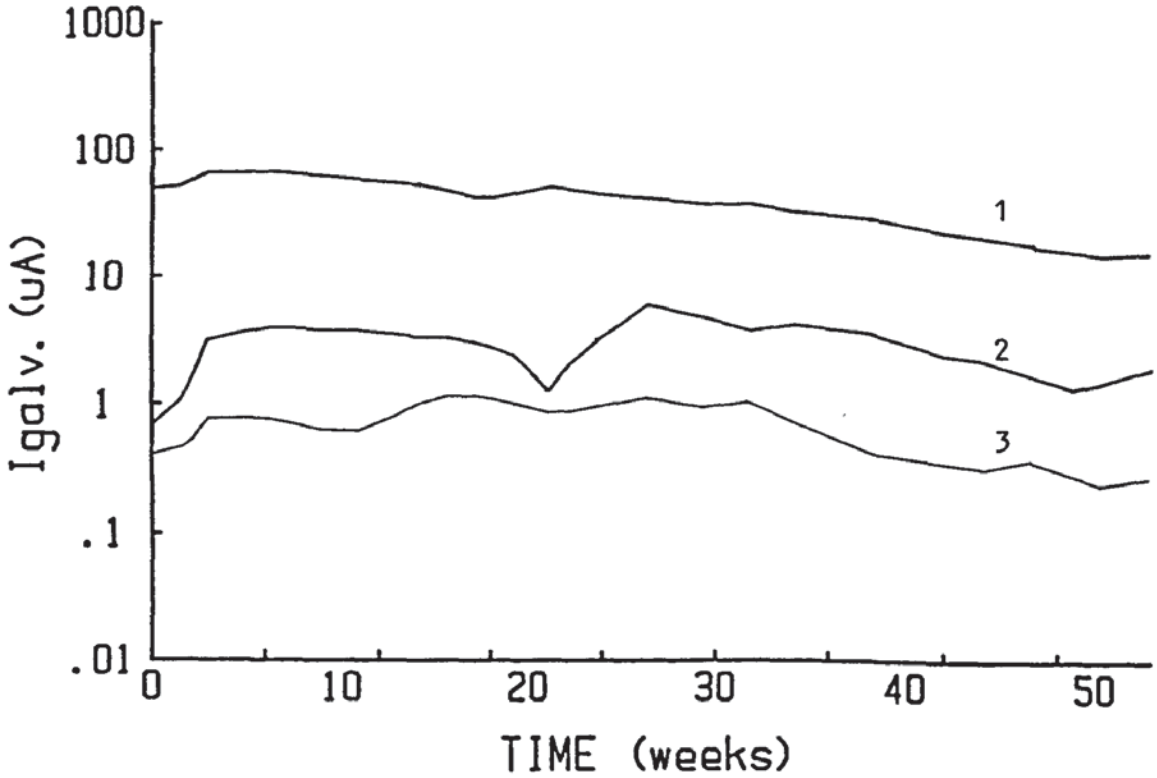

FIGURE 3.8 i_{galv}/time traces, dry condition, for the following segment combinations (% chloride ion by weight of cement); 1=5% vs 1% + 0.1% + 0.0%, 2 = 1% vs 0.1% + 0.0%, 3 = 0.1% vs 0.0%

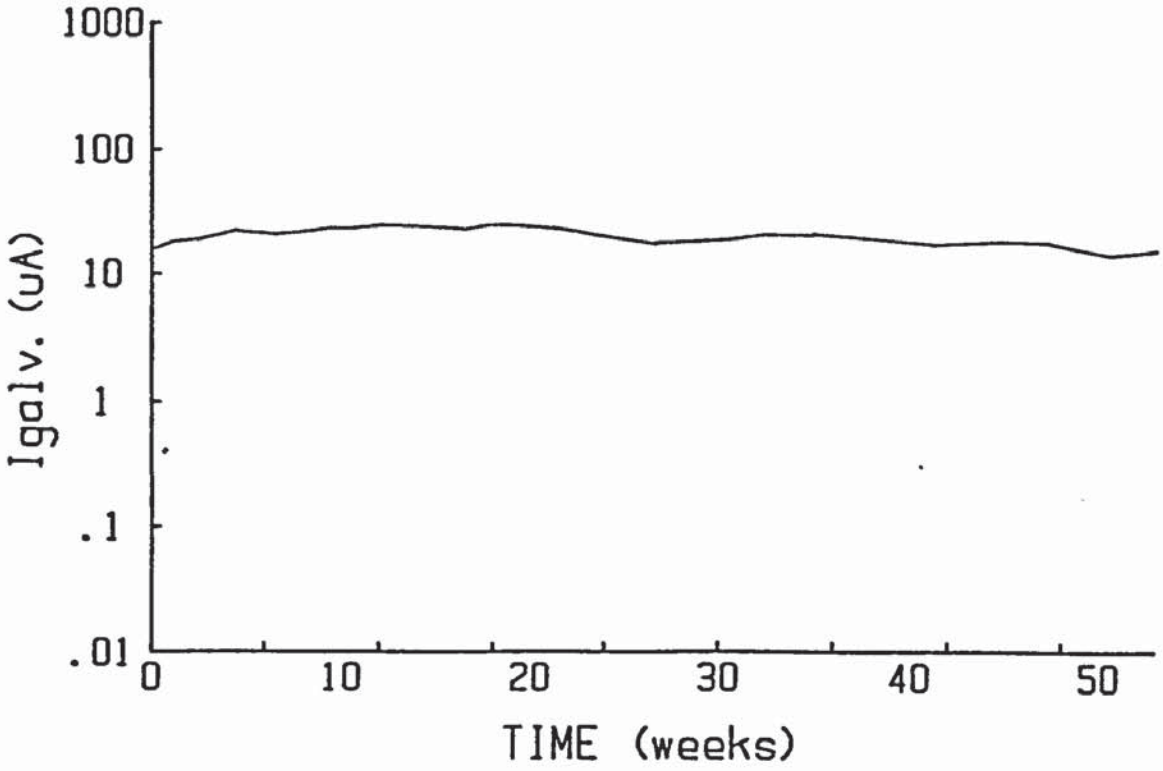

FIGURE 3.9 $\dot{\iota}_{galv}$ (cathodic)/time trace, wet condition, for the following segment combination (% chloride by weight of cement); 1% vs 5% + 0.1% + 0.0%

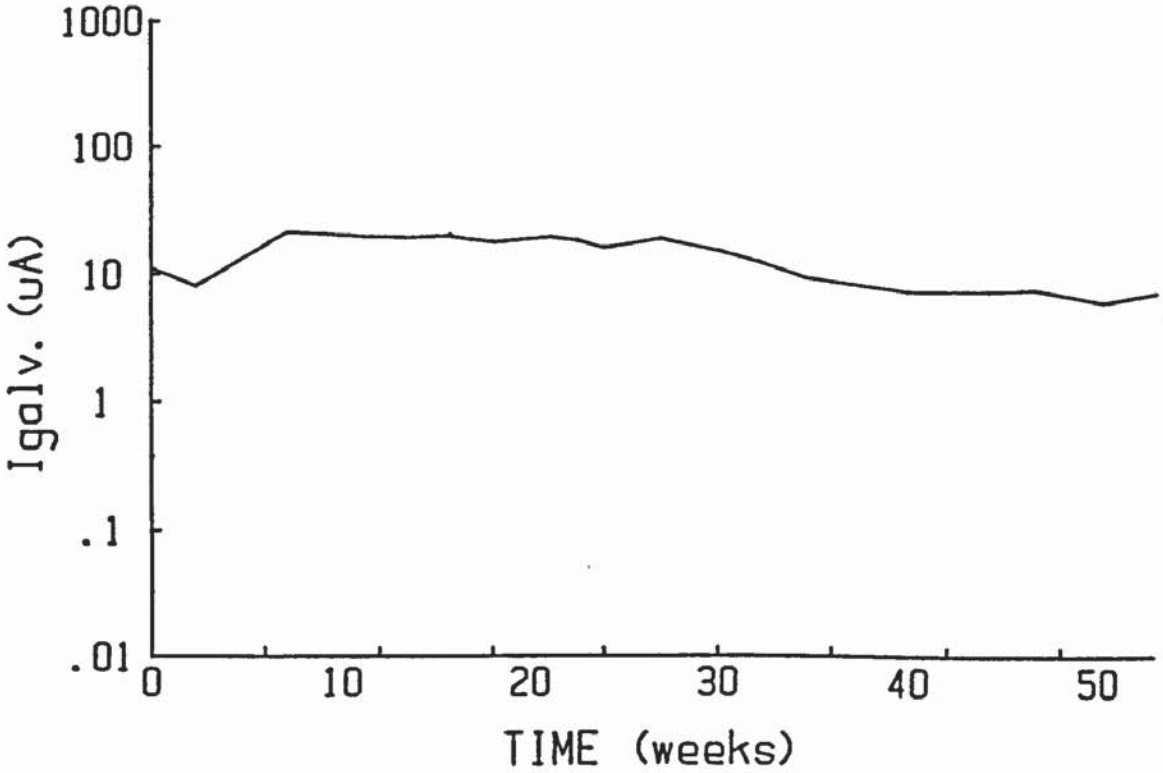

FIGURE 3.10 $\dot{\iota}_{galv}$ (cathodic)/time trace, dry condition, for the following segment combination (% chloride by weight of cement); 1% vs 5% + 0.1% + 0.0%

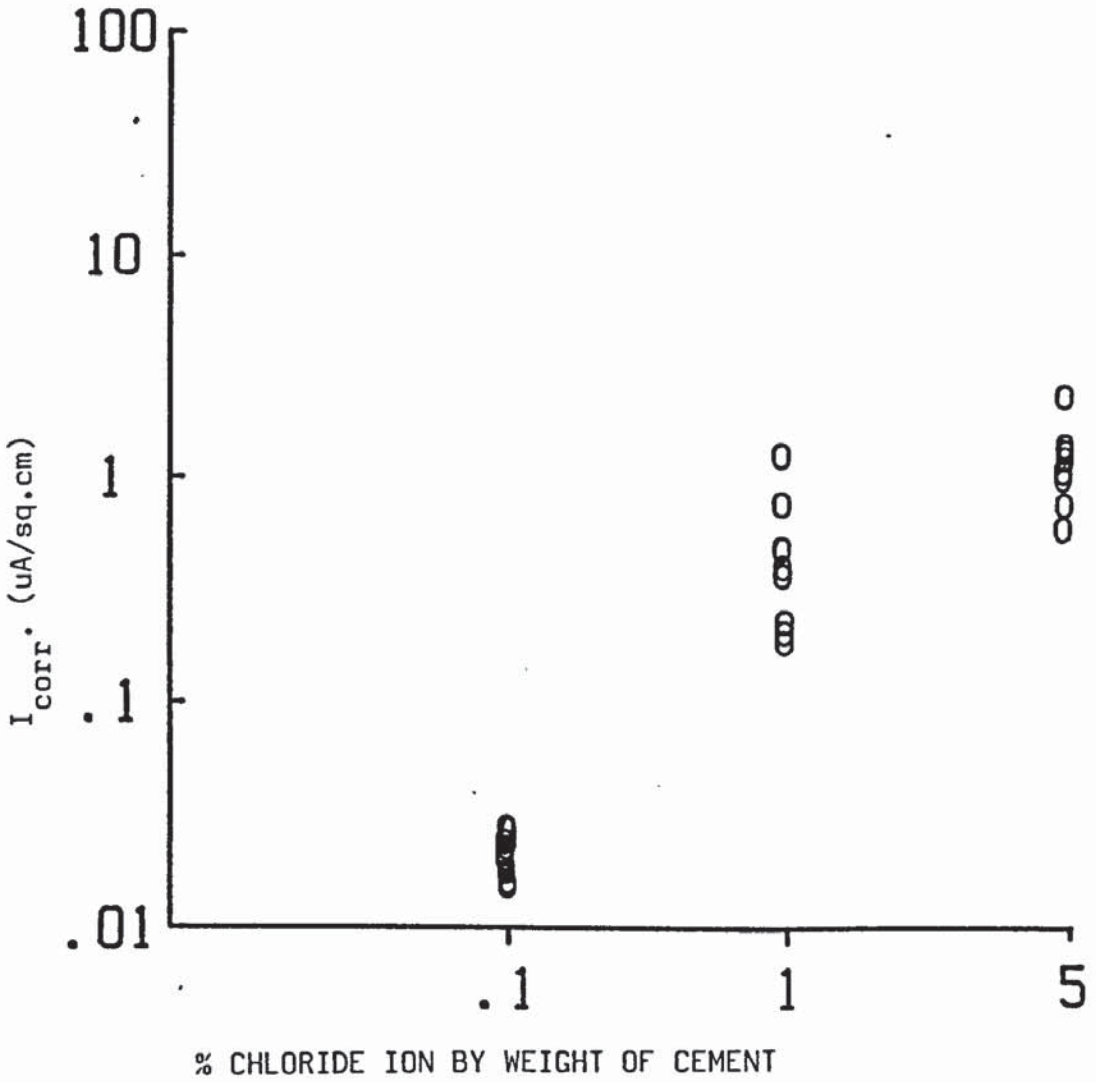

FIGURE 3.11 Values of i_{corr} for the micro-cell condition for individual isolated segments in wet conditions

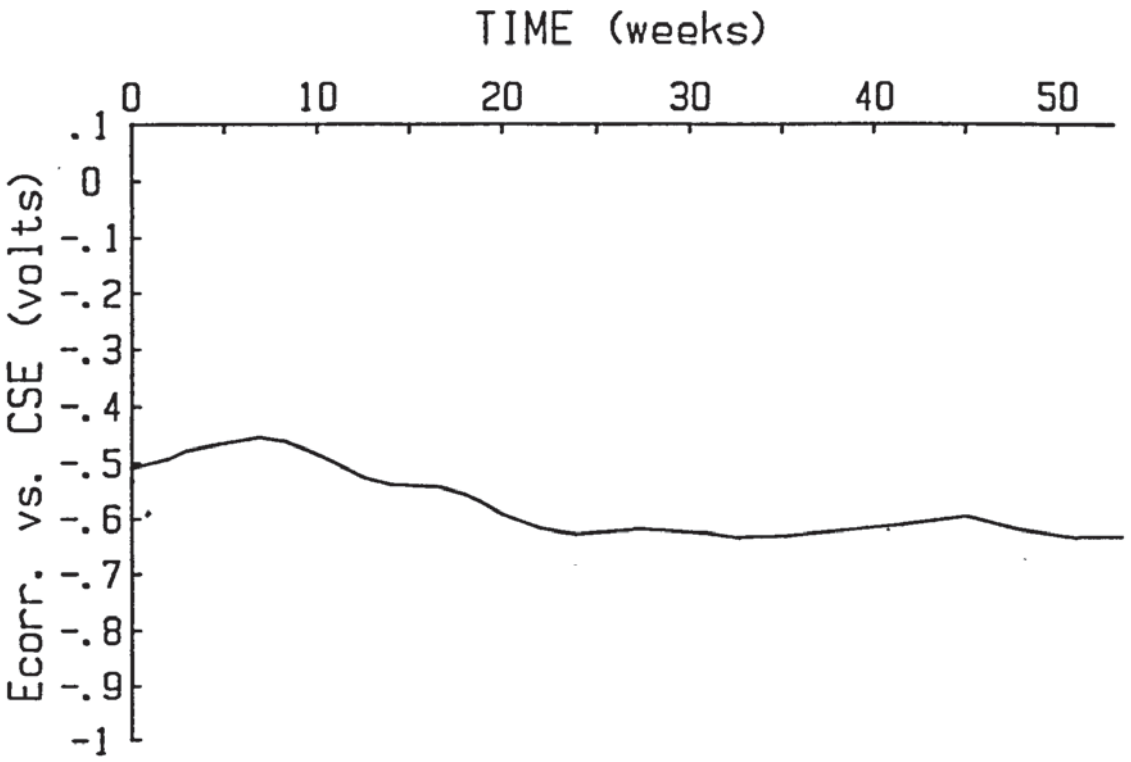

FIGURE 3.12 E_{corr}/time trace for the 5% chloride ion segment (by weight of cement) in wet conditions

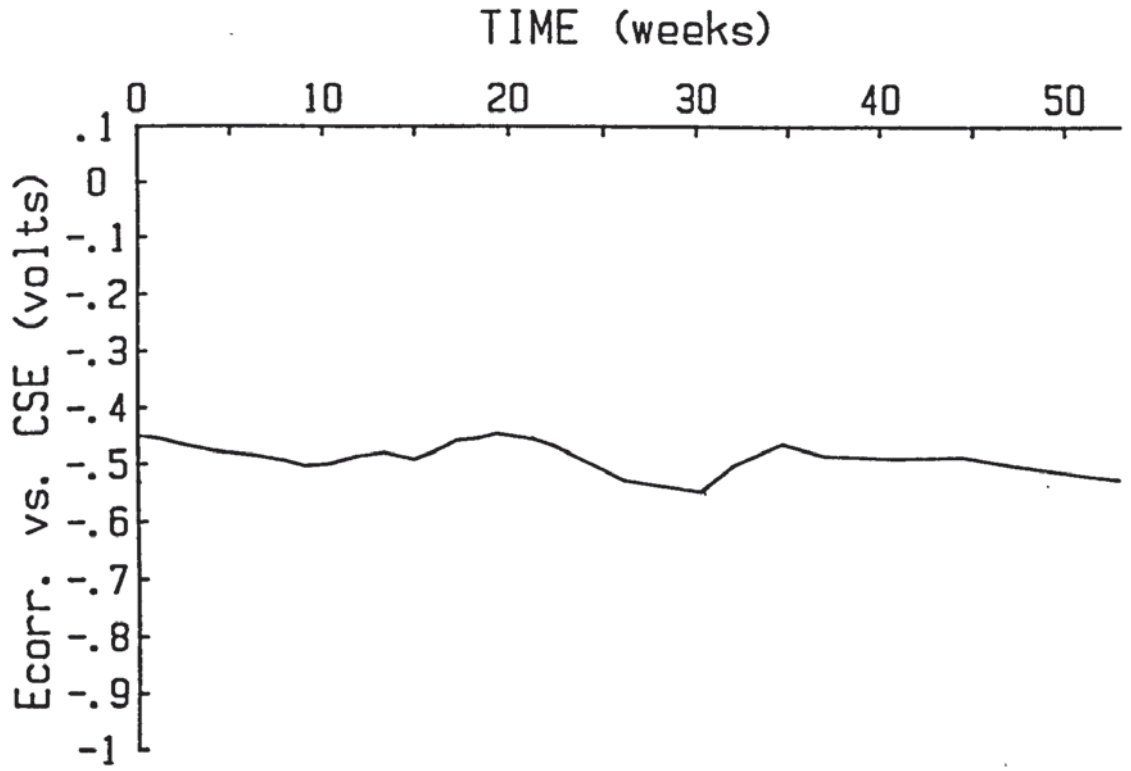

FIGURE 3.13 E_{corr}/time trace for the 5% chloride ion segment (by weight of cement) in dry conditions

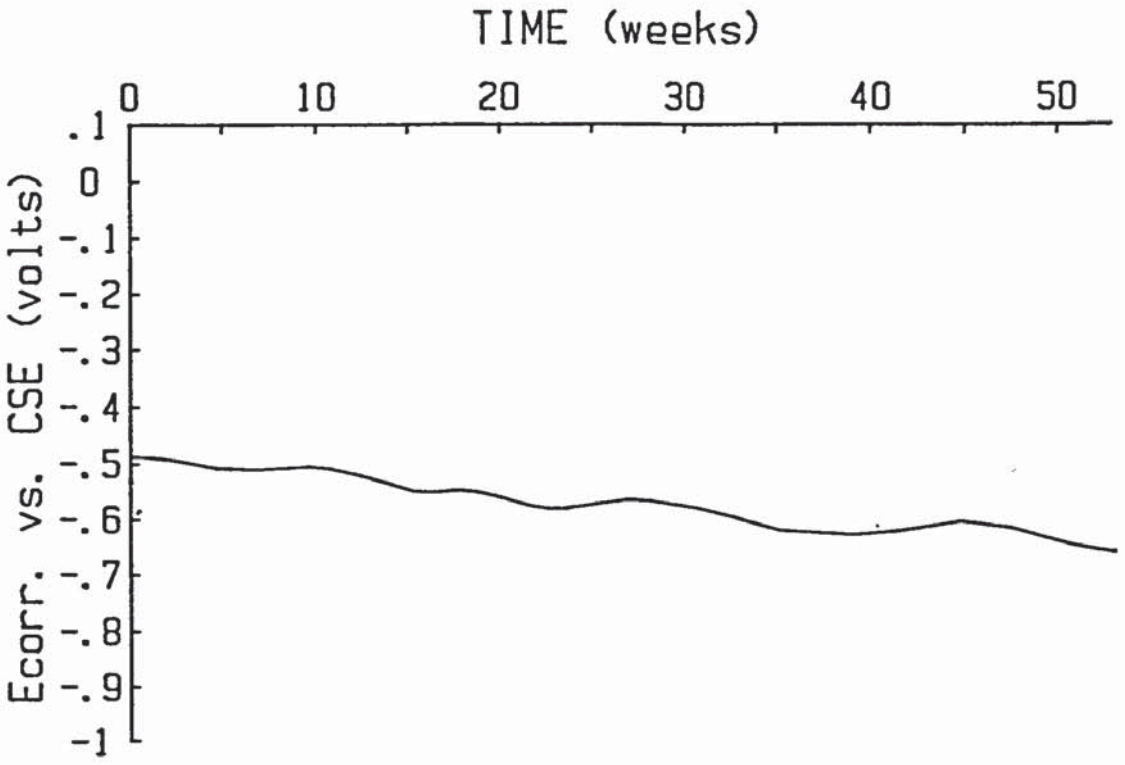

FIGURE 3.14 E_{corr}/time trace for the 1% chloride ion segment (by weight of cement) in wet conditions

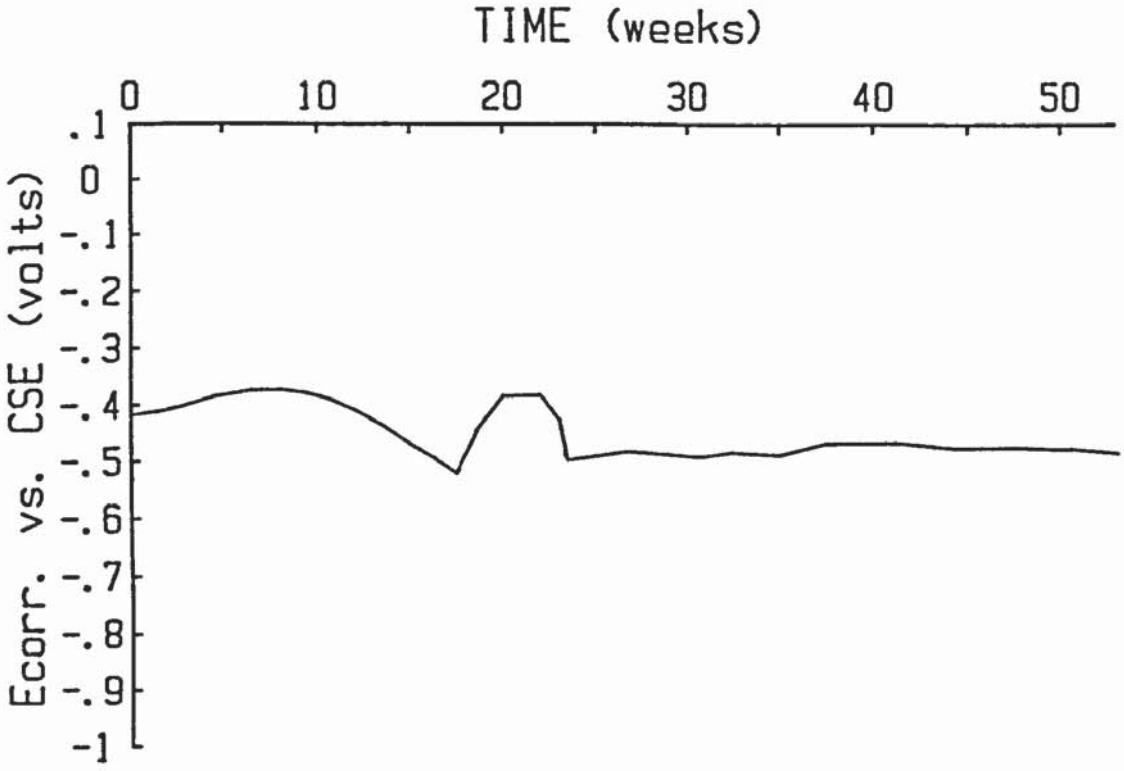

FIGURE 3.15 E_{corr}/time trace for the 1% chloride ion segment (by weight of cement) in dry conditions

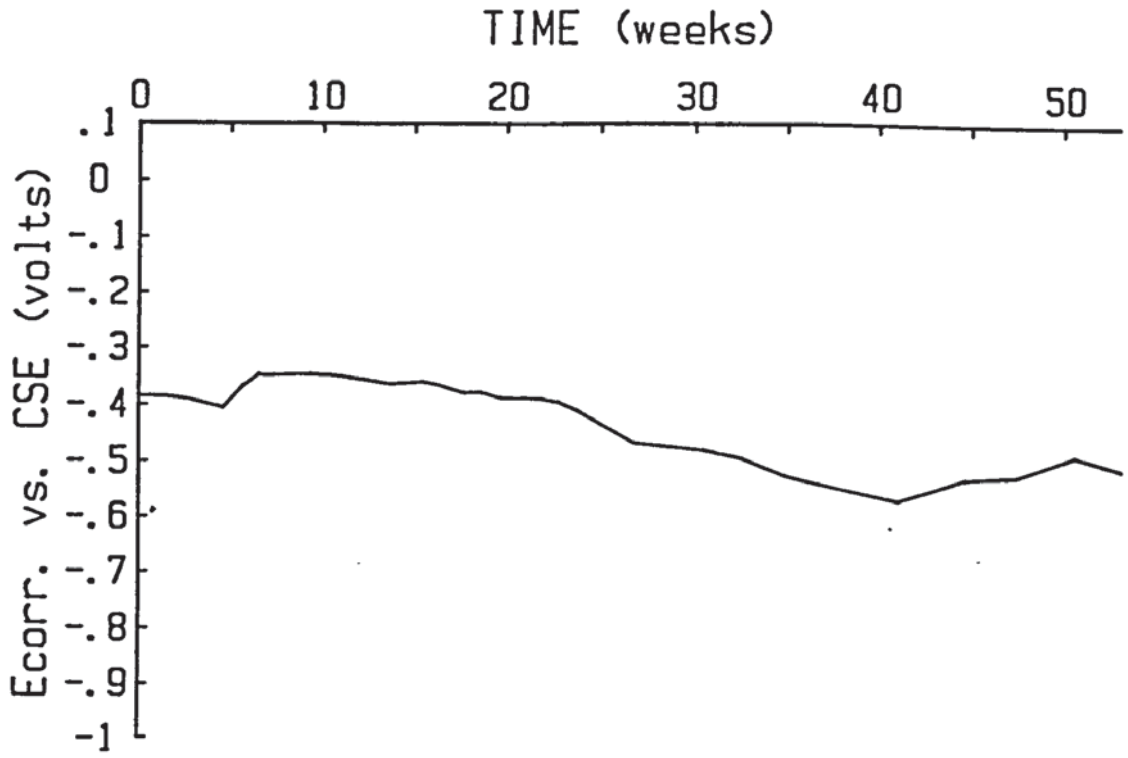

FIGURE 3.16 E_{corr}/time trace for the 0.1% chloride ion segment (by weight of cement) in wet conditions

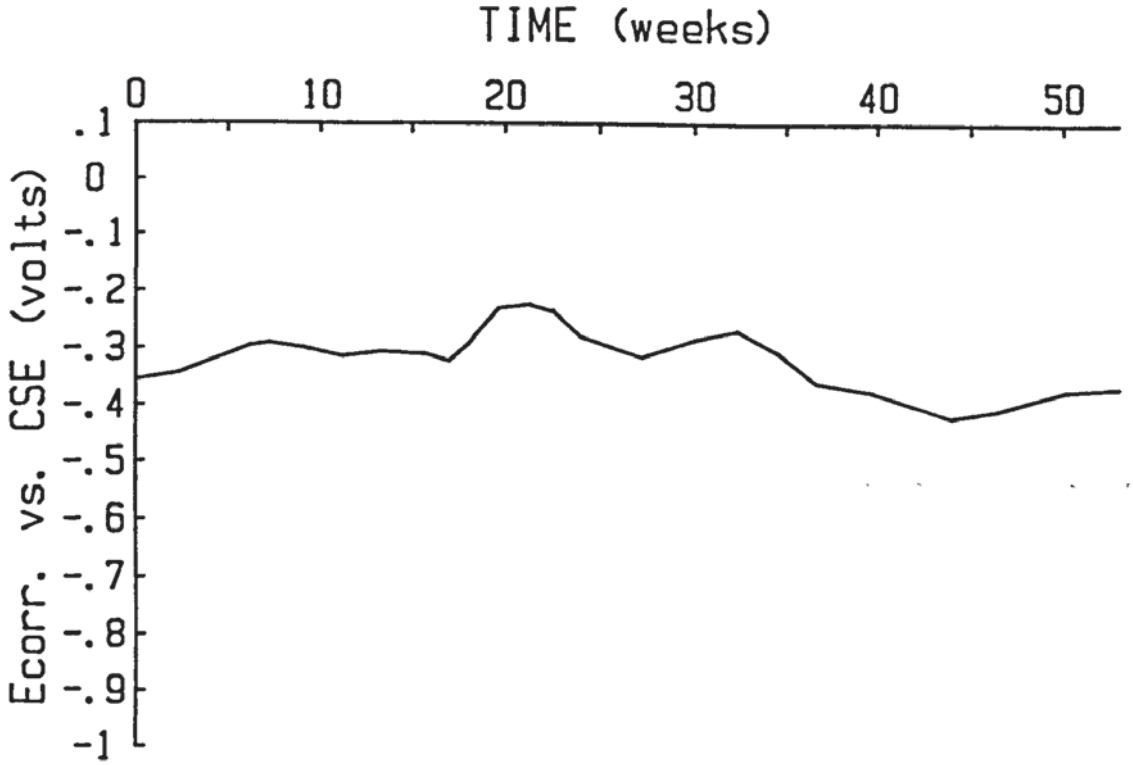

FIGURE 3.17 E_{corr}/time trace for the 0.1% chloride ion segment (by weight of cement) in dry conditions

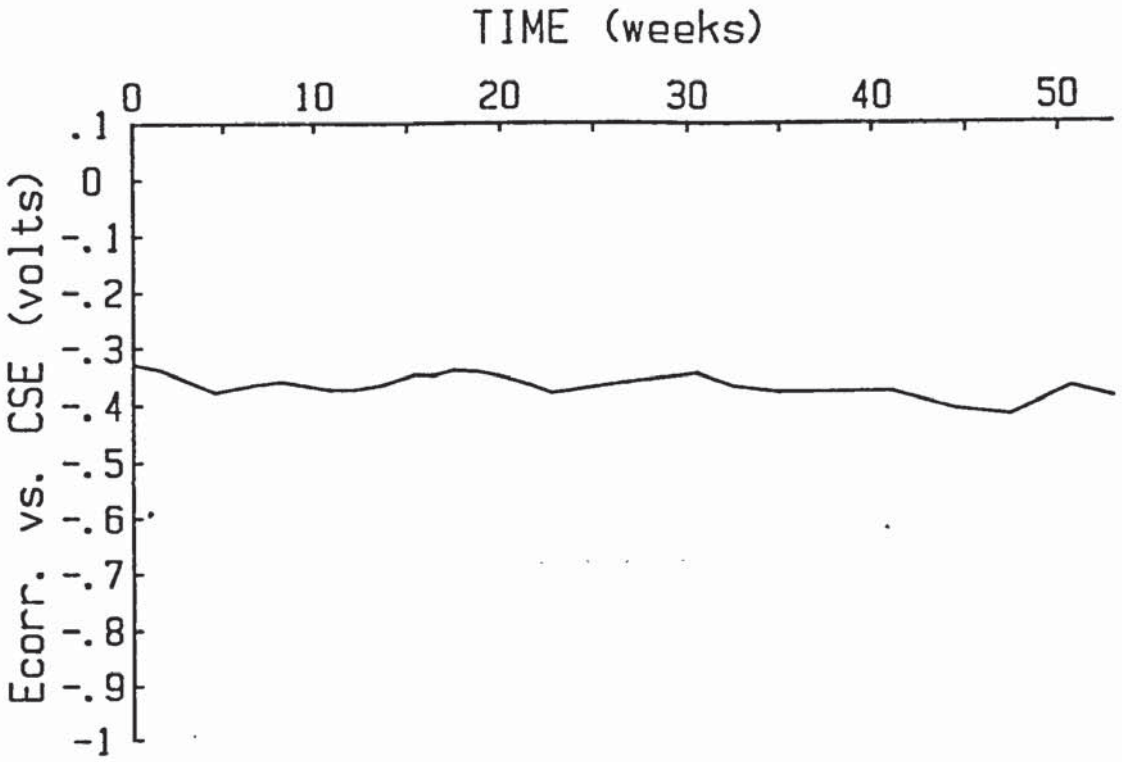

FIGURE 3.18 E_{corr}/time trace for the chloride free segment in wet conditions

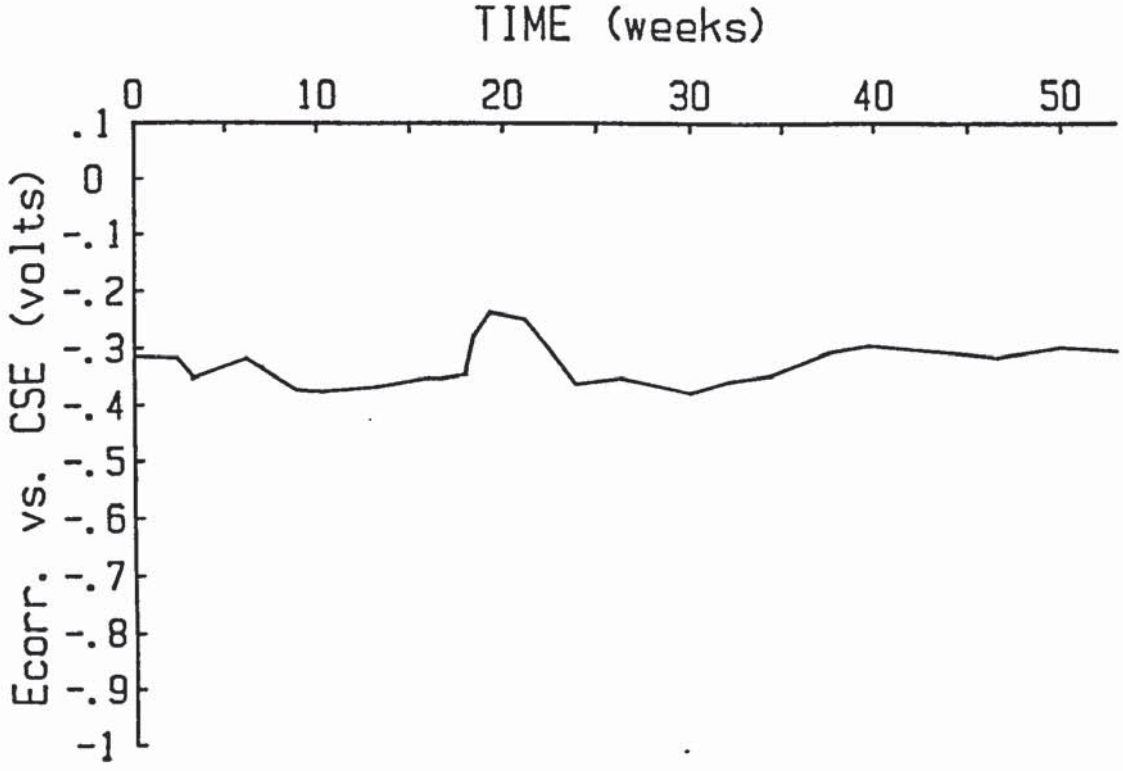

FIGURE 3.19 E_{corr}/time trace for the chloride free segment in dry conditions

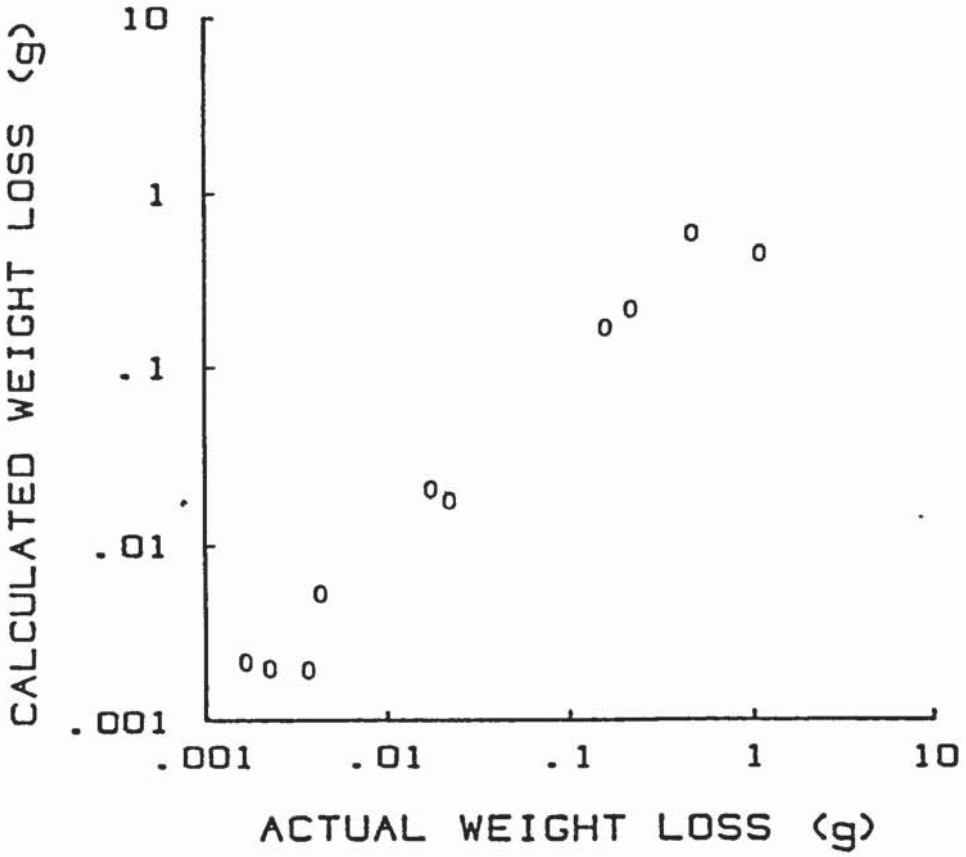

FIGURE 3.20 Calculated vs actual weight loss for segments at 5%, 1%, 0.1% and 0.0% chloride concentration

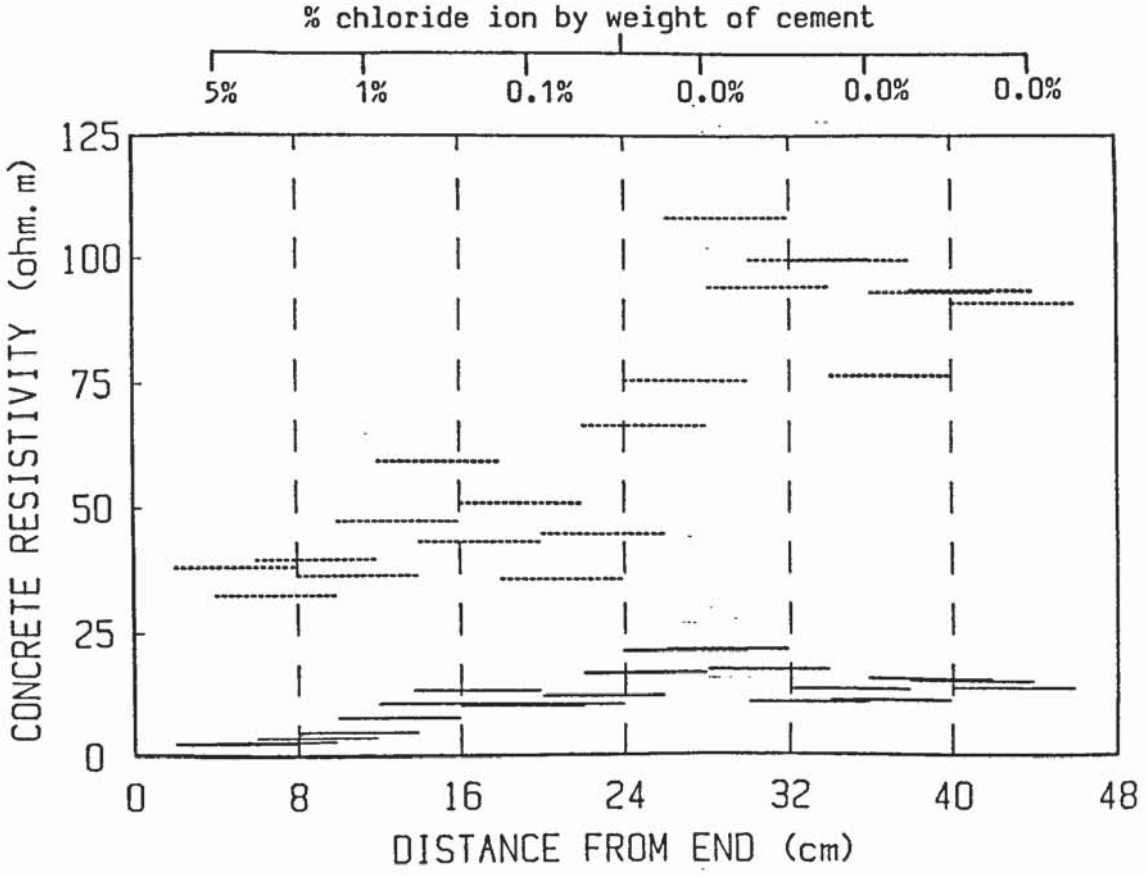

FIGURE 3.21 Resistance profile for the mortar, change in resistance as a function of mortar chloride concentration; solid line = wet conditions, broken line = dry conditions

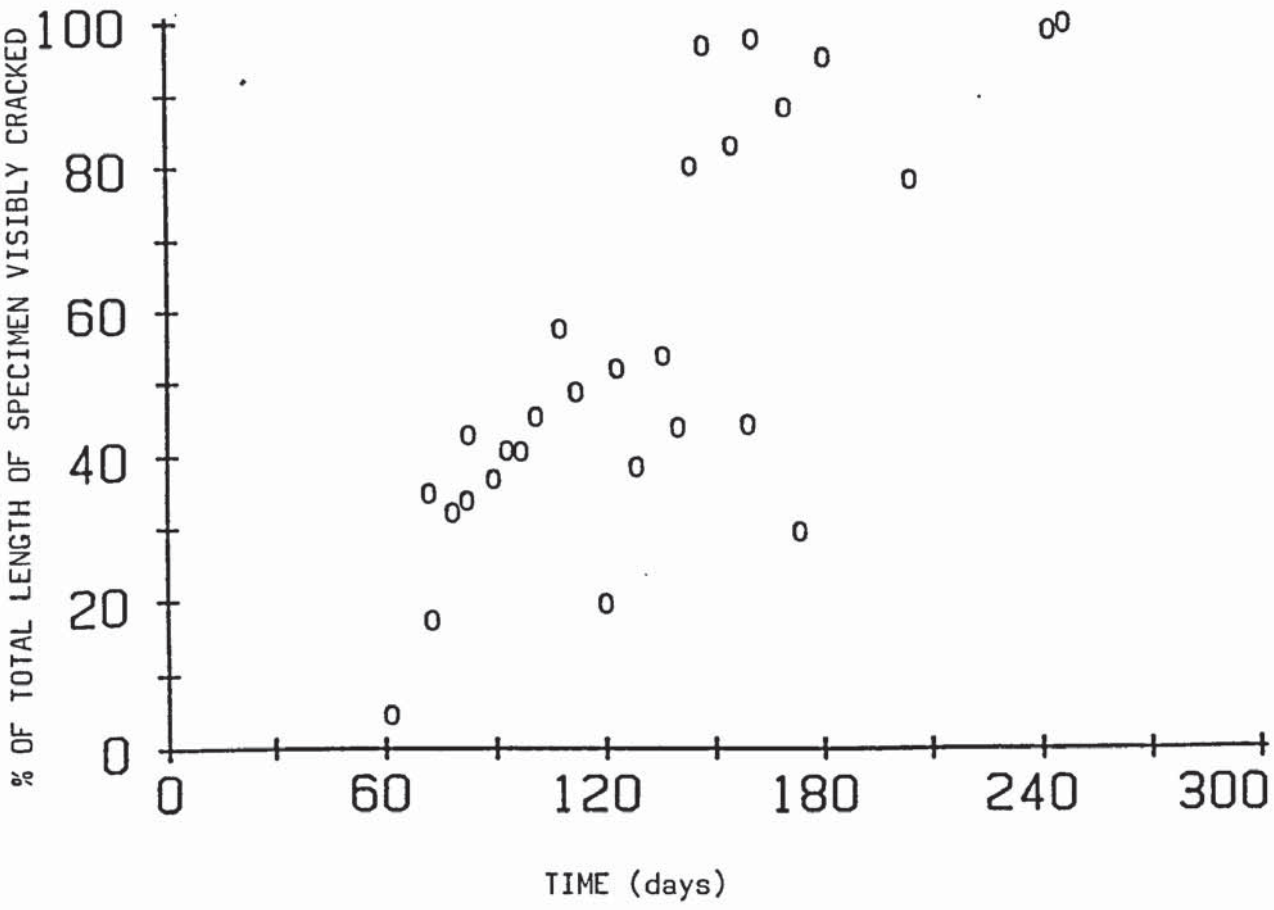

FIGURE 3.22 Proportion of longditudinal cracking visible at various times

FIGURE 3.23 Cracking within a mortar prism at end of exposure periods, the crack widths were; @ 0mm = 1.85mm, @ 90mm = 0.70mm and @ 190mm = 0.10mm

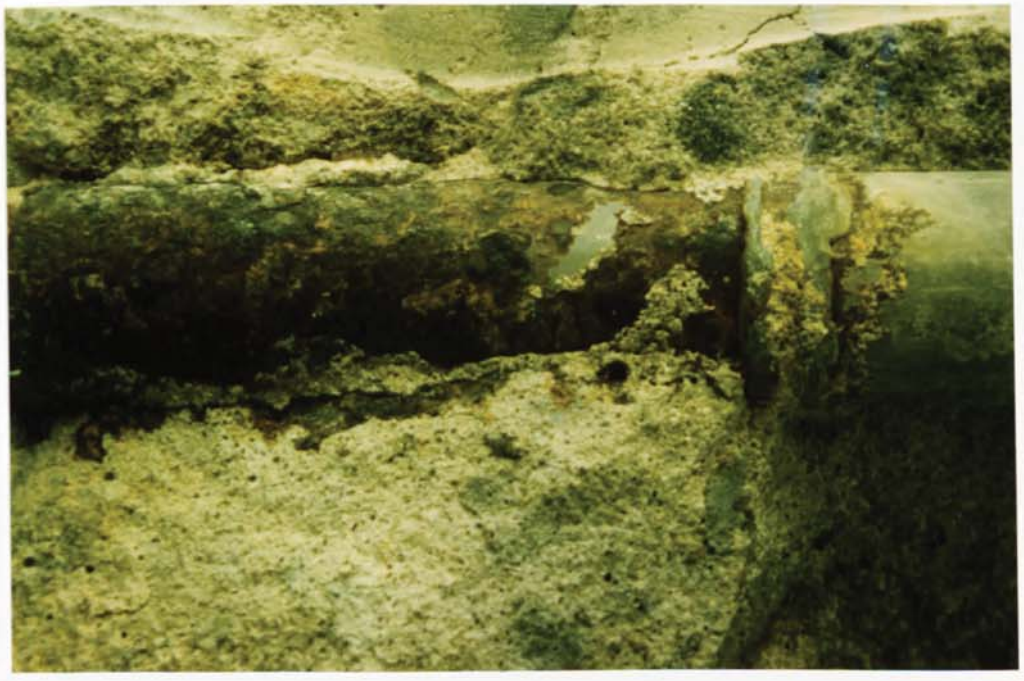

FIGURE 3.24 Extensive corrosion product both upon the 5% chloride segment, but also distant from the electrode, adherent to the mortar

FIGURE 3.25 Example of galvanic bar at end of exposure period; from left to right 5% and 1% segments

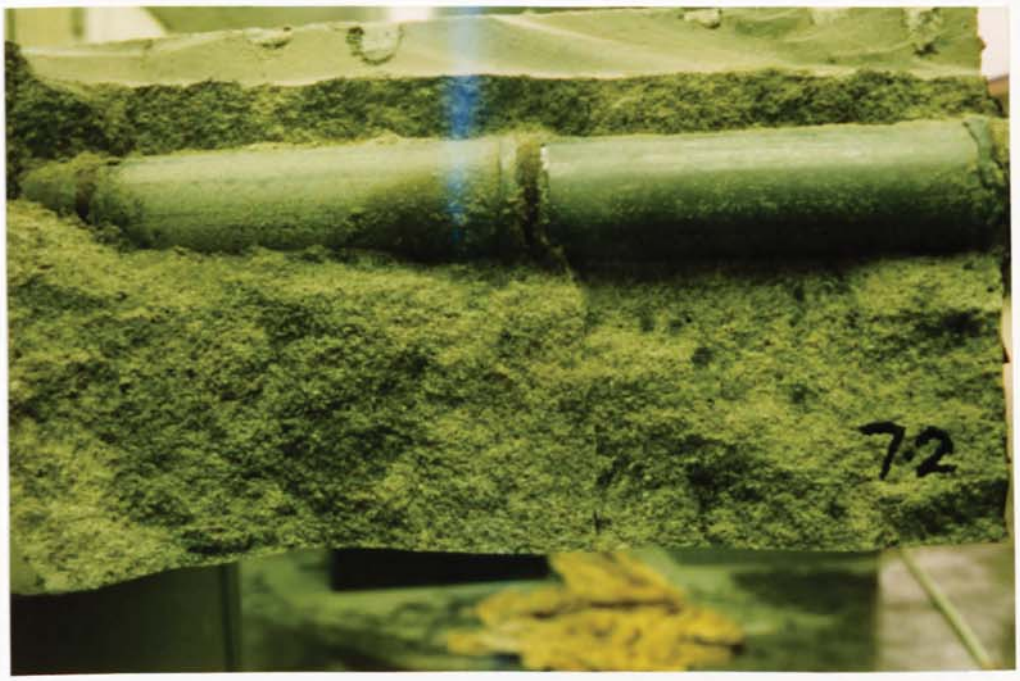

FIGURE 3.26 Example of galvanic bar at end of exposure period; chloride free segments

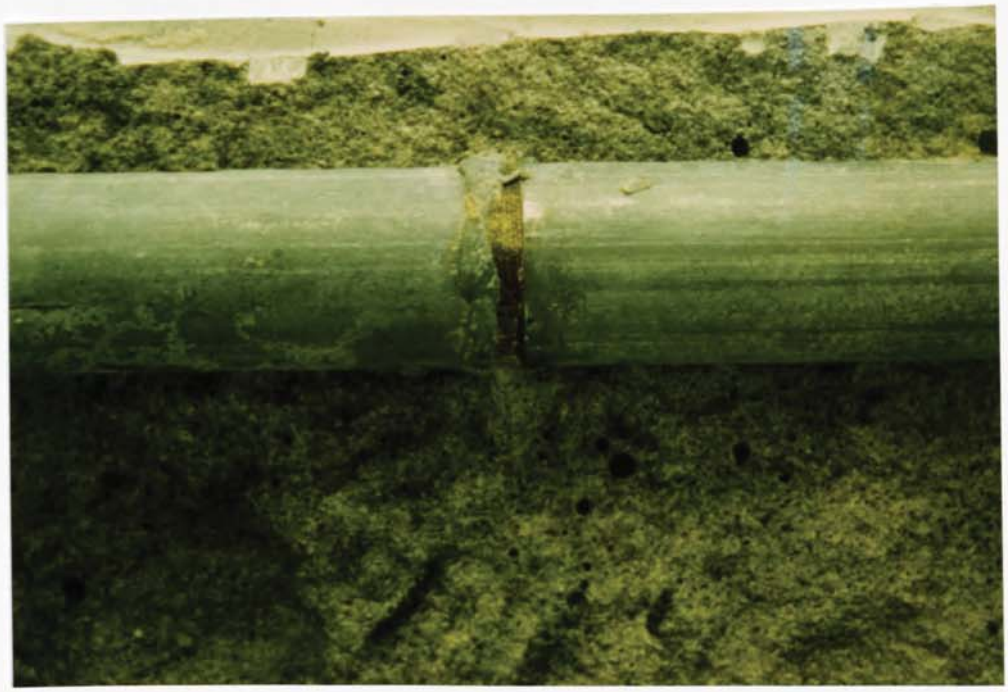

FIGURE 3.27 General condition of two chloride free segments showing no signs of corrosion

FIGURE 3.28 Example of end chloride free segment, free from signs of crevice corrosion

CHAPTER 4

PATCH REPAIRS AND PRIMERS - MICRO AND MACRO-CELL EFFECTS

4.1 INTRODUCTION

A repair and maintenance policy should be based upon a suitable investigation of the causes of the corrosion problem (4.1, 4.2). Such an appraisal is likely to identify regions of anodic activity. In the light of this information a method of repair may be selected.

Repair systems are diverse and include the following :

1. Sealing cracks - Wide cracks are closed by means of a suitable grout (4.3, 4.4).

2. Patching - Isolated regions of concrete are cut out and corrosion products removed from exposed reinforcement. A primer may be applied to cleaned reinforcements prior to the reinstatement of the patch which frequently comprises a proprietary polymer modified mortar (4.5).

3. Complete replacement - All contaminated concrete is removed and reinstated with new concrete of high quality (4.6).

4. Polymer impregnation - A monomer is applied to the surface of the structure and heat is used to initiate polymerisation (4.7).

5. Waterproof membranes - Asphaltic concrete is applied over a preformed mastic-asphalt sheet membrane (4.8).

6. Chloride ion removal - Electromigration of chloride ion is induced by the application of a d.c. current between temporary surface anodes and the reinforcement. Chloride ions migrate towards the surface where they are collected by an ion exchange resin (4.9).

7. Cathodic protection - Rebars are made cathodic relative to implanted surface anodes usually by the application of a d.c. current (4.10). The technology of cathodic protection for reinforced concrete is reviewed in Chapter 6.

It is apparent that a number of the above systems may prove difficult to apply to structures other than those consisting of predominantly horizontal surfaces.

The most simple and frequently used method of repairing a structure is patching. Guidelines have been suggested for selection of suitable materials to be used in this type of repair (4.11), but these do not consider potential problems involving incipient anodes, in the non-repaired areas. Corrosion interaction driven by the cathodic activity of repaired areas within a structure has been suggested (4.12), and it is possible that the net effect of this type of repair is to exacerbate corrosion in the non-repaired regions. Effects of this kind may be monitored by potential mapping techniques, though the data obtained only indicate the likelihood of incipient anodes, not the rate of metal dissolution. Whilst it

appears possible to repair structures durably and avoid incipient anodes by careful design of the patch repair (4.6), no quantitative data can be found to support the approach. Possible reasons for the lack of evidence are related to difficulties in devising a suitable laboratory methodology and the qualitative nature of data from field studies.

From the above, it is, therefore, unremarkable that there has been a widespread call for a better understanding of the science and practice of repair (4.12, 4.13, 4.14). It has been the purpose of this chapter to investigate a range of generic patch repair systems, in order to study their influence upon macro-cell corrosion of non-repaired steel under conditions conducive to an incipient anode condition. For this purpose, a well characterised specimen facilitating the measurement of macro-cell corrosion has been employed - see previous chapter.

4.2 PREVIOUS WORK

The properties of, and tests applicable to patch repair materials have recently been reviewed (4.15). Investigation of a repair material usually involves the study of both physical and mechanical properties of the systems' components. A study typical of this type involved an examination of adhesion/bond, thermal movement, permeability, mechanical strength, chemical resistance, freeze thaw resistance and ease of application (4.5). The use of surface treatments and modified mortars in order to reduce chloride ion ingress through repairs has been studied (4.16). The addition of polymeric materials to repair concretes has been evaluated terms of the mechanical and physical properties imparted (4.17).

The influence of primers applied to reinforcing steel, substrate primers, repair mortars, and also surface impregnation has been studied (4.18). The investigation of reinforcement primers showed that cement mortar slurry provided protection within the repair zone, but accelerated corrosion of reinforcement within the surrounding concrete. The phenomenon was attributed to the repair acting as a cathodic site, for adjacent non-repaired steel. Polymer modified cement slurry, non passivating epoxies and passivating epoxies (zinc phosphate and cement clinker) were found to suffer undercutting. It was suggested this undercutting was due to the primer isolating the rebar from the alkaline repair mortar. Passivating fillers were found to be ineffective, possibly as they were bound-up within the polymer matrix. A zinc rich primer was found to impart protection to steel embedded in concrete surrounding the repair. The effect was thought to be due to the zinc behaving anodically relative to the steel substrate, i.e. providing sacrificial cathodic protection to the substrate and surrounding steel.

Laboratory and field exposure studies evaluated five repair systems (4.19, 4.20). In both studies, the performance of repairs was monitored by periodic visual inspection and electrochemical testing (a.c. impedance). Finally, destructive testing was carried out in order to evaluate the condition of the repair, substrate concrete, and steel embedded in both repair and non-repair regions.

The experimental work to be described was aimed at providing a direct measurement of the galvanic interactions between steel in repaired and non-repaired regions of concretes. By using the specimens of the kind described in Chapter 3 it was intended to evaluate a range of generic patch repair systems typical of those

used in practice. In particular, the objective was to establish quantitatively the effects of certain reinforcement and concrete substrate primers, upon corrosion at the repair site, and also regions of steel near to the repair.

4.3 EXPERIMENTAL

The experimental approach in this chapter involves the use of the galvanic bar specimens devised in Chapter 3. These specimens had been monitored over a prolonged exposure period and were well characterised in terms of their macro and micro-cell corrosion behaviour. For the repair programme, a range of generic reinforcement priming systems were selected as described below :

Repair system one.	Ordinary Portland cement slurry applied to the reinforcement.
Repair system two.	System one plus an acrylic bonding agent applied over the OPC slurry and mortar substrate (see Chapter 2 and Appendix).
Repair system three.	Zinc rich epoxy primer applied to the reinforcement (see Chapter 2 and Appendix)
Repair system four.	System three plus an acrylic bonding agent applied over the zinc primer and mortar substrate.
Repair system five.	Ordinary Portland cement applied to the reinforcement plus an insulating epoxy resin applied over the OPC primer and mortar substrate (see Chapter 2 and Appendix).

Diagrams of the above systems are given in figures 4.1 to 4.5 and photographs of systems one, three and five in figures 4.6 and 4.8. System one was selected as the most convenient method of placing the electrode within a passivating highly alkaline medium. The use, in system two, of an acrylic bonding coat - employed in practice to improve the initial grab of the repair mortar to primer and substrate - was intended to simulate a more practical example and to elucidate any influences of the acrylic upon the electrochemical behaviour of the system. Zinc rich primers (system three) are used in practice as they are thought to impart sacrificial protection to both steel within a repair and also within a zone surrounding repaired concrete. The addition of the acrylic bonding coat, in system four, was for those reasons given for system two. In system five, the insulating epoxy was intended to isolate the entire repair from the remainder of the specimen whilst the OPC slurry, applied to the electrode, was included to promote passivity and to minimise any risk of corrosion undercutting the epoxy. Although not used in practice, it was thought that system five might be particularly effective in limiting any incipient anode effects.

In all cases, the mortar patching material comprised a proprietary polymer modified mortar - used at the specified water/pow der ratio. Details of the mortar are given in Chapter 2.

The method adopted for the physical execution of each repair was as follows. First, the mortar surrounding the most anodic segmental electrode of a galvanic bar was removed; in all instances this had previously been established as the electrode within the 5% chloride region (see previous chapter). Removal of existing mortar was achieved by cutting around the perimeter of the prism, then carefully breaking away the mortar from the electrode. It was

found that mortar could be removed with relative ease and no electrode surface was inadvertently damaged by mechanical action. The ease of removal was, in part, due to the extensive corrosion product on the electrode, which was found to comprise a friable interfacial layer between the electrode and mortar. An example of this layer is shown in figure 4.9.

In order to remove adherent corrosion product from the electrode, the surface was sand-blasted in two stages, first using particles $\not>1000\mu m$ in size, and secondly particles $\not>600\mu m$. The second treatment was found to be effective for the removal of strongly adherent corrosion products. Finally, a pencil device, containing tightly bunched, fine glass fibre strands, was carefully worked over the entire sand-blasted surface. In a limited number of instances exceptionally hard black corrosion product remained after the above treatment. This product, thought to be magnetite (figure 4.10) would remain insoluble and consequently be unlikely to influence the completed repair.

With all electrodes suitably prepared, the primer systems previously described were applied. In systems where more than one coat of primer was applied, approximately 48 hours was allowed to elapse between coats. All primers were applied by hand. Curing was carried out under ambient laboratory conditions. Having inspected completed primed electrodes for any visual defects, the specimens were arranged in moulds ready for casting. In the case of those specimens where an acrylic bonding coat was to be included, application was carried out immediately prior to casting. In practice this is the normal procedure to maximise grab of the coating. The polymer modified mortar was compacted by hand and cured within the mould for 24 hours at $22^{\circ}C \pm 2^{\circ}C$, 100% relative

humidity. The mould was then stripped, specimens were cured for a further 21 days and the anti-crevice masking (Chapter 3) was applied to the end of each specimen.

The prisms had suffered cracking due to the voluminous corrosion products formed during the earlier exposure programme and it was decided to seal these cracks. This was necessary in order to minimise any possibility of differential corrosion cells, e.g. differential aeration etc. Although it had previously been noted that corrosion products had tended to block cracks, deliberately sealing cracks was more representative of site practice. Sealing was effected with a low viscosity resin grout, able to penetrate cracks under its own hydrostatic head. Details of the grout are given in the Appendices.

Corrosion activity for the macro-cell study was monitored by measurement of the galvanic current, and linear polarisation was used for the micro-cell investigation. Corrosion potentials were monitored at the locations used in Chapter 3. Specimens were subjected to alternate cycles of wetting and drying, as in Chapter 3.

4.4 RESULTS AND DISCUSSION

The mean results obtained for the macro-cell corrosion study, in wet and dry conditions, are shown as current/time traces in figures 4.11 to 4.15. The three traces show anodic currents, i_{galv}, for the following sets of measurements :

Trace one. i_{galv} measured between 1% segments and all others, including the repaired segment.

Trace two. i_{galv} measured between 1% segments and all others, except the repaired segment.

Trace three. i_{galv} measured between 0.1% segments and those in a lower chloride environment, except the repaired segment.

Mean cathodic galvanic currents, i_{galv} (cathodic) measured between the repaired segments and all others, for both wet and dry conditions, are given in figures 4.16 to 4.20. Micro-cell corrosion has been determined for individual, isolated, 1% segments, by linear polarisation (Chapter 2), the values obtained being compared to the pre-repair condition in table 4.1. Linear polarisation measurements were carried out after the disconnected segments had settled for $\leq$ 30 minutes, in order to allow their potential to stabilise. Mean values of corrosion potential, E_{corr}, for repaired segments are given in figures 4.21 to 4.25, and 1% segments in figures 4.26 to 4.30. Traces of E_{corr} for 0.1% segments are shown in figures 4.31 to 4.35 and for chloride free segments in figures 4.36 to 4.40.

Considering the macro-cell corrosion data for the 1% segments first. From the previous chapter it has been established that 1% segments were undergoing partial cathodic protection, due to the influence of the adjacent strongly anodic 5% segment. The effect of removing the 5% segments' influence has been to promote an incipient anode condition at the 1% segment. The intensity of the anode at the 1% segment, in terms of i_{galv}, is shown by trace one in figures 4.11 to 4.15. By comparison of traces one and two (figures 4.11 to 4.15), it is apparent that the magnitude of i_{galv} has been

increased by the availability of the nearby cathode at the repair site. Exacerbation of the incipient anode can be clearly seen for all repair systems, except the insulating epoxy system, shown in figure 4.15, where the effect is far less pronounced.

The influence of the various repair primers upon the corrosion rate of the 1% segment incipient anode, has been assessed by comparison of changes in i_{galv} for the 1% segment coupled with and without the repair (table 4.2).

From table 4.2 it can be seen that, in terms of restraining incipient anode activity, the insulating epoxy system has proven to be the most effective of those systems investigated. Passivity of the repaired segment was engendered by the OPC slurry (beneath the epoxy) which was in intimate contact with the electrode providing a strongly buffered alkaline region. Such conditions are conducive to the promotion of the passivating oxide layer. Very little evidence of crevice corrosion was found at the interface between the repair and 1% chloride region. This system's ability to limit the intensity of the incipient anode at the 1% segment may be attributed to the epoxy reducing the rate of movement of the reactants involved in the cathodic process. The insulating properties of the epoxy provide an effective barrier to ionic migration.

It is possible that the above explanation is also applicable to the OPC and acrylic bonding coat system. Here the acrylic acted in a similar manner to the epoxy, albeit less effectively. A visual comparison of the repaired and 1% segments for the OPC systems, with and without the acrylic bonding coat, is shown in figures 4.41 and 4.42. A greater area of corrosion product can be seen on the 1% segment of the OPC system without the acrylic. The visual

observations tend to confirm the comparison of the micro and macro-cell intensities for the OPC acrylic and non-acrylic systems. The pre-repair micro-cell intensities were very similar; $\sim 0.6 \mu A/cm^2$ for each set of specimens. After repairing the adjacent segment the micro-cell intensities increased to $1.02 \mu A/cm^2$ and $2.33 \mu A/cm^2$ for the OPC with acrylic and OPC without acrylic system respectively.

The macro-cell corrosion currents for both zinc primer systems (with and without an acrylic bonding agent) indicate an acceleration of the incipient anode at the 1% segment. There appears to be no significant difference in terms of i_{galv}, between zinc primers with and without an acrylic bonding coat. Sacrificial corrosion of the zinc, and possible cathodic protection of the nearby 1% region, would not appear to have played a significant role in the electrochemical process. Figure 4.43 shows the presence of a brown corrosion product of steel upon the zinc rich paint surface. These regions of corrosion product were, however, limited to a very small number of isolated sites. A surface more typical of the exposed zinc coated electrode is shown in figure 4.44. Examples of the surfaces of 1% segment corresponding to a zinc coated electrode are shown in figures 4.45 and 4.46. The portion of electrode visible at the right hand side of figure 4.45 corresponds to a 0.1% electrode. Figures 4.47 and 4.48 show a well developed pitted region present on a 1% segment, the electrode corresponding to a zinc primer and acrylic bonding agent repair.

On the basis of these results, it would appear that the zinc has not imparted any significant sacrificial cathodic protection to the 1% segment. This finding conflicts with a previous investigation in which the results suggested sacrificial dissolution of the zinc giving rise to cathodic protection to

nearby areas of steel (4.18). It is therefore necessary to examine possible reasons for this variable behaviour. Figure 4.49 shows the influence of pH upon the corrosion rate of zinc; it can be seen that the rate of dissolution increases at pH values below 6 and above 12.5, becoming increasingly rapid as the pH is raised from the latter value. By using the pore press technique (Chapter 2) and titrating the pore solution expressed, the pH of the pore solution from the repair mortar was found to be pH 13.38, which is relatively low compared with that of mortars containing moderate to high alkali Portland cements (4.23) and such as to indicate that passivation of zinc might occur for an embedded electrode (4.24-4.26). It has been found that cell reversal can occur in zinc-iron galvanic cells (4.21) under conditions which favour the formation on the zinc of a surface film that hinders dissolution by limiting the diffusion of zinc ions. It was also found that the stability of this inhibitive film was dependent upon the activation of anodic sites, upon the iron surface, supported by the action of aggressive nitrate ions. In the present case, it seems probable that a similar mechanism may have been at work, with the zinc in a passivating medium and chloride available to activate the steel.

In order to further elucidate the behaviour of the zinc rich systems, an investigation by scanning electron microscopy (SEM) used in conjunction with a microanalysis system - energy dispersive x-ray analysis (EDXA) - was performed. For this purpose, sample material was taken from a number of dismantled segmental bars.

Initially, repair mortar/zinc coating interfacial regions were examined from zinc specimens with and without acrylic bonding agent. A comparison of these surfaces showed their appearance and composition to be similar. However, a feature found to be peculiar

to the acrylic coated zinc specimen involved regions of smooth appearance (figure 4.50). It is possible that these areas were associated with acrylic coating. In order to simplify the investigation, further study was limited to specimens comprising zinc-primer without the acrylic bonding agent.

Figures 4.51 and 4.52 show surfaces typical of the samples investigated. The lightly textured background surface was covered with random, rough, cratered, spheroidal features. The crater features when examined closely were found to comprise two main forms; those with intact spheroids and those showing spheroid debris; both features are evident in figure 4.52. A spot EDXA analysis was carried out on a collapsed spheroid and an empty crater (electron photomicrograph, shown in figure 4.53); the x-ray traces are given in figure 4.54. The crater composition was mainly calcium and zinc, the collapsed sphere was substantially zinc, with a lower level of calcium, but with higher levels of silicon and aluminium. In order to establish the source of the silicon and aluminium, intact and broken spheroids were examined (figures 4.55 and 4.56). The x-ray traces, (figure 4.57) show high levels of silicon and aluminium to be present for both cases. The appearance and composition of these objects was suggestive of a pozzolanic material, possibly pulverised fuel ash (PFA). The composition of the broken sphere was very similar to that found for the intact sphere. The presence of these elements upon the zinc primer's surface may be accounted for by the likely inclusion of a pozzolanic material within the formulation of the repair mortar.

Having excluded the larger spheroids as forming a part of the zinc coating layer, the background textured surface was examined in more detail. This was found to comprise much smaller, closely

packed and irregularly sized spheroids (figure 4.58). The EDXA analysis indicates the most abundant element to be zinc though lower levels of silicon oxide, potassium and calcium were present (figure 4.59).

The zinc layer was investigated at the location of a fracture through the coating, where the underlying steel substrate was exposed (figures 4.60 and 4.61). From figure 4.61 the spheroidal arrangement comprising the coating can be seen, one side in close contact with the substrate, and the other side overlaid with an intimate layer of cementitious mortar hydrates.

In order to examine further the nature of the zinc layer, a specimen of zinc primer coated rod was specially prepared with a thicker than usual coating. The nature of a fracture surface is shown in figures 4.62 and 4.63. E.D.X.A analysis confirmed a high zinc loading of the layer (figure 4.64). From figures 4.65-4.67, the spheroids appear irregularly, closely packed and randomly cross linked.

It is possible that the layer of mortar hydrates found to be in intimate contact with the zinc has served as a barrier to the diffusion of reactants involved in the dissolution of the zinc. Previous studies involving galvanised steel in alkaline solutions established the presence of a passivating layer comprising; calcium hydroxyzincate in the case of saturated calcium hydroxide (4.24), and zinc hydroxide for sodium or potassium hydroxide solutions within the range $12.8 \pm 0.1 < pH < 13.4 \pm 0.1$ (4.26). Furthermore, the presence of a pozzolan - thought to be PFA - would tend to remove free alkali from the pore solution. Any reduction in alkalinity is likely to reduce the rate of zinc dissolution, and so its effectiveness as a sacrificial coating.

The i_{galv} traces for 0.1% segments coupled with chloride free electrodes (except the repair), do not show any significantly different trends to the pre-repair traces. The surface condition of these electrodes was not dissimilar from that of the chloride free electrodes. An example of an electrode is shown in figure 4.68 showing 1%, 0.1% and chloride free segments.

The mean values of i_{galv} determined for the repaired electrodes, measured against all other segments, are given in figures 4.16 to 4.20. In all cases the magnitude of the cathodic currents reflect the difference between trace one and two for i_{galv} (anodic) in figures 4.11 to 4.15.

Corrosion potential/time traces for repaired segments (figures 4.21 to 4.25) indicate a shift to less negative potentials as a result of repair. Values of E_{corr} obtained for the OPC slurry and epoxy system (figure 4.25) are generally as negative as those measured for the pre-repair 5% chloride environment. It is possible that the epoxy layer has restricted oxygen access to the electrode. This being the case, the condition may be analogous with a submerged structure where the potential is depressed and the corrosion limited by oxygen availability. The values of E_{corr} for 1% segments (figures 4.26 to 4.30) indicate negative potentials of similar range to those recorded for the pre-repair condition, where corrosion was restrained by the cathodic protection afforded by the highly active 5% electrodes. The apparent similarity of pre and post-repair corrosion potentials is not reflected by the macro and micro-cell corrosion current data.

For the zinc primer system the values of E_{corr} for the 1% segments were more negative than those potentials determined for the zinc coated electrodes. This finding confirms the theory of the

zinc behaving cathodically relative to the 1% electrode.

The traces of E_{corr} recorded for the 0.1% and chloride free segments show no significant change in trend from the pre-repair condition.

The i_{galv} and E_{corr} traces show a reduction in i_{galv} and a shift to less negative potentials, when specimens are in a dry condition. This indication of macro-cells being subject to resistance control agrees with the findings of the previous chapter.

4.5 CONCLUSIONS

Several primer systems have been investigated within a patch repair under conditions conducive to the activation of an incipient anode.

It was found that electrodes in a 1% chloride environment previously experiencing cathodic protection, due to the influence of a nearby and high active macro-cell, became active due to the removal of the near anode. The intensity of the macro-cell, at the 1% chloride electrode, was further increased due to the introduction of a cathodic region viz. the repaired electrode. However, the intensity of the macro-cell was found to be influenced by the particular priming system used at the repair site.

A system involving ordinary Portland cement slurry overcoated with insulating epoxy was found to be effective in limiting macro-cell intensities. A zinc rich epoxy primer, found to comprise tightly packed, randomly sized spheres, was found to exacerbate the incipient macro-cell condition. This phenomenon was thought to be due to a combination of factors involving the suppression of zinc dissolution and a cell reversal process associated with the

corrosion of the nearby electrode within the 1% chloride environment. However, the zinc was studied under specific conditions involving chloride levels considered high in terms of desirable on-site concrete repair practice. Changes in the experimental conditions, e.g. involving reduced chloride levels near to the zinc and/or an increase in the pH of the pore solution at the zinc, may well produce a quite different response, in keeping with other investigators, i.e. sacrificial protection.

Increases in micro-cell intensity were found at the incipient anode electrode, although no correlation for increased micro and macro-cell corrosion rates were established.

Whilst the visual condition of the electrodes was generally supportive of corrosion current data, in certain instances the corrosion potentials measured tended to be more negative than would normally be expected for a passive electrode.

From these findings several phenomena relating to the on-site practice of concrete repair are suggested. The presence and possibility of incipient anodes has been established and emphasises the necessity for the thorough removal of chloride contaminated concrete. Failure to do so may result in the promotion of significant corrosion currents within unrepaired regions of a structure. The requirement for complete chloride removal will prove impracticable in many instances, for reasons of cost, structural integrity, etc. Under these circumstances the use of reinforcement primers will significantly influence the net electrochemical behaviour within the structure. It would appear that primers which cause electrochemical isolation of the reinforcement are most likely to suppress incipient anodes in the unrepaired zones. However, whilst such systems exhibit desirable features under

strictly controlled laboratory conditions, it may prove difficult to develop them for reliable on-site application. This is an area where further work is required.

Primer Repair System	Pre-Repair Corrosion Intensity at 1% Electrode $\mu A/cm^2$	Post-Repair Corrosion Intensity at 1% Electrode $\mu A/cm^2$	Pre to Post Repair Increase in Micro-Cell Intensity %
Ordinary Portland Cement Slurry	0.61	2.33	282
Ordinary Portland Cement Slurry plus Acrylic Bonding Agent	0.62	1.02	64
Zinc Rich Primer	0.14	0.66	371
Zinc Rich Primer plus Acrylic Bonding Agent	0.49	2.29	367
Ordinary Portland Cement Slurry plus Insulating Epoxy	0.32	0.94	194

TABLE 4.1 Comparison of micro-cell corrosion intensities pre and post repair

Primer Repair System	Pre to Post Repair Increase in Macro-Cell Corrosion Intensity (dry condition) %	Pre to Post Repair Increase in Macro-Cell Corrosion Intensity (wet condition) %
Ordinary Portland Cement Slurry	166	103
Ordinary Portland Cement Slurry Plus Acrylic Bonding Agent	54	57
Zinc Rich Primer	238	123
Zinc Rich Primer Plus Acrylic Bonding Agent	182	121
Ordinary Portland Cement Slurry Plus Insulating Epoxy	24	17

TABLE 4.2 Comparison of increase in macro-cell corrosion intensities, pre to post repair, for dry and wet conditions

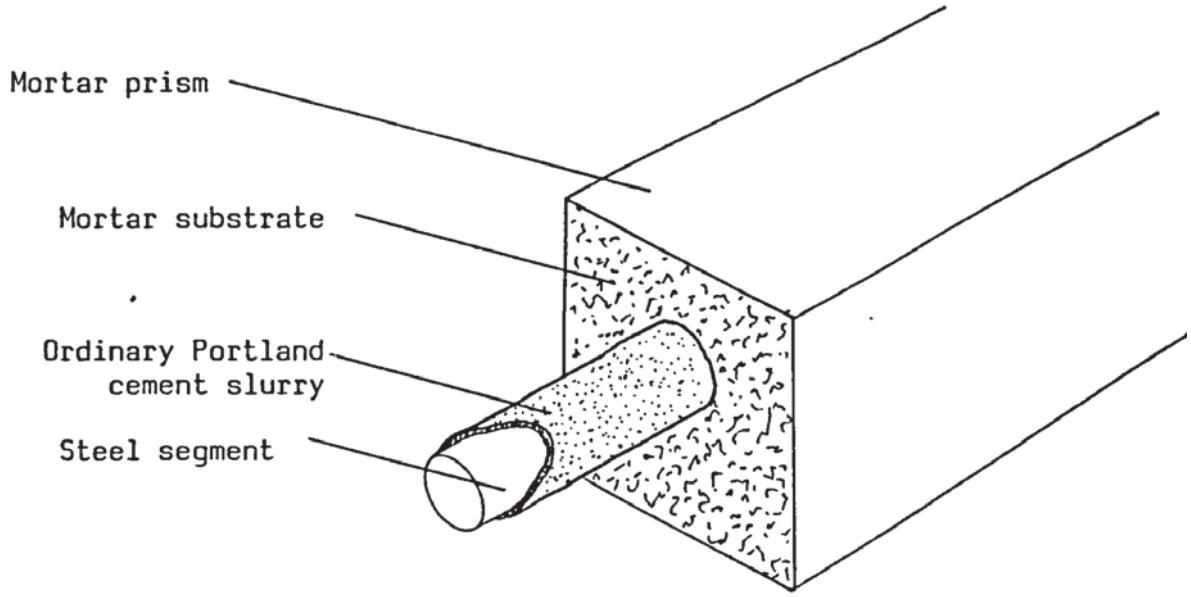

FIGURE 4.1 Cut-away isometric showing repair system one

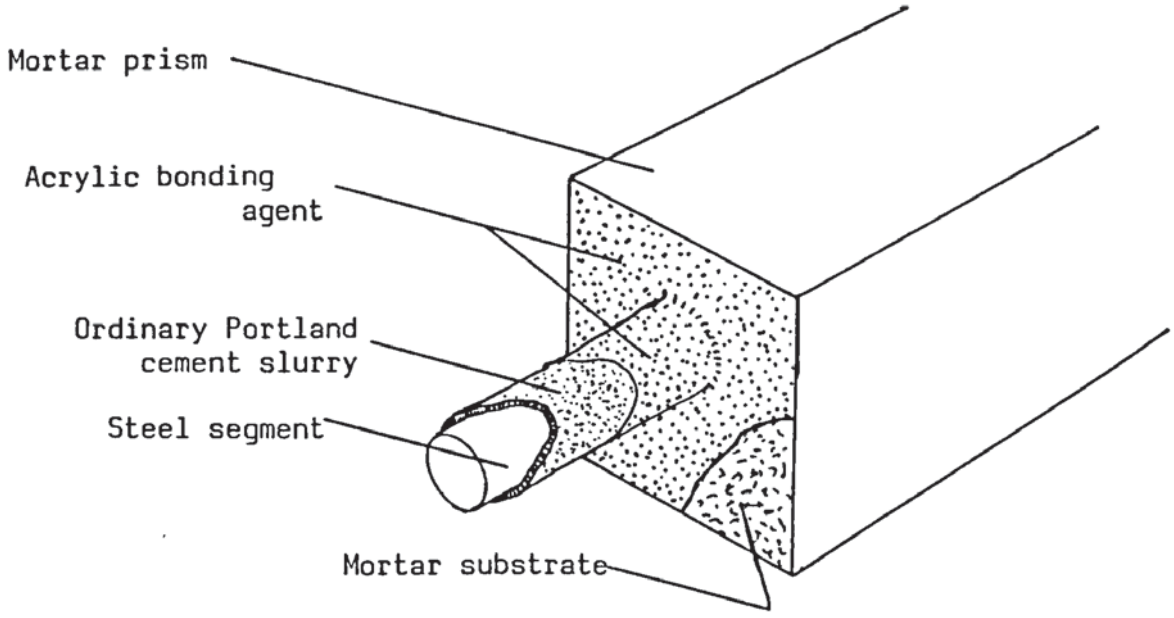

FIGURE 4.2 Cut-away isometric showing repair system two

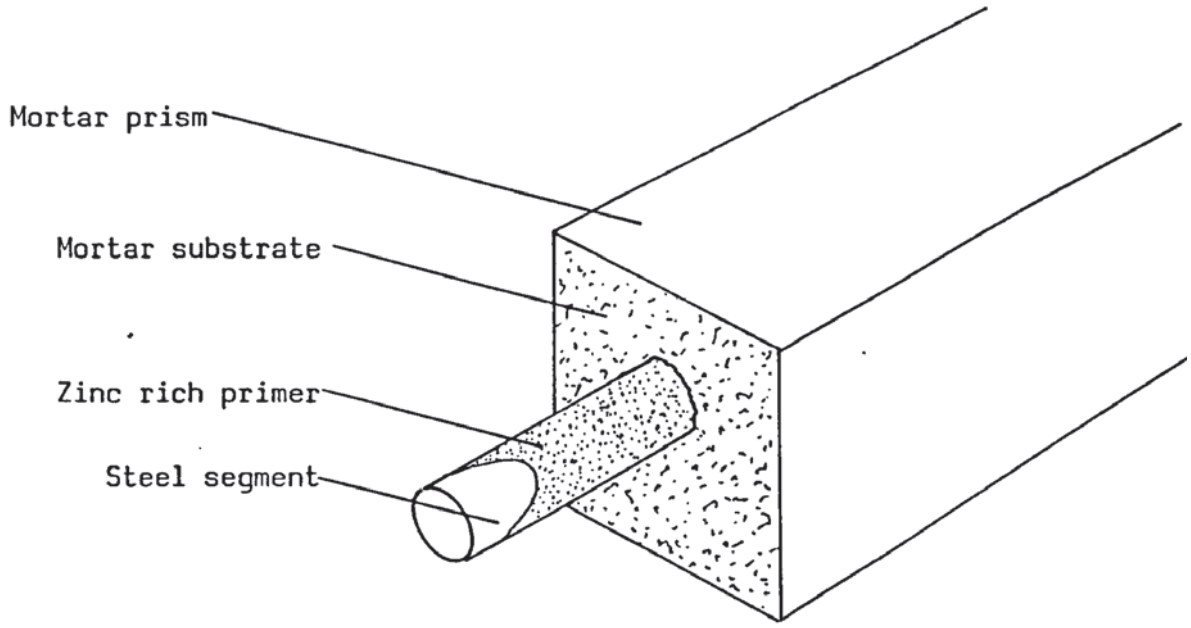

FIGURE 4.3 Cut-away isometric showing repair system three

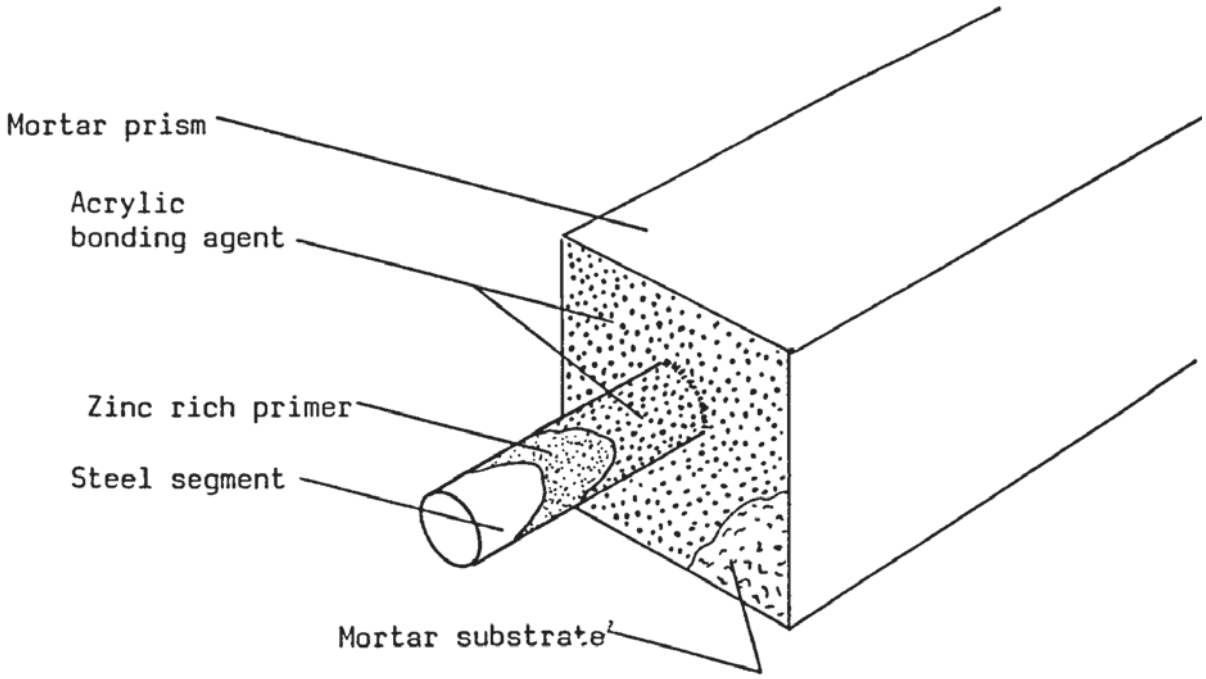

FIGURE 4.4 Cut-away isometric showing repair system four

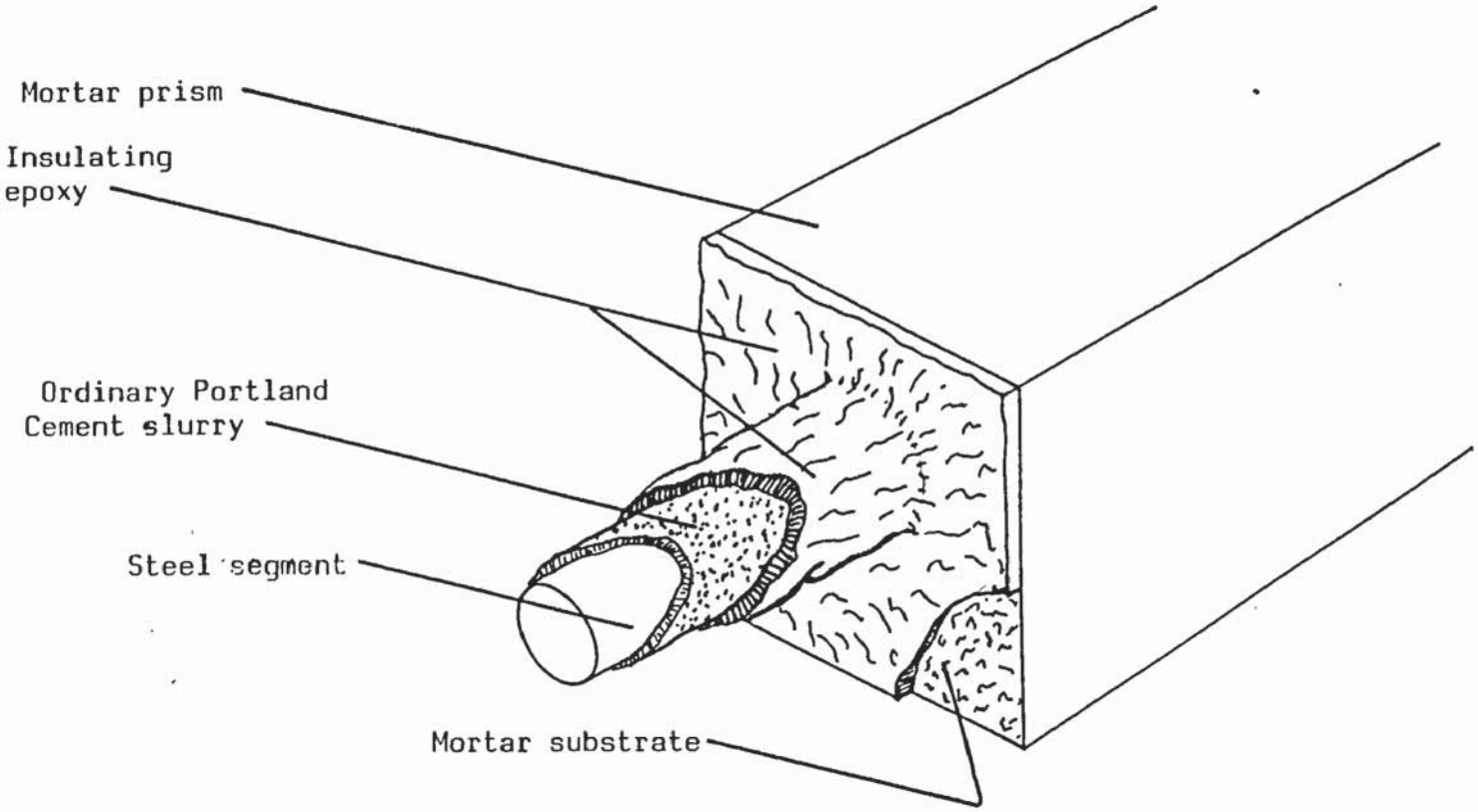

FIGURE 4.5 Cut-away isometric showing repair system five

FIGURE 4.6 Repair system one comprising ordinary Portland cement slurry applied to the steel segment

FIGURE 4.7 Repair system three comprising zinc rich epoxy primer applied to the steel segment

FIGURE 4.8 Repair system five comprising ordinary Portland cement slurry applied to steel segment, OPC slurry and mortar substrate overcoated with insulating epoxy

FIGURE 4.9 Friable layer comprising corrosion products found at 5% chloride segment/mortar interface

FIGURE 4.10 Macro (x6.5) showing black regions thought to comprise magnetite, in this instance within a ordinary Portland cement slurry and insulating epoxy repair, after completion of the exposure period

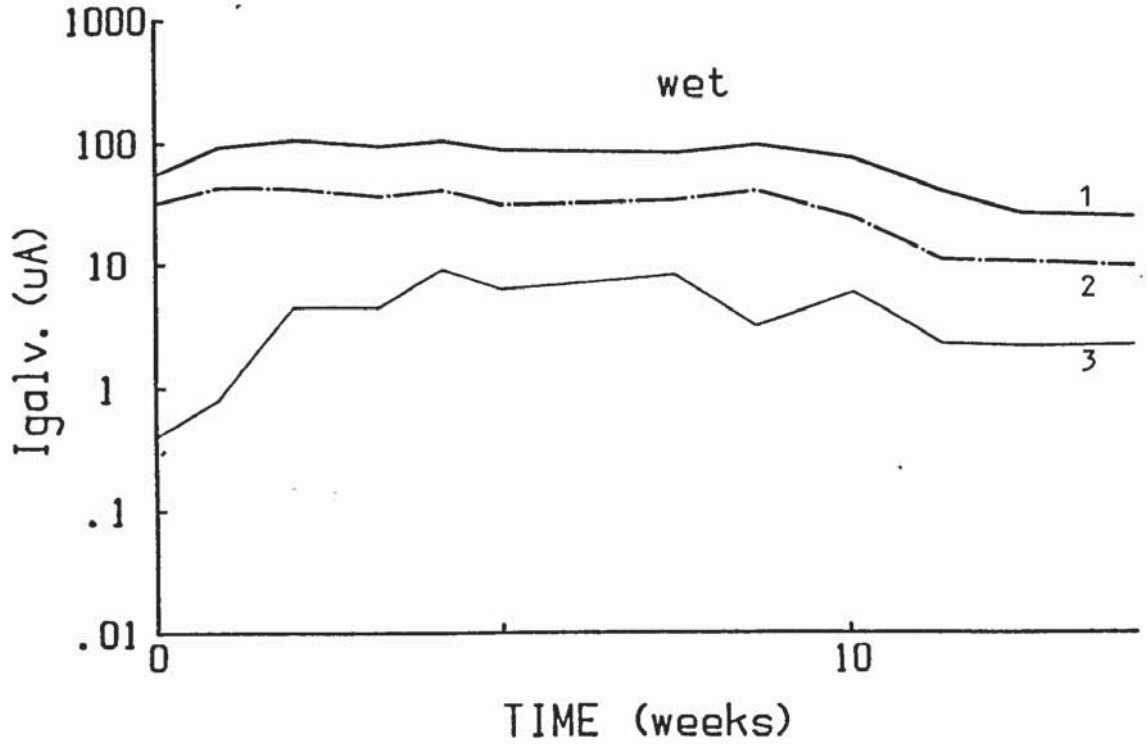

FIGURE 4.11 a

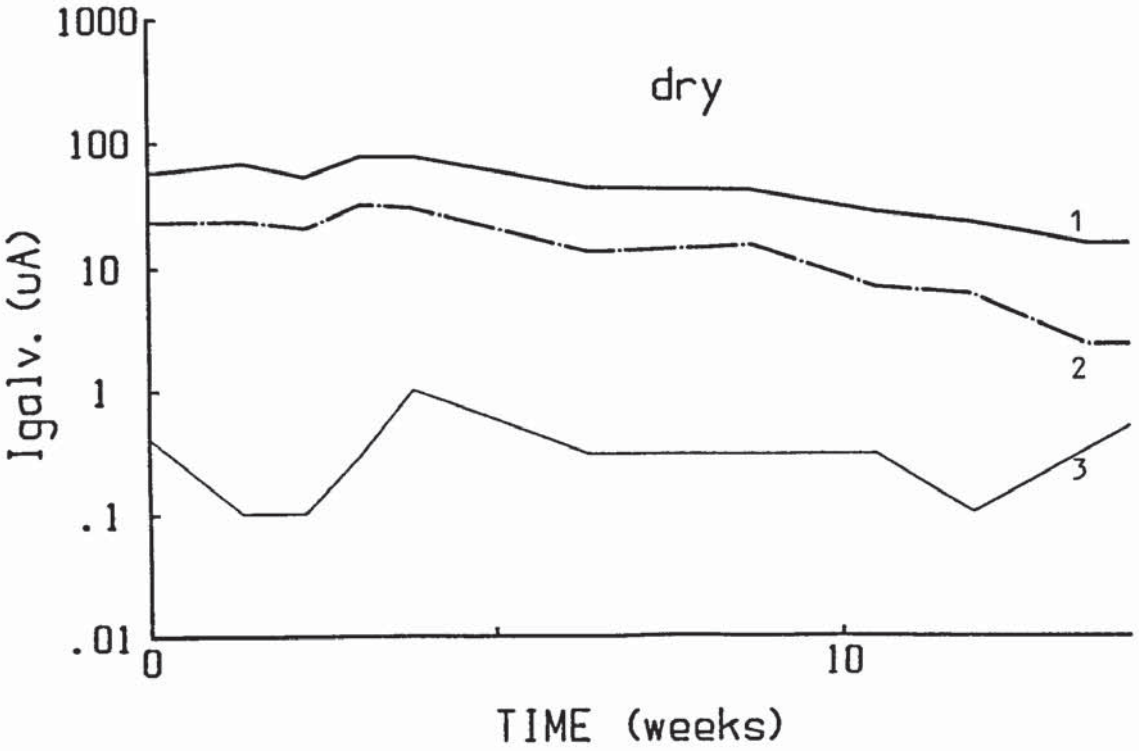

FIGURE 4.11b

FIGURE 4.11 Repair system one (OPC slurry); i_{galv}/time traces for wet (a) and dry (b) conditions for the segment combinations; 1 = 1% vs repair + 0.1% + 0.0%, 2 = 1% vs 0.1% + 0.0%, 3 = 0.1% vs 0.0%

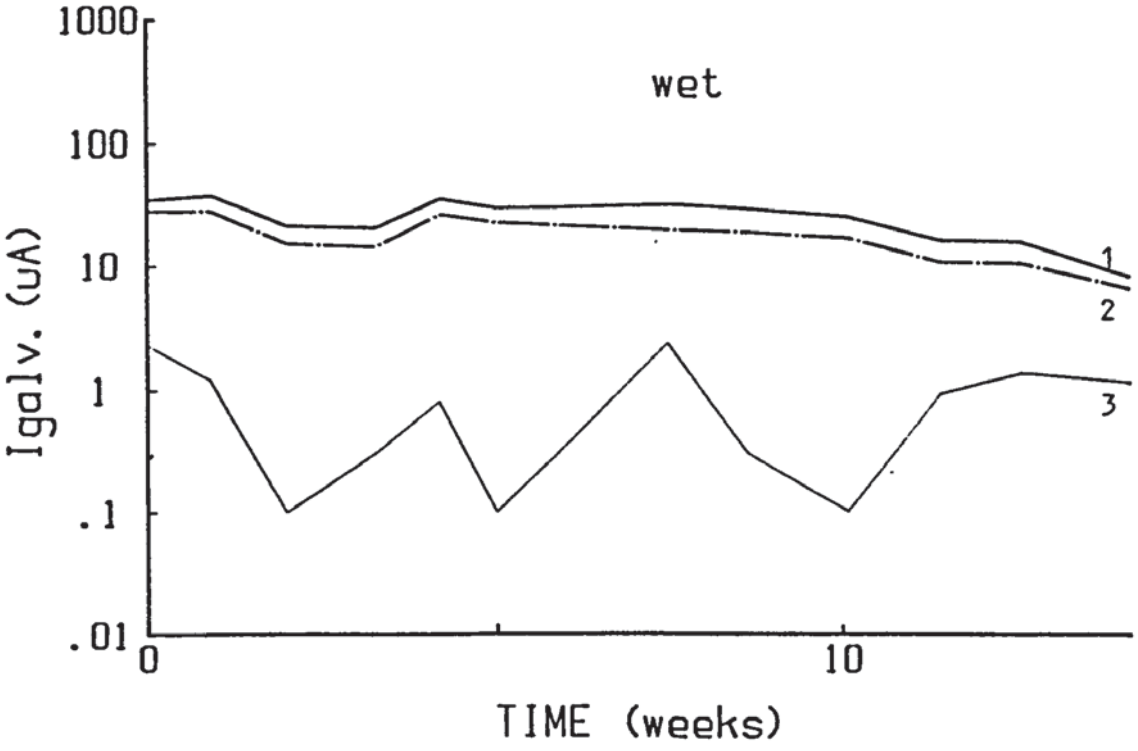

FIGURE 4.12 a

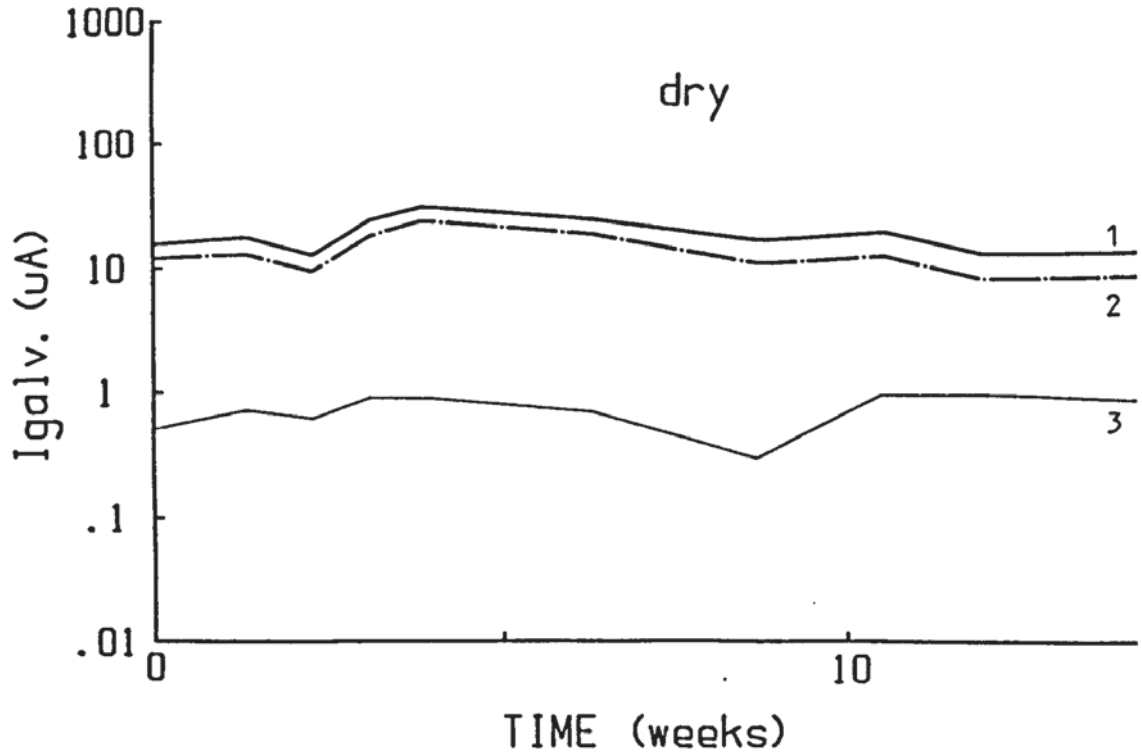

FIGURE 4.12 b

FIGURE 4.12 Repair system two (OPC slurry and acrylic bonding agent) ι_{galv}/time traces for wet (a) and dry (b) conditions for the segment combinations; 1 = 1% vs repair + 0.1% + 0.0%, 2 = 1% vs 0.1% + 0.0%, 3 = 0.1% vs 0.0%

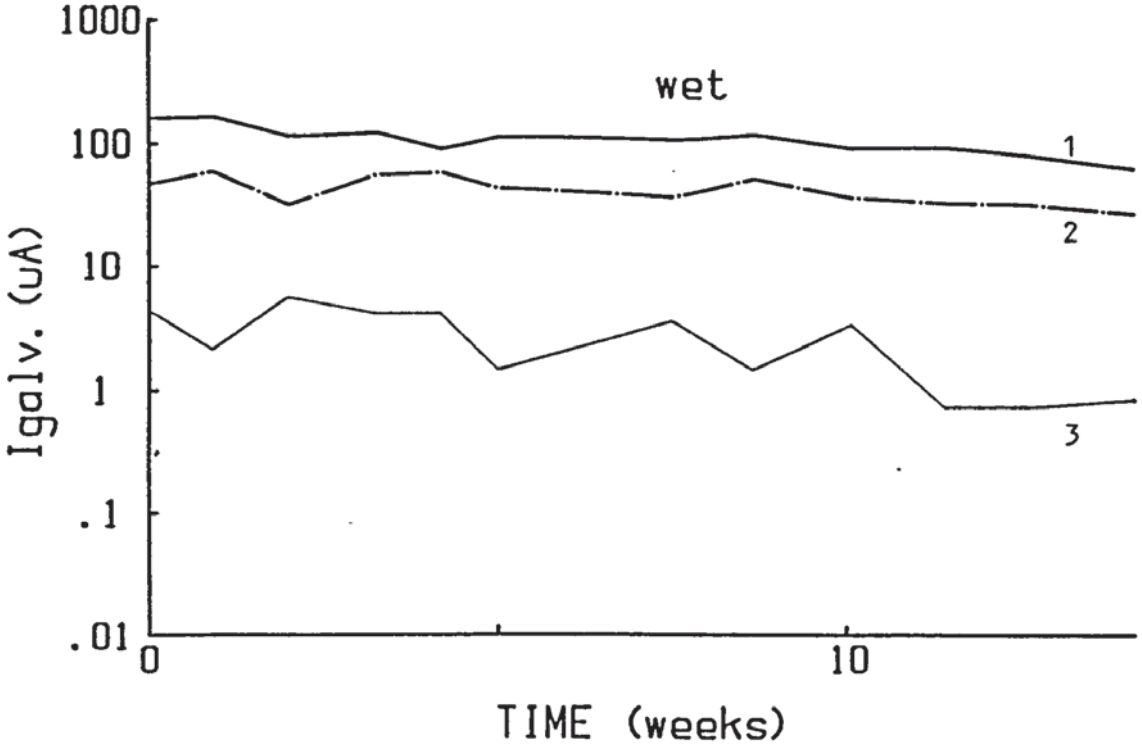

FIGURE 4.13 a

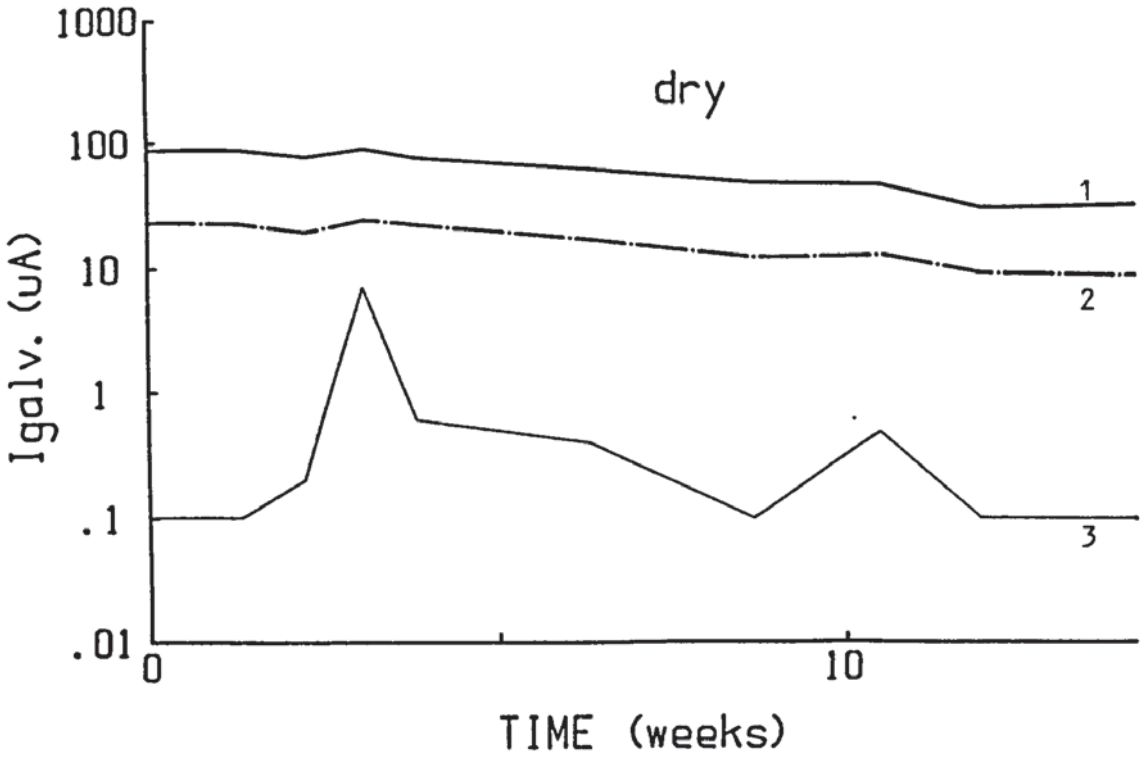

FIGURE 4.13 b

FIGURE 4.13 Repair system three (zinc rich primer) i_{galv}/ time traces for wet (a) and dry (b) conditions for the segment combinations; 1 = 1% vs repair + 0.1% + 0.0%, 2 = 1% vs 0.1% + 0.0%, 3 = 0.1% vs 0.0%

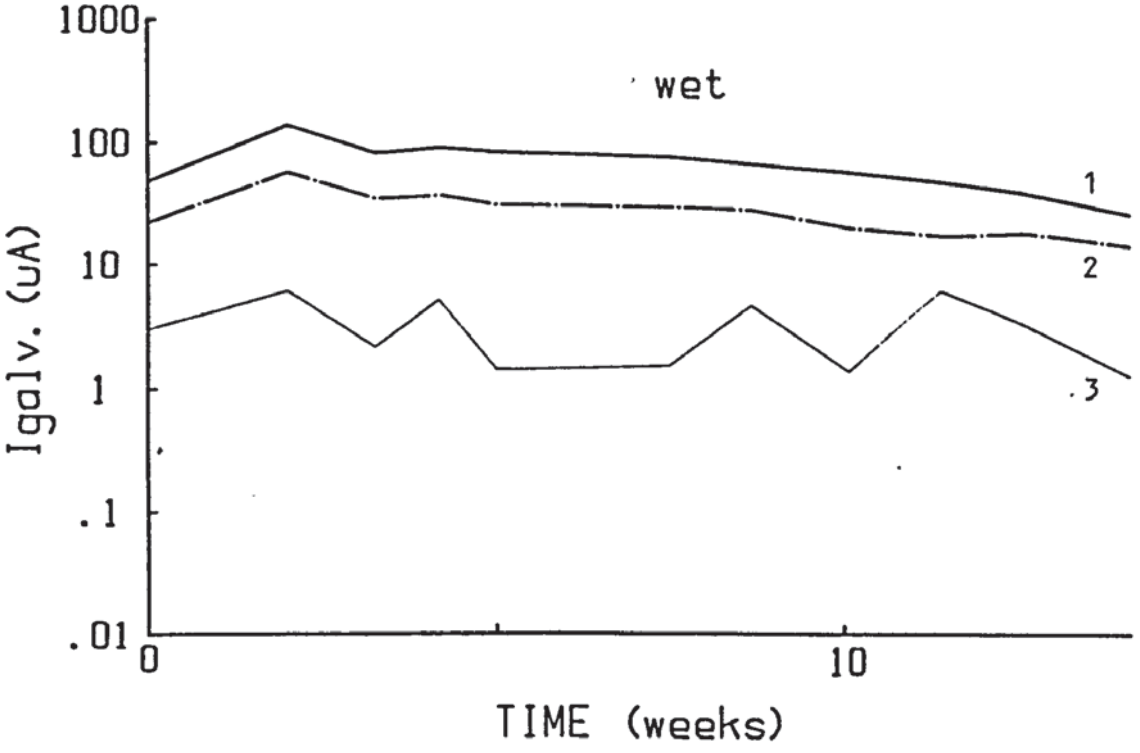

FIGURE 4.14 a

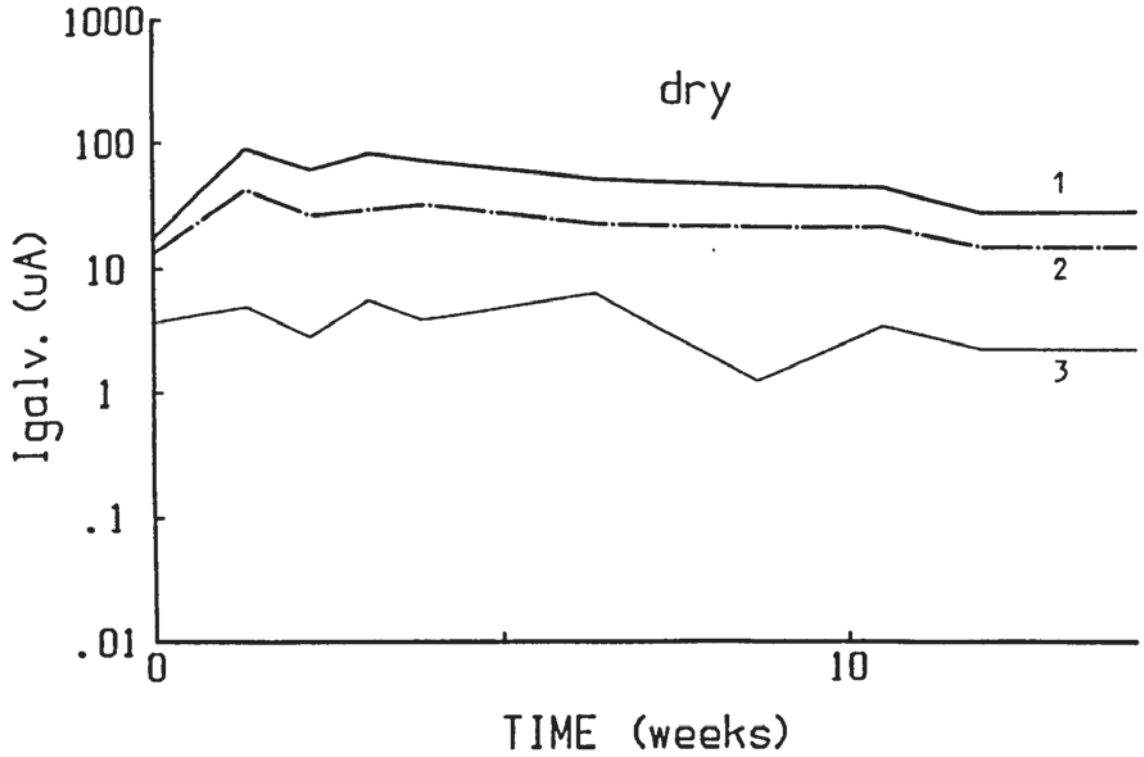

FIGURE 4.14 b

FIGURE 4.14 Repair system four (zinc rich primer and acrylic bonding agent); i_{galv}/time traces for wet (a) and dry (b) conditions for the segment combinations; 1 = 1% vs repair+ 0.1% + 0.0%, 2 = 1% vs 0.1% + 0.0%, 3 = 0.1% vs 0.0%

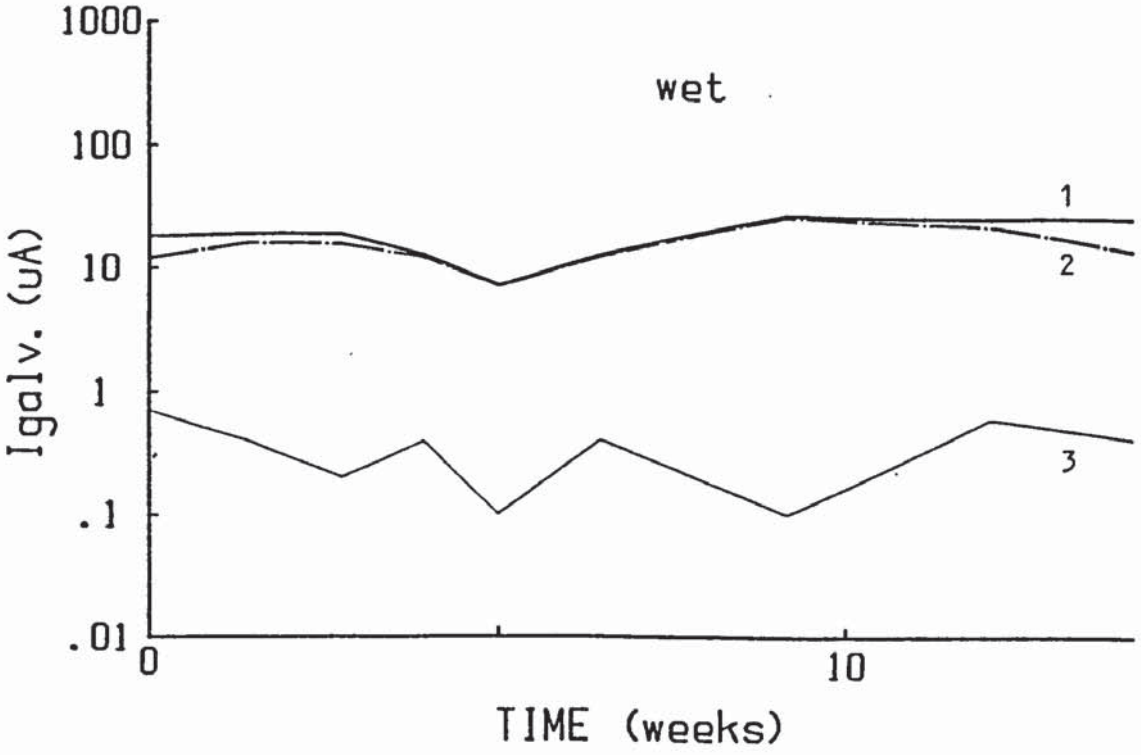

FIGURE 4.15 a

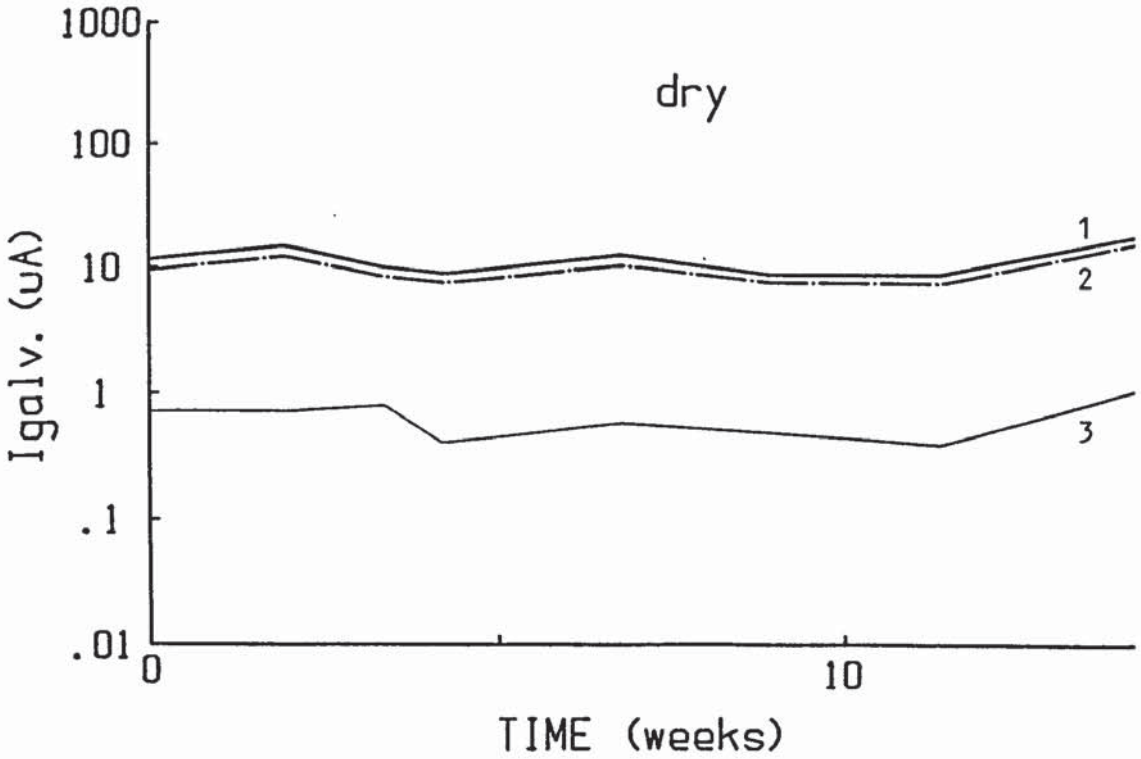

FIGURE 4.15b

FIGURE 4.15 Repair system five (OPC slurry + insulating epoxy) i_{galv}/time traces for wet (a) and dry (b) conditions; 1 = 1% vs repair + 0.1% + 0.0%, 2 = 1% vs 0.1% + 0.0%, 3 = 0.1% vs 0.0%

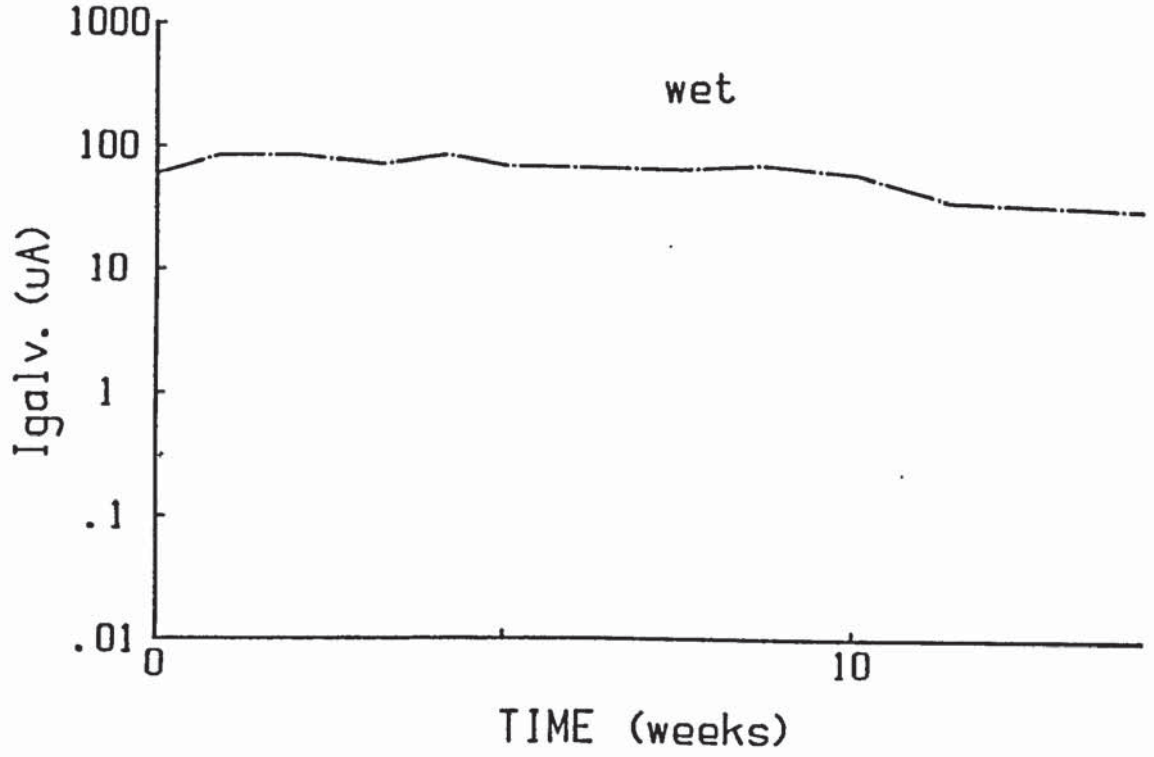

FIGURE 4.16 a

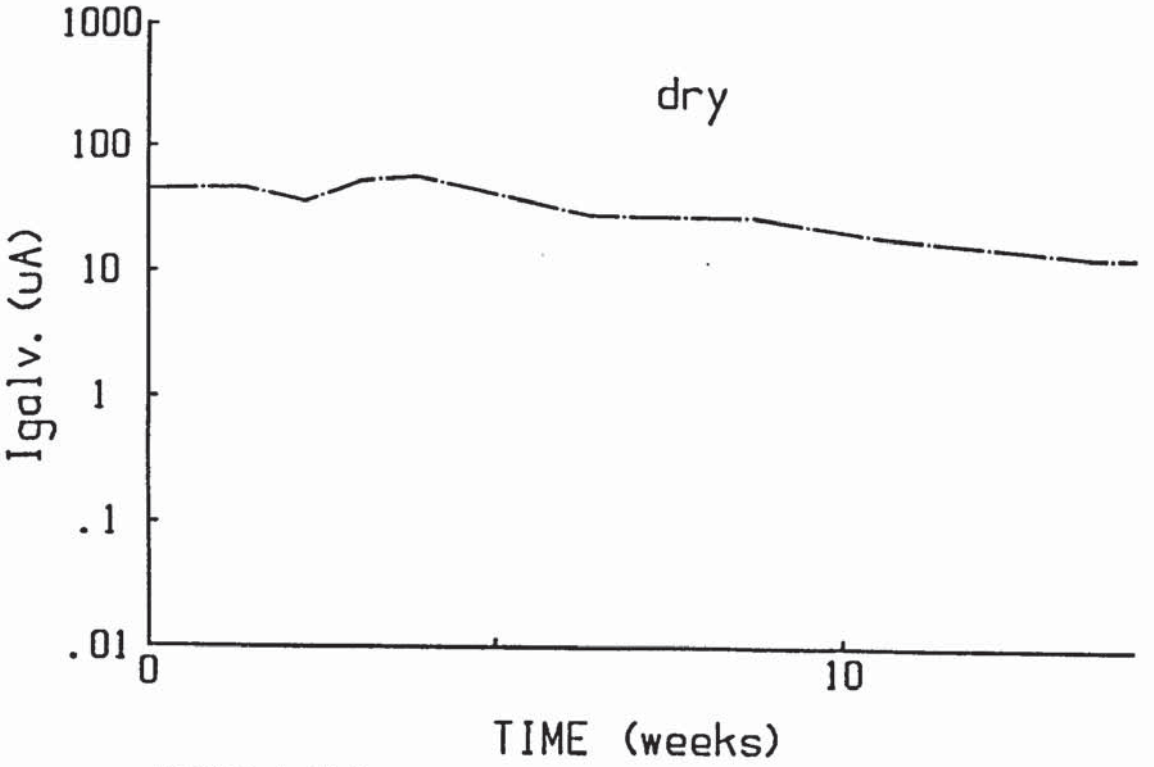

FIGURE 4.16 b

FIGURE 4.16 Repair system one (OPC slurry) i_{galv} (cathodic)/ time traces for wet (a) and dry (b) conditions for the segment combination repair vs 1% + 0.1% + 0.0%

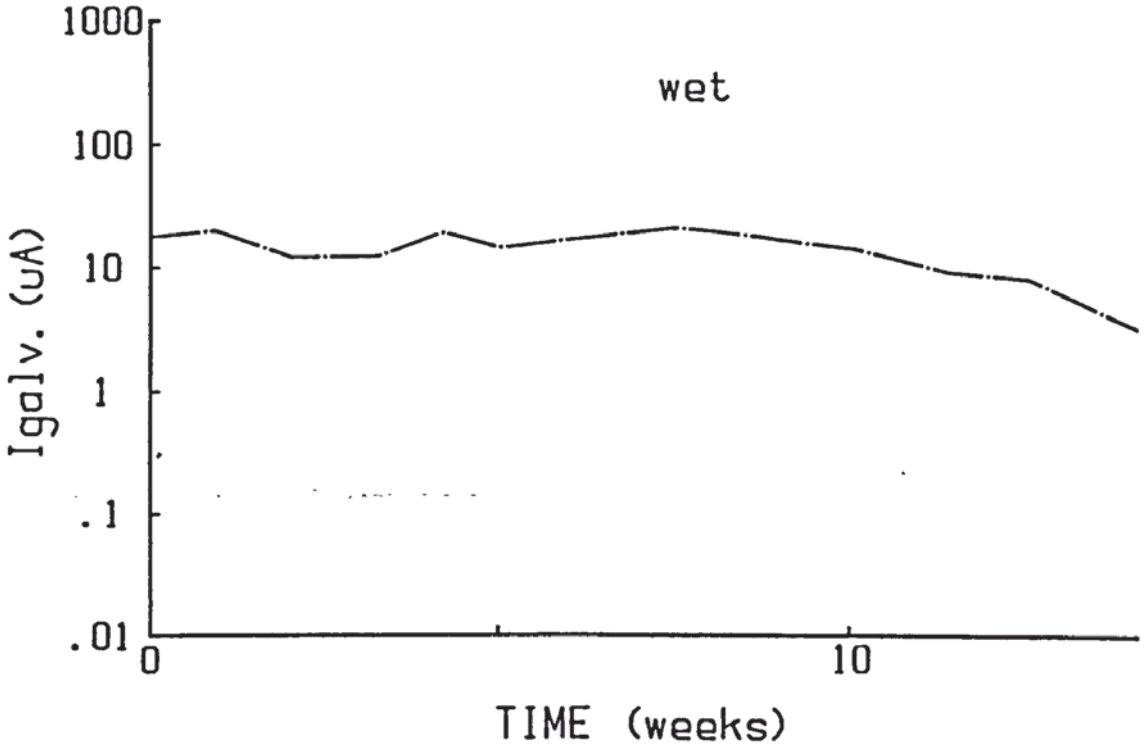

FIGURE 4.17 a

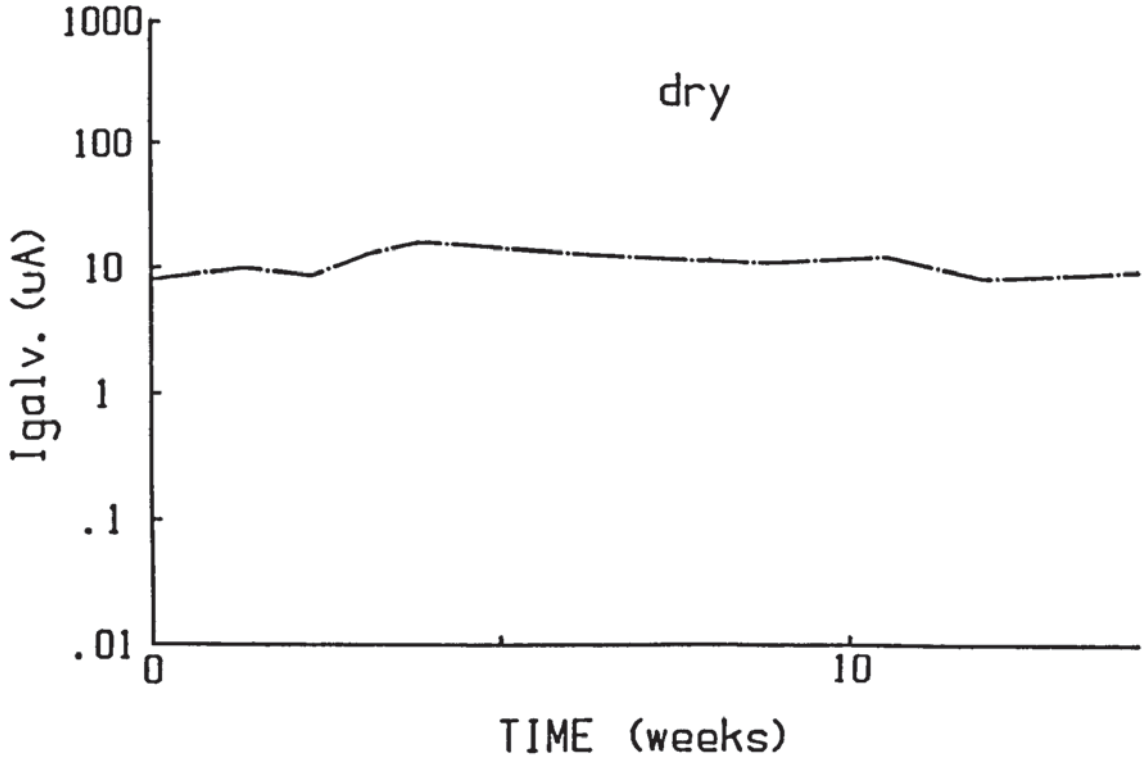

FIGURE 4.17 b

FIGURE 4.17 Repair system two (OPC slurry and acrylic bonding agent) i_{galv} (cathodic)/time traces for the segment combination repair vs 1% + 0.1% + 0.0%

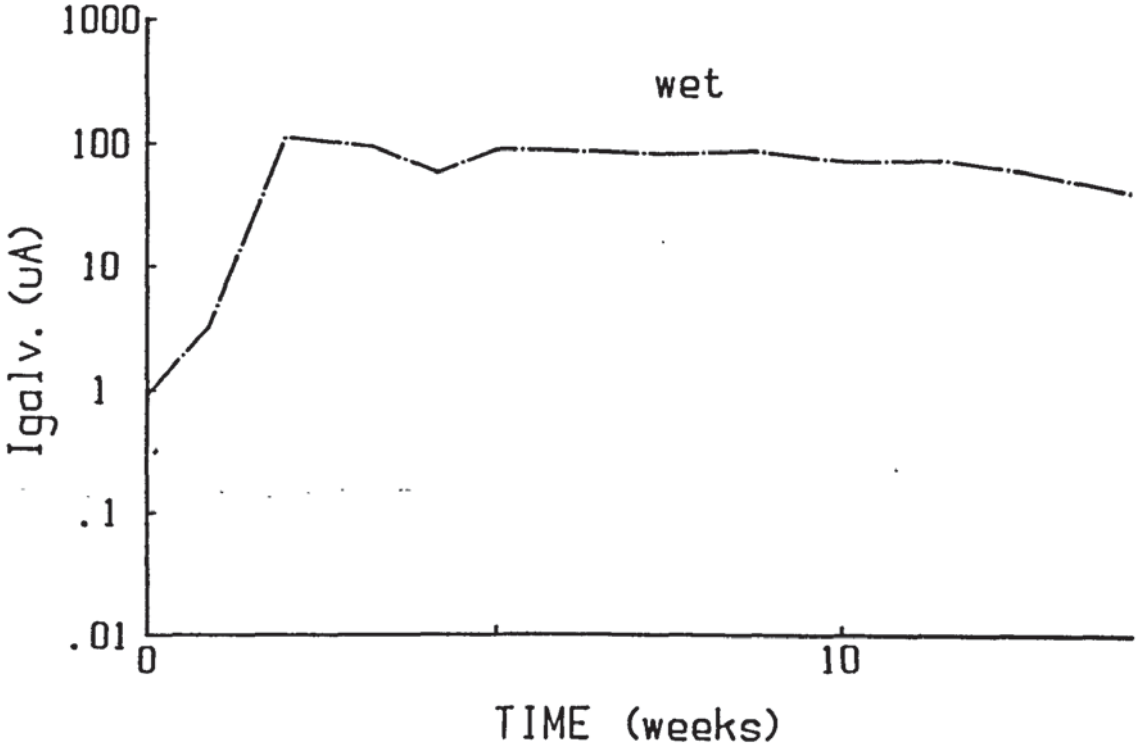

FIGURE 4.18 a

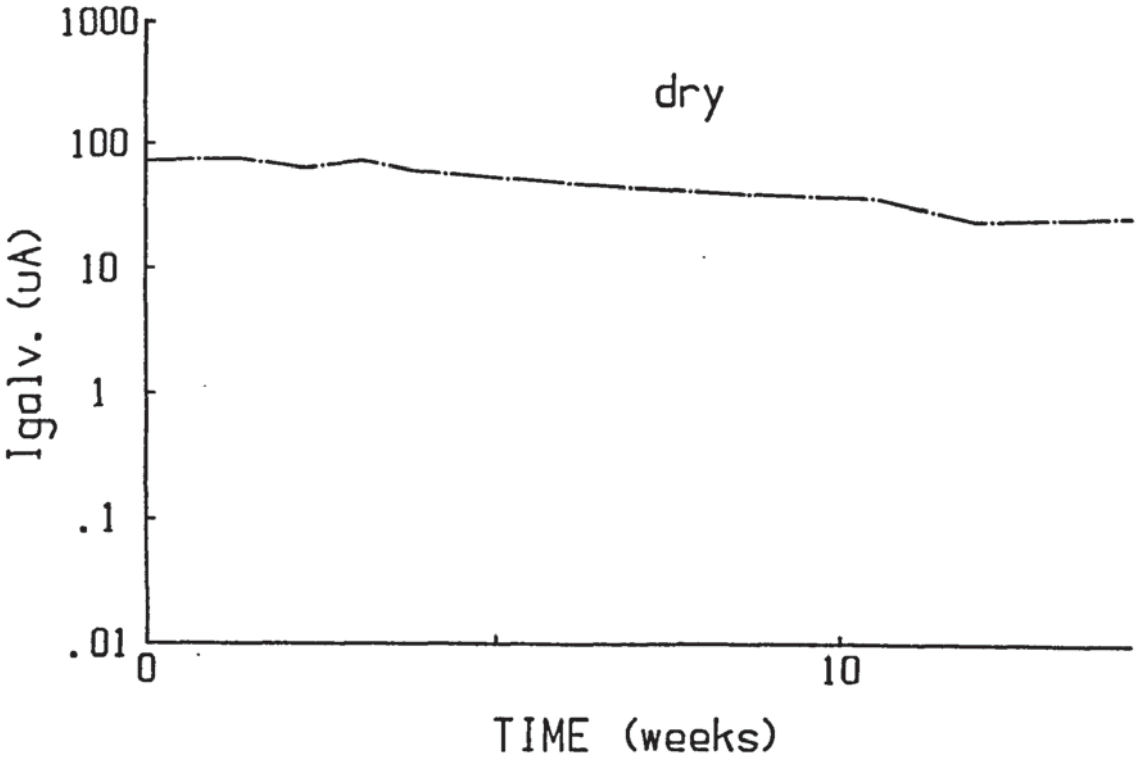

FIGURE 4.18 b

FIGURE 4.18 Repair system three (zinc rich expoxy primer) i_{galv} (cathodic)/time traces for wet (a) and dry (b) conditions for the segment combination repair vs 1% + 0.1% + 0.0%

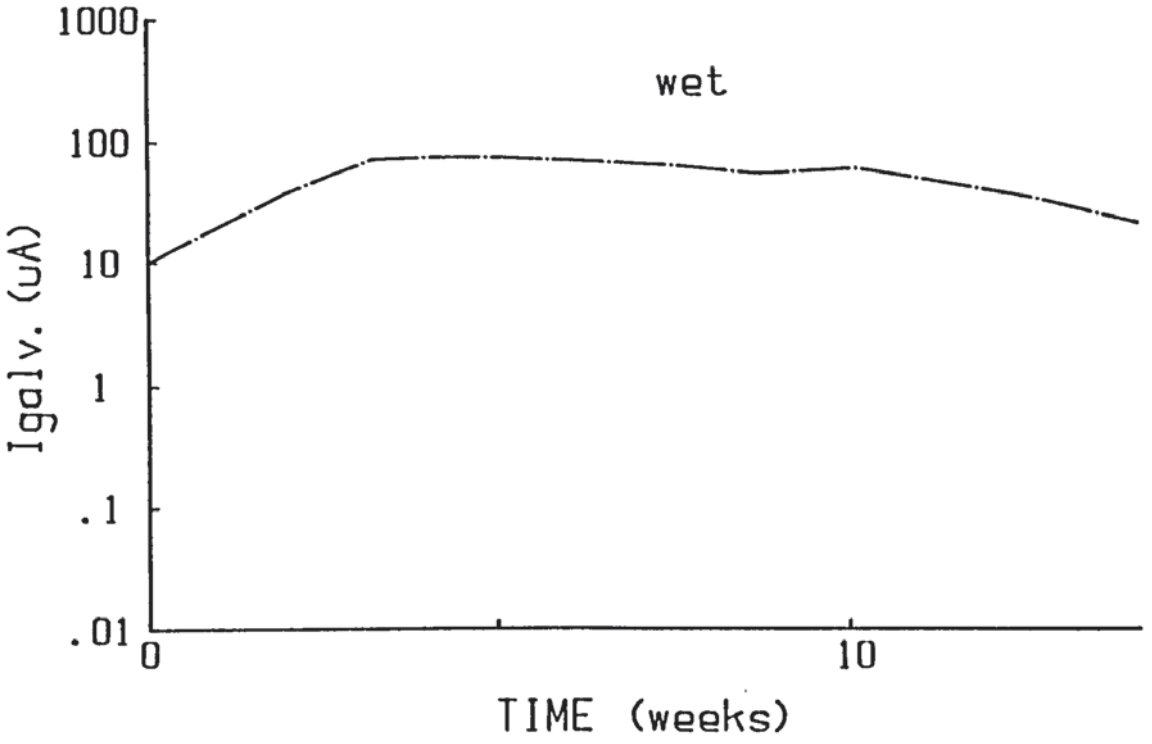

FIGURE 4.19 a

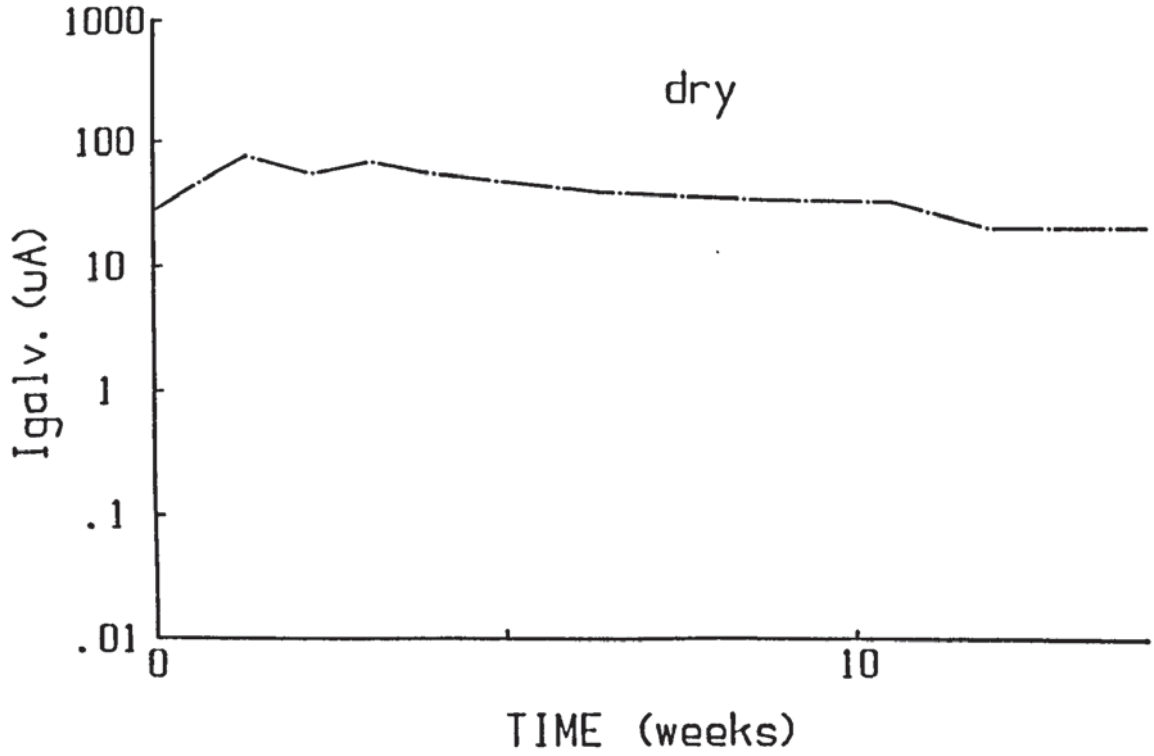

FIGURE 4.19 b

FIGURE 4.19 Repair system four (zinc rich epoxy primer + acrylic bonding agent) i_{galv} (cathodic)/time traces for wet (a) and dry (b) conditions for the segment combination repair vs 1% + 0.1% + 0.0%

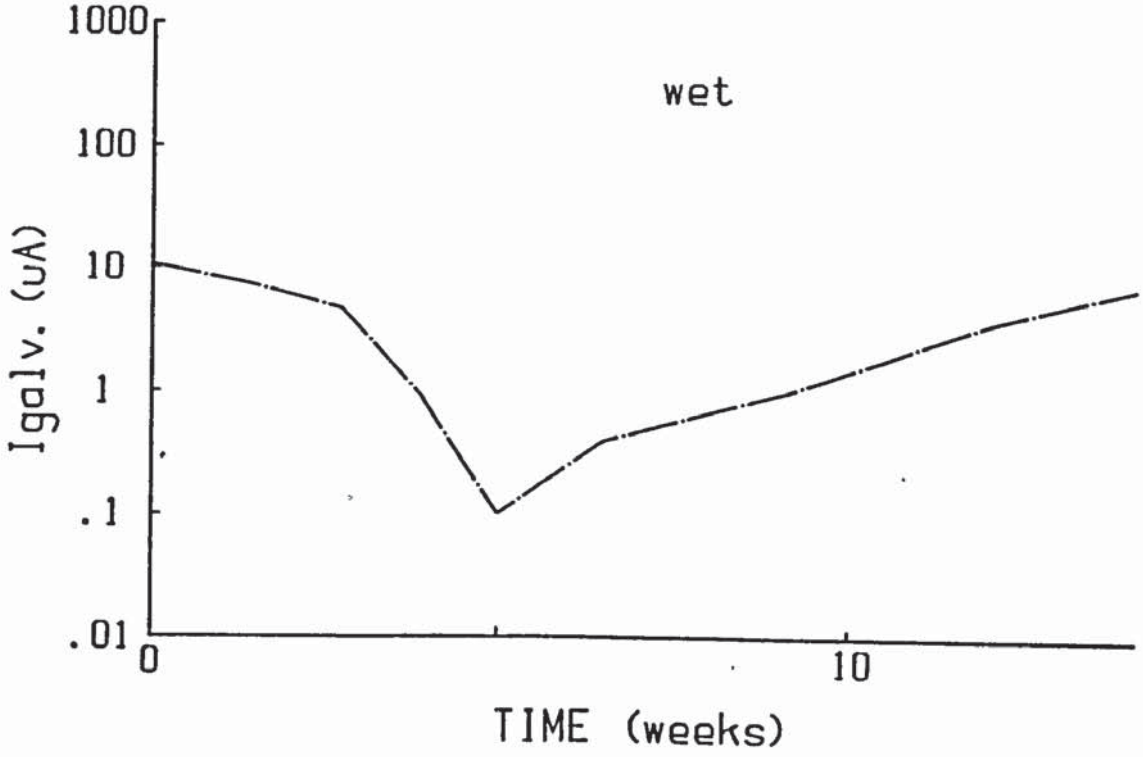

FIGURE 4.20 a

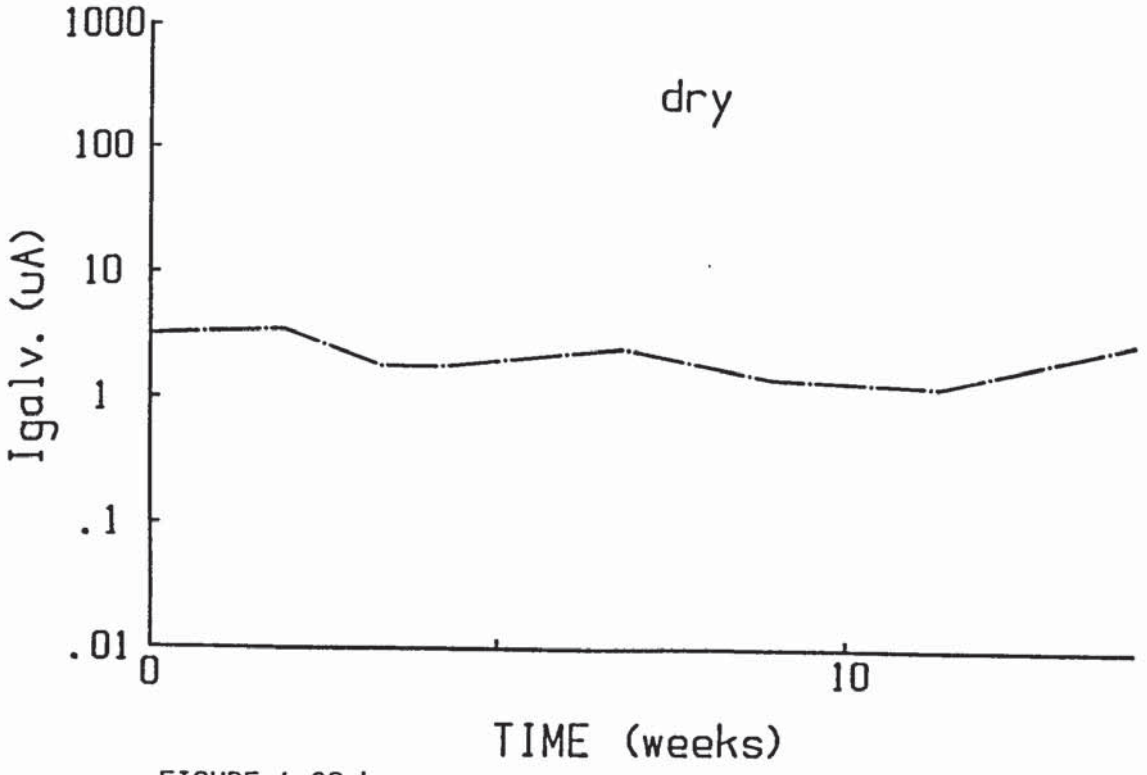

FIGURE 4.20 b

FIGURE 4.20 Repair system five (OPC slurry + insulating epoxy) i_{galv} (cathodic)/time traces for wet (a) and dry (b) conditions for the segment combination repair vs 1% + 0.1% + 0.0%

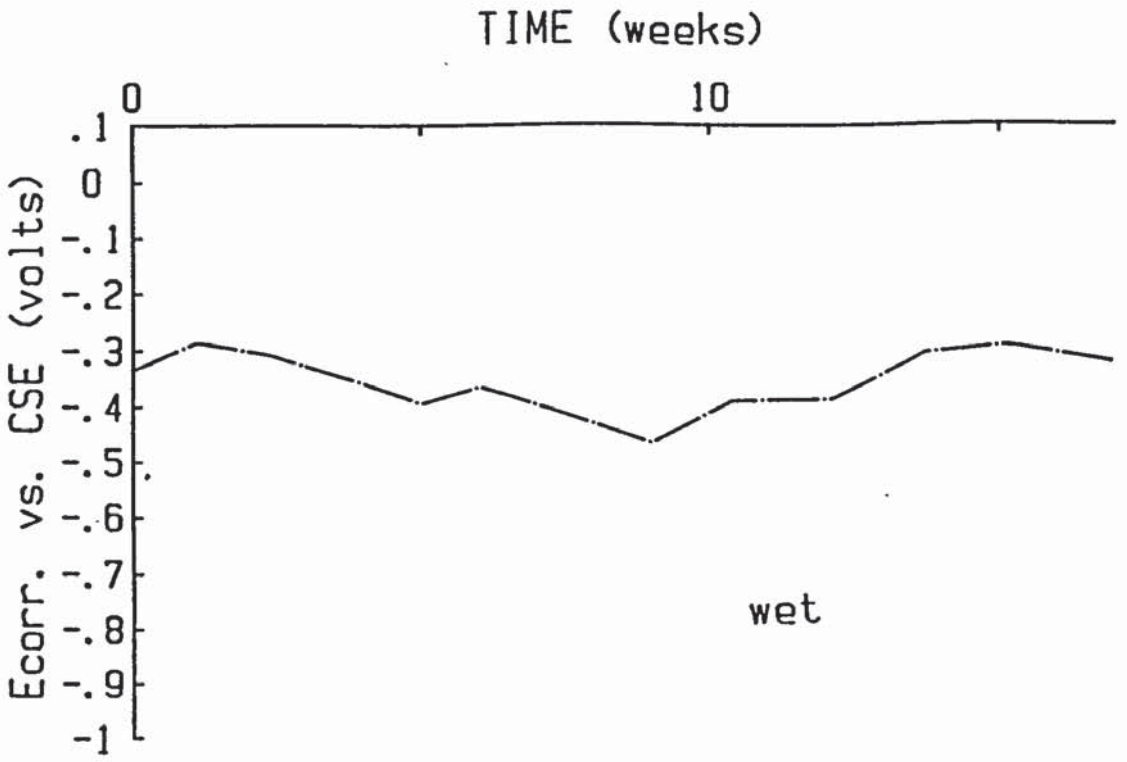

FIGURE 4.21 a

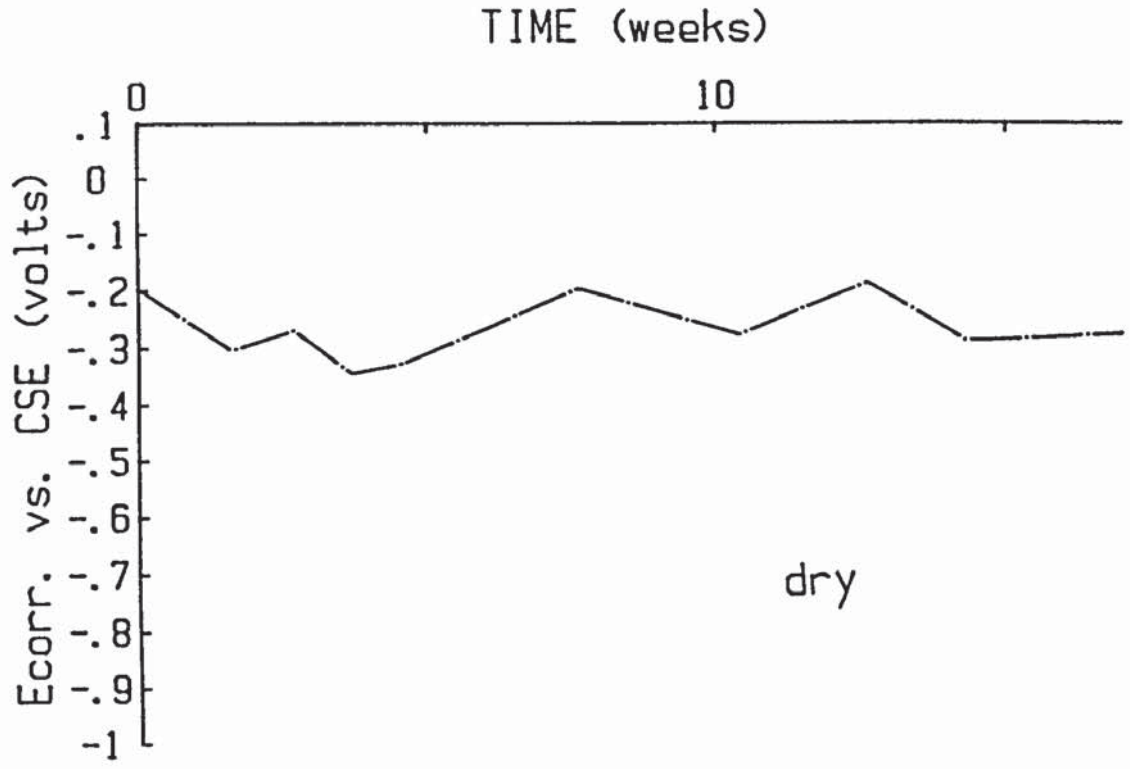

FIGURE 4.21 b

FIGURE 4.21 Repair system one (OPC slurry) E_{corr}/time traces for repaired segment in wet (a) and dry (b) conditions

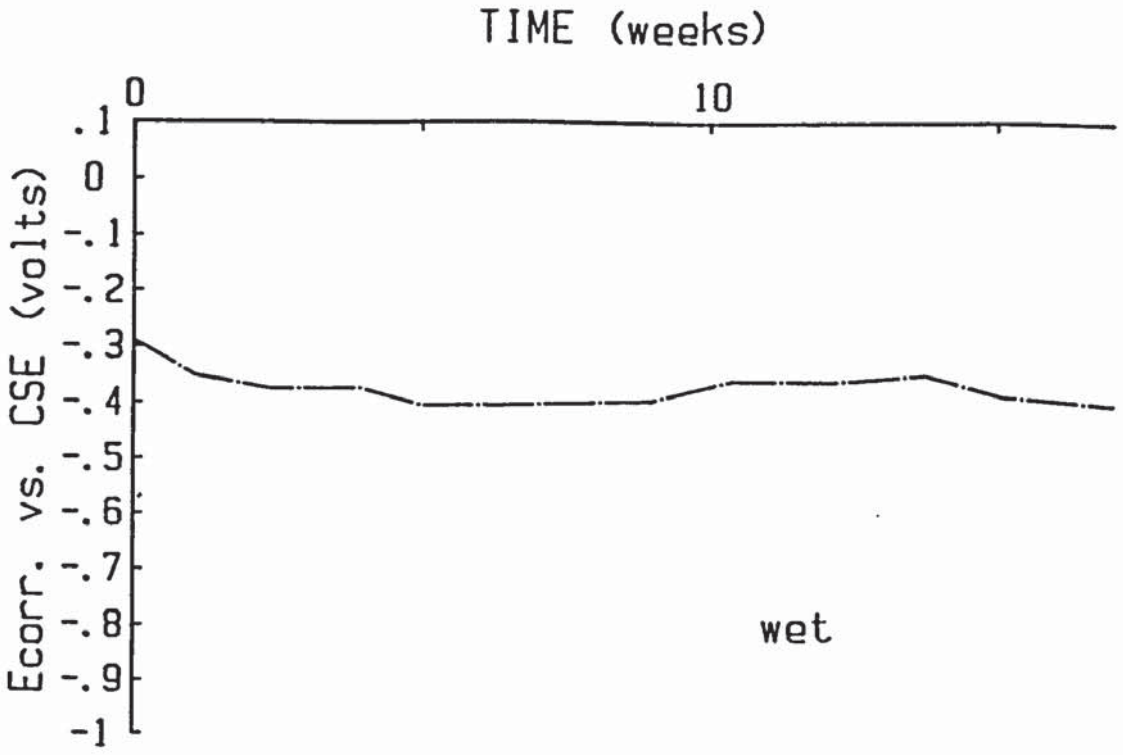

FIGURE 4.22 a

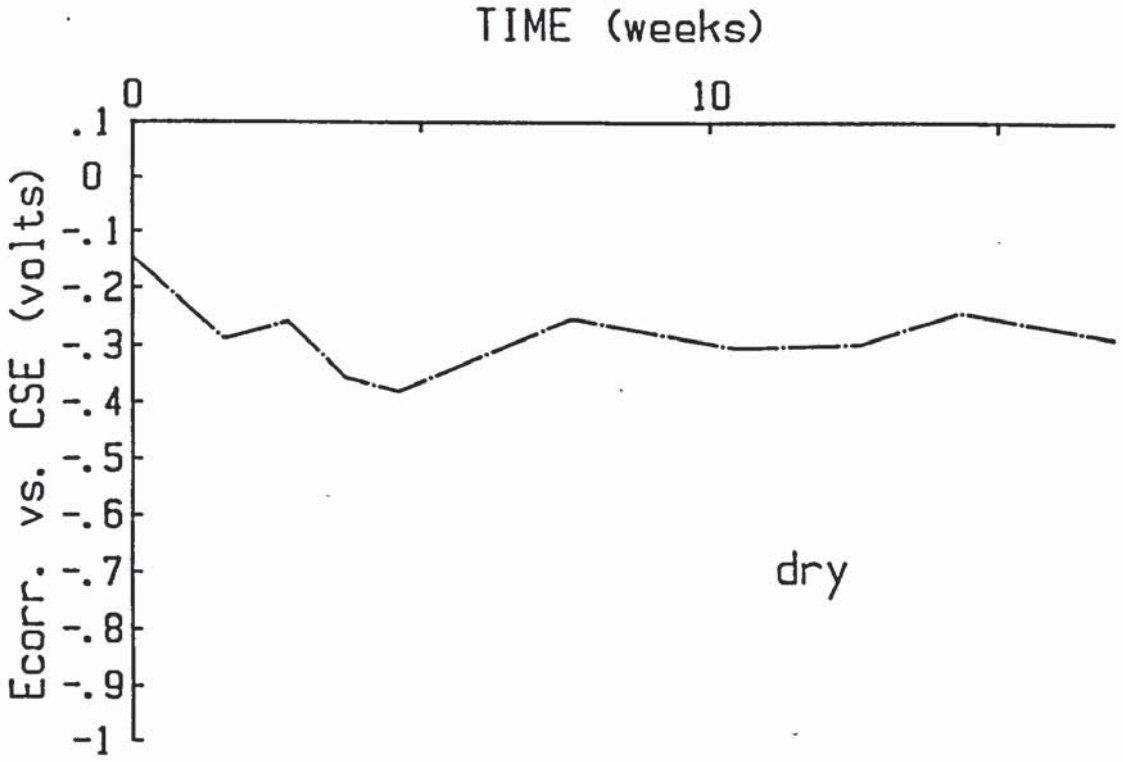

FIGURE 4.22 b

FIGURE 4.22 Repair system two (OPC slurry + acrylic bonding agent) E_{corr}/time traces for repaired segment in wet (a) and dry (b) conditions

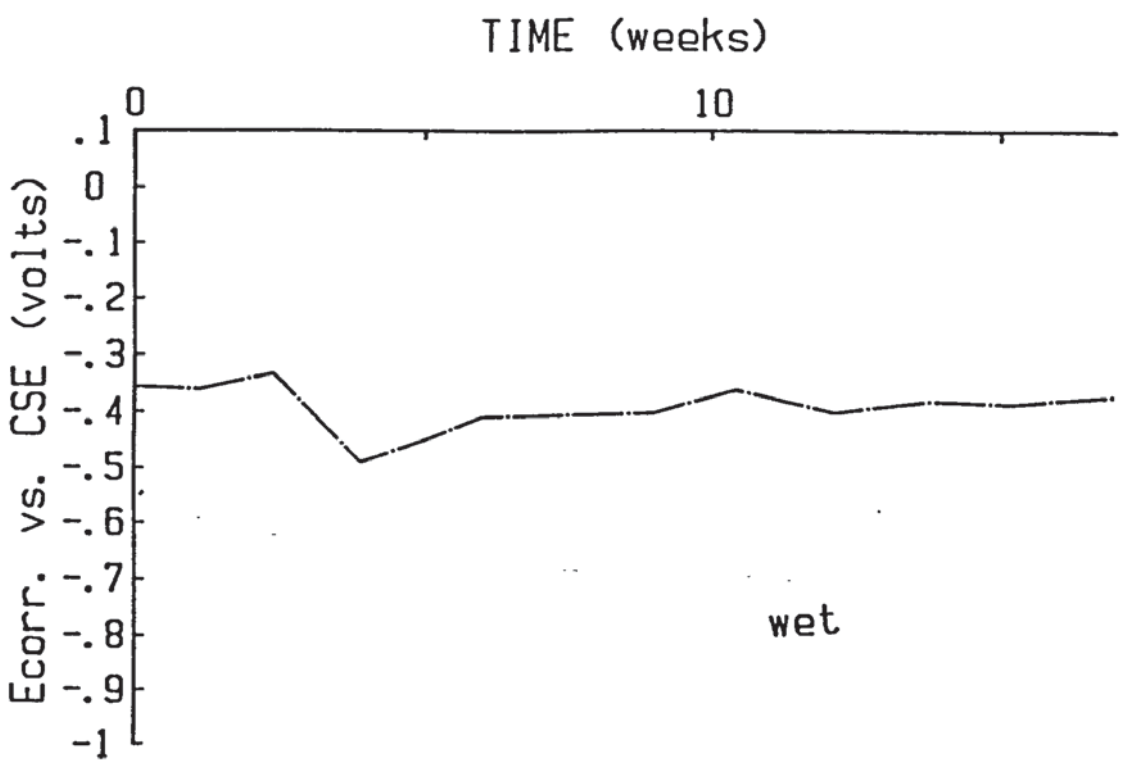

FIGURE 4.23 a

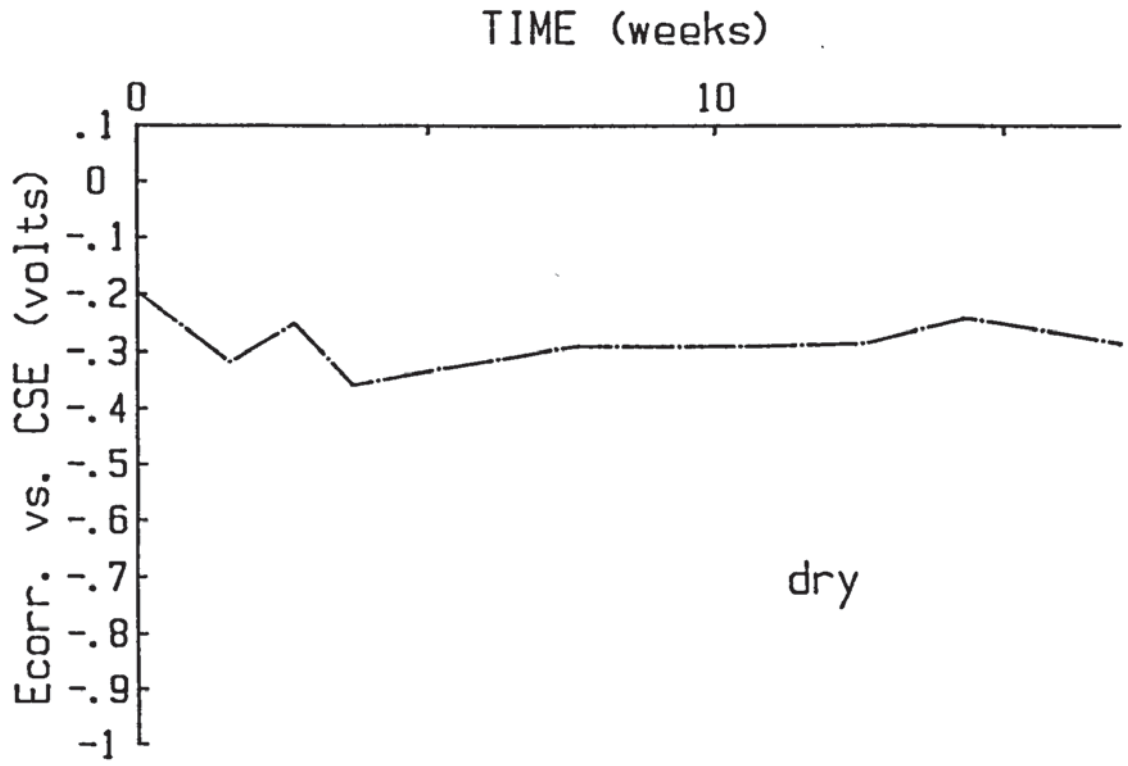

FIGURE 4.23 b

FIGURE 4.23 Repair system three (zinc rich primer) E_{corr}/ time traces for repaired segment in wet (a) and dry (b) conditions

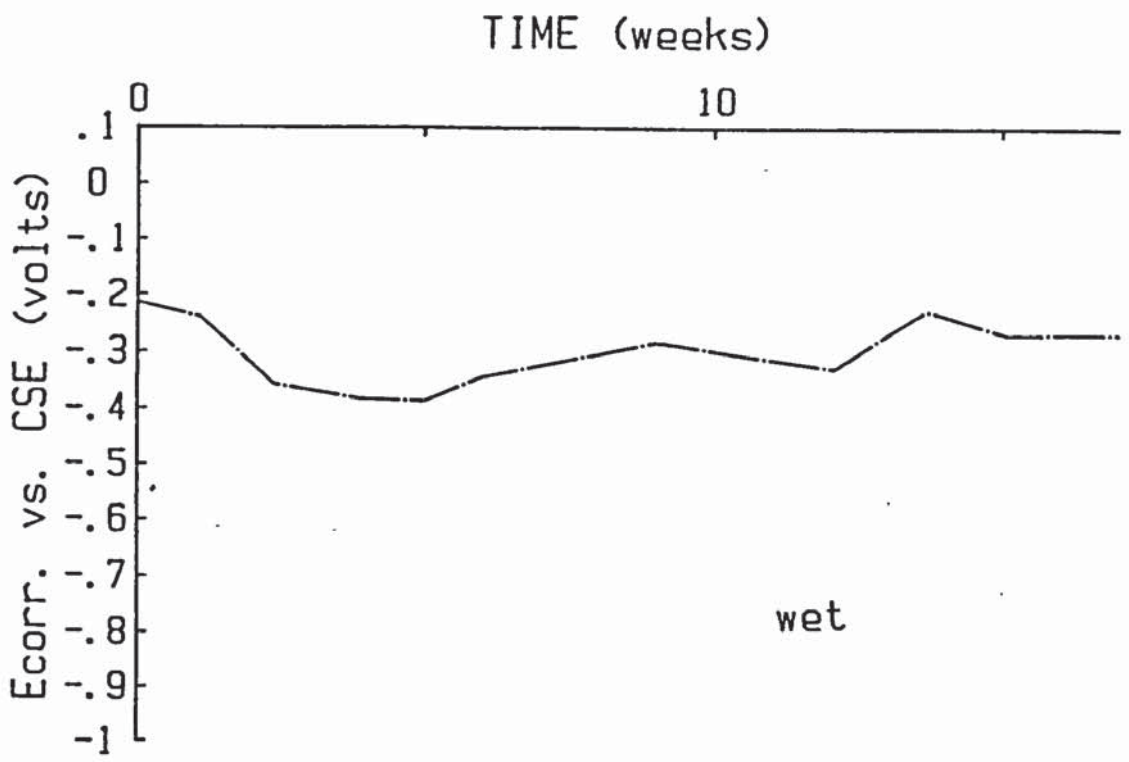

FIGURE 4.24 a

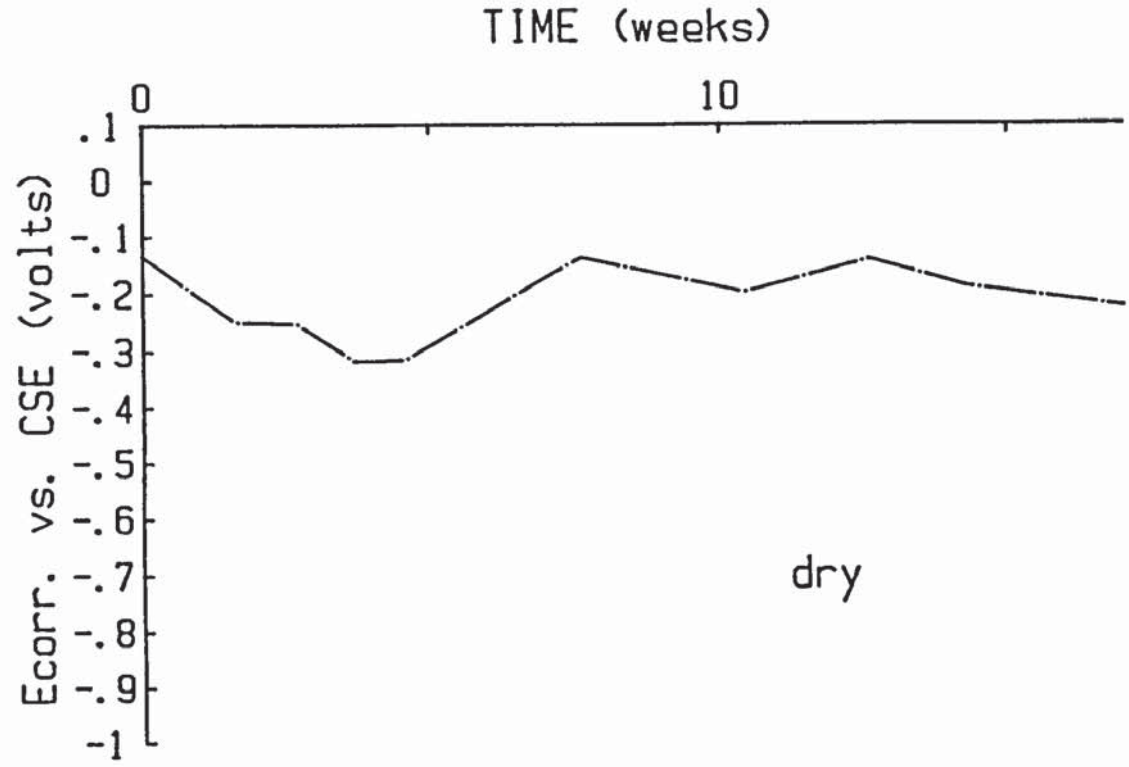

FIGURE 4.24 b

FIGURE 4.24 Repair system four (zinc rich primer + acrylic bonding agent) E_{corr}/time traces for repaired segment in wet (a) and dry (b) conditions

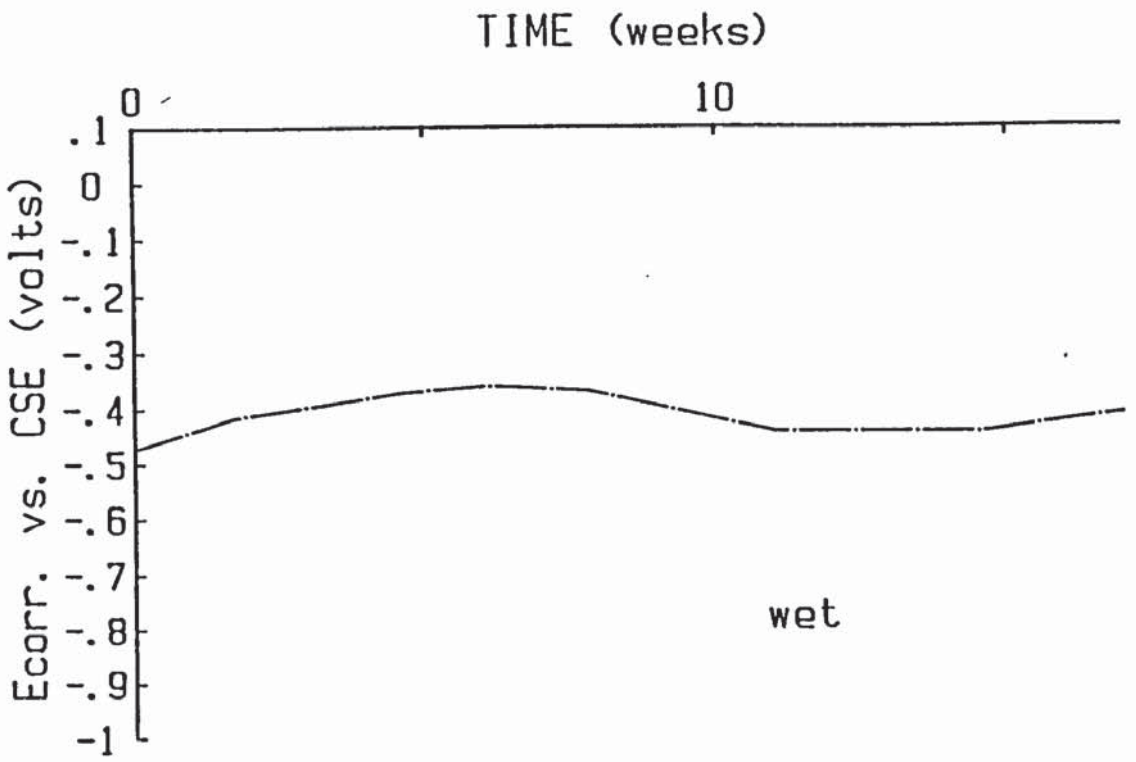

FIGURE 4.25 a

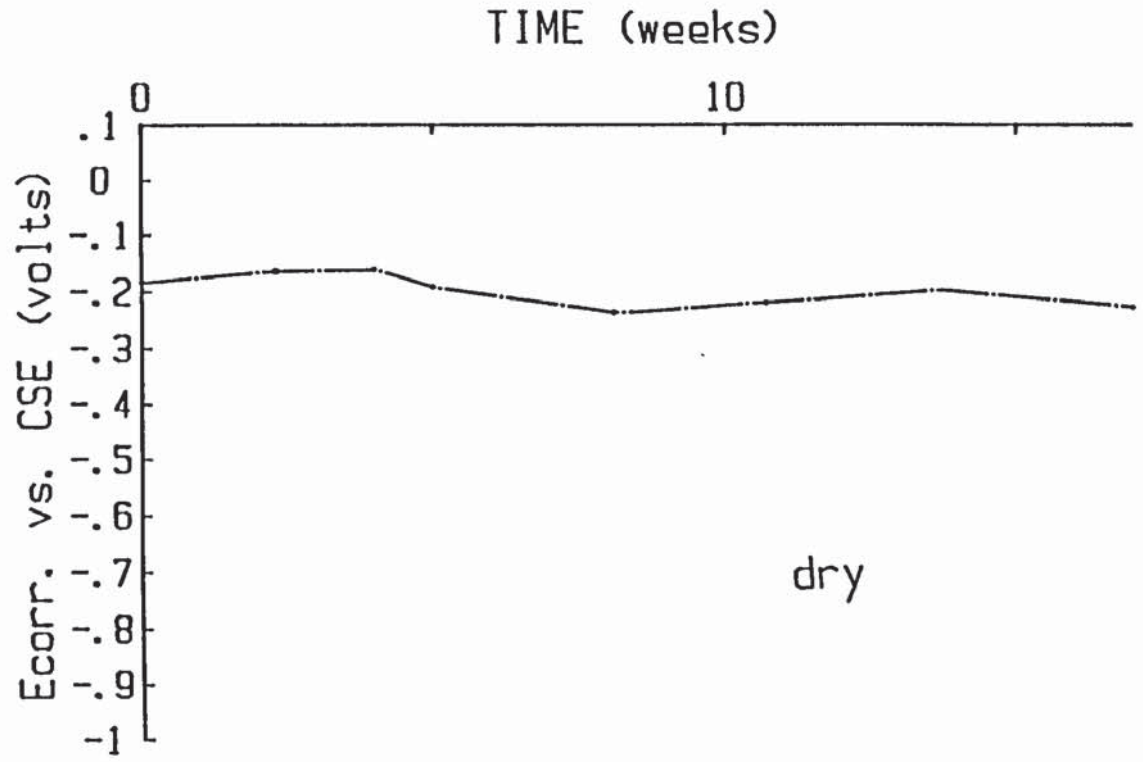

FIGURE 4.25 b

FIGURE 4.25 Repair system five (OPC slurry + insulating epoxy) E_{corr}/time traces for repaired segment in wet (a) and dry (b) conditions

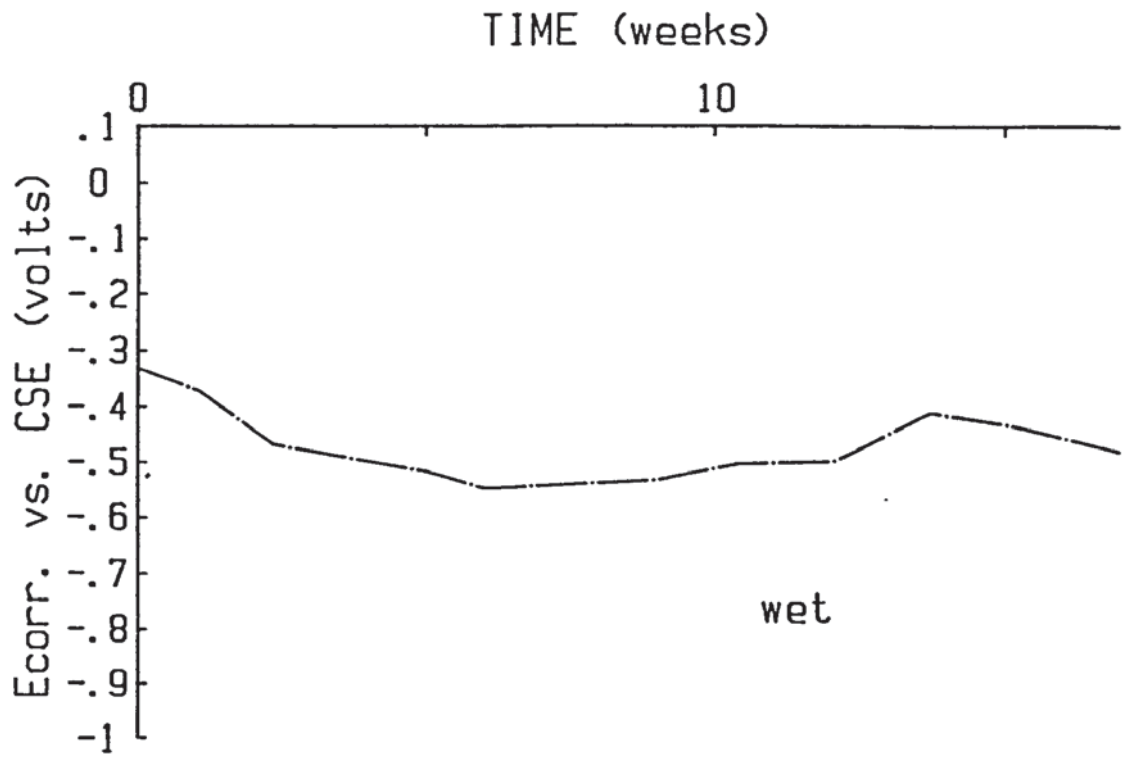

FIGURE 4.26 a

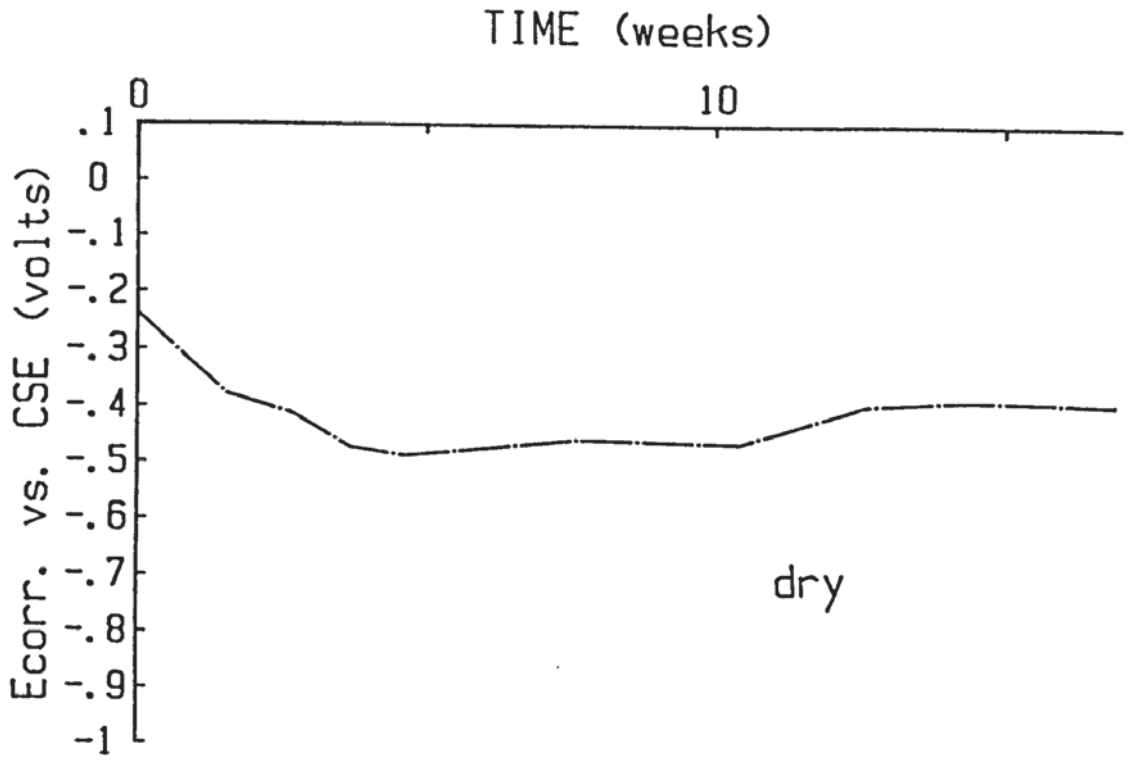

FIGURE 4.26 b

FIGURE 4.26 Repair system one (OPC slurry) E_{corr}/time traces for 1% chloride segments in wet (a) and dry (b) conditions

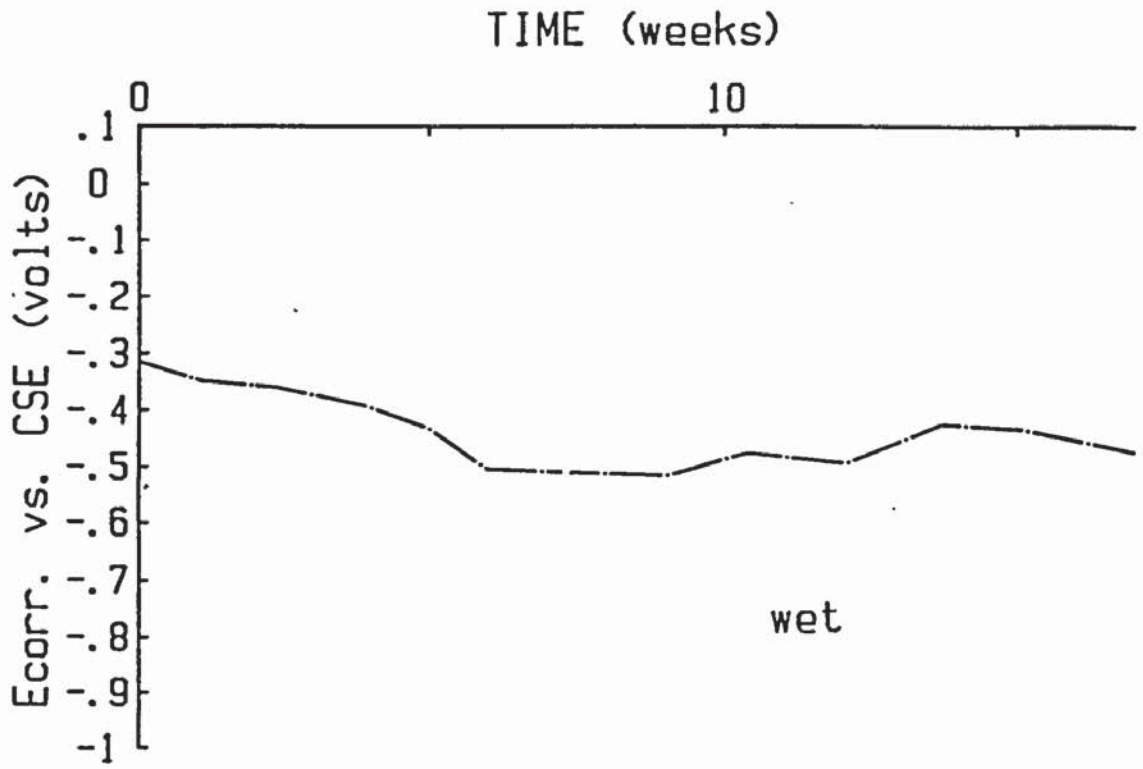

FIGURE 4.27 a

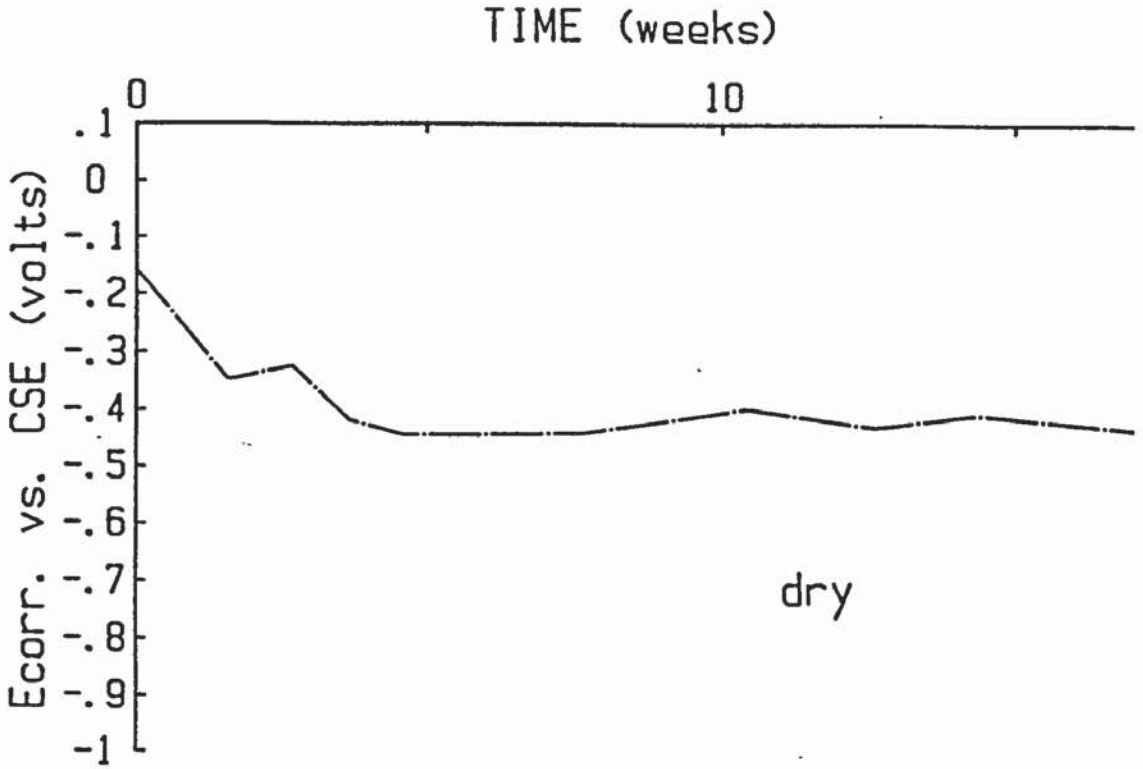

FIGURE 4.27 b

FIGURE 4.27 Repair system two (OPC slurry + acrylic bonding agent) E_{corr}/time traces for 1% chloride segments in wet (a) and dry (b) conditions

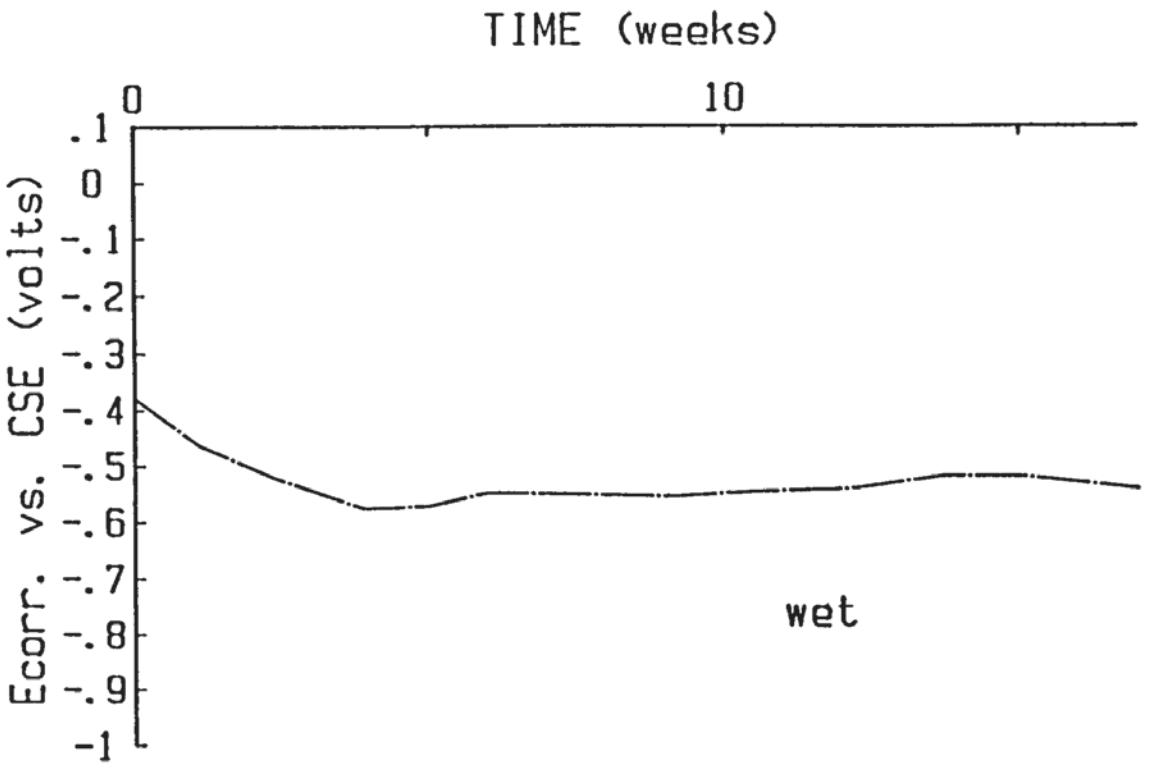

FIGURE 4.28 a

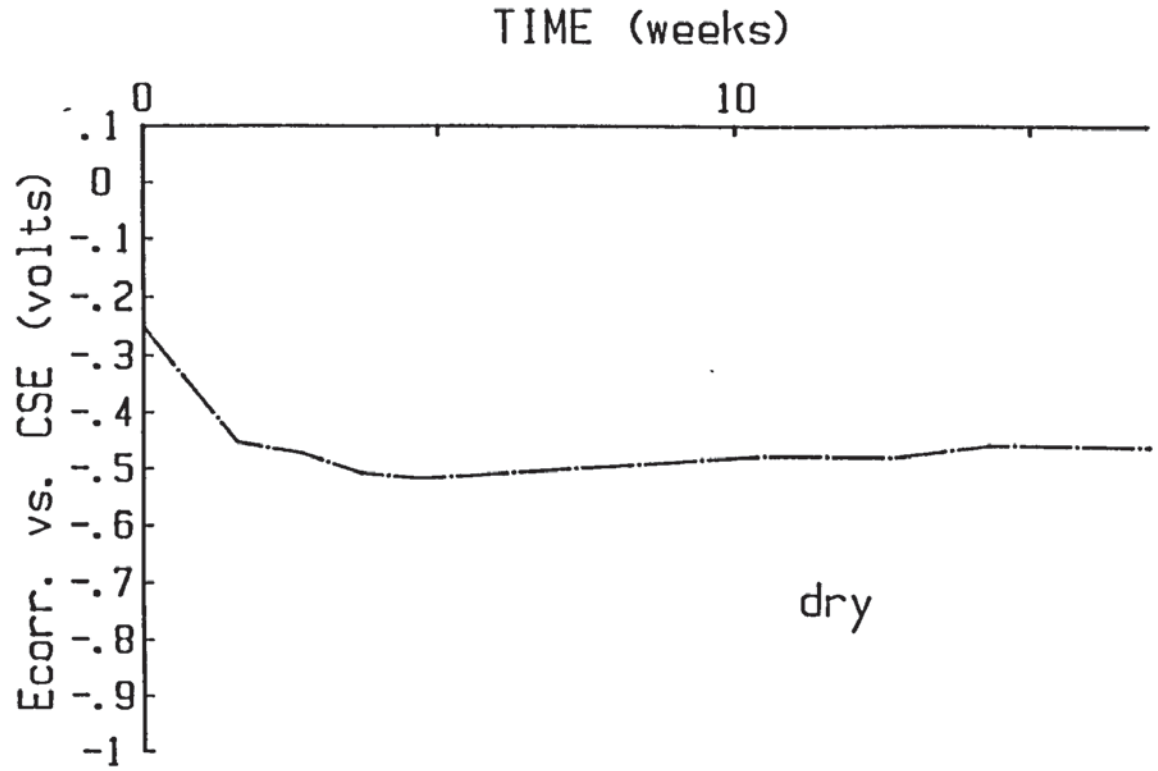

FIGURE 4.28 b

FIGURE 4.28 Repair system three (zinc rich epoxy primer) E_{corr}/time traces for 1% chloride segments in wet (a) and dry (b) conditions.

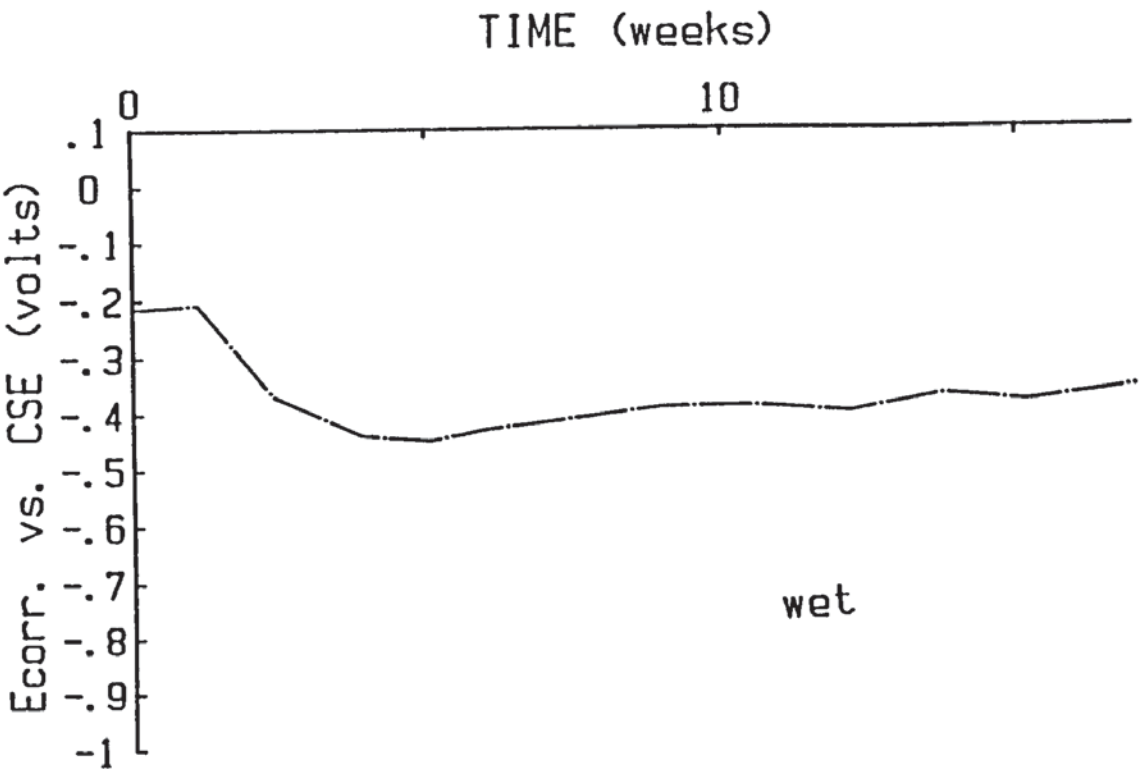

FIGURE 4.29 a

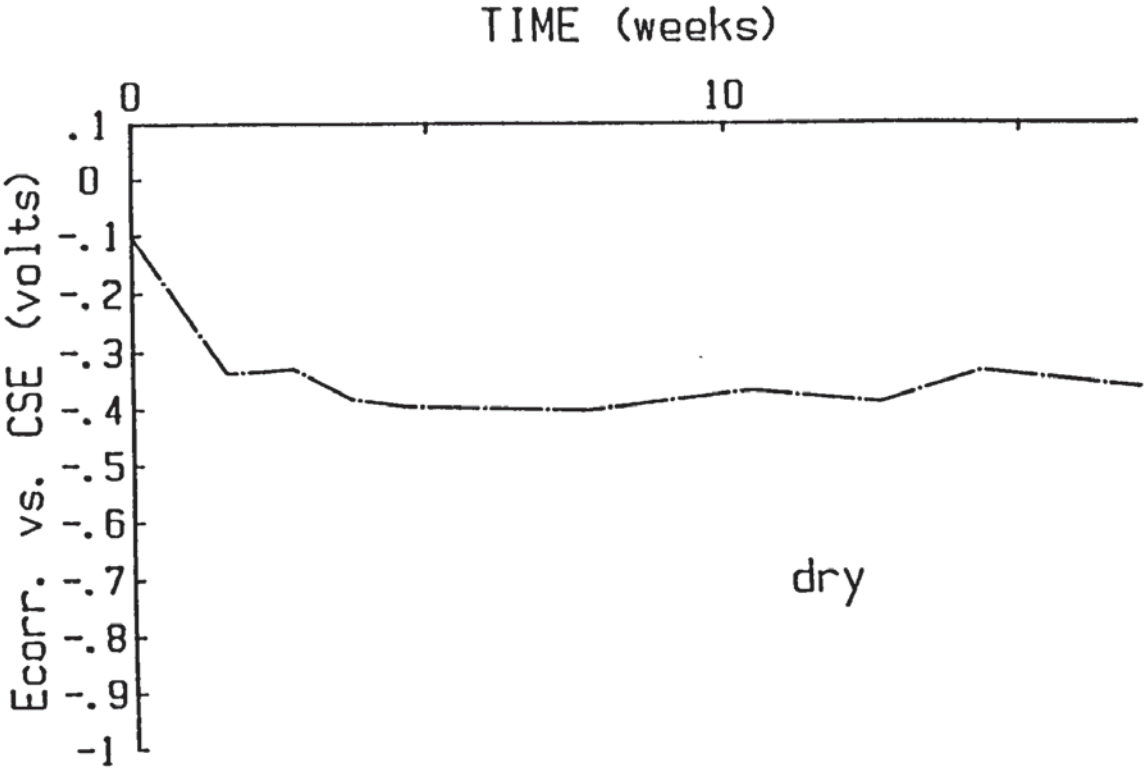

FIGURE 4.29 b

FIGURE 4.29 Repair system four (zinc rich epoxy primer and acrylic bonding agent) E_{corr}/time traces for 1% chloride segments in wet (a) and dry (b) conditions

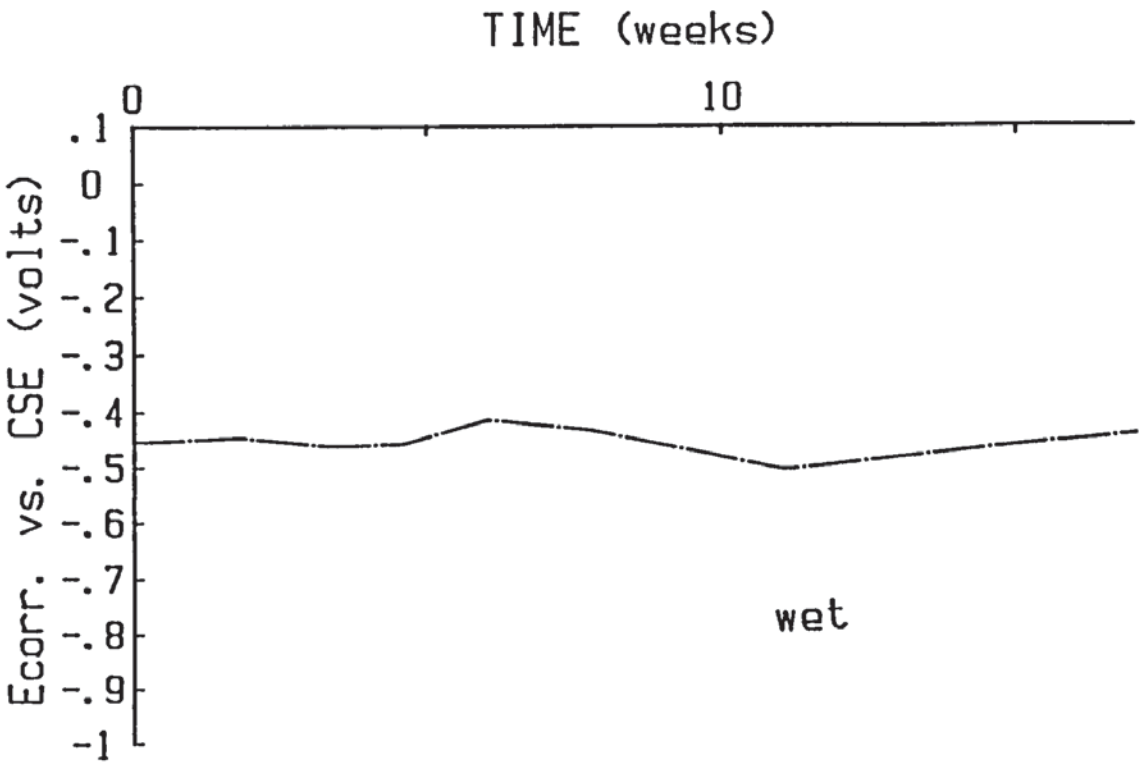

FIGURE 4.30 a

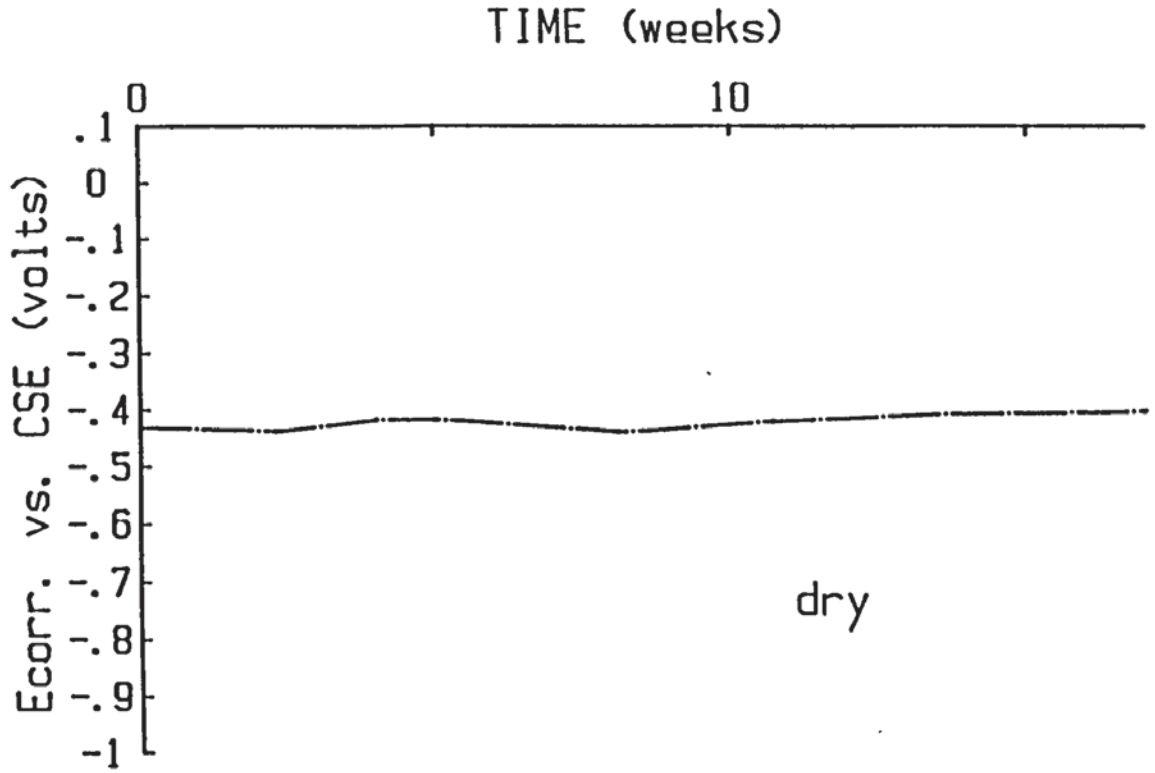

FIGURE 4.30 b

FIGURE 4.30 Repair system five (OPC slurry + insulating epoxy) E_{corr}/time traces for 1% chloride segments in wet (a) and dry (b) conditions

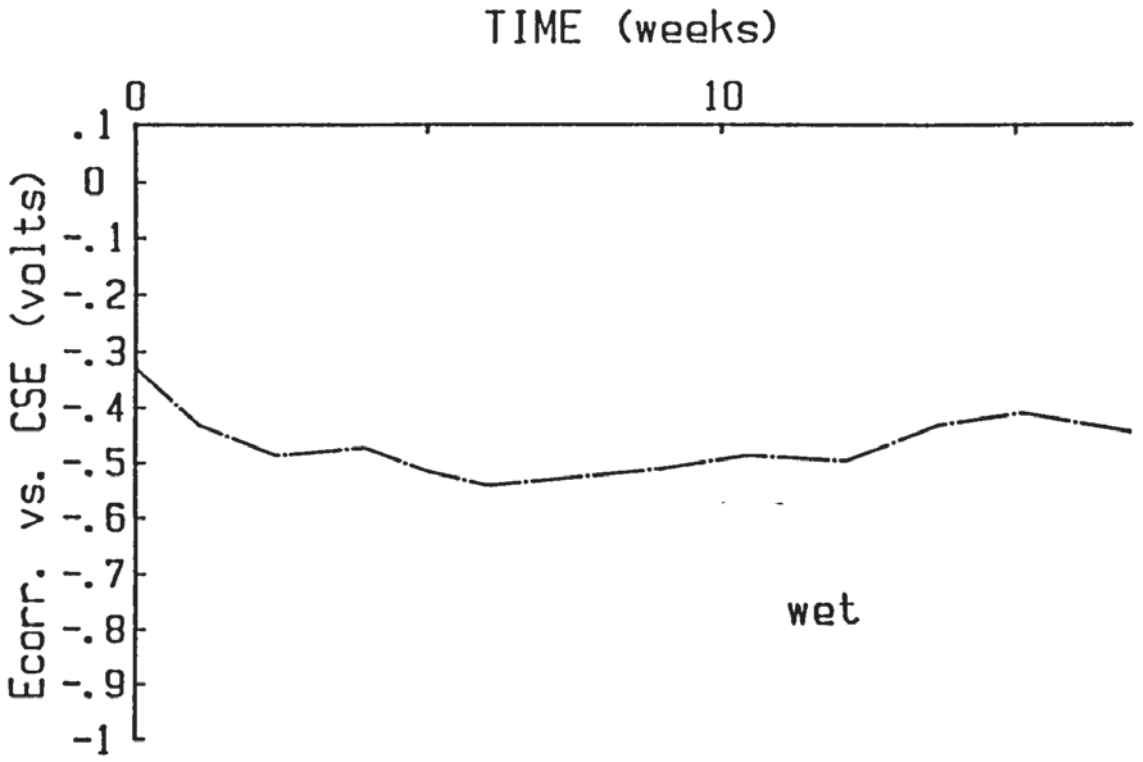

FIGURE 4.31 a

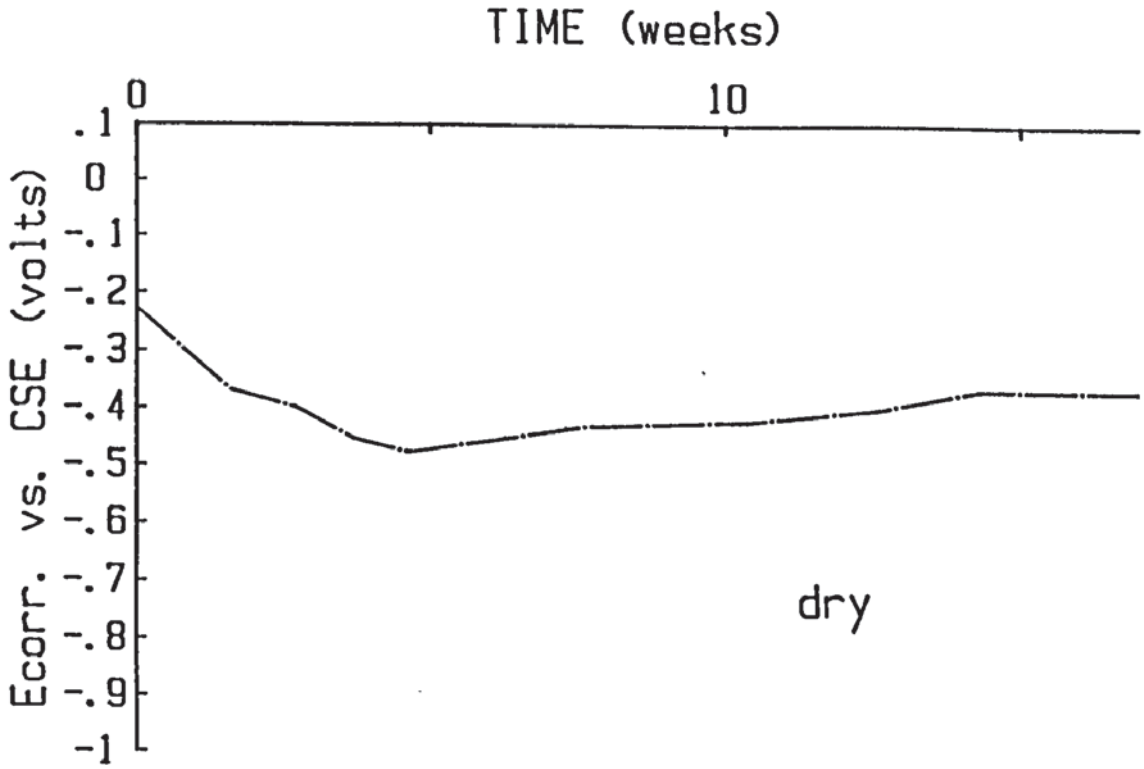

FIGURE 4.31 b

FIGURE 4.31 Repair system one (OPC slurry) E_{corr}/time traces for 0.1% chloride segments in wet (a) and dry (b) conditions

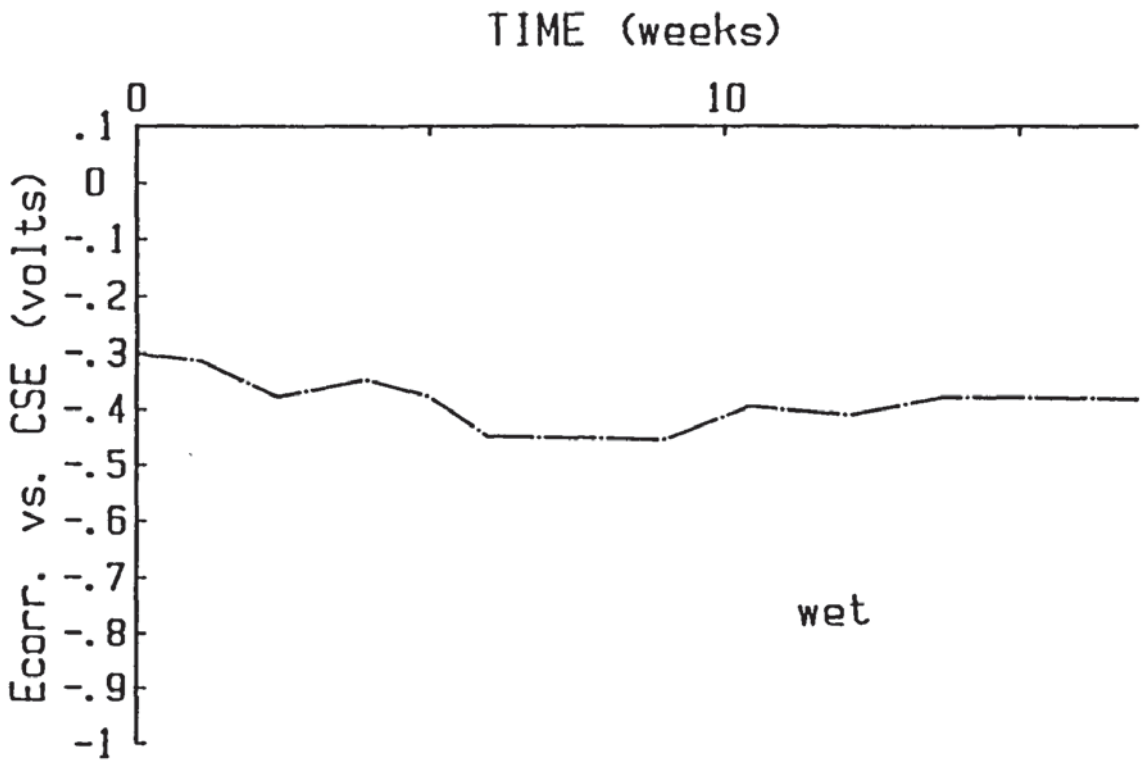

FIGURE 4.32 a

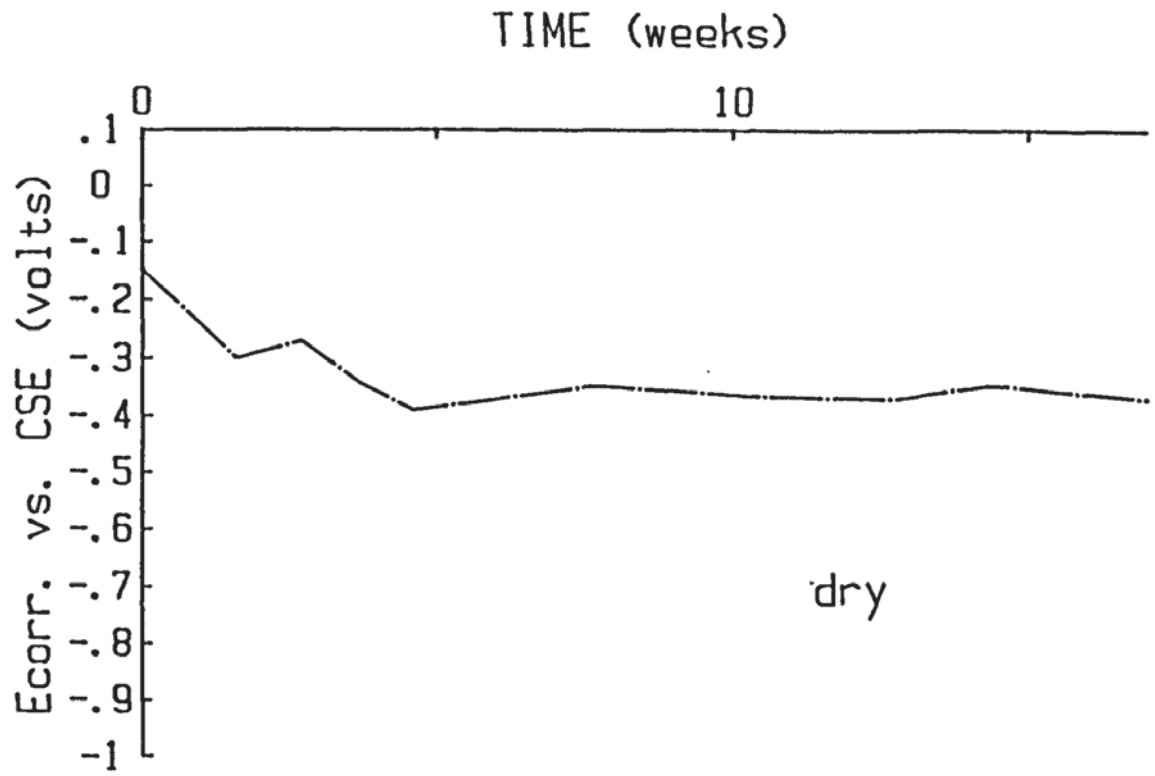

FIGURE 4.32 b

FIGURE 4.32 Repair system two (OPC slurry + acrylic bonding agent) E_{corr}/time traces for 0.1% chloride segments in wet (a) and dry (b) conditions

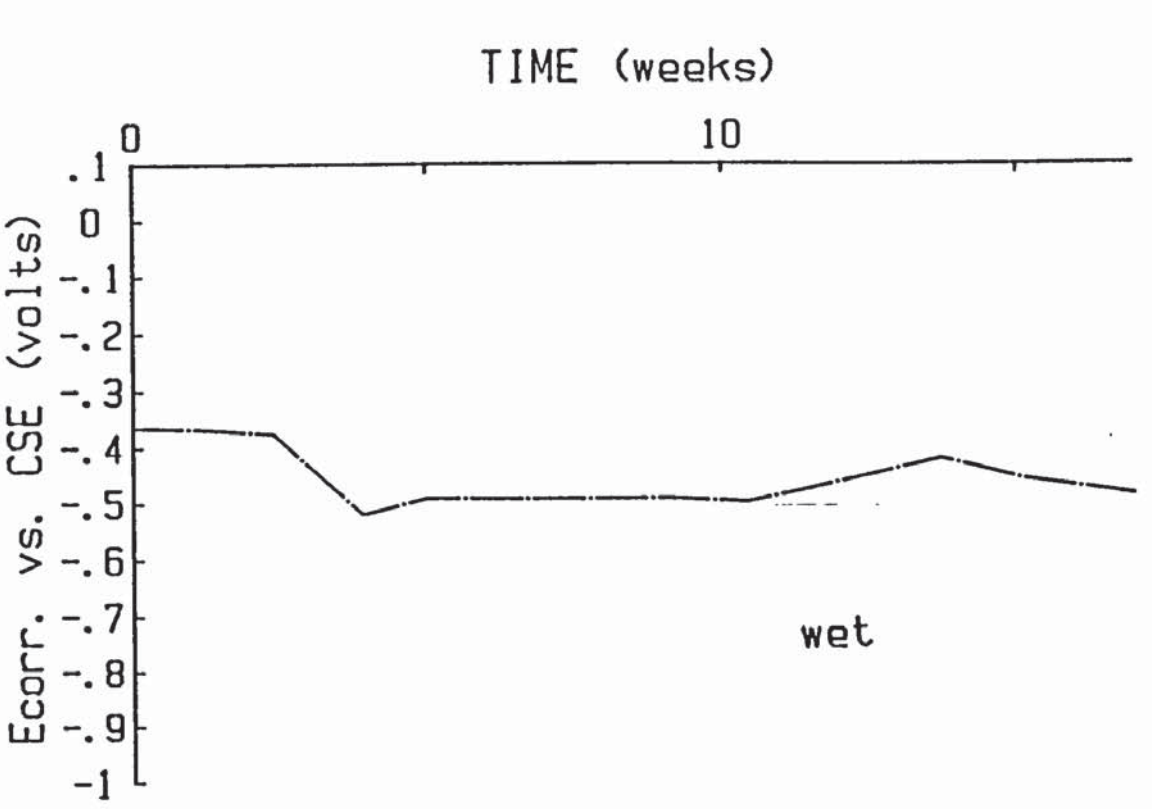

FIGURE 4.33 a

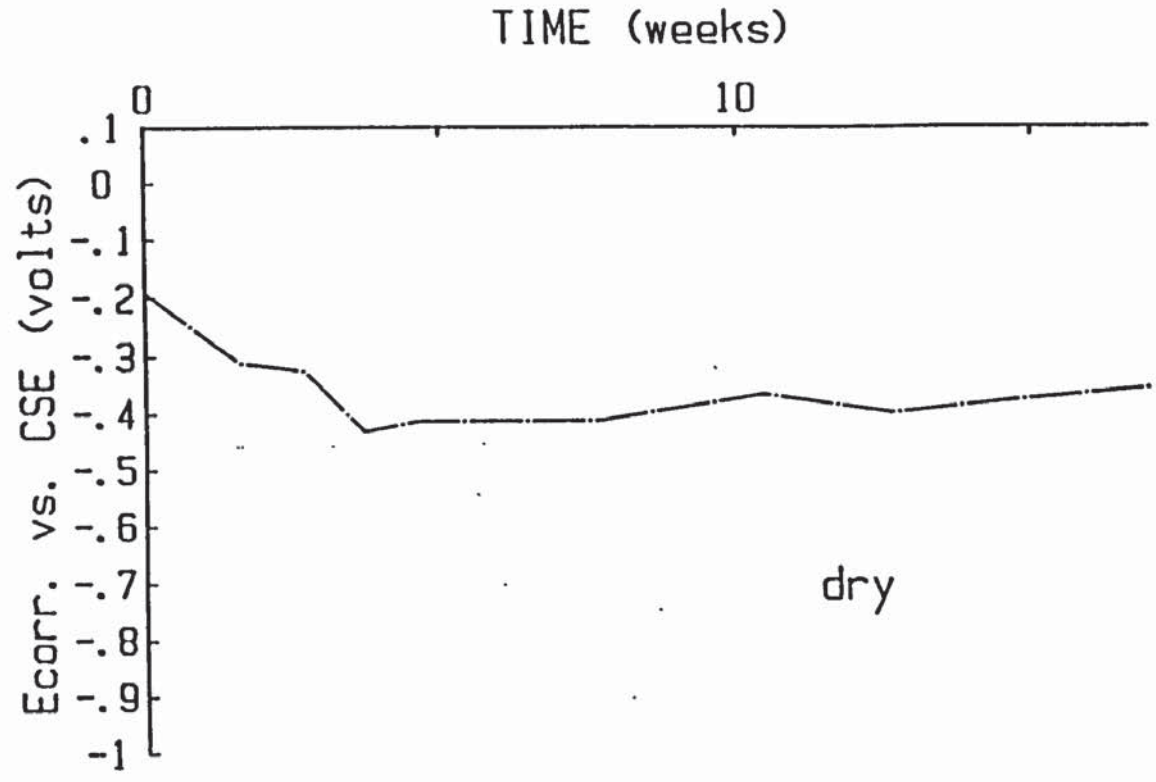

FIGURE 4.33 b

FIGURE 4.33 Repair system three (zinc rich epoxy primer) E_{corr}/time traces for 0.1% chloride segments in wet (a) and dry (b) conditions

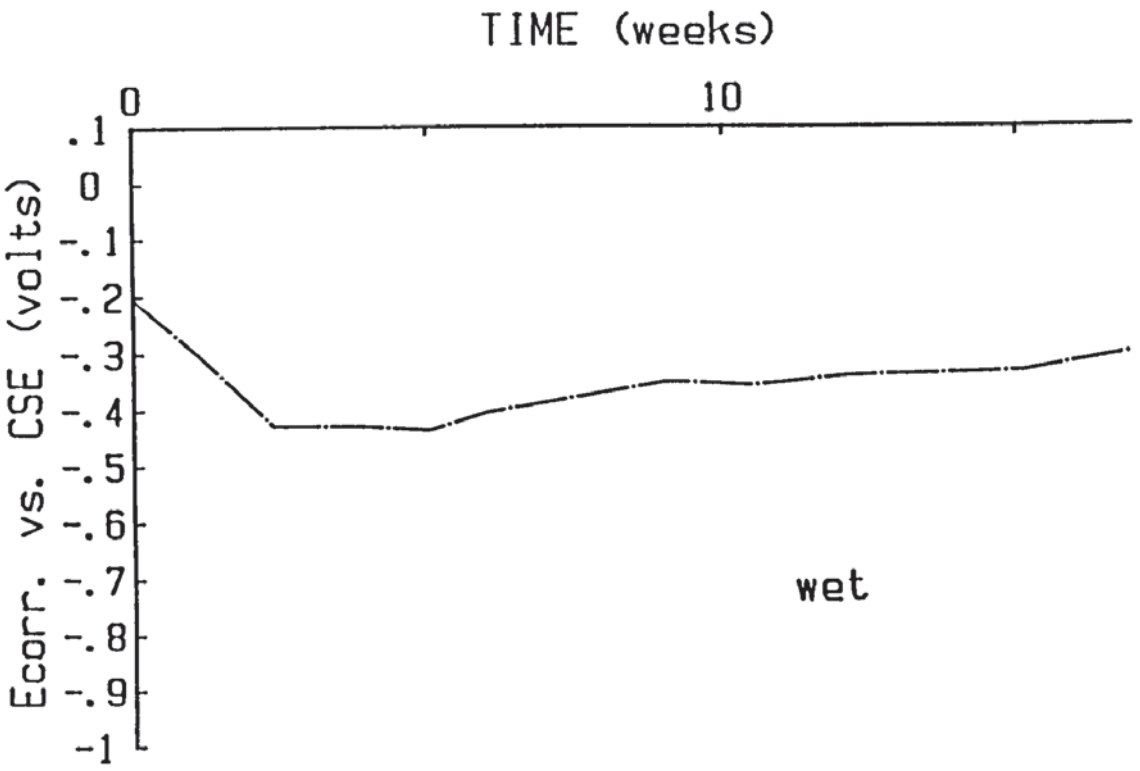

FIGURE 4.34 a

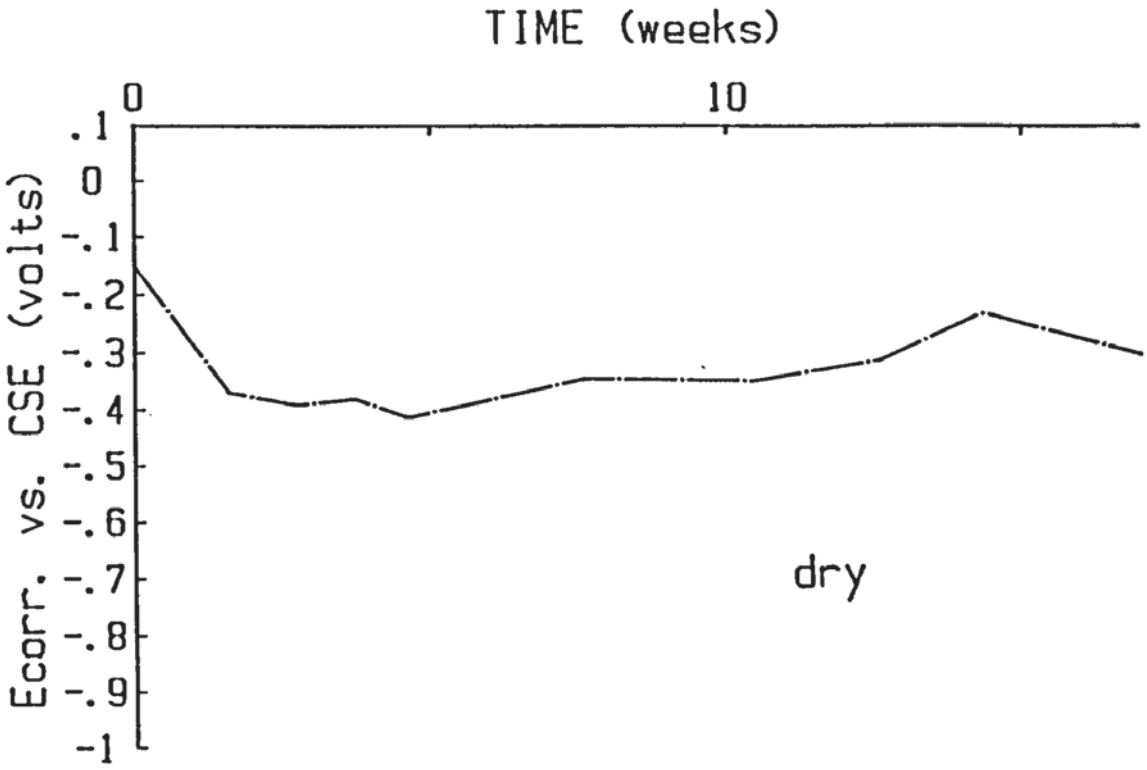

FIGURE 4.34 b

FIGURE 4.34 Repair system four (zinc rich epoxy primer + acrylic bonding agent) E_{corr}/time traces for 0.1% chloride segments in wet (a) and dry (b) conditions

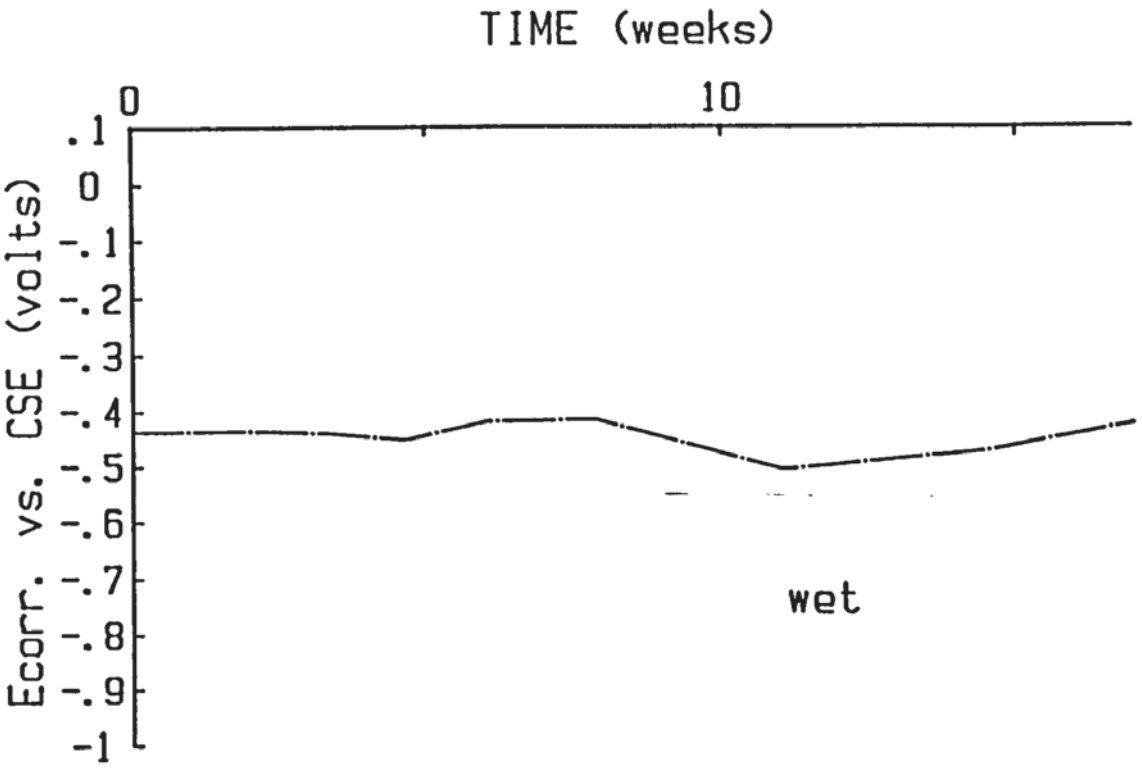

FIGURE 4.35 a

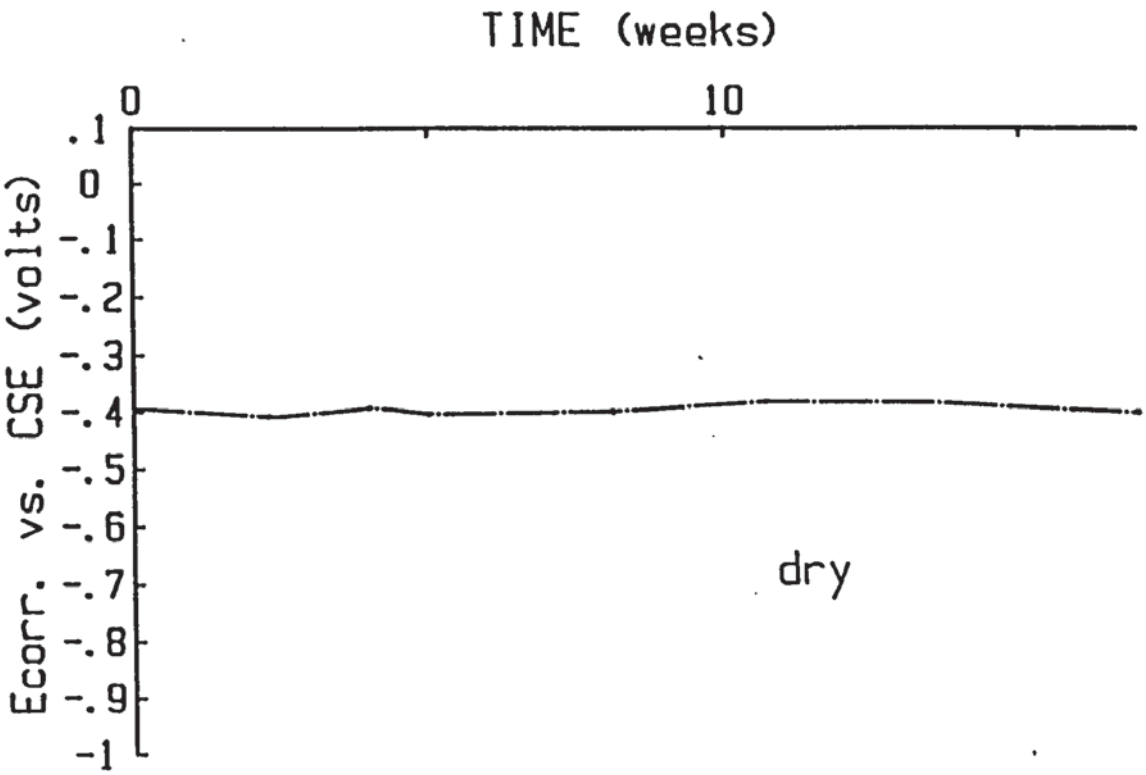

FIGURE 4.35 b

FIGURE 4.35 Repair system five (OPC slurry + insulating epoxy) E_{corr}/time traces for 0.1% chloride segments in wet (a) and dry (b) conditions

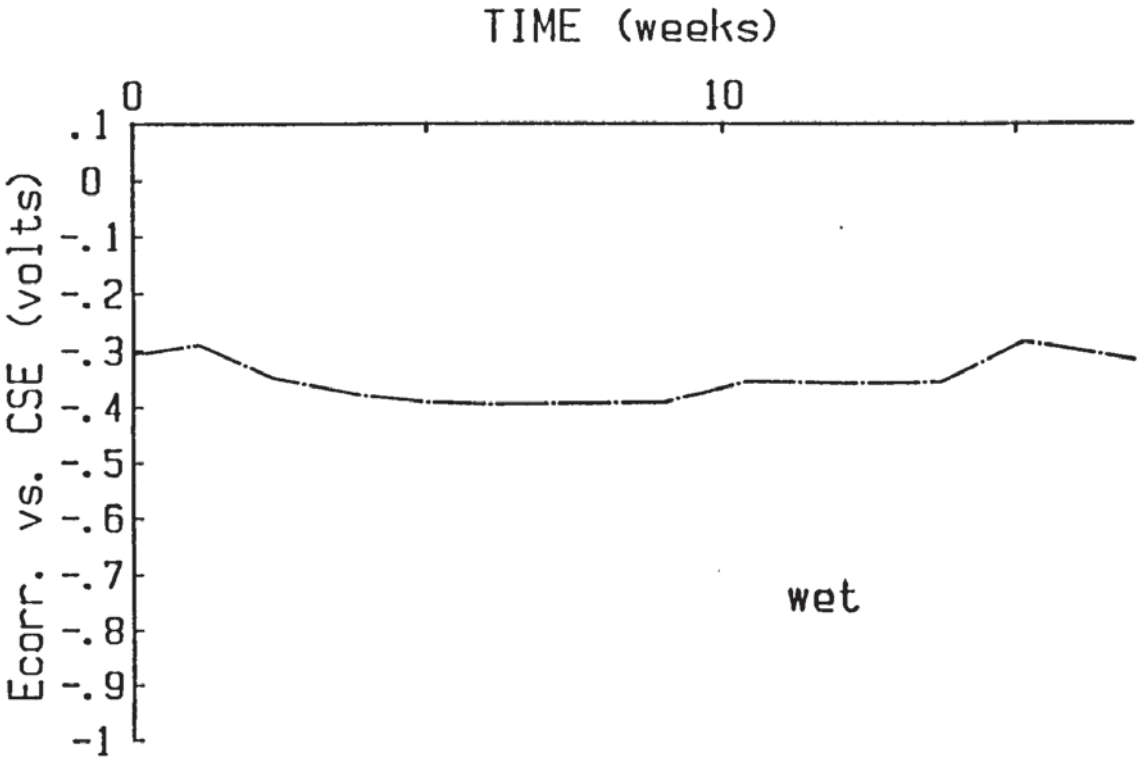

FIGURE 4.36 a

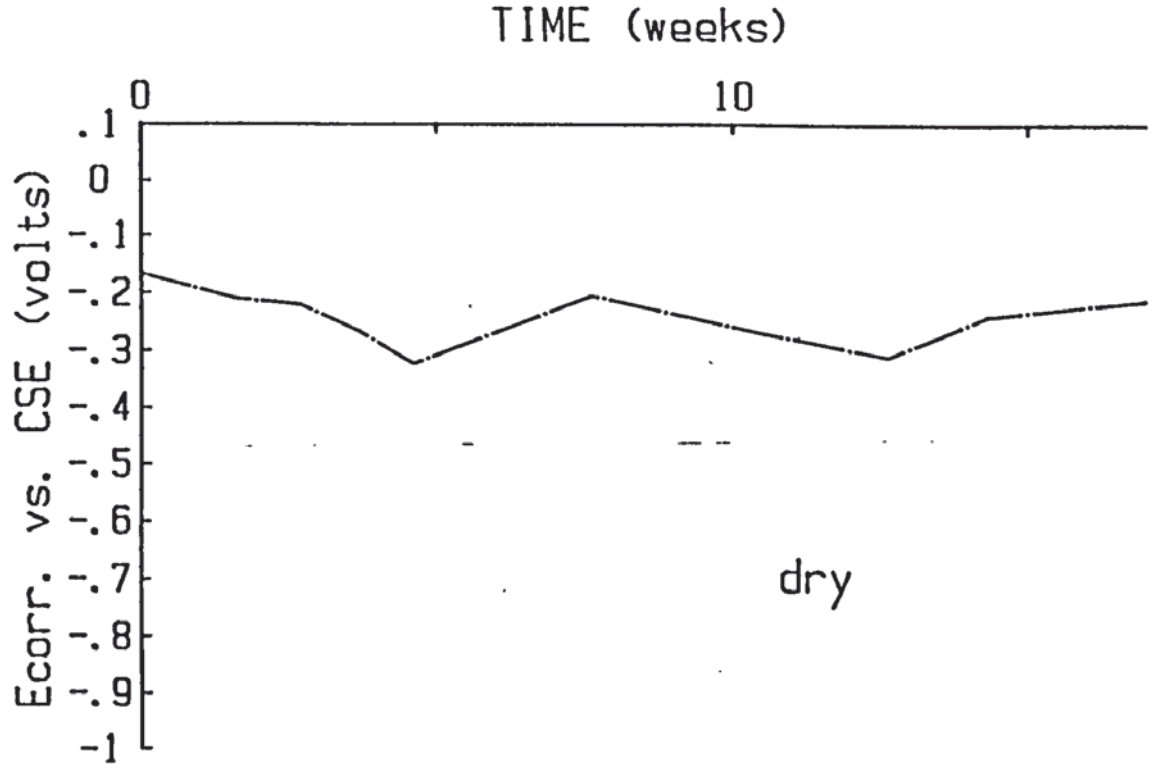

FIGURE 4.36 b

FIGURE 4.36 Repair system one (OPC slurry) E_{corr}/time traces for 0.0% chloride segments in wet (a) and dry (b) conditions

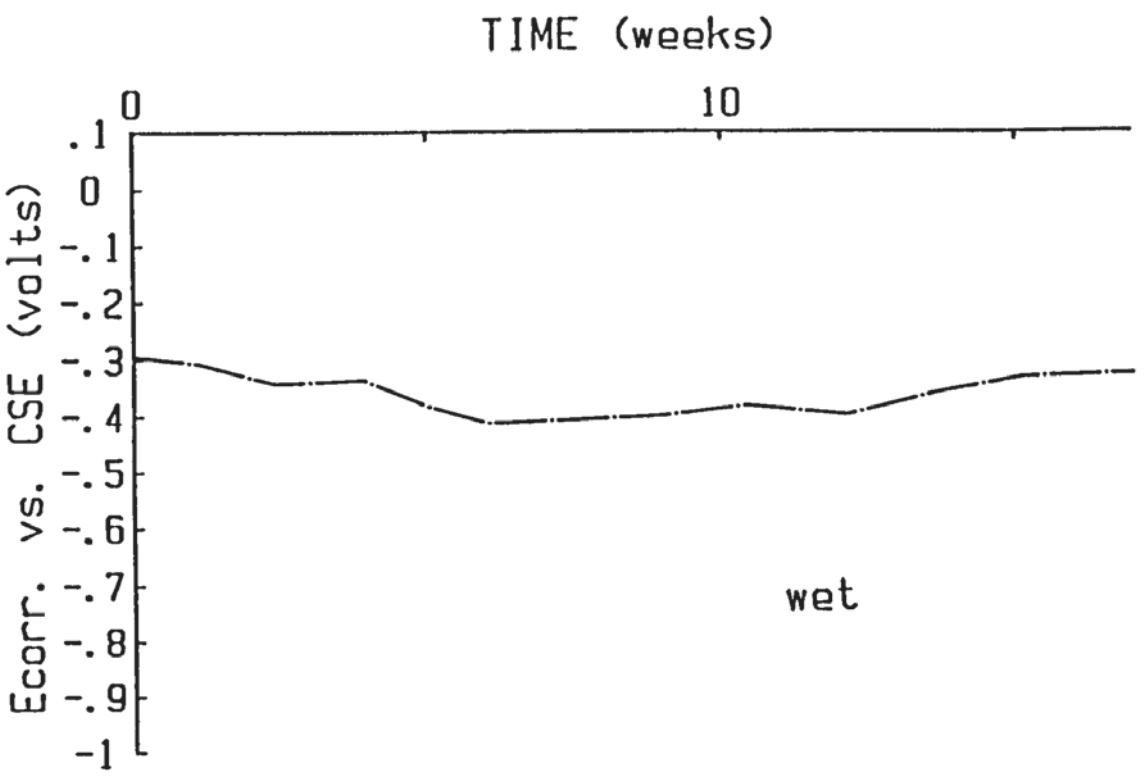

FIGURE 4.37 a

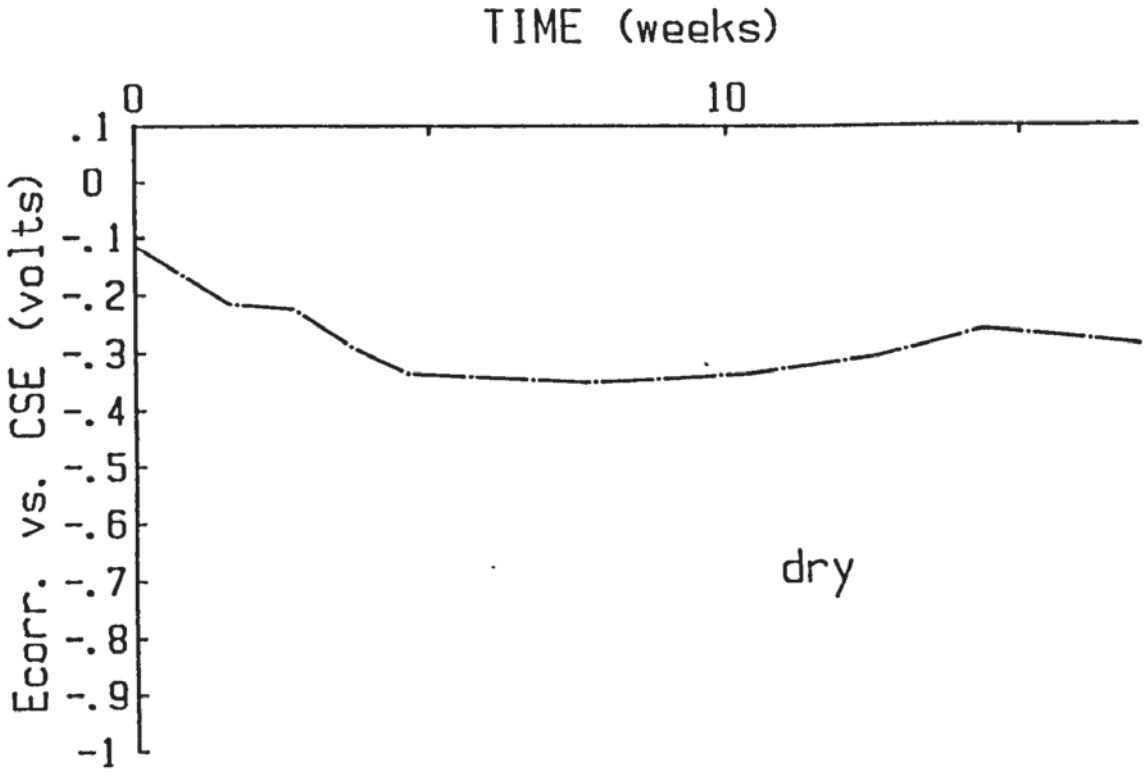

FIGURE 4.37 b

FIGURE 4.37 Repair system two (OPC slurry + acrylic bonding agent) E_{corr}/time traces for 0.0% chloride segments in wet (a) and dry (b) conditions

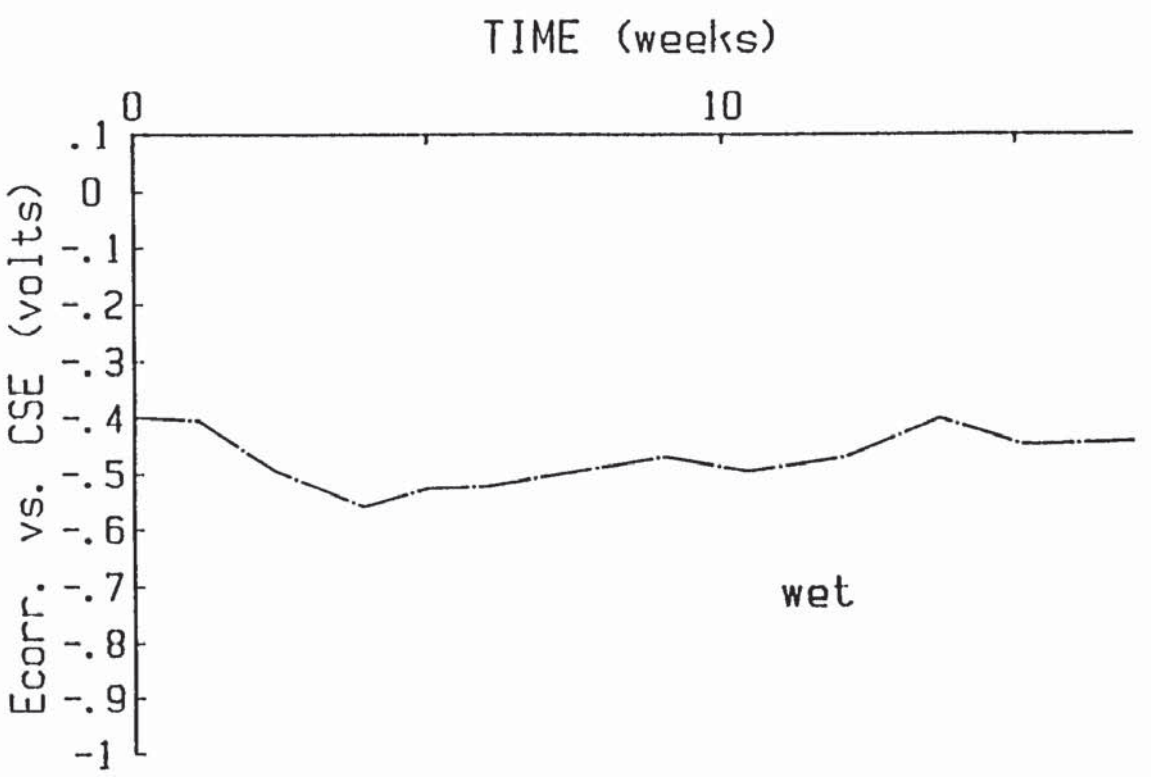

FIGURE 4.38 a

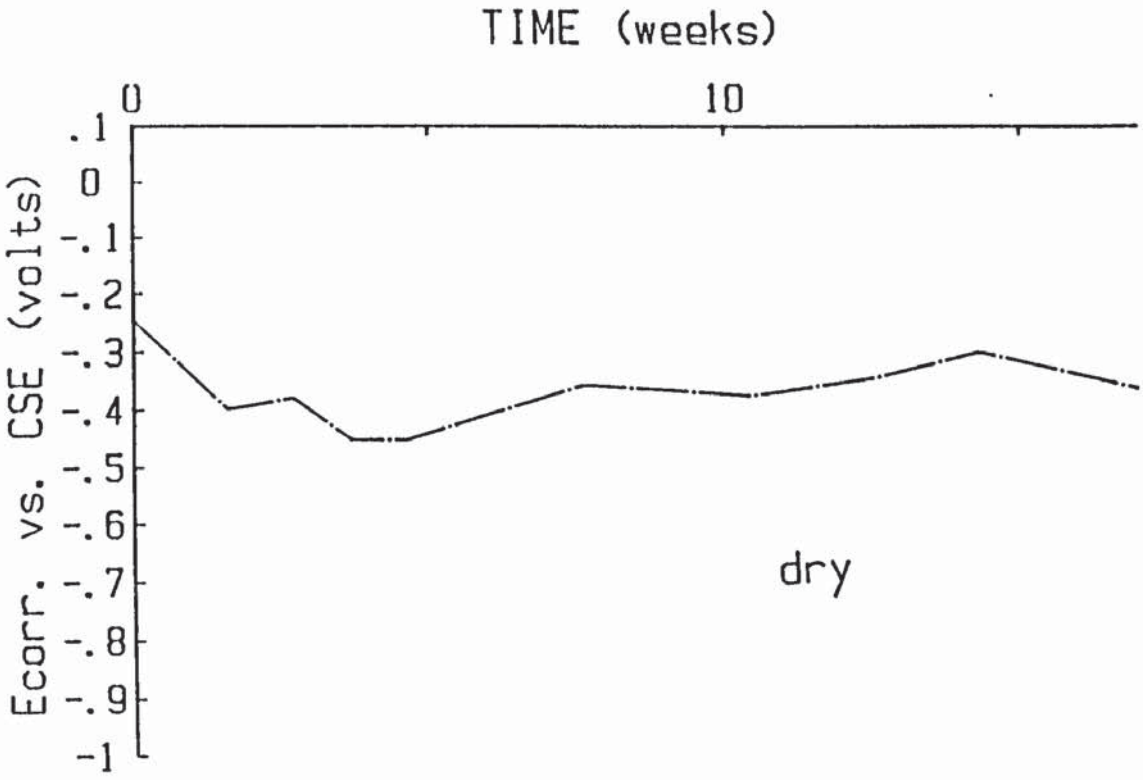

FIGURE 4.38 b

FIGURE 4.38 Repair system three (zinc rich epoxy primer) E_{corr}/time traces for 0.0% chloride segments in wet (a) and dry (b) conditions

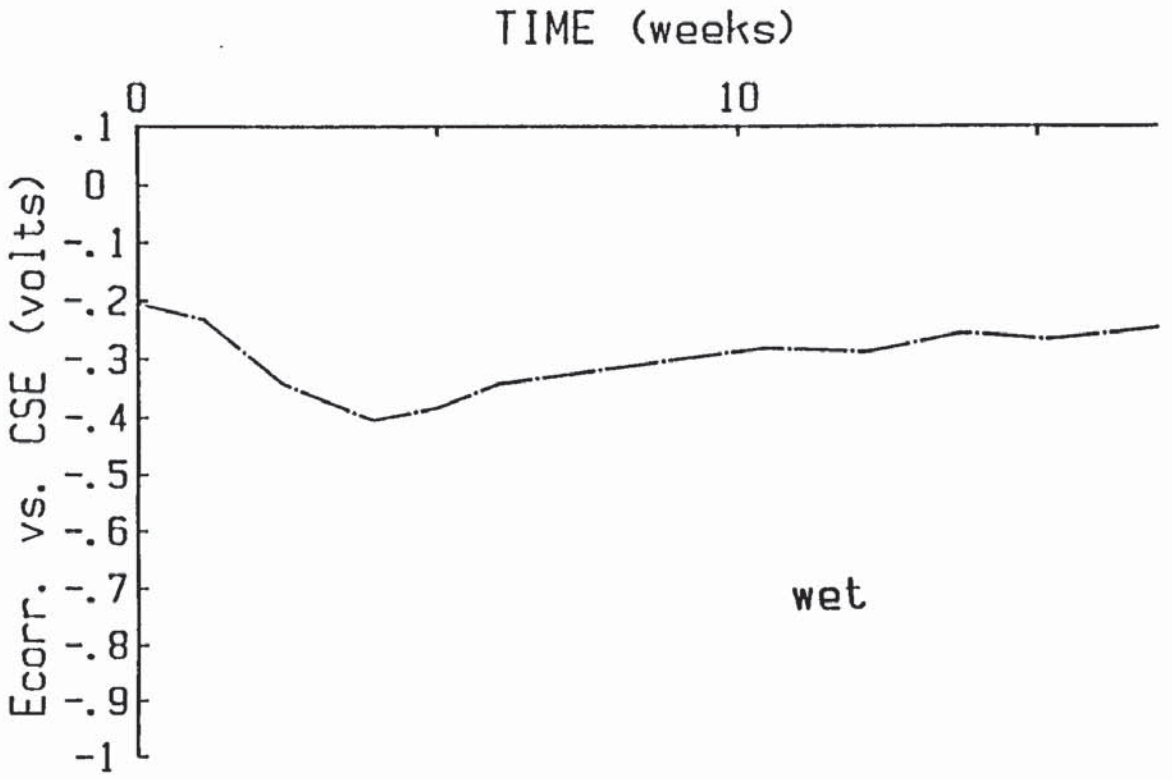

FIGURE 4.39 a

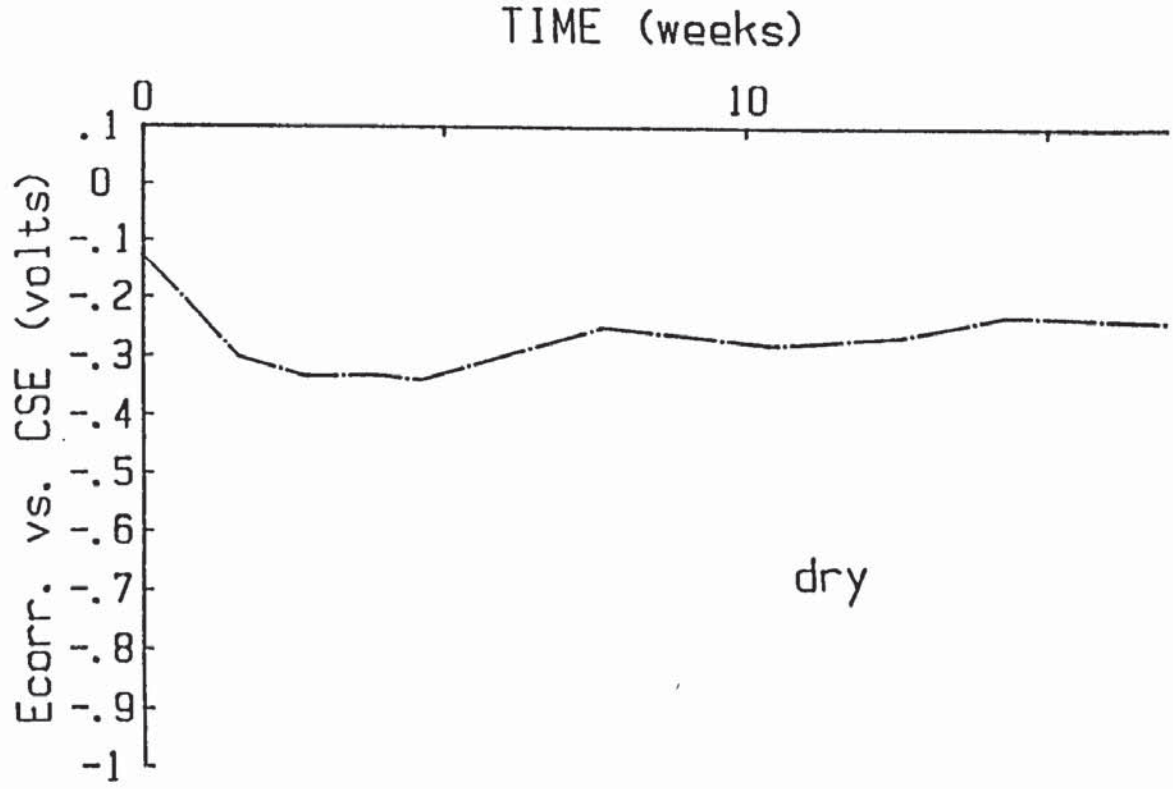

FIGURE 4.39 b

FIGURE 4.39 Repair system four (zinc rich epoxy primer and acrylic bonding agent) E_{corr}/time traces for 0.0% chloride segments in wet (a) and dry (b) conditions

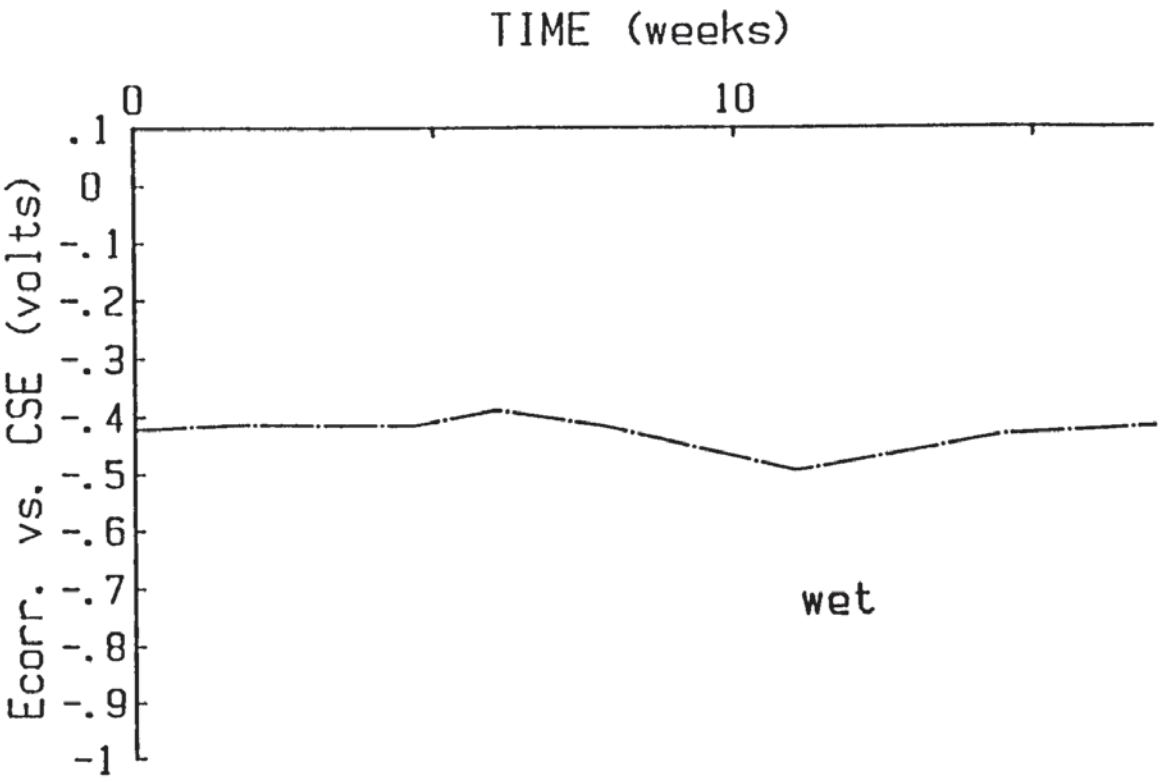

FIGURE 4.40 a

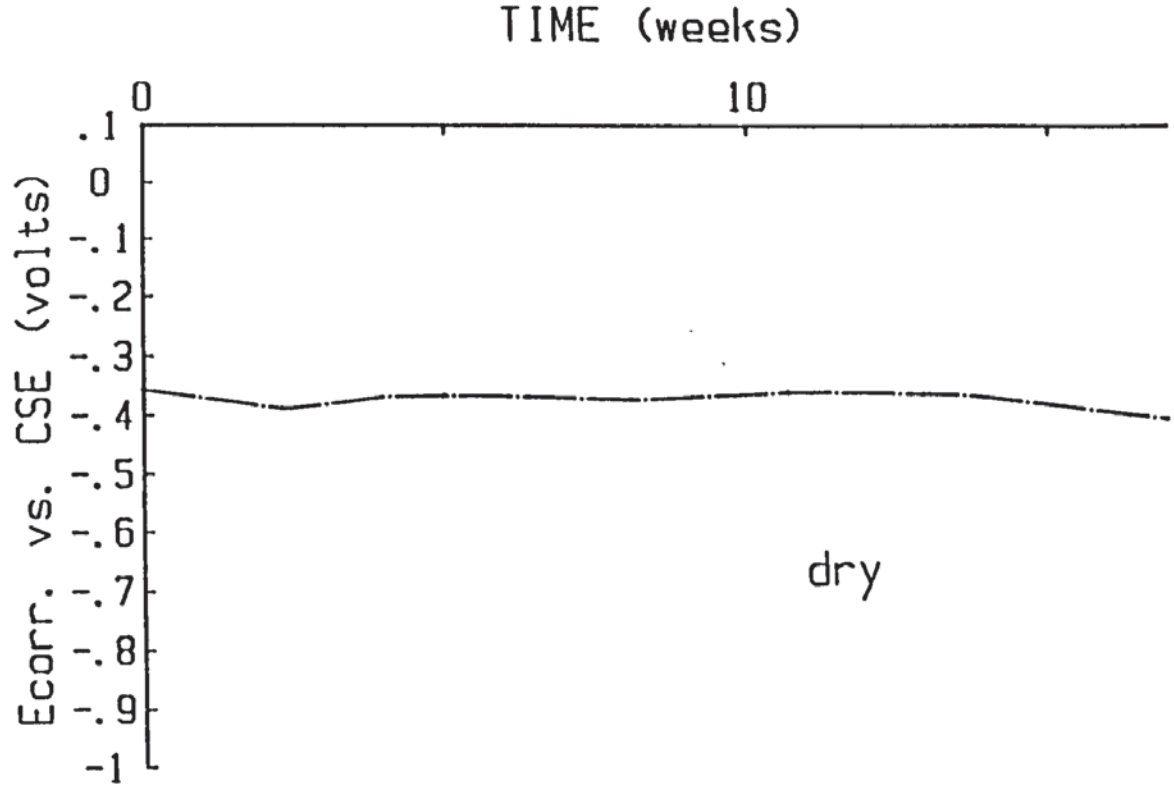

FIGURE 4.40 b

FIGURE 4.40 Repair system five (OPC slurry + insulating epoxy) E_{corr}/time traces for 0.0% chloride segments in wet (a) and dry (b) conditions

FIGURE 4.41 Ordinary Portland cement slurry and acrylic bonding agent repair primer with adjacent 1% chloride electrode. Slurry coat has been broken away in order to expose electrode

FIGURE 4.42 As figure 4.41, but repair comprising only ordinary Portland cement slurry

FIGURE 4.43 Macro (x6.5) zinc rich primer, showing light brown coloured corrosion product. Underlying steel substrate is visible

FIGURE 4.44 Macro (x6.5) zinc rich primer, typical surface of zinc primer after removal from mortar prism

FIGURE 4.45 Zinc rich primer and acrylic bonding agent repair. Repaired electrode (LHS) and 1% chloride electrode (RHS)

FIGURE 4.46 Zinc rich primer repair. Comparison of zinc coating, exposed segment substrate and adjacent 1% chloride electrode

FIGURE 4.47 Macro (x6.5) pitted region present at 1% chloride electrode, corresponding to an electrode adjacent to a zinc rich primer and acrylic bonding agent repair

FIGURE 4.48 Macro (x25) of well developed pitting site visible at top RHS of figure 4.47

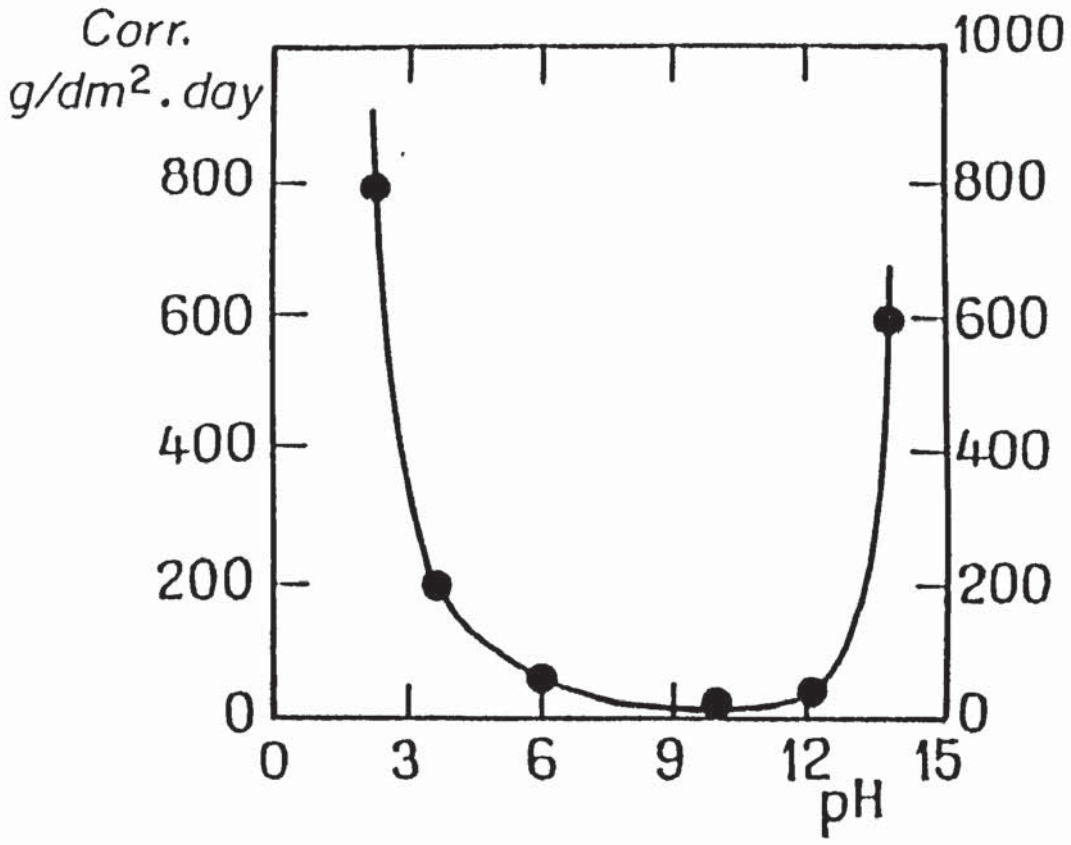

FIGURE 4.49 Influence of pH upon the rate of dissolution of zinc (after Chatalov, 4.22)

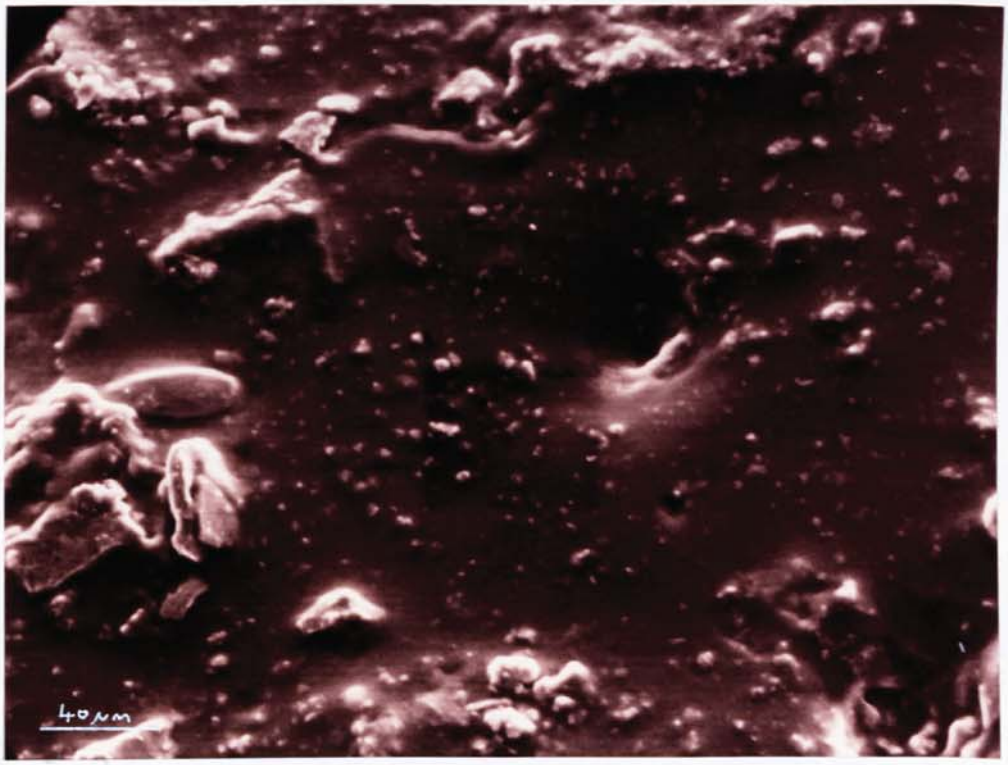

FIGURE 4.50 Electron photomicrograph of zinc rich primer and acrylic bonding agent. Smooth surface, thought to be associated with the acrylic layer

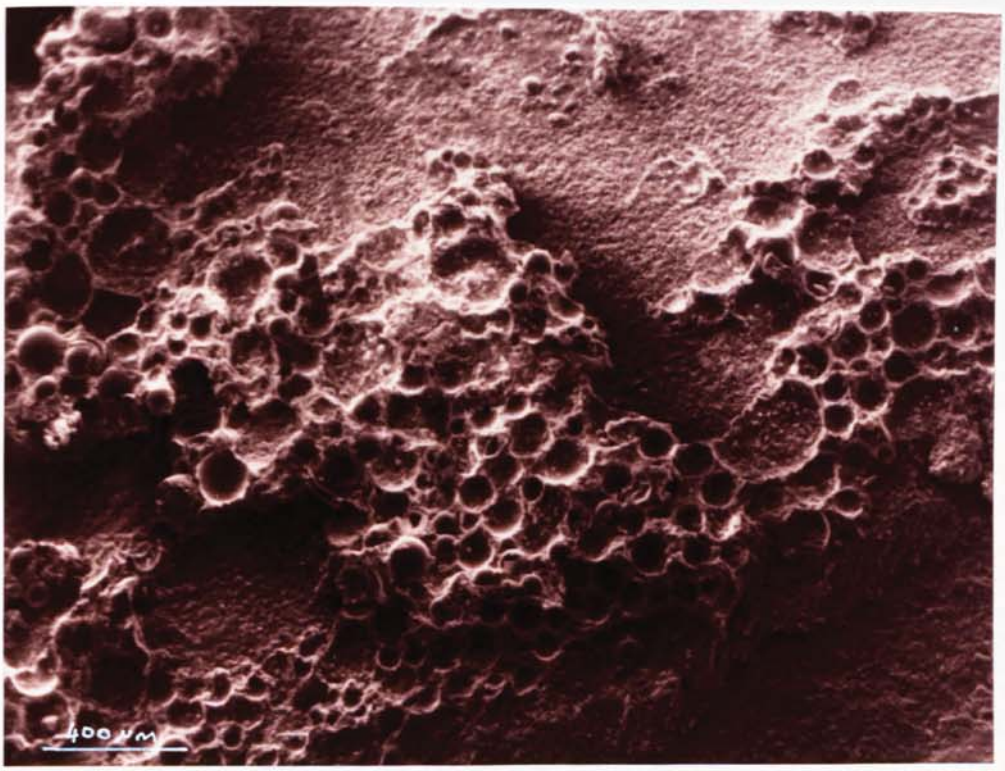

FIGURE 4.51 Electron photomicrograph of zinc rich primer surface showing cratered regions

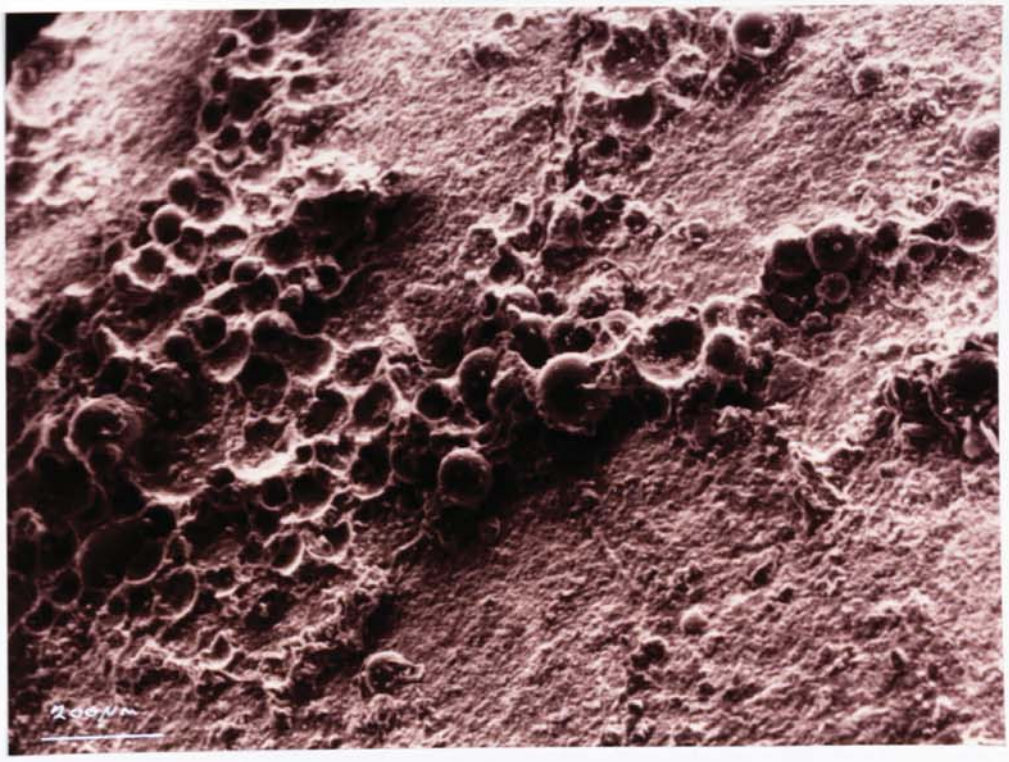

FIGURE 4.52 Electron photomicrograph showing typical surface of zinc primer specimen, note : spheroid present within cratered region

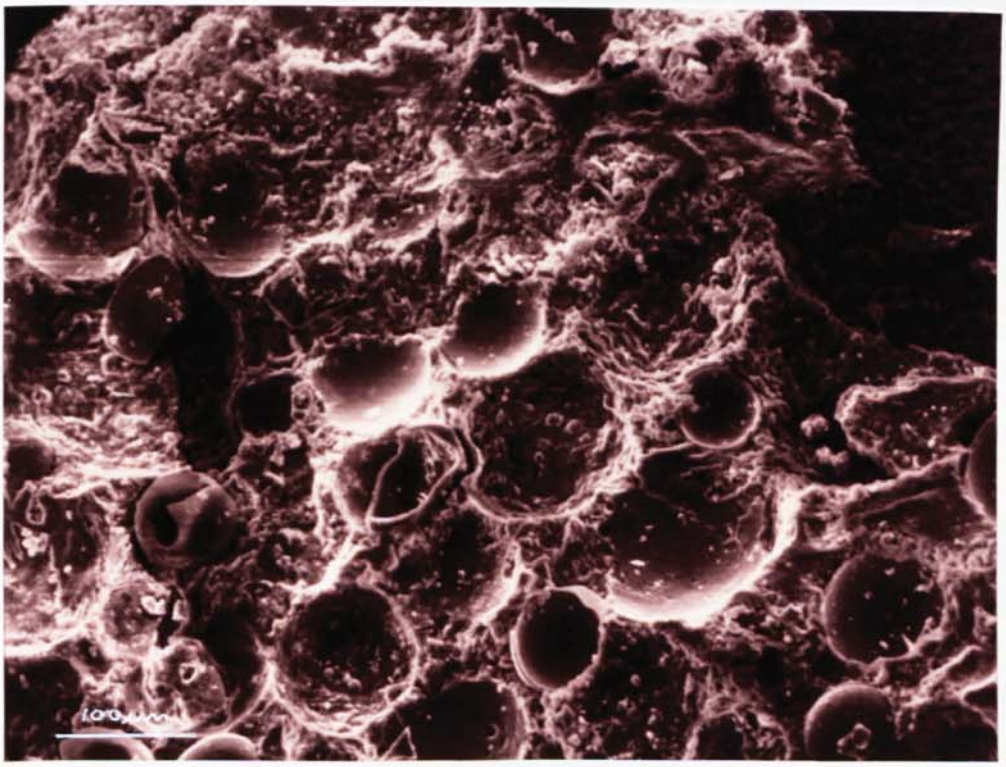

FIGURE 4.53 Electron photomicrograph showing the region comprising collapsed spheroid (bottom LHS corner) and empty crater (bottom and centre) analysed using EDXA spot technique

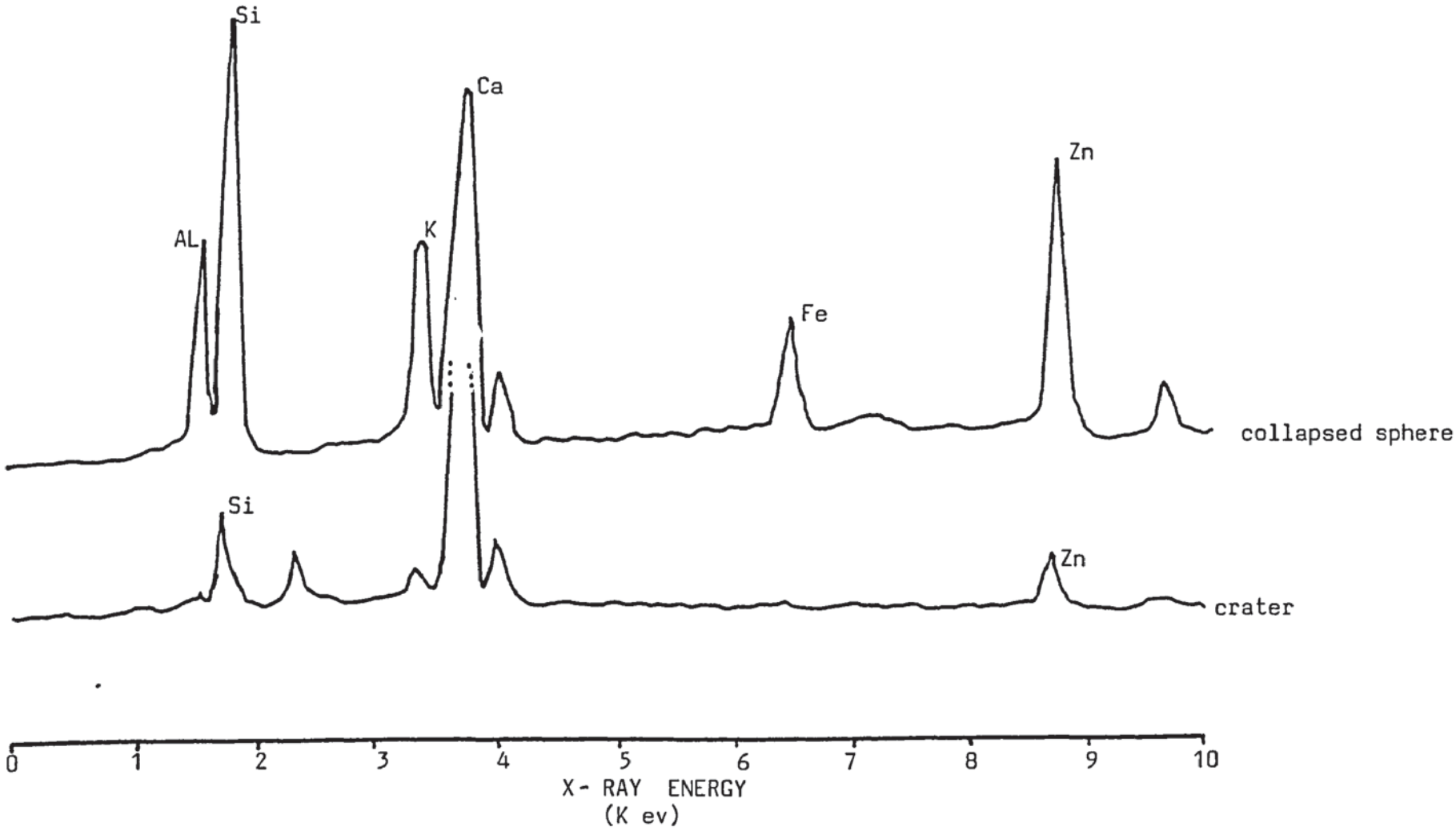

FIGURE 4.54 E.D.X.A. traces for the collapsed sphere and empty crater

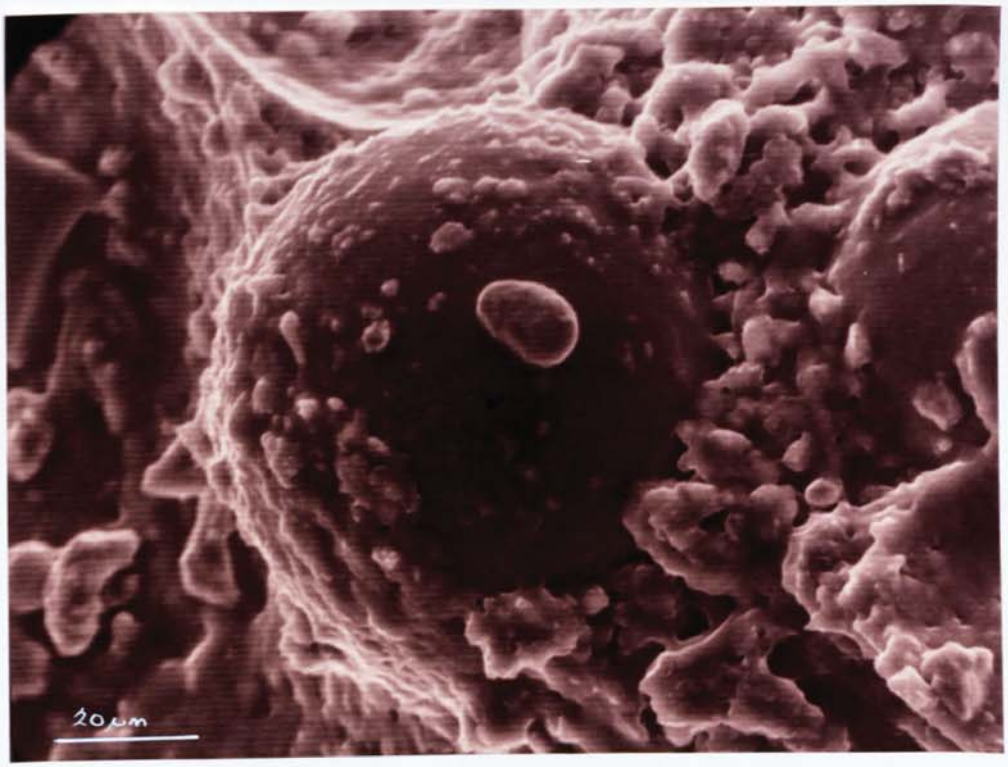

FIGURE 4.55 Electro photomicrograph clearly showing intact spheroid examined for presence of silicon and aluminium

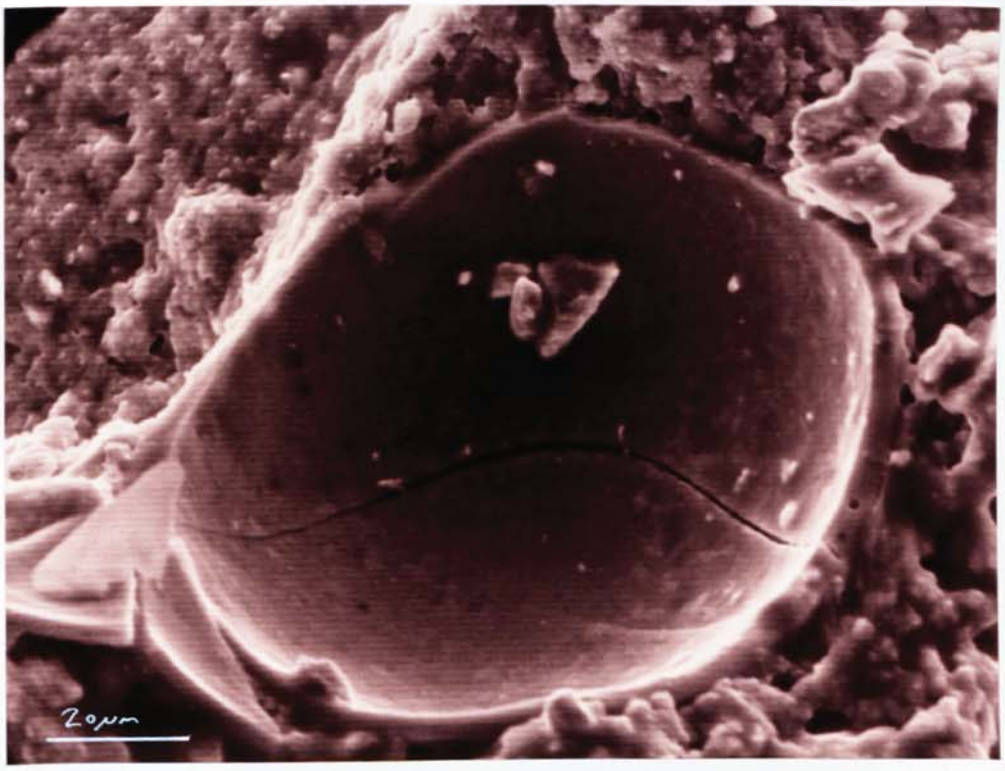

FIGURE 4.56 Electron photomicrograph showing well defined broken sphere smooth lining examined for presence of silicon and aluminium

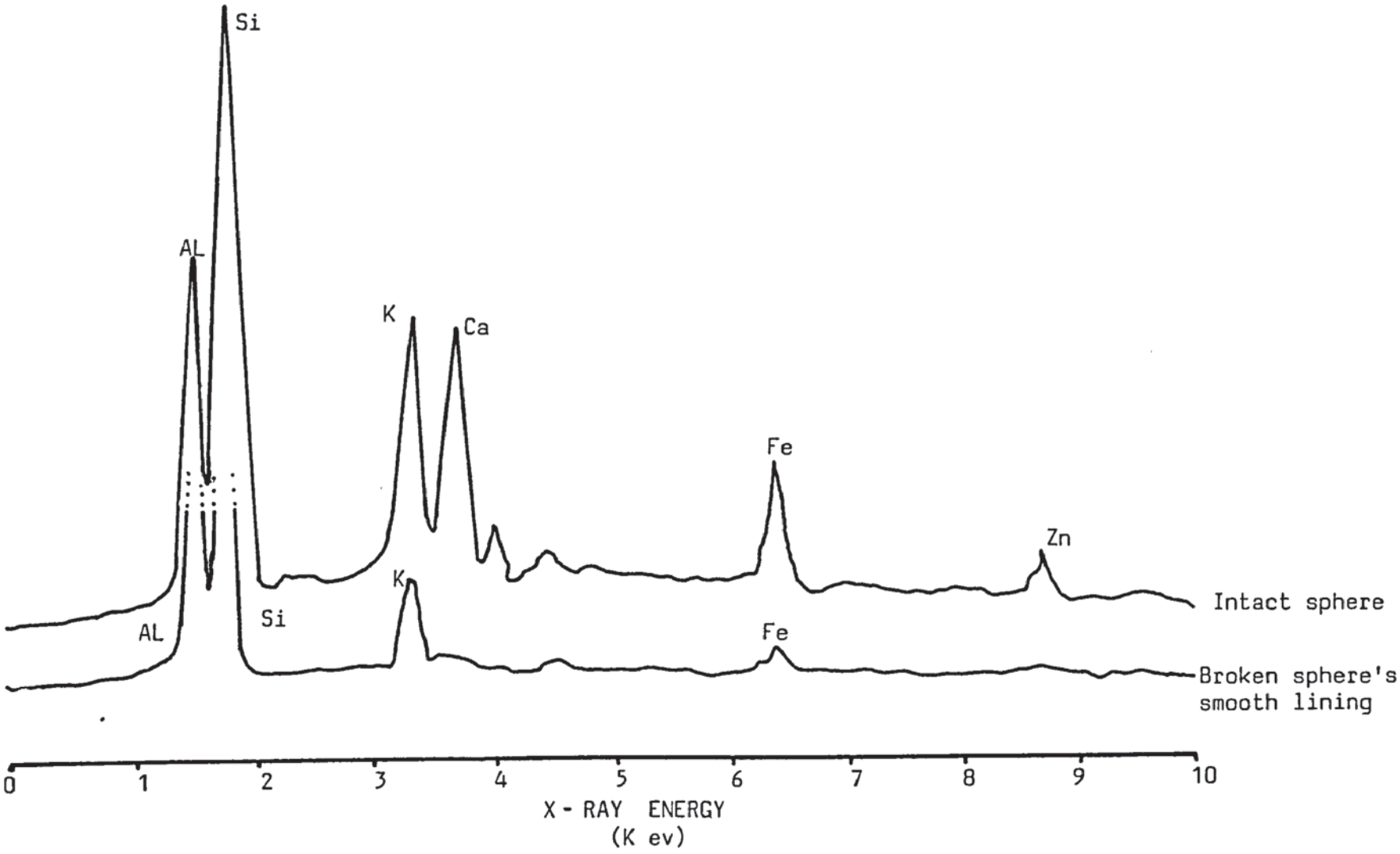

FIGURE 4.57 E.D.X.A. traces for intact sphere and broken sphere's smooth lining

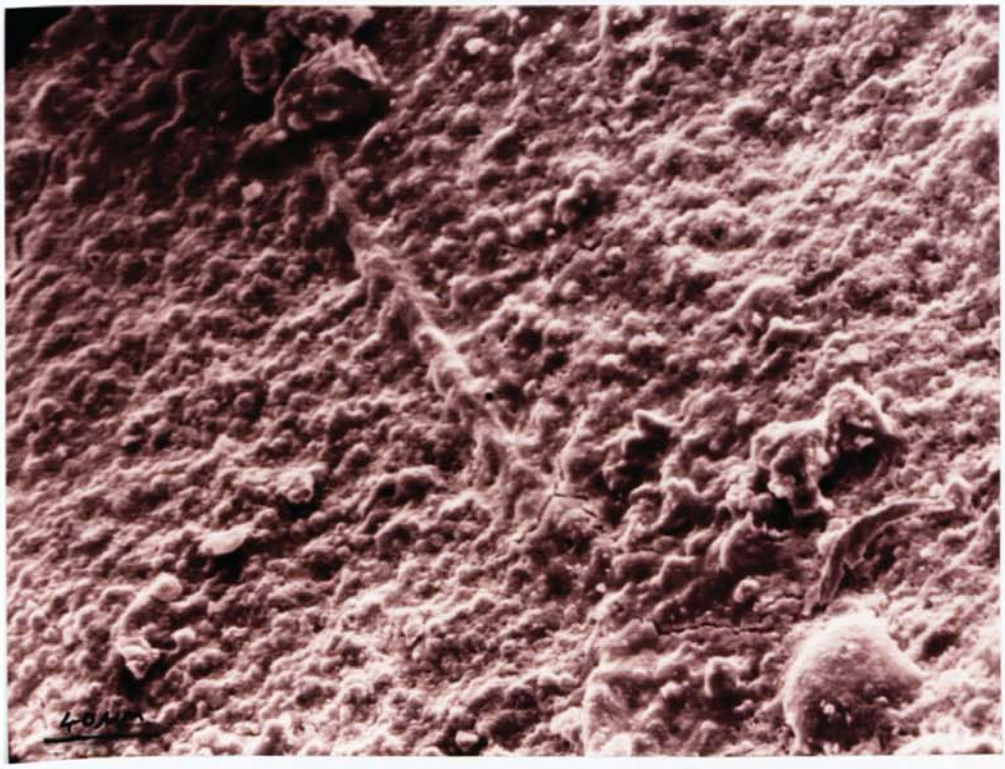

FIGURE 4.58 Electron photomicrograph of rough textured surface found to comprise tightly packed spheres

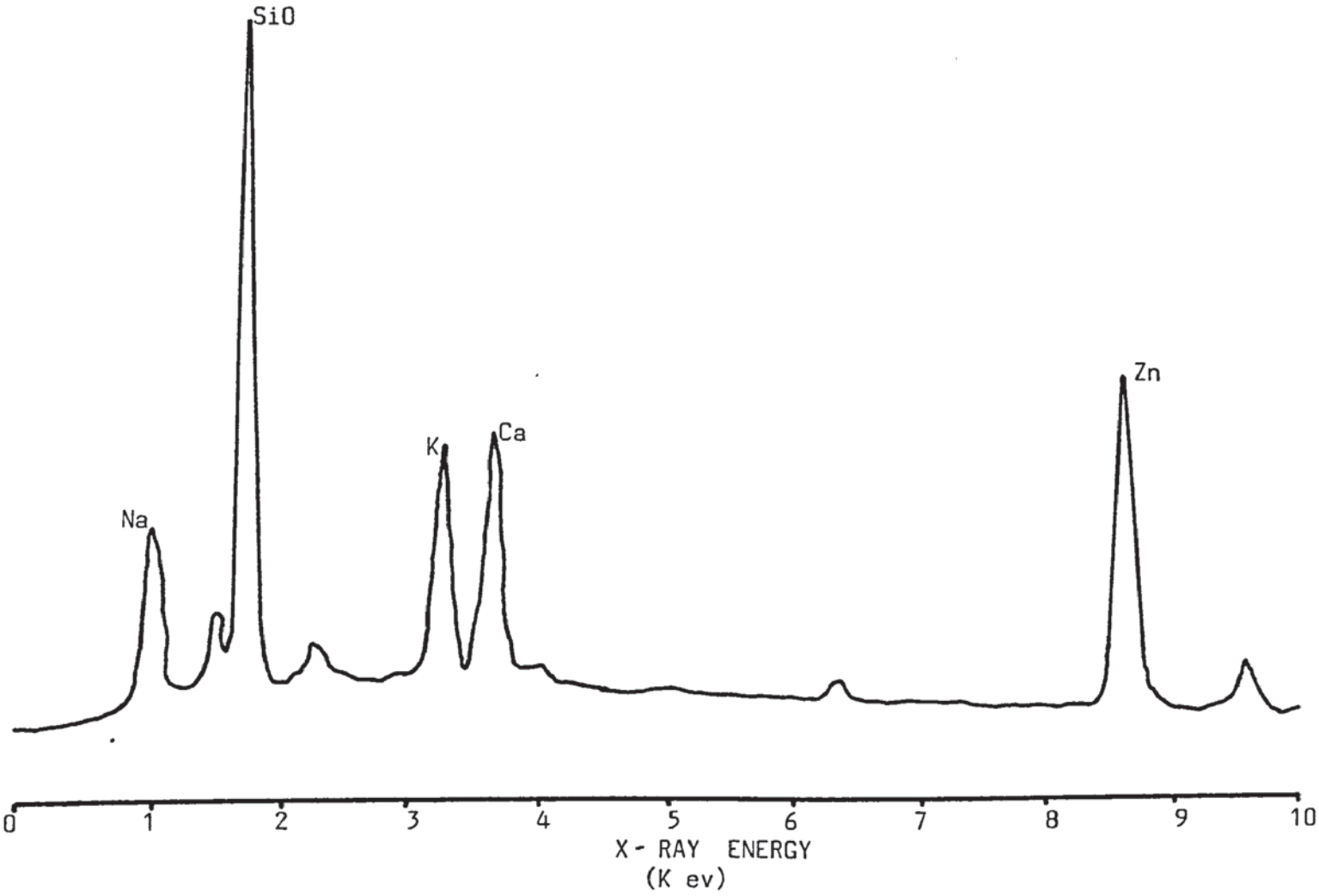

FIGURE 4.59 E.D.X.A. trace for the zinc primer surface

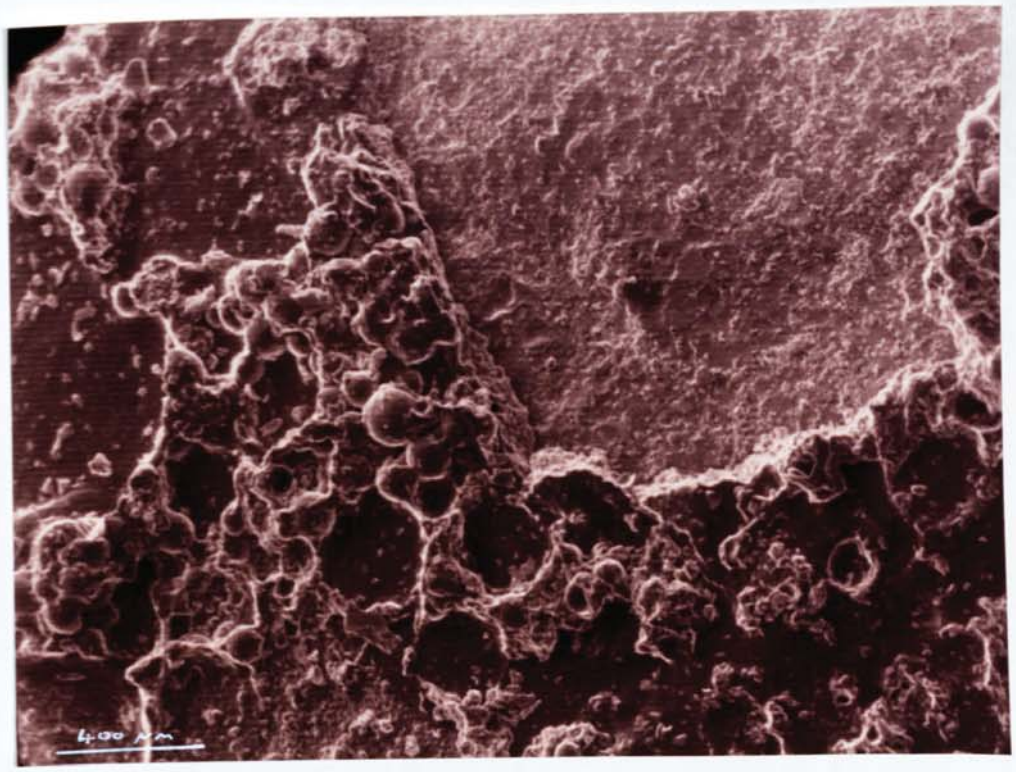

FIGURE 4.60 Electron photomicrograph showing fracture through zinc rich primer coating exposing underlying steel substrate

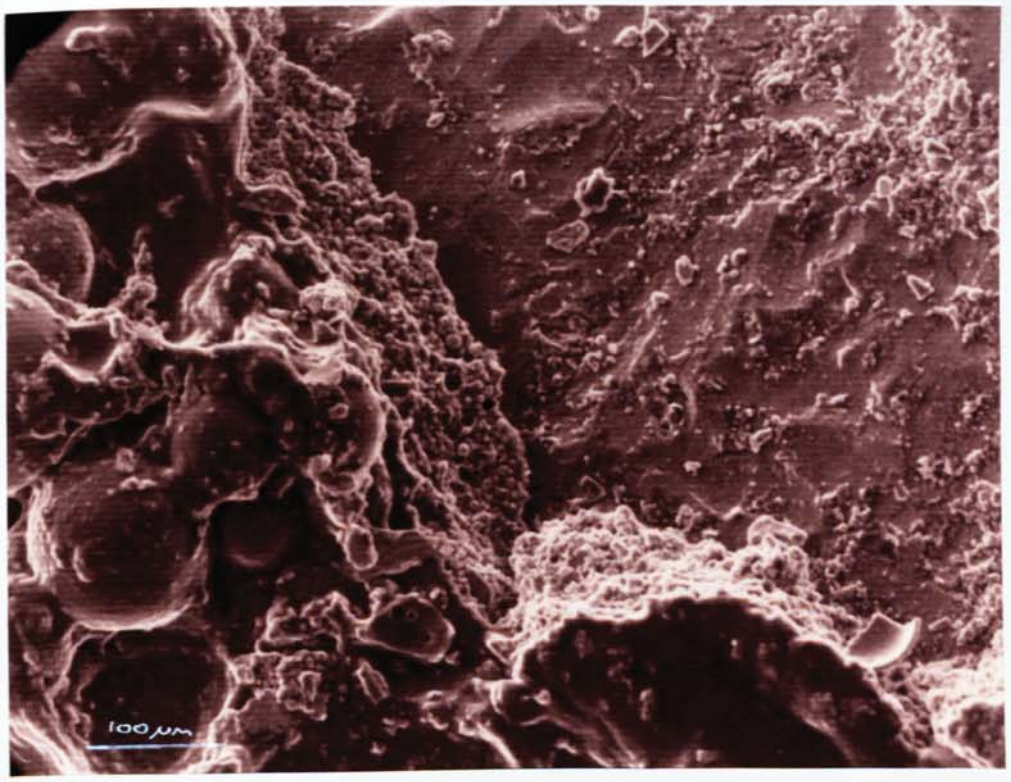

FIGURE 4.61 Electron photomicrograph showing the zinc layer in close contact with the steel substrate and a cementitious layer present upon the zinc surface

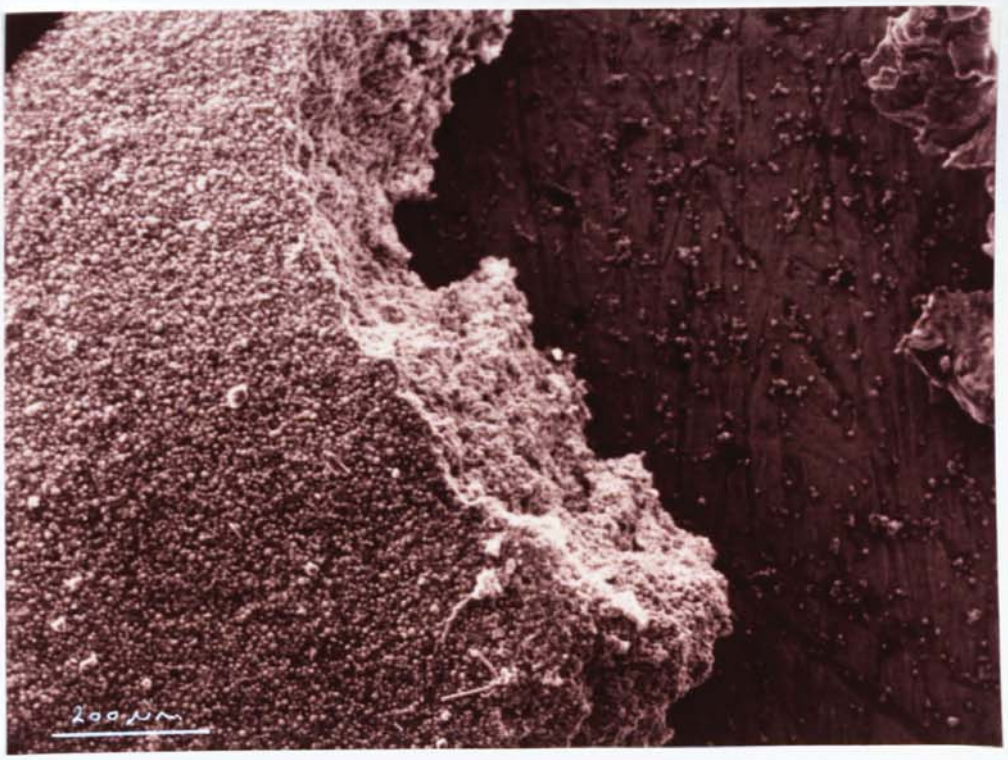

FIGURE 4.62 Electron photomicrograph showing nature of "thick" zinc primer layer with steel rod substrate exposed on RHS

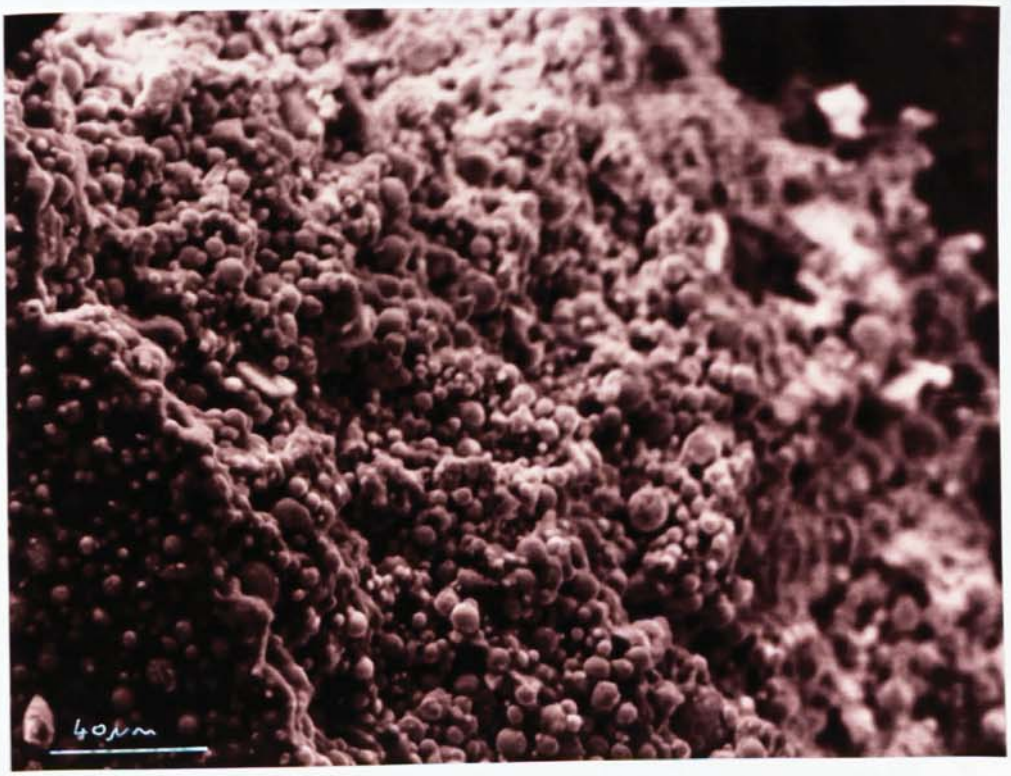

FIGURE 4.63 Electron photomicrograph showing the spheroidal nature of the zinc primer layer

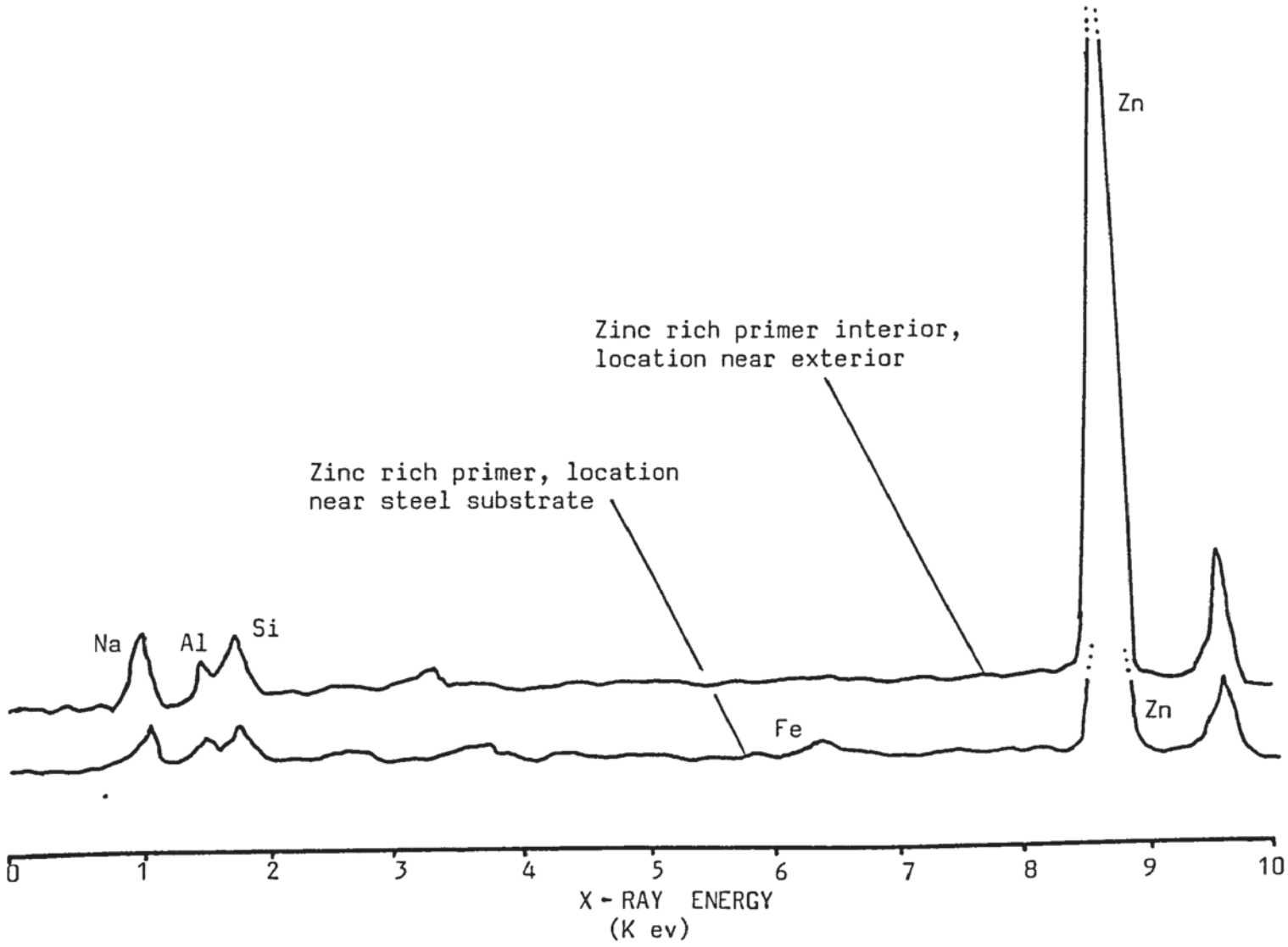

FIGURE 4.64 E.D.X.A. traces for the interior of the zinc rich primer layer

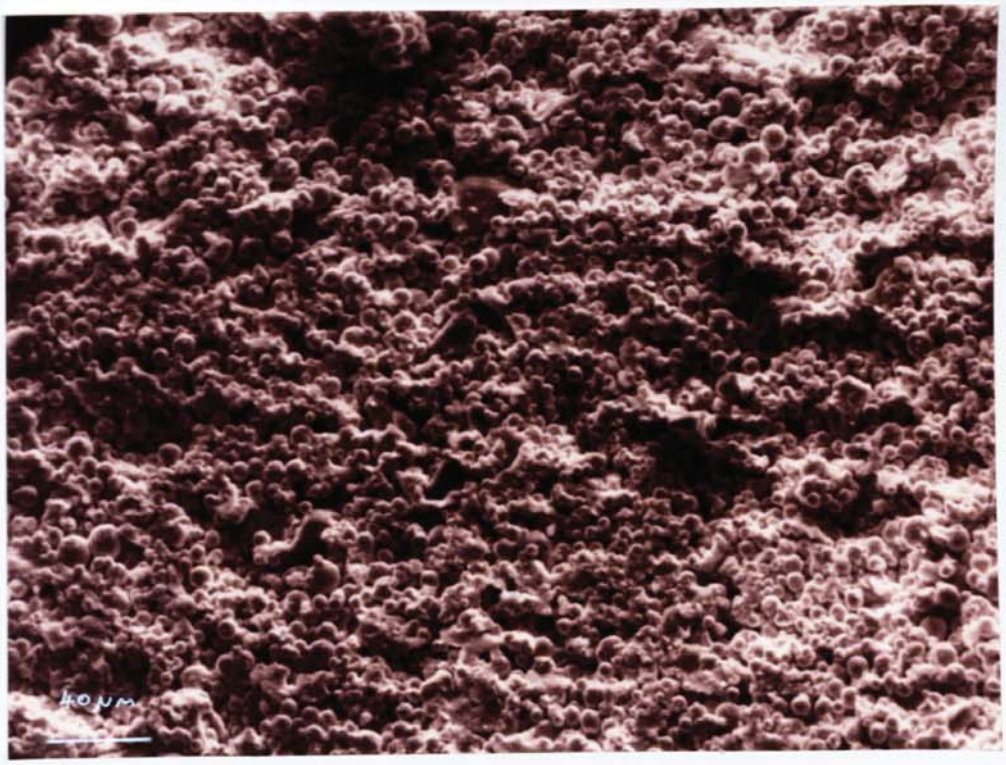

FIGURE 4.65 Electron photomicrograph showing structure of zinc layer at a fractured surface

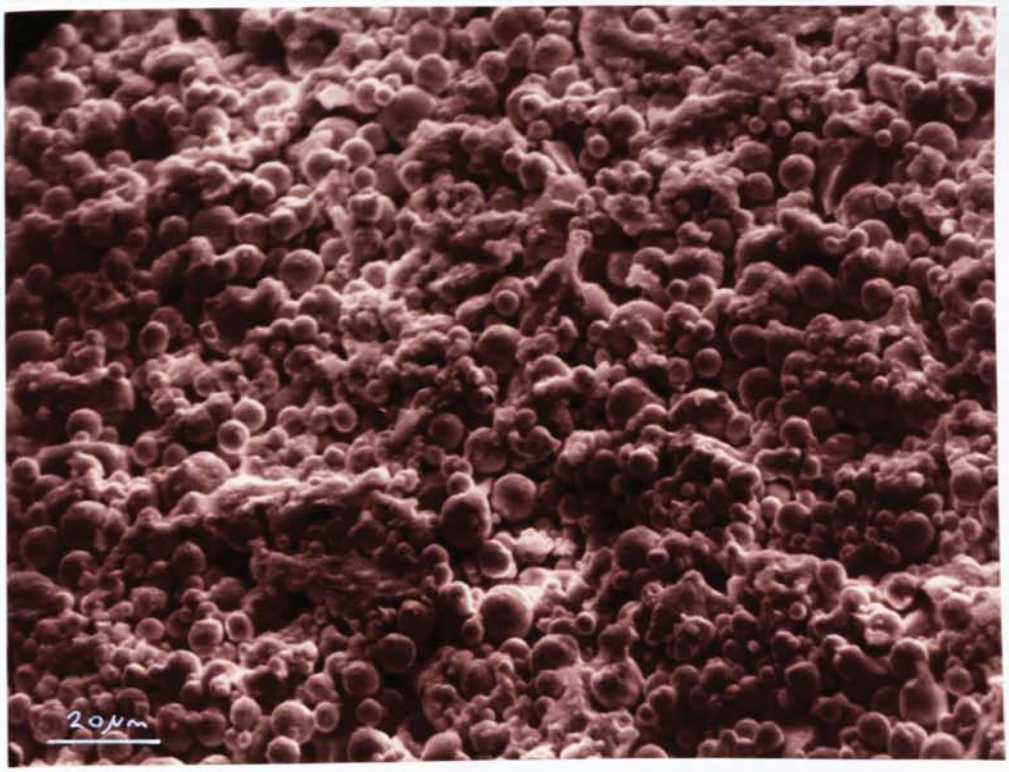

FIGURE 4.66 Electron photomicrograph showing tightly packed spheroids comprising the zinc coating

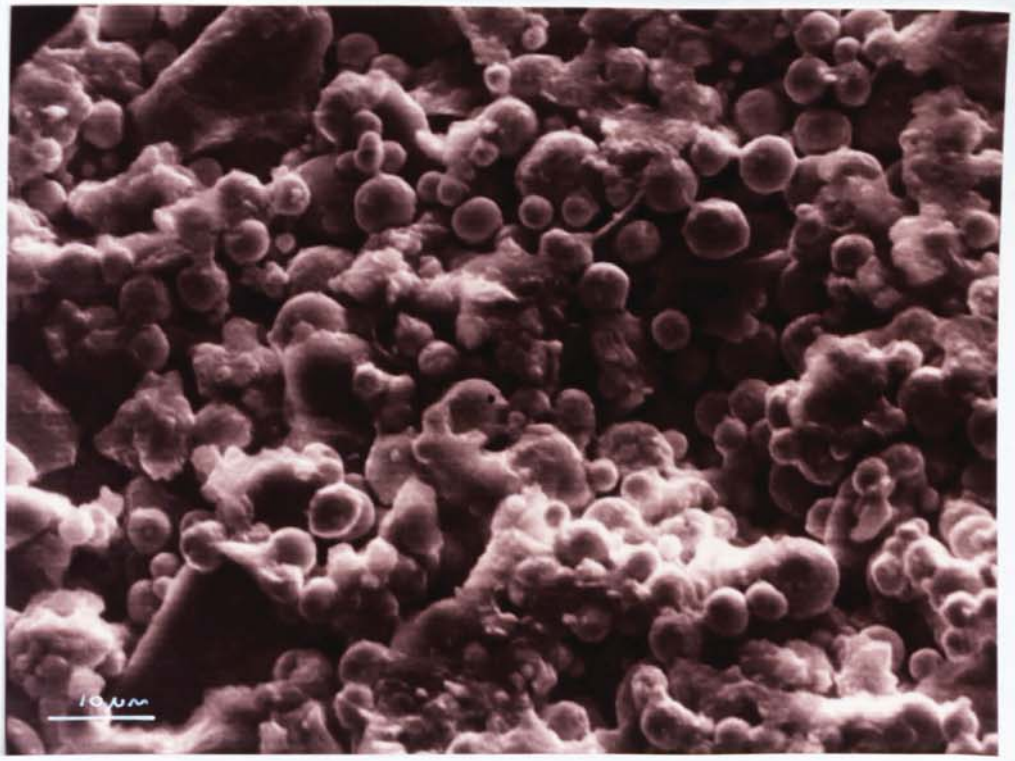

FIGURE 4.67 Electron photomicrograph showing the range of spheroid sizes and cross linking within the zinc coating

FIGURE 4.68 From left to right; 1%, 0.1% and 0% chloride segments corresponding to a zinc rich primer and acrylic bonding agent repair

CHAPTER 5

A STUDY OF ELECTROCHEMICAL NOISE GENERATED BY STEEL EMBEDDED IN A CHLORIDE CONTAMINATED ENVIRONMENT

5.1 INTRODUCTION

In many reinforced concrete durability-related problems, the investigator has at his disposal techniques capable of providing data, upon which, a decision may be made in order that remedial measures can be taken (e.g. reinforcement cover depths assessed using a cover meter).

Specifically, in the case of steel reinforcement corrosion, carbonation and/or chlorides are the most common causes and established techniques are available for the identification of such conditions (5.1-5.4). Merely identifying the cause of corrosion is, however, inadequate in terms of providing a basis for the cost effective rehabilitation of a corroding structure. It is necessary, also to determine the areas undergoing corrosion and the relative rates at which corrosion is taking place.

Whilst it is possible to identify likely areas undergoing corrosion - by taking half cell measurements (5.5) - no direct information as to the intensity of corrosion can be gained. The results obtained by this method are also open to serious errors of interpretation, e.g. in the cases of embedded or submerged structures where corrosion rates may be under cathodic control.

Although the methods available for investigations of corrosion on-site are rather limited, in the laboratory a number of established electrochemical techniques are available for the study

of steel embedded in cementitious materials (5.6). One application for data obtained from such studies is the construction of service life prediction models (5.7). It is apparent, however, that prediction of service life based upon data derived from laboratory studies cannot take full account of the many variables that may be encountered in practice. It would, therefore, be desirable to develop a more quantitative technique for the assessment of corrosion rate on-site. Towards this end, work has previously been carried out on two possible techniques, polarisation resistance (5.8-5.11) and electrochemical noise (5.12).

The work described in this chapter has sought to assess the merits of electrochemical noise measurement, as an on-site technique, by establishing a relationship with micro and macro-cell corrosion rates in specimens of the sort described in Chapter 3.

5.2 PREVIOUS WORK

Non destructive methods available for corrosion studies of steel embedded in cementitious materials include half cell potential monitoring, a.c impedance and linear polarisation (polarisation resistance). These techniques have been reviewed (5.13). A relatively recent development is electrochemical noise measurement.

Half cell potential measurement (Chapter 2) is the most simple of the above techniques. A suitable reference electrode and high input impedance voltmeter is required (5.5). Measurements are obtained instantaneously; there is no requirement to know the area of steel under investigation and so technique is appropriate for

on-site applications.

The evaluation of half cell potentials is frequently performed with reference to criteria, developed in the United States, based on the survey of 473 bridge decks (5.14). Structures of large surface area can be investigated by moving the half cell over a reference grid, enabling the construction of an equipotential contour map, from which, likely sites of anodic activity may be identified (5.15, 5.16). It should be noted that the electrochemical environment found within a bridge deck is a specific set of conditions, and great care should therefore be exercised when applying such criteria in order to evaluate potential surveys from structures other than bridge decks. For example, under conditions of restricted oxygen availability, (e.g. submerged marine structures), large negative potentials may be mistakenly thought to indicate corrosion, when they are actually due to a rate of limiting cathodic reaction (5.17).

Linear polarisation (also referred to as polarisation resistance), is a d.c. perturbative technique (Chapter 2) involving the calculation of corrosion intensity, i_{corr}, from the Stern-Geary relationship (5.18). The technique has been used since the 1970's for studies involving steel in concrete (5.8). Comparisons of corrosion rate determined by this technique and gravimetric methods have given reasonable agreement (5.19-5.22).

The technique of a.c. impedance involves applying a signal of small amplitude (10 to 20 mV) of known variable frequency (100KHz) to 1MHz) in order to determine values of the charge transfer resistance (R_T) - analogous to the d.c. polarisation resistance (R_p). Charge transfer resistance values are then used to determine values of corrosion rate from the Stern-Geary expression. This

technique has been used to estimate corrosion rates of steel in concrete (5.23-5.25), but when compared to linear polarisation, it is more time consuming, requires more sophisticated equipment and is prone to larger errors.

Electrochemical noise techniques involve the measurement of small fluctuations of corrosion current or potential (5.26, 5.27). Such fluctuations in the electrochemical processes are thought to be related to the formation and repassivation of pits. Several theoretical treatments of electrochemical noise have been proposed (5.28 - 5.30). Electrochemical noise has been used to investigate certain electrode processes including; surface effects (5.31), initiation of pitting or crevice corrosion (5.32), passive film local breakdown and repassivation (5.33), initiation of crevice corrosion and repassivation (5.34). A previous study at Aston involving large numbers of specimens containing steel electrodes embedded in cement pastes and concretes, exposed to an external source of chloride, determined a relationship between corrosion rate and standard deviation of electrochemical noise (5.21).

Electrochemical noise measurements do not depend on a knowledge of electrode areas concerned. Thus the technique, if successfully developed for on-site applications would be of considerable value.

For reasons of reliability, linear polarisation has been used in this study as a method of providing an independent measure of corrosion rate, with which to compare electrochemical noise data.

5.3 EXPERIMENTAL

In order to study electrochemical noise generated under

conditions of chloride contamination, and also investigate the influence of several anode/cathode combinations, the specimens required were as described in Chapter 3. These were intended to provide a simplified model of a structure containing several levels of chloride contamination. Their important feature was the facility to monitor macro and micro-cell corrosion activity both in terms of corrosion current and potential noise.

The equipment used throughout this study was based upon a system previously developed at Aston (5.21). The system comprised several devices used for the acquisition and processing of data. A software component was required in order to programme the equipment and subsequently process collected data.

The individual elements of hardware comprise a high resolution digital voltmeter (Solartron 7060A), a microprocessor/control unit (Hewlett Packard HP85B), and an output device (Hewlett Packard 7470A x-y line plotter). The arrangement is shown schematically in figure 5.1. The voltmeter measured the corrosion potential of the electrode to a resolution of 1 μ V. The frequency at which individual measurements were taken was controlled by the microprocessor which also compiled acquired data, and subsequently performed an analysis of the collected data.

Based upon an empirical model (5.21), a prediction of corrosion rate, $\dot{C}_{pred}$, was made after analysis of collected data. After completion of each run all information was recorded by means of the output device. Integration of the system was achieved through an I.E.E.E. interface and the equipment operated as a single device.

Where a reference electrode was used, the saturated calomel half cell (SCE) was adopted. The calomel electrode has been found

to be the most suitable in other studies as it exhibits less noise and drift than other reference electrodes, such as, copper/copper sulphate and silver/silver chloride (5.12, 5.34).

Having experimented with various combinations of measurement interval period and total run time, measurements were taken over a 1000 second period at intervals of 1 second. By monitoring specimens in a variety of moisture conditions it was shown that the most reproducible results were obtained from specimens in a saturated condition. It was found to be of considerable importance that specimens were maintained in a uniform condition, both in terms of saturation and temperature, not only during monitoring but also for an equilibration period prior to a run. Rapid linear drift of the potential signal was frequently observed immediately after connection of the specimen to the measuring equipment. It was, therefore, found necessary to allow the specimen-equipment system a period of approximately 30 minutes to settle.

Owing to the high sensitivity of the measuring equipment some external intermittent interference was experienced. Such interference was manifested by sudden transient changes in the potential signal. Sources of interference were identified as switching of other electrical apparatus within the immediate vicinity of the test rig. The problem was eliminated by powering the measuring equipment through a mains smoothing device and using a grounded metal guard to shield specimens during monitoring periods.

With the system fully operational, and free from interference, measurement of potential noise was undertaken. Noise was measured in the systems described:

System one. Noise between an individual segment and external reference electrode (figure 5.2).

System two. Noise between an individual segment and an adjacent single segment in material of lower chloride concentration (figure 5.3).

System three. Noise between a single segment and all those segments in material of lower chloride concentrations (figure 5.4).

For all of the above systems the individual measurements of potential were compiled and computed as a standard deviation (SD mV). Standard deviation (mV) was used throughout this study as the measure of electrochemical noise.

In order to compare values of SD (mV) with values of corrosion rate ($\dot{\iota}_{corr}$), as determined by an independent means, two methods were used. For system one, linear polarisation (Chapter 2) was used to determine values of $\dot{\iota}_{corr}$. In order to establish any possible effects of the counter electrode, geometry and orientation to the working electrode, a double prong carbon rod and an adjacent steel segment were both used as counters (figure 5.5). For systems two and three, the galvanic macro-cell currents, $\dot{\iota}_{galv}$, flowing between the same coupled segments used for noise measurements were employed. For this purpose a high resolution ammeter, resolving to 1 μA, was used. Readings were taken after an initial decay period had elapsed, from the time of initially connecting to the couple. Measurements of $\dot{\iota}_{corr}$ and $\dot{\iota}_{galv}$ were taken immediately after the acquisition of noise data for each configuration, in order to minimise any possible influences arising from changes in the

specimens' condition.

An investigation of current noise had been planned for systems two and three. This investigation proved impractical however, because of the very low amplitude of current fluctuations which were not resolvable with the equipment available.

5.4 RESULTS AND DISCUSSION

The results for the micro-cell investigation, in system one, involving the measurement of potential noise between a single segment and an external reference electrode are presented graphically in figures 5.6 and 5.7 using a logarithmic scale. The corrosion rates in figure 5.6 have been determined by linear polarisation using the double prong counter electrode. Figure 5.7 shows noise determined by the same system (single segment, external SCE) but plotted against i_{corr} determined by linear polarisation using an adjacent segment as counter electrode.

From comparison of the forms of figure 5.6 and 5.7 it would appear that the different arrangements of counter electrode have made little difference to the values obtained for i_{corr}. This is probably due to the specimens being maintained in a near saturated condition which served to minimise their resistivity. Thus measurements of i_{corr} were not affected by a significant iR drop.

From figures 5.6 and 5.7 there exists a linear relationship between corrosion rate and standard deviation of potential noise. This relationship holds true at both high and low corrosion rates. The good agreement found at low values of corrosion rate (<0.1 $\mu A/cm^2$) is of interest as it would suggest that the data obtained was free from artefacts originating from unwanted external sources

of noise.

Values of standard deviation of potential noise have been used in a previously determined relationship (5.21) in order to calculate values of predicted corrosion rate, i_{pred}. The calculated values of i_{pred}, given in table 5.1, tend to overestimate i_{corr}. This variation is likely to be due, in part at least, to the differences between the specimens investigated here and those used to establish the empirical relationship.

The results from systems two and three, the macro-cell involving measurement of potential noise between two arrangements of segments, are given in figures 5.8 and 5.9. In both cases the corrosion rate was measured in terms of the galvanic current, i_{galv}, flowing between the same arrangement of coupled segments used to determine the potential noise. The values of i_{galv} were converted into corrosion rates by dividing the galvanic current (μA) by the total area of the anodic segment (cm^2). In doing so, it was assumed that a purely anodic segment was coupled with a purely cathodic segment(s). Making such assumptions is an oversimplification of the true electrochemical nature of individual segments. However, in net terms, it is reasonable to assume that, for instance, a segment in a 5% chloride environment will be anodic relative to segments in significantly lower chloride environments.

From figures 5.8 and 5.9 there exists a definite relationship between standard deviation of potential noise and i_{galv}. The relationship appears to be as well defined as the potential noise (SD) and i_{corr} relationship in the micro-cell system except at low values of standard deviation and i_{galv}. The increased scatter found at the low values may be attributed to an increasing error in the assumption of net anodic and cathodic segments at the lower levels

of chloride concentration.

Values of i_{pred} have been calculated, using the previously determined relationship (5.21), and are shown in table 5.2 A tendency for i_{pred} to overestimate i_{galv} has been found, as for system one where i_{pred} overestimated i_{corr}. The reason for this is not clear, but several factors may be involved. It is possible that due to significant differences in specimen composition, the corrosion current/potential relationship for the galvanic bar specimens was not comparable to those used previously. This possibility being the case, the previously devised relationship, upon which i_{pred} calculations were based, would not hold true.

5.5 CONCLUSIONS

The study of potential noise, determined for systems representing macro and micro-cell corrosion systems, has been supported by measurement of corrosion rate by linear polarisation (i_{corr}) and galvanic current density (i_{galv}). Good correlations have been found between standard deviation of potential noise for both i_{corr}(micro-cell) and i_{galv}(macro-cell).

For the macro-cell system, a linear relationship between standard deviation (mV) and i_{galv}($\mu A/cm^2$) was found where there was a clear distinction between coupled anodic (assumed) and cathodic (assumed) segments. This relationship became less clear as the definition between assumed anodes and cathodes diminished.

Using values of standard deviation in a previously determined relationship, values of predicted corrosion rate, i_{pred}, were calculated. Predicted corrosion rates tended to overestimate corrosion rates when compared to those measured in terms of

$\dot{\iota}_{galv}$ and $\dot{\iota}_{corr}$. A definite explanation for this was not established, but it was thought possible that variation in a corrosion current/potential relationship, due to specimen differences, may have contributed.

The clear relationship found between standard deviation of potential noise and corrosion rate, for the systems investigated, was thought to be largely due to the care taken in specimen preparation and maintaining stable conditions throughout the study. Sources of external interference would also appear to have been eliminated.

It is apparent that the conditions maintained throughout this study, found to be necessary in order to achieve success with the technique, are far removed from on-site conditions. It is, therefore, thought unlikely that potential noise can be utilised as a reliable method for determining corrosion rates in real structures.

SEGMENT (% chloride ion by weight of cement)	STANDARD DEVIATION (mV)	i_{pred} $\mu A/cm^2$	i_{corr} $\mu A/cm^2$		i_{pred} $\mu A/cm^2$	STANDARD DEVIATION (mV)
			external counter electrode	adjacent segment counter		
5.0	1.20	1.72	1.47	0.99	2.13	1.55
5.0	1.47	2.04	1.45	0.64	0.75	0.44
5.0	1.15	1.66	1.07	0.78	1.48	1.00
1.0	0.38	0.58	1.37	0.11	0.43	0.22
1.0	0.37	0.67	0.33	0.12	0.44	0.23
1.0	0.14	0.65	0.21	0.04	0.11	0.04
0.1	0.23	0.29	0.11	0.02	0.06	0.02
0.1	0.14	0.44	0.20	0.03	0.06	0.02
0.1	0.14	0.29	0.17	0.04	0.11	0.04
0.0	0.02	0.06	0.01	0.03	0.06	0.02
0.0	0.02	0.06	0.01	0.05	0.10	0.04
0.0	0.02	0.06	0.14	0.09	0.20	0.09

TABLE 5.1 Values of corrosion rate, i_{corr}, and predicted corrosion rate, i_{pred}, for the micro-cell system

SEGMENTS COUPLED (% chloride ion by weight of cement)	SINGLE VS MULTIPLE SEGMENTS			SINGLE VS SINGLE SEGMENT		
	STANDARD DEVIATION (mV)	i_{pred} $\mu A/cm^2$	i_{galv} $\mu A/cm^2$	i_{galv} $\mu A/cm^2$	i_{pred} $\mu A/cm^2$	STANDARD DEVIATION (mV)
5.0 vs 1.0 + 0.1 + 0.0	3.64	4.19	2.19	0.45	0.74	0.43
5.0 vs 1.0	1.04	1.53	1.02	0.42	0.71	0.41
	2.45	3.10	1.28	0.41	0.68	0.39
1.0 vs 0.1 + 0.0	0.06	0.15	0.09	0.03	0.13	0.05
1.0 vs 0.1	0.41	0.71	0.41	0.23	0.43	0.22
	0.43	0.74	0.22	0.06	0.17	0.07
0.1 vs 0.0	0.03	0.08	0.01	0.01	0.08	0.03
0.1 vs 0.0	0.09	0.20	0.01	0.01	0.08	0.03
	0.08	0.18	0.02	0.01	0.13	0.05

TABLE 5.2 Values of corrosion rate, i_{galv}, and predicted corrosion rate, i_{pred}, for the macro-cell system

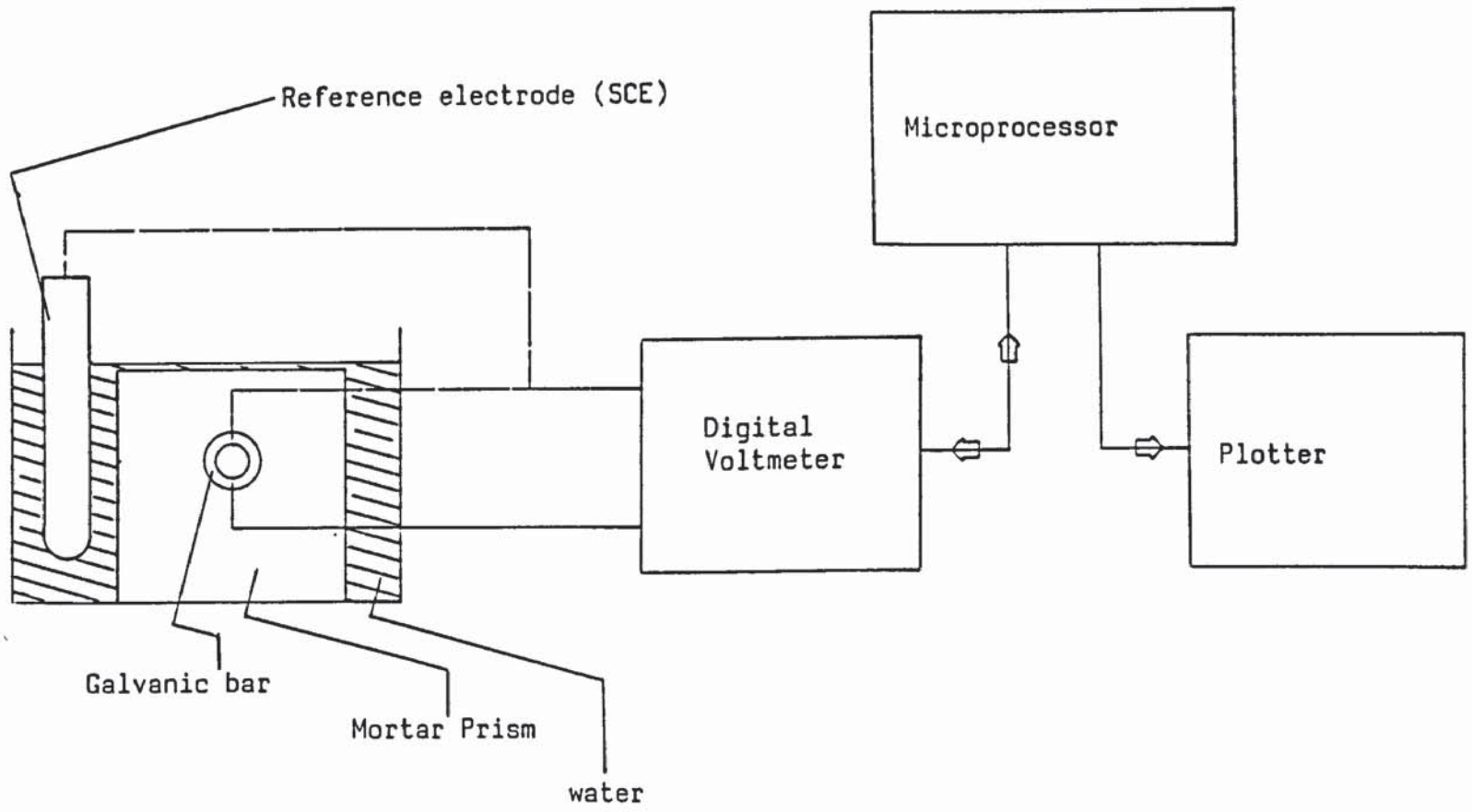

FIGURE 5.1 Schematic diagram of the experimental arrangement used for the measurement of potential noise

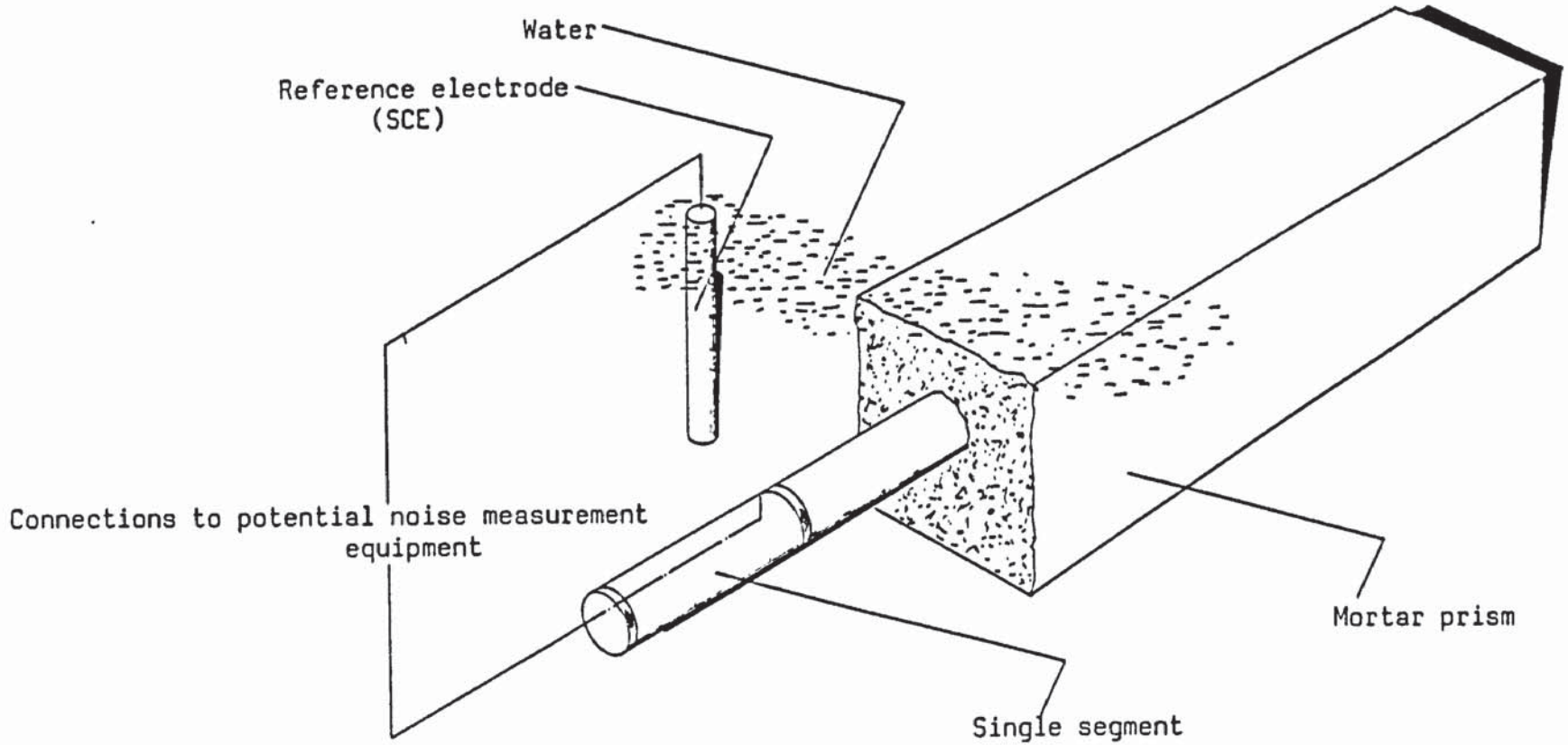

FIGURE 5.2 The general arrangement for potential noise measurement for system one ie. noise between single segment and external reference electrode

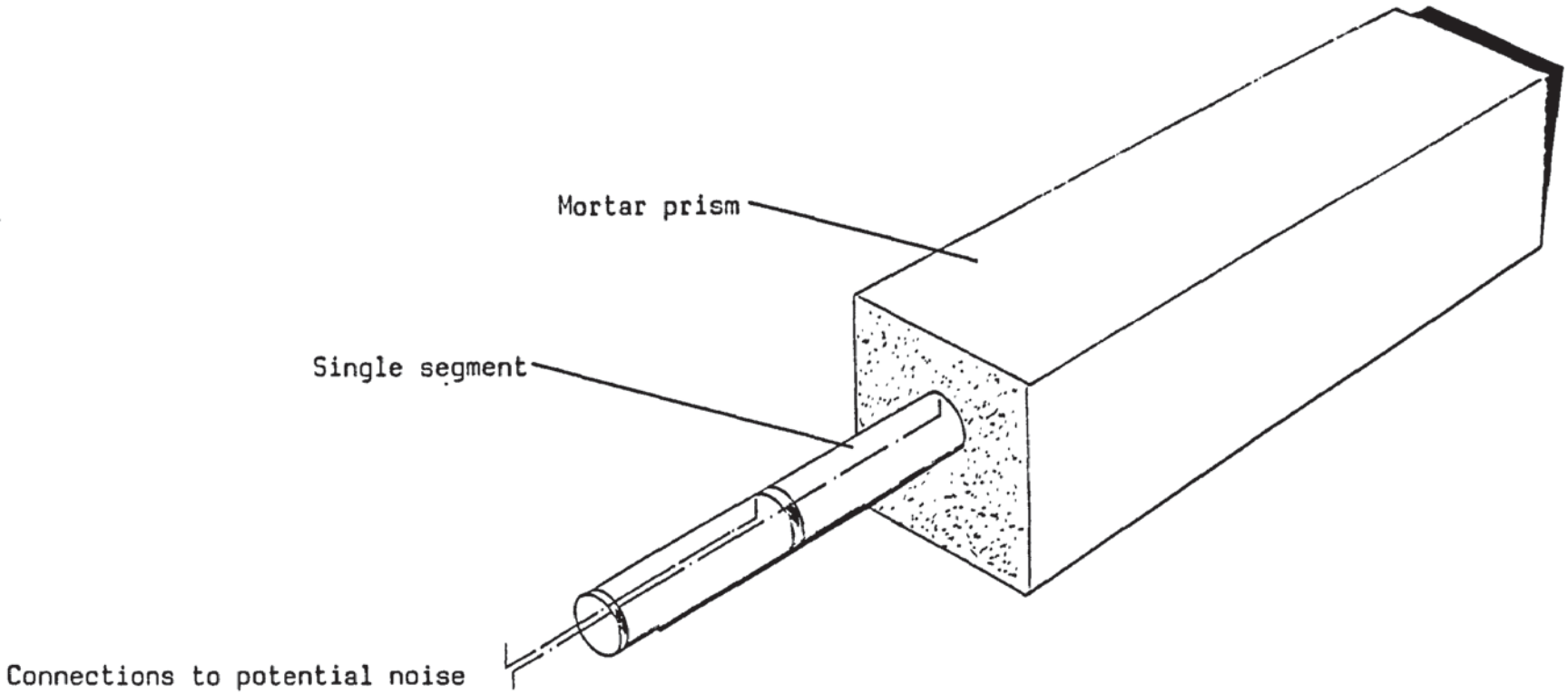

FIGURE 5.3 The general arrangement for potential noise measurement for system two ie. noise between an individual segment and an adjacent single segment in material of lower chloride concentration

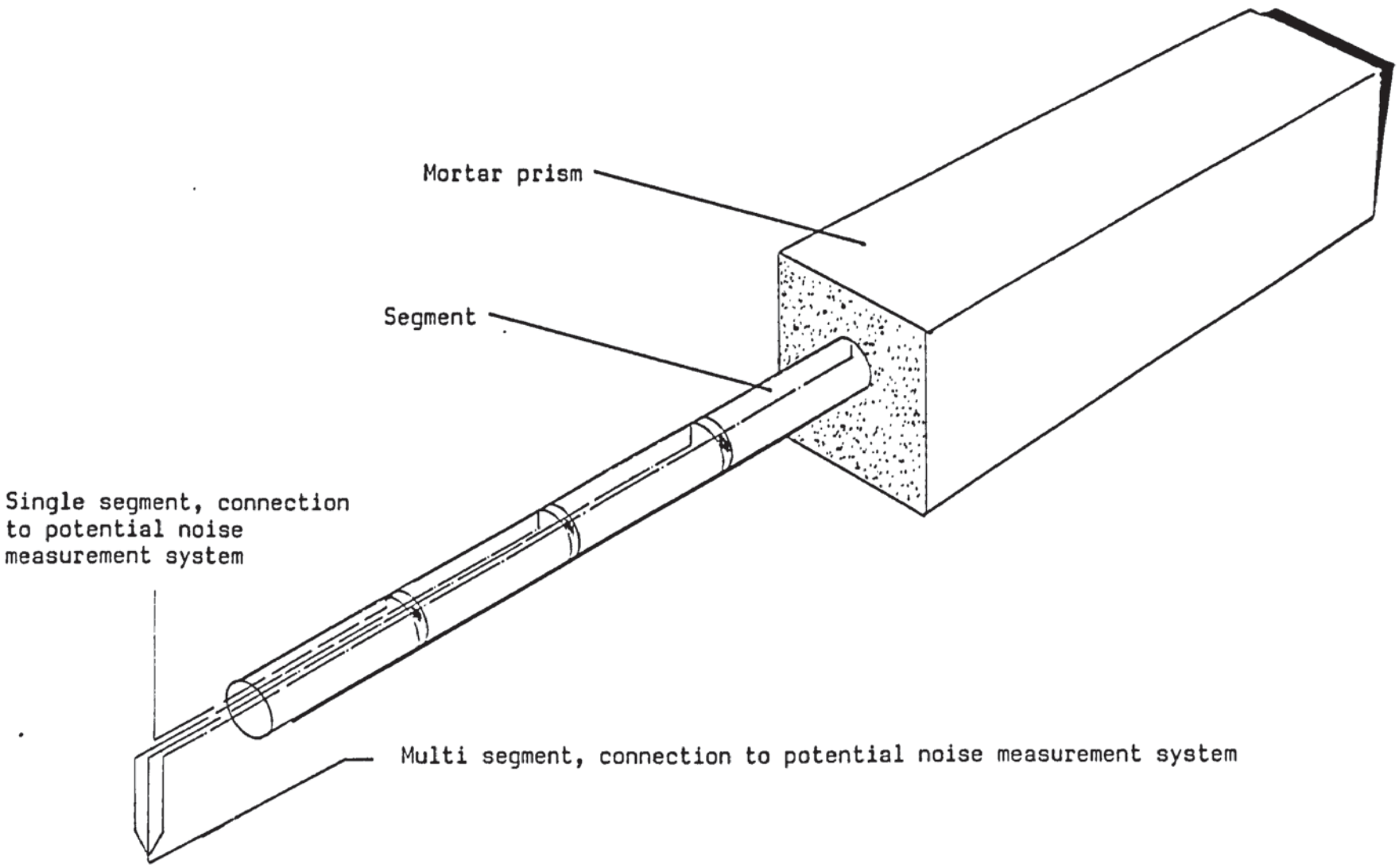

FIGURE 5.4 The general arrangement for potential noise measurement for system three ie. noise between single segment and all those segments in material of lower chloride concentration

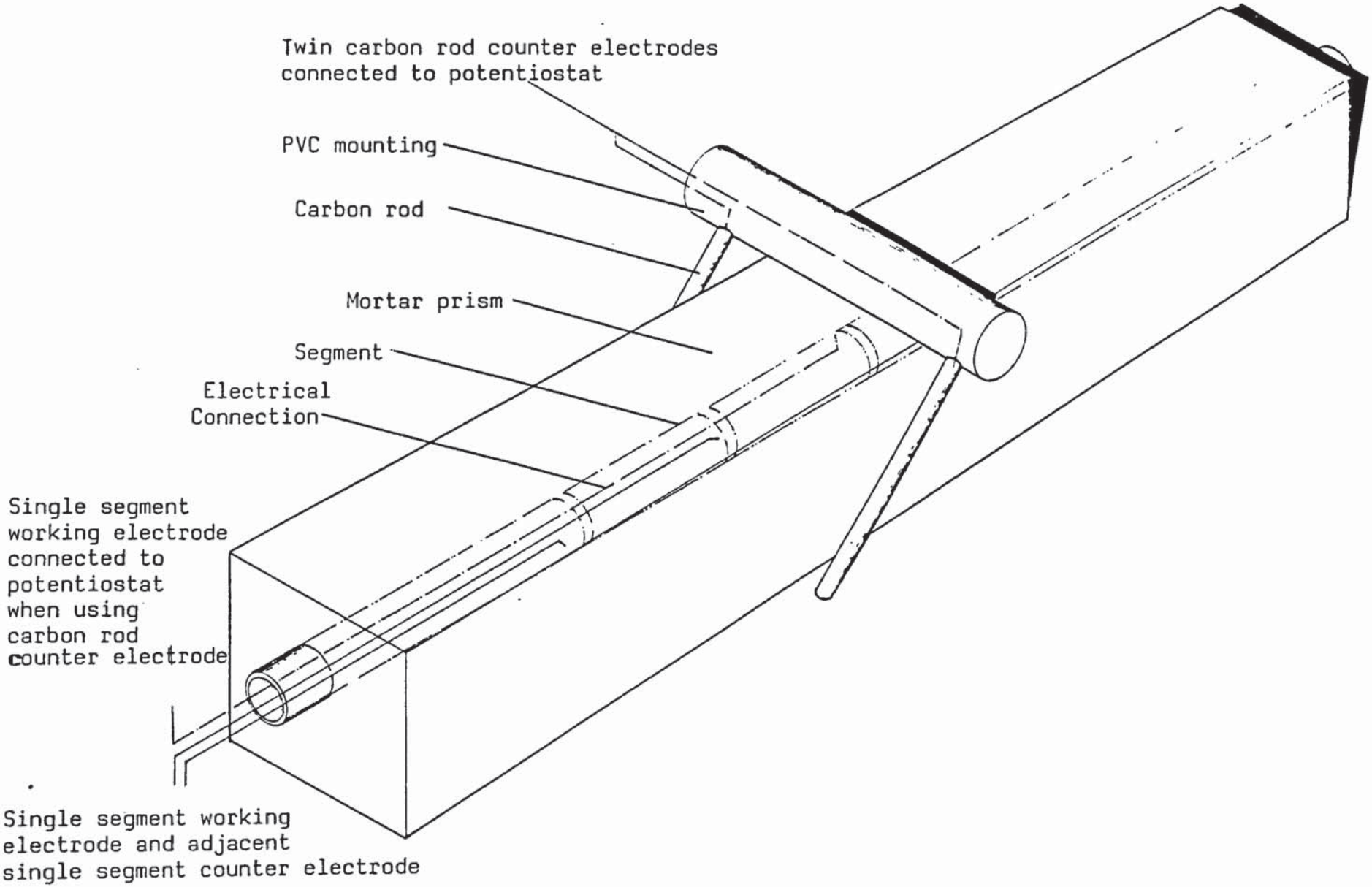

FIGURE 5.5 Counter electrodes used during linear polarisation measurement ie. carbon counter or adjacent segment counter electrode

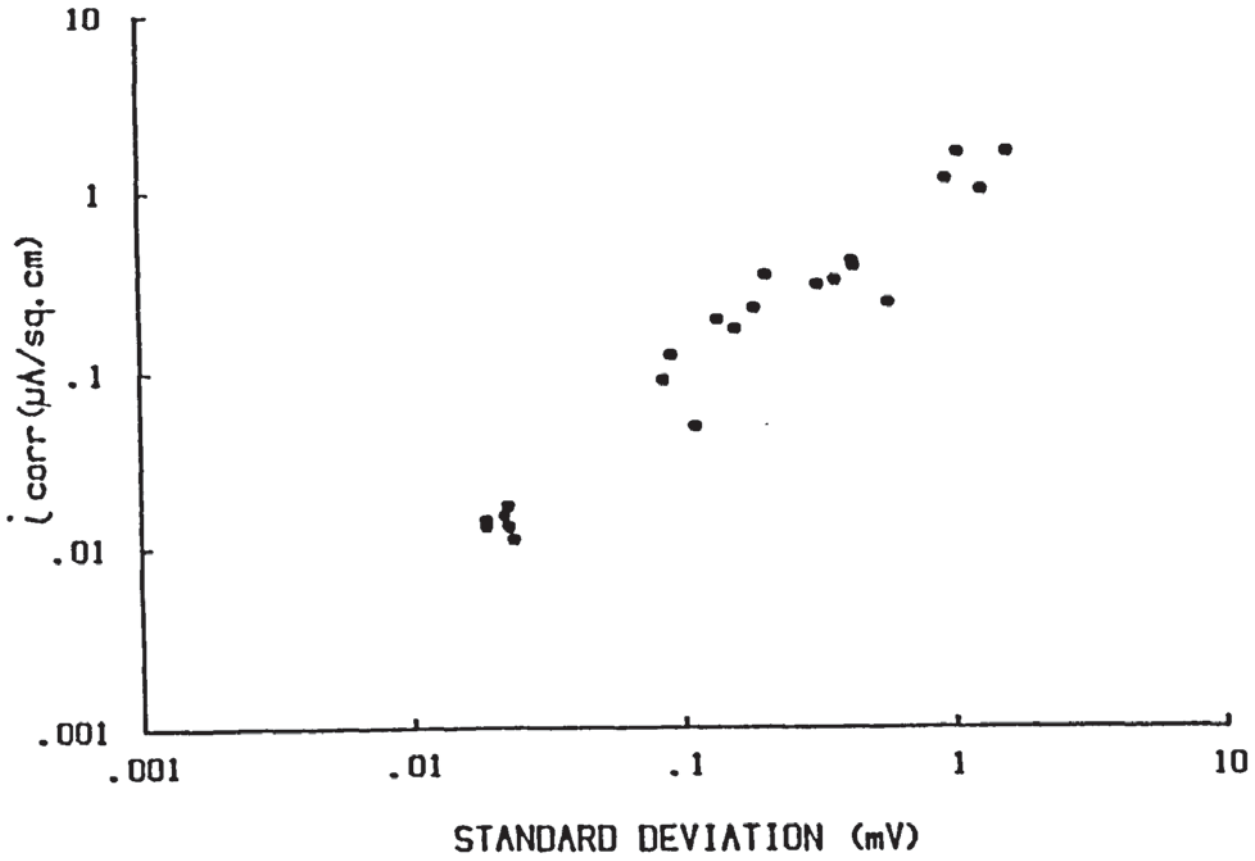

FIGURE 5.6 Results of the potential noise micro-cell study (system one), corrosion rate using carbon rod counter electrode

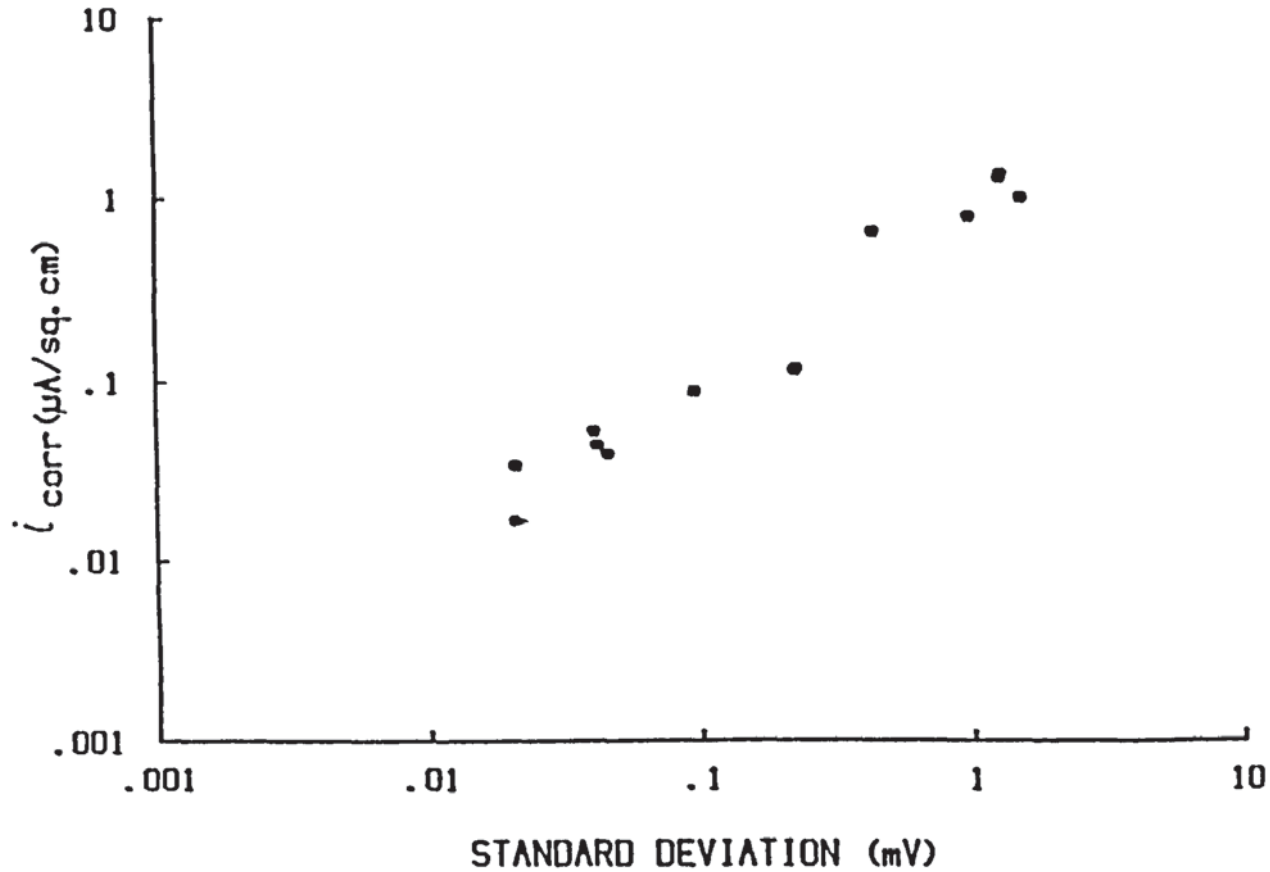

FIGURE 5.7 Results of the potential noise micro-cell study (system one), corrosion rate using an adjacent segment as counter electrode

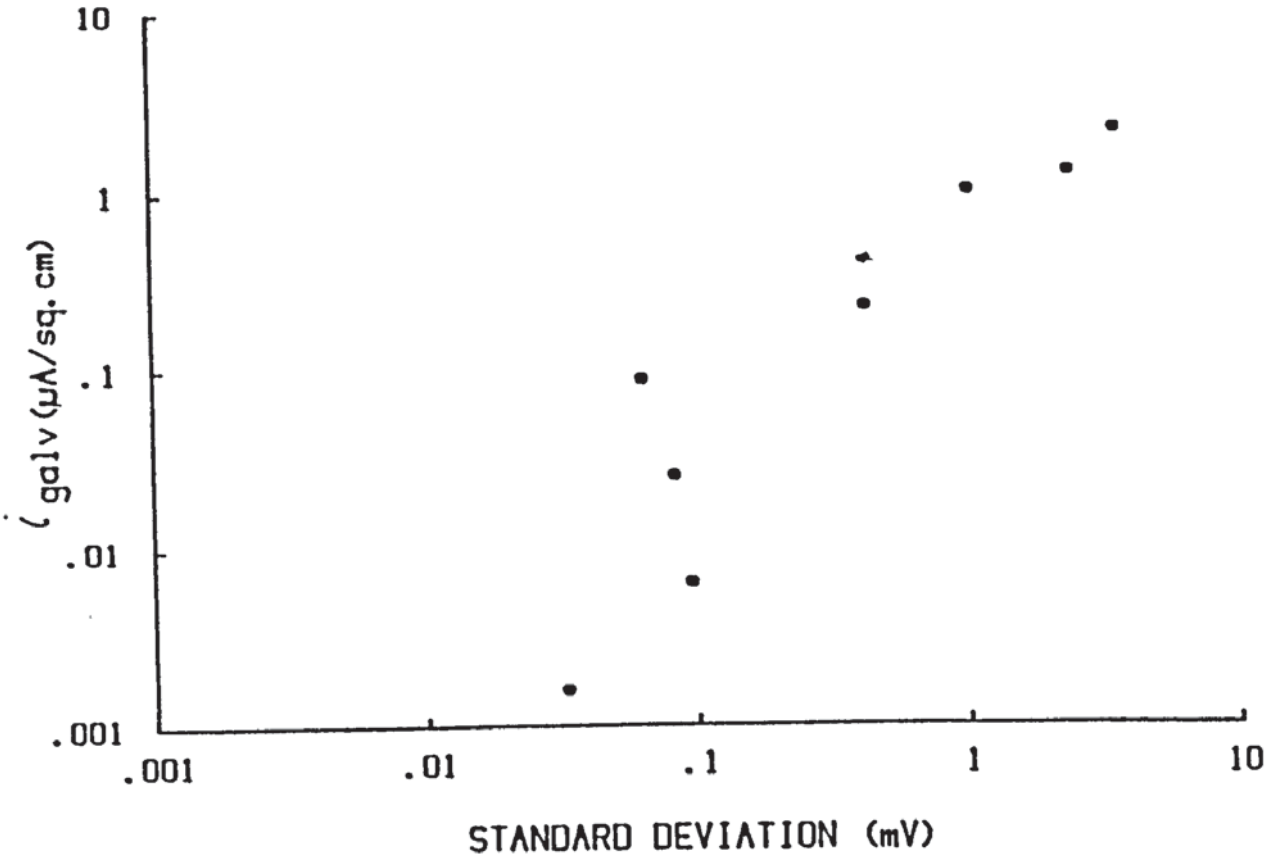

FIGURE 5.8 Results of potential noise macro-cell study (system two) for adjacent single segments and galvanic current measured for the same segments

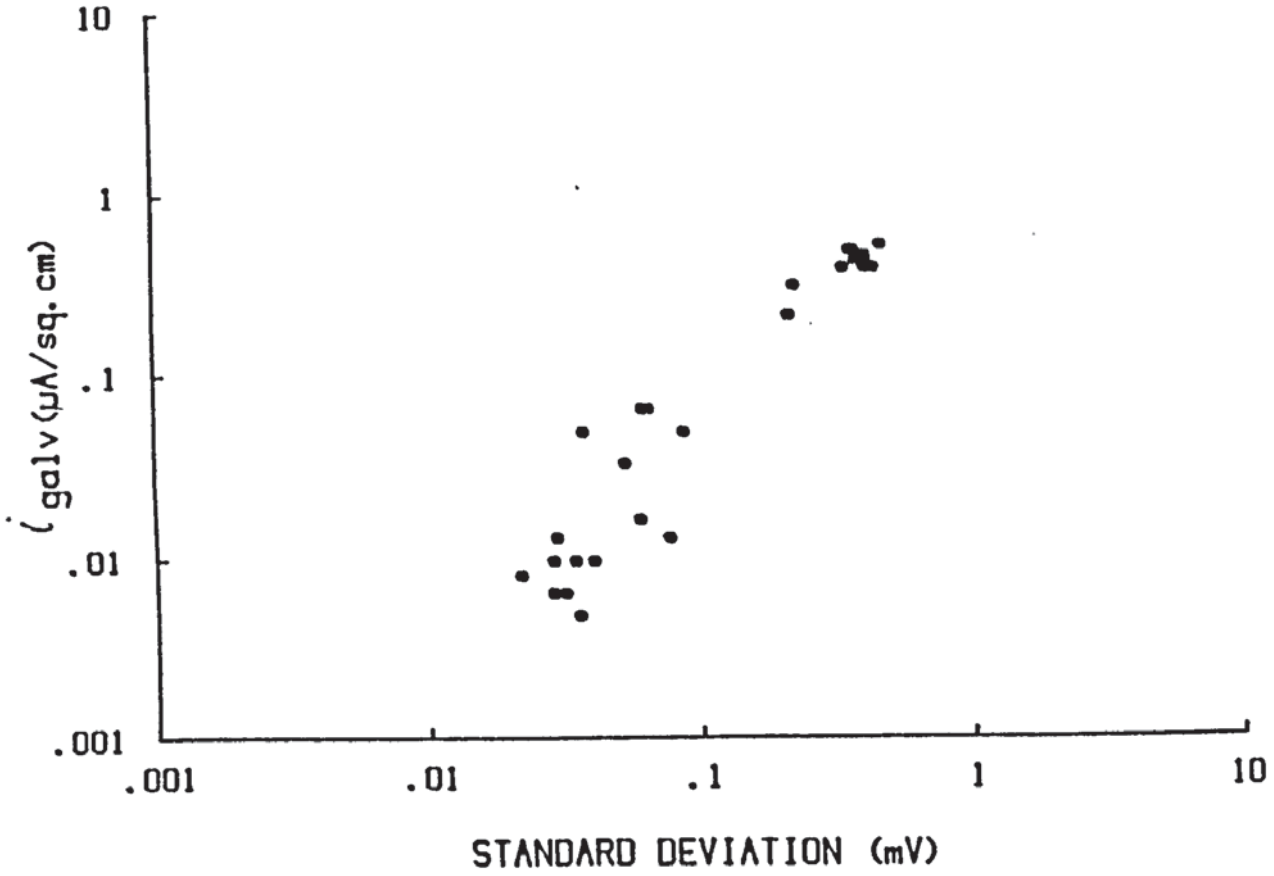

FIGURE 5.9 Results of the potential noise macro-cell study (system three) for single segments and all those segments in material of lower chloride concentration, galvanic corrosion current measured for the same segments

CHAPTER 6

THE INFLUENCE OF CATHODIC PROTECTION ON HYDROXYL ION CONCENTRATIONS IN CONCRETE PORE SOLUTIONS

6.1 INTRODUCTION

Cathodic protection, involving a displacement of the metal potential in the negative direction, is one of the most important and most widely used methods of corrosion control (6.1). The application of cathodic protection to reinforced concrete, however, is a comparatively recent application of an established technique.

The first recorded use of a cathodic protection system is attributed to Sir Humphrey Davy. Davy presented a paper to the Royal Society in 1824 (6.2) in which he described how the corrosion of copper sheathed ship hulls could be appreciably reduced. This was achieved by attaching sacrificial blocks of iron to the hull of the vessel in the ratio of iron to copper surface of 1 : 100. Although this was effective in preventing corrosion, cathodically protected copper vessels are prone to marine fouling and a consequential reduction in speed; hence the idea was not adopted for over a hundred years when marine anti-fouling paints became available.

Cathodic protection by means of an impressed current, as opposed to a sacrificial anode system, started to be used in the United Kingdom and United States around 1910-1912 when it was applied to underground structures (6.3). Today, cathodic protection has applications as diverse as marine steel sheet piles (6.4) and aircraft fuel systems (6.5).

To elucidate the rationale for the investigation undertaken in this chapter, it is first necessary to provide a theoretical explanation of the mechanism of cathodic protection. The interpretation given here is based upon the original theories of Mears and Brown (6.6) and Hoar (6.7).

Corrosion (within an aqueous environment) proceeds by coupled electrochemical reactions; an anodic (oxidation) reaction involving the dissolution of metal and a cathodic (reduction) reaction. An arbitar system is given below

$$M \longrightarrow M^{+} + e^{-} \quad \text{anodic} \quad (6.1)$$

$$Z^{2+} + e^{-} \longrightarrow Z^{+} \quad \text{cathodic} \quad (6.2)$$

The reaction given by equation (6.1) involves metal atoms (M) dissolving as metal ion (M^{+}), the metal liberating an electron (e^{-}). In order to maintain electrical neutrality the reaction given by equation (6.2) occurs simultaneously, the reduction of an arbitary species Z^{2+} (present in the electrolyte) to Z^{+} ions which consumes an electron (e^{-}). Both of these reactions (6.1) and (6.2) involve electrons, thus it is possible to express rates of reaction (i.e. rate of corrosion) in terms of charge passed (Columbs per second or amps), usually referred to as current densities i_a and i_c . It has been established for many cases that these reaction rates obey a logarithmic (Tafel) relationship when expressed as a function of potential (6.8):

$$\eta a = \beta a \log i_a / i_{o,a} \quad (6.3)$$

$$\eta c = \beta c \log i_c / i_{o,c} \quad (6.4)$$

where ηa and ηc are changes in potential from the equilibrium potentials of the two reactions (known as polarisation or overpotential) caused by i_a and i_c. The constants $\beta a, \beta c, i_{o,a}$ and $i_{o,c}$ can be explained in terms of the plot given in figure 6.1 of

current density/potential (6.9). The reaction rates of the processes in equations (6.1) and (6.2) are shown on a logarithmic scale as a function of potential, and are straight lines. Where the rates of reduction and oxidation are found to be equal ($i_a = i_c$) a steady state corrosion potential E_{corr} is found and the rate of dissolution (i_a) of metal atoms (M) equals the corrosion rate, i_{corr} , of the metal. Thus at E_{corr} , $i_a = i_c = i_{corr}$.

The slopes of the semilogarithmic polarisation curves of the reactions (6.1) and (6.2) are denoted by βa and βc, referred to as Tafel coefficients, with units of potential (volts per decade on the log scale).

If the potential of the metal is forced in a negative direction (cathodic polarisation) by applying an overvoltage, more electrons are made available to both anodic and cathodic reactions. The result is to depress reaction (6.1) and accelerate reaction (6.2), so that the net rate of dissolution is diminished and the metal is said to be cathodically protected. This condition is illustrated in figure 6.1 where the externally impressed overvoltage ε_c is produced by applying a current i_{app} to the corroding metal. The anodic reaction is depressed to i'_a with a corresponding increase in the cathodic reaction i'_c . As $i_{app} = i'_c - i'_a$ charge neutrality is maintained. The ideal rate of current supply i_{app} is that which reduces the corrosion rate i'_a to an 'effective zero' at potential $E_{o,a}$.

The data points in figure 6.1 (Δ and o) represent imaginary anodic (Δ) and cathodic (o) polarisation curves of i_{app} vs potential. These curves provide a basis for the determination of i_{app}.

Extraneous factors will seriously reduce the validity of theoretical cathodic polarisation curves. In situations where the reactants involved in the electrode oxidation and reduction processes are in short supply the reaction rate will be limited by mass transport processes such as diffusion. An example of concentration polarisation would be limited oxygen availability at the cathode in which case the rate limiting diffusion current could not be exceeded by i_{app} (6.10). Resistance polarisation, ohmic or resistance potential drop (i_{app} R), due to the resistance R of the electrolytic medium, can be responsible as a major source of error in applying theoretical cathodic polarisation curves. Resistance polarisation prevents the accurate measurement of the potential of the metal, thus hindering the accurate calculation of the cathodic polarisation necessary to achieve a 'zero' rate of corrosion.

The general cathodic reaction given in (6.2) will in practice involve hydrogen ions or dissolved oxygen :

$$2H^+ + 2e^- \rightarrow H_2 \qquad (6.5)$$

$$O_2 + 2H_2O + 4e^- \rightarrow 4OH^- \qquad (6.6)$$

In each case these reactions will result in an increase in pH within the electrolyte at the metal interface owing to the removal of hydrogen ions or the production of hydroxyl ions. In the case of steel subjected to cathodic protection in concrete, it is reaction (6.6) involving the production of hydroxyl ions that is of most interest.

Generally in cathodic protection engineering a rise in pH can cause effects such as saponification of paints, or, cathodic corrosion in the case of amphoteric metals such as aluminium and lead. Large negative potentials may also promote reaction (6.5), a

consequence of this being hydrogen embrittlement of high strength steels. Additionally, overprotection at unnecessarily large negative potentials will lead to increased power consumption and increased running costs. It becomes apparent that protection potentials should not be allowed to become too negative. In the case of steel in certain types of concrete, excessively negative potentials may be equally deleterious if associated with a significant increase in pH within the already alkaline pore electrolyte phase of the concrete (6.11). The mechanism associated with alkali-aggregate reactions in concrete involves the imbibition of water by an expansive alkali-silica gel formed as reaction with alkali proceeds (6.12 and 6.13). Unstable aggregates and high pH are required for this phenomenon to proceed. The possible implications of inordinately large cathodic potentials become apparent for structures containing marginal aggregates.

Customarily, a protection potential of -850mV ($Cu/CuSO_4$) is specified as the optimum protection potential for ferrous structures in soil (6.14) and sea water (6.15). However, a survey of actual installations found no particular protection potential to be superior for all applications (6.16).

Considerable experience has been gained in protecting buried structures, for which early recommendations date from 1933 (6.17), and yet there is a diversity of opinion as to the optimum protection potential for such applications. Perhaps it is, therefore, not surprising that universal agreement cannot be found regarding the optimum protection potential for steel in concrete, since this is a relatively new application of the technique.

The increasing usage of de-icing salt in the United States (6.18, 6.19) has been responsible for premature deterioration of

reinforced concrete road bridges. This has been due to chloride induced corrosion of embedded reinforcements. A considerable volume of research work has been carried out in the United States in applying cathodic protection systems to reinforced concrete bridge structures (6.20-6.24).

Development of new cathodic protection methods and materials are now providing a technology for the application of the technique to reinforced concrete structures of various geometry (6.25, 6.26). The individual components of a system will vary between installations but the prerequisites for a successful system are common:

1. A souce of current, usually ac rectified to dc.

2. A means of distributing the current evenly over the surface of the structure.

3. A structure in which all the reinforcing steel is continuous.

4. A predetermined protection potential at which to operate the system.

It is perhaps this last requirement (4) that is of most interest and of fundamental importance. In the absence of a unified approach to the optimum protection potential for reinforced concrete structures it was decided to cathodically protect chloride-contaminated specimens, over a range of polarisation potentials, in order to establish whether the generation of

hydroxyl ion at the cathode could be detected and also be related to the polarisation potential applied.

6.2 PREVIOUS WORK

A review of work published on protection potentials, E_{cp}, has revealed that a wide range of values of E_{cp} have been used in the study of cathodic protection for reinforced concrete.

The most commonly used value of E_{cp}, -850mV (CSE), has been adopted as a consequence of the experience gained by the steel pipeline protection industry. It is apparent however, that the pore electrolyte phase of concrete does not resemble the electrolyte phase of a soil medium.

It has been shown that steel, with damaged concrete cover, can be protected over a range of E_{cp} -710 to -810mV (CSE) (6.27). Studies of uncorroded and corroded steel (both in chloride environments) suggested that protection could be achieved at -500mV (CSE)for uncorroded steel and -710mV (CSE) for protection of active steel (6.28). It was also suggested that E_{cp} -850mV (CSE) for steel in a passivating Portland cement environment, is not applicable and may result in overprotection.

Studies using a 0.4% carbon steel in a saturated calcium hydroxide solution containing sodium chloride, up to a 5 molar concentration, revealed that protection could be achieved at -770mV (CSE) (6.29). The same investigation showed that values of E_{cp} -770mV imparted protection against pitting and crevice corrosion. It should be noted that these studies (6.28, 6.29) were carried out on steel immersed in solutions designed to represent the composition of the pore electrolyte phase of hydrated Portland

cement and therefore did not reflect the diffusive or resistive characteristics of hardened concretes. Figure 6.2 suggests potentials of approximately -700mV (CSE) would be sufficient to maintain steel within the domain of 'perfect passivity' and prevent corrosion even in the presence of high chloride concentrations.

It has been suggested that in conditions of high alkalinity, values of E_{cp} -900mV (CSE) are required for protection (6.31, 6.32). As indicated in figure 6.2 values of E_{cp} more negative than approximately -1100mV (CSE) are likely to evolve hydrogen (as a gas) and promote bond failure at the steel concrete interface (6.18, 6.27). There is also the risk of hydrogen embrittlement of the steel, particularly in the case of prestressed tendons. Studies were carried out to determine the value of E_{cp} at which hydrogen evolution occurred (6.33). This involved observations of the potential ($E_{B(H_2)}$) of hydrogen gas bubble formation on the steel. The work was carried out in solutions of various composition (based on $Ca(OH)_2$ containing chlorides), and showed $E_{B(H_2)}$ to fall between -970 and -1170mV (CSE) and to be solution composition dependent. Other workers have reported that potentials significantly more negative produced no deleterious effect upon bond strength. Experiments involving applied potentials of -740, -1140 and -1540mV, vs saturated calomel electrode (SCE), did not indicate bond failure after two and a half years exposure (6.34). A recent study remarkably reported a 61% increase in bond corresponding to E_{cp} -1350mV (SCE) (6.35). An early investigation of bond thought that the increase in bond was attributable to the gradual dissolution of the passive layer. The products of the dissolution were thought to 'clog' concrete around the steel, hence increasing bond strength (6.36). However, this suggestion is

at variance with the findings of a study involving mechanical characteristics and electrocapillarity of steel/mortar interfaces (6.50). Part of this study involved the potentiostatic polarisation of steel electrodes embedded in cement paste of 0.3 water/cement ratio. The most negative potential applied was -1100mV (SCE) which induced a reduction in the tensile bond strength. This finding was attributed, in part, to hydrogen evolution giving rise to increased porosity within the steel/cement interfacial zone.

Measurements of ionic migration in cathodically protected specimens (E_{cp} -680 to -780mV (CSE)) have indicated an accumulation of sodium and potassium ions in the region near to the reinforcement (6.37). Despite these relatively modest values of E_{cp}, a degradation in bond was found. This was attributed to the high concentrations of sodium and potassium ions giving rise to a softening within the cement matrix in the vicinity of the reinforcement. An investigation of anodic reactions reported a lowering of pH near the anode, and also, an accumulation of chloride ions - due to their migration from the cathodic region (6.51). A study currently in progress has the objectives of measuring the diffusion of alkali ions (sodium and potassium), under the influence of applied potential. Additionally, it is intended to examine the possibility of increased concentrations of sodium and potassium ions, in the vicinity of the reinforcing steel, initiating alkali aggregate reactions (6.52).

Currently in preparation is the draft of recommendations for the protection criteria for reinforced concrete structures above ground. The bodies involved are the National Association of Corrosion Engineers (NACE), and the Institute of Corrosion Science and Technology (I Corr ST). Both the NACE committee (T-3K-2) and

the NACE/I Corr ST joint venture task group (E4-9), are likely to recommend a 100mV depolarisation decay of potential, over a four hour period, subject to a minimum potential of -1100mV (Ag/AgCl) (6.53, 6.54).

It is apparent from the above review that considerable divergence of opinion exists with regard to (a) protection criteria, (b) as to whether degradation occurs within the region of the cathodic reaction and (c) if it does, as to the precise mechanism responsible.

Whilst previous workers have investigated the effects of hydrogen evolution and the migration of alkali metal ions, there appears to be a lack of work relating to the distribution of hydroxyl ion in reinforced concrete subjected to cathodic protection. This is considered to be an important issue since hydroxyl ions (rather than sodium or potassium) are believed to initiate alkali silica reaction in concretes containing reactive aggregates (6.55). The experimental work to be described in the following section was therefore aimed at elucidating changes in hydroxyl concentration of the pore fluid in concrete immediately adjacent to steel mesh subjected to cathodic protection at various potentials. The method of sampling pore solutions was based on the technique devised by Longuet (6.38) and used by several other researchers studying aspects of pore solution chemistry (6.39-6.41).

6.3 EXPERIMENTAL

The study undertaken involved a number of cathodically protected (chloride contaminated) specimens. The protection

potentials (E_{cp}) selected, were those thought to cover a range of values of cathodic polarisation likely to be used in practice. A total of fourteen specimens of uniform design were prepared, representing triplicate specimens at each of the four values of E_{cp}, plus two control specimens.

Specimen geometry was based upon the 500 x 100 x 100 mm British Standard prism mould. The reinforcement, which was selected on the basis that it represented a scaled down model of BS reinforcement mesh, was mild steel of 1.6 mm bar diameter, with a 12 x 12 mm square spacing. Mesh sheets were prepared to the dimensions shown in figure 6.3. In order that electrical connection could be effected, and also to provide uniform concrete cover depths, the following procedure was followed. Sheets of mesh were trimmed in order to provide two tails of wire which could later serve for external electrical connection. In order to avoid crevice corrosion at the steel/environment interface, a masking technique was adopted similar to that described in Chapter 3. Prepared mesh reinforcement was then fixed within the moulds at the required depth using brick chairs. Prior to the pre-casting procedure all mesh sheets were grit blasted and degreased with 'Inhibisol' to produce a consistent surface finish.

The mortar was a mix of two parts sand and one part cement with a water/cement ratio of 0.5. The sand was a zone 2 concreting sand and the cement was an ordinary Portland cement, an analysis of which is given in Chapter 2. The procedure for mixing, casting and vibrating are given in Chapter 2. In order to initiate corrosion of the steel reinforcement at an early stage, the mix was contaminated by dissolving chloride ion (4% sodium chloride by weight of cement) in the mix water. This necessitated speed and care during the

casting operation, in view of the set accelerating effect of the contaminant. Specimens were demoulded twenty four hours after casting and then cured in saturated air for twenty eight days. After this curing period, specimens were connected to the cathodic protection system.

In order to apply a current to the steel reinforcement mesh, a cathodic protection system as shown in figure 6.4 was employed. The system comprised primary anode strips of austenitic stainless steel type 316 arranged longitudinally on the top surface of each protected specimen (stainless steel analysis given in Chapter 2). To aid even current distribution across the entire top surface of each specimen the primary anodes were sandwiched between two layers of cotton wool. The specimens were kept permanently wet with an approximately 0.5 molar sodium chloride solution which maintained the cotton wool in a conductive state.

The four values of E_{cp} selected were: -700, -850, -1000 and -1150mV (SCE). At each value three parallel specimens were polarised by applying variable current to them from a proprietary dc stabilised current/voltage source.

Values of E_{cp} were checked on a regular basis by measuring the actual value of E_{cp} of the steel against a reference electrode (SCE). Any discrepancy between the desired value of E_{cp}, and that measured, was corrected by manual adjustment to the power supply. These measurements and adjustments were carried out with the currents switched on. All specimens were maintained at their respective levels of polarisation for a period of five weeks. It was considered that any errors in controlling the applied potential, due to the IR drop, would be small in view of the conductive nature of the chloride solution and saturated condition

of the specimens.

In addition to the triplicates of cathodically protected specimens, duplicate control specimens (no cathodic protection) were maintained within the same environment as those protected.

In order to investigate the nature of the pore solution near the electrode, material, from the near vicinity of the mesh, required examination. For this purpose a crush-sectioning technique, previously developed at Aston was utilised (6.42). This technique involved wrapping individual prisms within flexible polythene jackets and loading them in a compression machine, the platens of the machine having first been lubricated in order to reduce the frictional restraint at the polythene/plattern interface. The prism was then loaded to failure, such that a uniformly shattered specimen with many longitudinal fracture planes was produced. Material from a zone extending approximately 4 mm either side of the reinforcement was then removed, in order to provide debris material for pore solution expression. Hydroxyl ion concentrations were determined by titrating the pore solution expression against nitric acid (see Chapter 2). A minimum of time was allowed to elapse between crush sectioning and titrating the pore solution in order to minimise the neutralising influence of atmospheric gases.

6.4 RESULTS AND DISCUSSION

The results obtained from the hydroxyl ion analysis are presented in table 6.1, where ionic concentration and equivalent pH are given as a function of polarisation potential.

From table 6.1 it is clear that the pore solution of the

cement/mortar matrix, near to the reinforcement, has developed significantly greater hydroxyl ion concentrations than that of the reference set of specimens. The alkalinity of the control mortar is itself unremarkable and is in line with other Portland cements (table 6.2).

Whilst an elevation in hydroxyl ion concentration of approximately 50% was observed at all applied potentials, it has not been possible to establish a relationship between change in potential and change in ionic concentration. Variations in concentration found between the individual sets of cathodically protected specimens are not significant and are likely to have been associated with sample variability and experimental error.

The apparent consistency of the increase in hydroxyl ion concentration is itself notable. It suggests that for the practical application of cathodic protection to steel in concrete, significant changes in hydroxyl ion concentration are likely to be induced. In practical terms a threshold potential above which the phenomenon becomes insignificant is unlikely to exist considering the range of potentials typically used on site.

During the experiment, the current density at the cathode was no greater than 80 mA/m^2. This value compares with initial switch-on cathode current densities which can be as high as 90 mA/m^2 under certain on-site conditions (6.43). However, values more typical for a fully operational on-site system are in the range 2 to 8 mA/m^2 (6.43).

The avoidance of alkali-silica reaction in new construction normally involves the limitation of alkali levels within the cement. It is usual to express the alkali level in terms of sodium oxide equivalent, the upper limit being 0.6% sodium oxide equivalent.

By assessing the hydroxyl ion concentrations in terms of sodium oxide equivalent, the control specimens were moderate (figure 6.5). However, the significant shift from pH 13.74 to 13.92 for the cathodically protected specimens equates to a sodium oxide equivalent of 1.1% sodium oxide equivalent (6.55), which is considerably in excess of the 0.6% sodium oxide equivalent upper limit. It is possible therefore, that under very specific conditions the application of cathodic protection would activate an incipient alkali aggregate reaction. These conditions would include; a cement of naturally low alkalinity, reactive aggregate and sufficient available moisture.

In considering the reactants involved in the reduction reaction at the cathode, an explanation for the phenomenon may be found. Of most interest is the reduction of oxygen and water to form hydroxyl ions, and the possibility that one of these species may have played a reaction rate limiting role. Specimens were maintained in a water saturated state throughout the duration of the experiments, hence it is inconceivable that the cathodic reaction would be stifled by the limited availability of water. It is more likely that oxygen access may have been rate limiting.

It has been shown that significant reductions in oxygen diffusion are found as relative humidity is increased in cement specimens of various type (6.44). Whilst the specific values given in figure 6.6 cannot be applied to this work, the possibility of reduced oxygen diffusion rates in the 'water saturated' condition applied to the cathodically protected specimens used in this study is apparent. Whilst there is some variation in the data relating to oxygen diffusion kinetics in cement systems (6.44-6.46), it was suggested that oxygen diffusion may be responsible, under certain

conditions, for promoting cathodically restrained dissolution in water saturated specimens of certain dimensions (6.47).

It would, therefore, appear plausible that for each of the cathodically protected specimens, the velocity of the cathodic reaction was not rate limited by E_{cp}, but by the availability of dissolved oxygen diffusing within the pore structure of the cement mortar matrix. As all cathodically protected specimens were subject to a relatively uniform environment this concentration polarisation, of the reduction reaction, may have been responsible for restraining i_{app} to i_{lim}.

It is of interest to consider the value of hydroxyl ion concentration measured for the -1150mV (SCE) specimen. This value of polarisation is equivalent to -909mV on the standard hydrogen scale (SHE) which is below the expected value required to allow cathodic production of hydrogen, -1170mV CSE (-854mV SHE). It would seem, however, that this additional reaction did not significantly enhance the development of a high pH zone near the cathode and that the main effect was due to oxygen reduction.

The implications of the results for cathodic protection applied to structures containing marginally reactive aggregates may be significant. The significant increases in alkalinity as were found in the pore solution could, under adverse conditions, be expected to initiate the expansive alkali silica reaction. It is, therefore, of some importance to determine if the increase in hydroxyl is restricted to a small region of matrix surrounding the reinforcement. Ions will diffuse away from the site of generation due to the imbalance in ionic concentration, and the effect of the applied electric field. The ionic gradient lying between the cathode and surface anode will be influenced by the rate of

hydroxyl ion diffusion, the effect of neutralisation caused by acidity produced at the surface anode and atmospheric gases. An ionic gradient of counter diffusing sodium and potassium ions has been found by other workers, when applying potentials within the range -680 to -780mV (CSE) (6.37). A reduction in pH near to the anode together with reduction in chloride at the cathode has also been observed (6.51).

The increase in concentration of hydroxyl ions near the cathode has been found to be independent of the polarisation potentials used in this study. Considering that the least negative potential applied in the present investigation (-700mV SCE) is likely to be more positive than the values of polarisation often used in practice, there is some cause for concern in the event of cathodic protection being applied to structures containing potentially reactive aggregates. It is notable that early cases of ASR identified in the United Kingdom were found at a number of power generating sub stations (6.48). It was indicated that direct "earth-loop" currents, a few amps in magnitude, could flow in the absence of an applied alternating current. It has also been found that the passage of a dc current appeared to accelerate the disruptive reaction between siliceous aggregate and alkali (6.49). Studies are currently in progress to determine the influence of cathodic protection on alkali-aggregate reactions using mortar bar expansion tests, and, also by determining diffusion of sodium and potassium ions as influenced by applied potential (6.52).

It was not the intention of this investigation to produce data on bond stress as a function of E_{cp}. However, a subjective assessment of the specimens after crush-sectioning suggested a softening of the cement matrix within the vicinity of the

reinforcement mesh. This assessment involved a very simple subjective measure of the comparative ease by which the cement/mortar matrix adhering to the mesh could be removed, when compared to the reference specimens.

The following visual observations were made regarding the condition of the reinforcement mesh taken from the specimens. The reference specimens showed extensive pitting, as would be expected for steel in such an aggressive environment. The -700mV SCE series displayed some slight evidence of pitting. This limited amount of corrosion may be due to pits initiated during the twenty eight day curing period, which were subsequently unable to repassivate during the period of cathodic protection. The remainder of the reinforcement sets (-850, -1000, -1150mV SCE) exhibited a surface oxide free from pitting, when initially removed from the mortar matrix.

6.5 CONCLUSIONS

By carefully extracting mortar from within the vicinity of the reinforcements in cathodically protected specimens, pore fluid expressions were achieved by means of a high pressure device. Subsequent analysis of the pore fluids revealed similar increases in hydroxyl ion concentration for each set of specimens containing steel polarised to different potentials in the range -700 to -1150mV (SCE). The lack of correlation between specific cathodic polarisation potentials and change in hydroxyl ion concentration is believed to signify a rate limiting oxygen diffusion step, associated with the near saturated condition of the specimens.

From a practical standpoint, the results suggest that under

certain circumstances an elevation in pore solution hydroxyl ion concentration may be possible. Of particular importance would be the influence of any such changes within the pore solution chemistry upon potentially reactive aggregates. It is not inconceivable that, under certain conditions, the application of cathodic protection, used in order to arrest the reinforcement corrosion, may trigger an incipient alkali silica reaction. This would, however, require the presence of a reactive aggregate in a concrete of insufficient natural alkalinity to cause alkali-aggregate reaction in the absence of cathodic protection.

A more positive conclusion was that cathodic protection greatly reduced the pitting of steel in concrete containing 4% sodium chloride by weight of cement when potentials of -700mV SCE were applied and completely suppressed pitting at more negative applied potentials.

Polarisation Potential E_{cp} mV vs SCE	Mean hydroxyl ion concentration OH^- m/l^{-1}	pH
-700	0.837	13.92
-850	0.836	13.92
-1000	0.835	13.92
-1150	0.829	13.92
Reference	0.550	13.74

TABLE 6.1 Results of hydroxyl ion pore solution analysis for various polarisation potentials

Description of Material	Alkalinity OH^- mmol/l^{-1} / pH	Age days	W/C	Analytical Procedure	Source of Data
OPC mortar + 4% NaCl	550 / 13.74	64	0.5	Pore press titration	Hardon, 1988
OPC 'A' + 0.4% Cl^-	741 / 13.87	84	0.5	ditto	Page, Short and Holden, 1986
OPC 'B' + 0.4% Cl^-	661 / 13.82	84	0.5	ditto	Page, Short and Holden, 1986
ASTM 1 OPC	600 / 13.78	174	0.4	ditto	Diamond, 1983
OPC + 1.0% Cl^-	836 / 13.92	56	0.5	ditto	Page and Vennesland, 1983
'British' OPC + 0.4% Cl^-	620 / 13.79	28	0.5	ditto	Andrade and Page, 1986
'British' OPC + 1.0% Cl^-	620 / 13.79	28	0.5	ditto	Andrade and Page, 1986

TABLE 6.2 Comparison of hydroxyl ion concentration for various cements and chloride levels

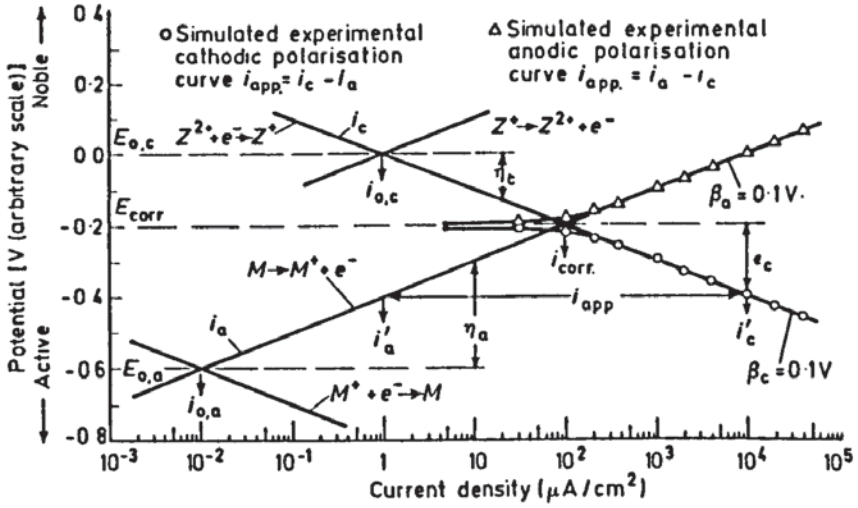

FIGURE 6.1 Theoretical basis for cathodic protection (after Jones (6.9))

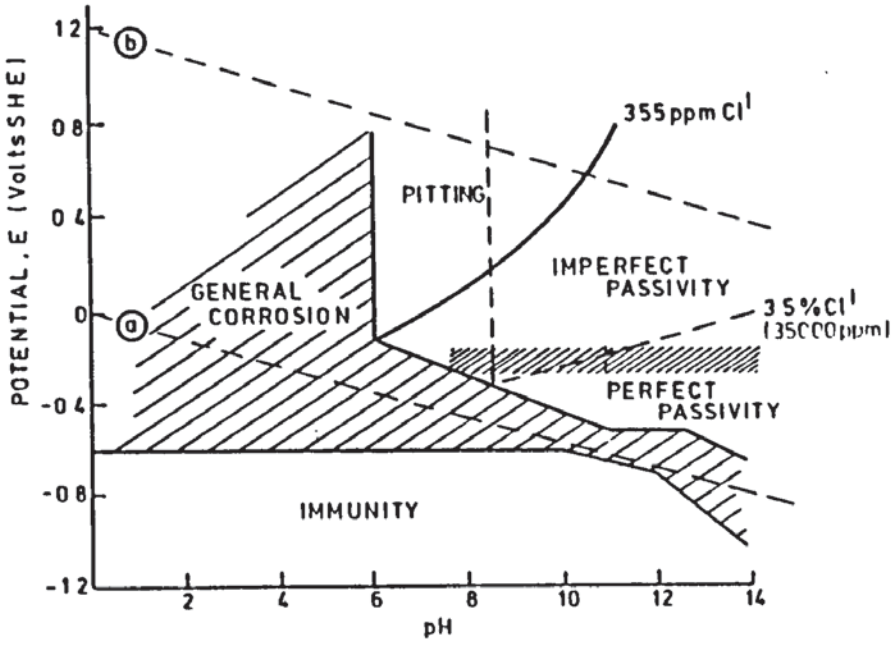

FIGURE 6.2 Influence of chloride on the passivation and corrosion of iron (after Pourbaix (6.30))

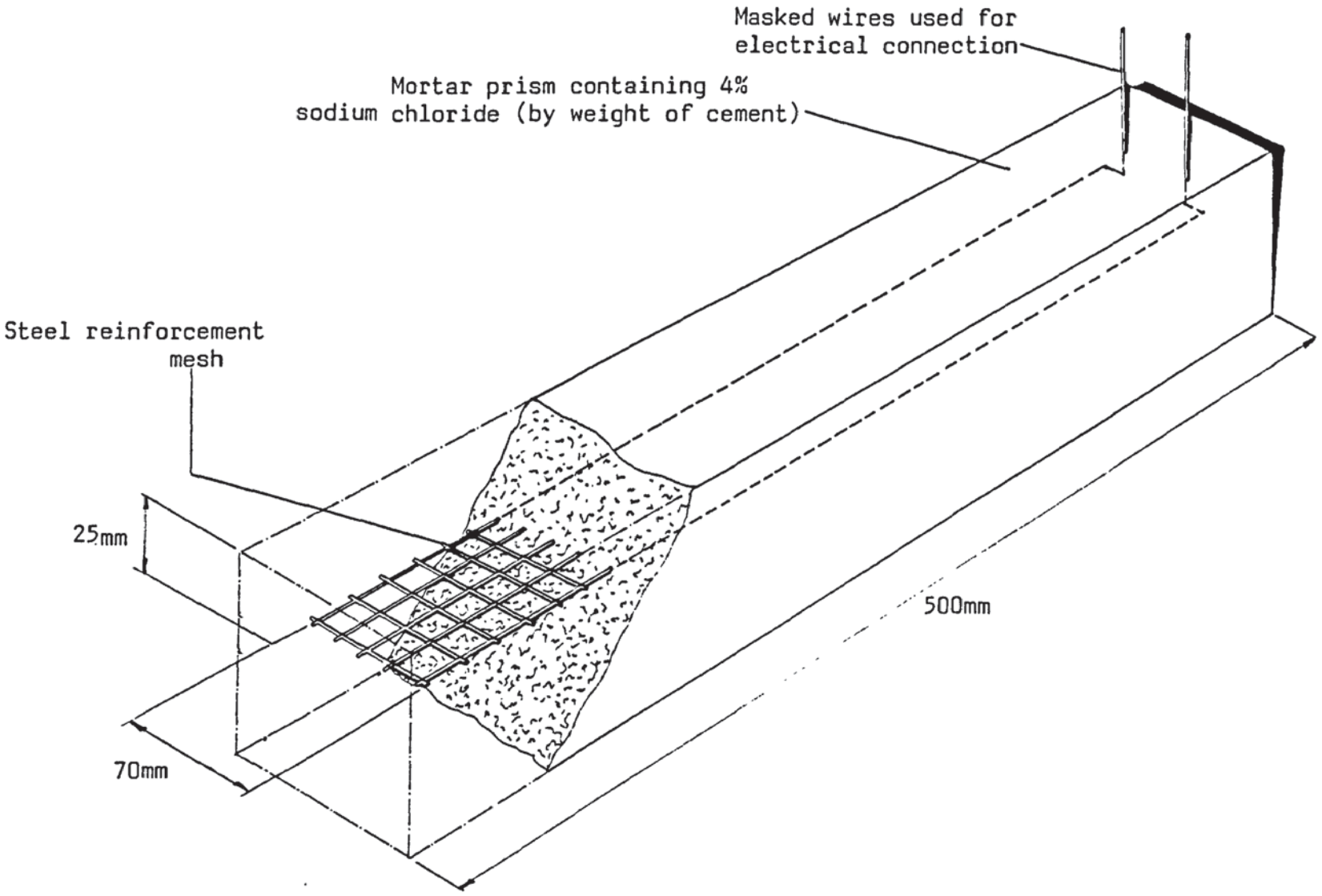

FIGURE 6.3 Cut-away isometric showing the cathodically protected mortar prism

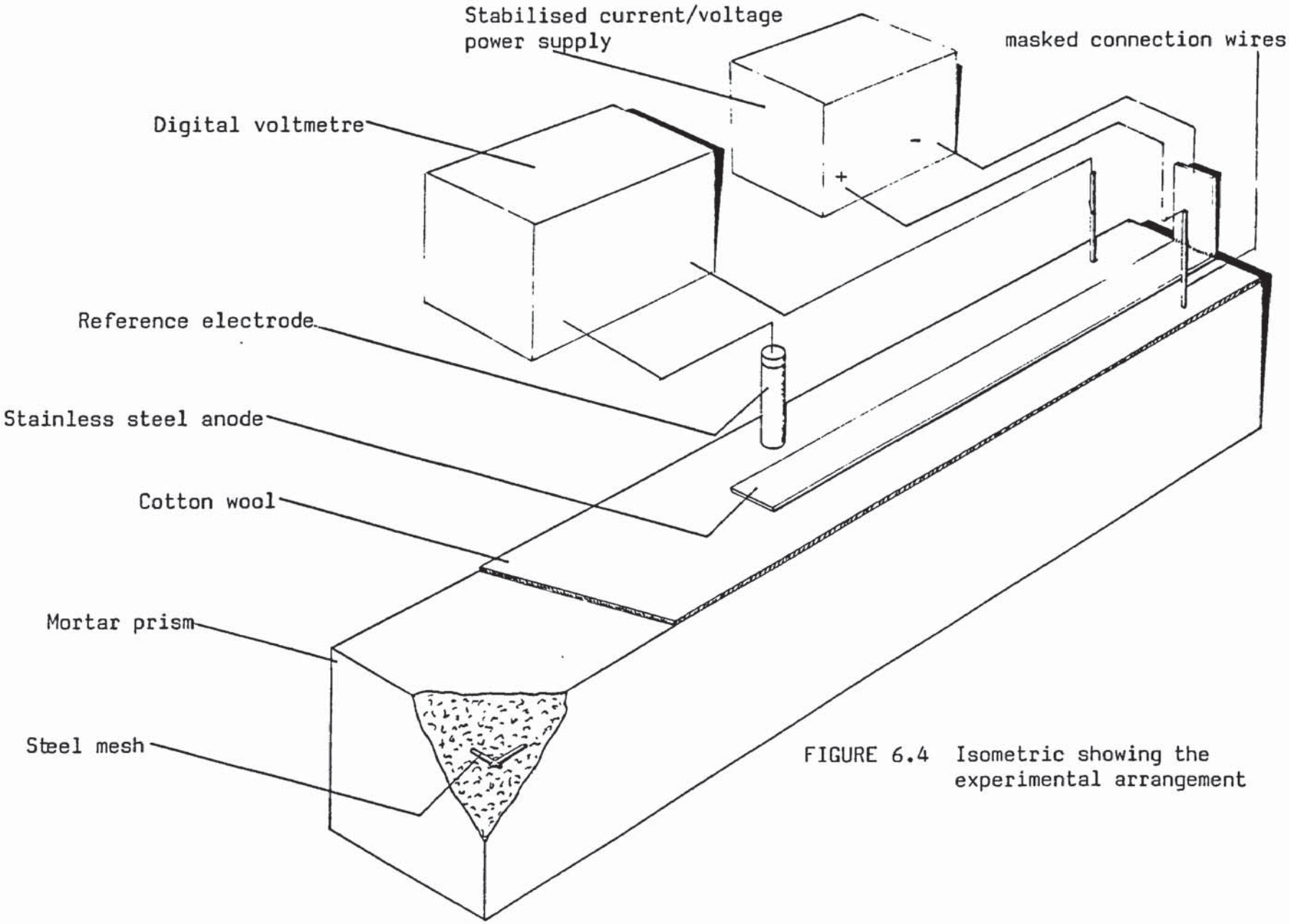

FIGURE 6.4 Isometric showing the experimental arrangement

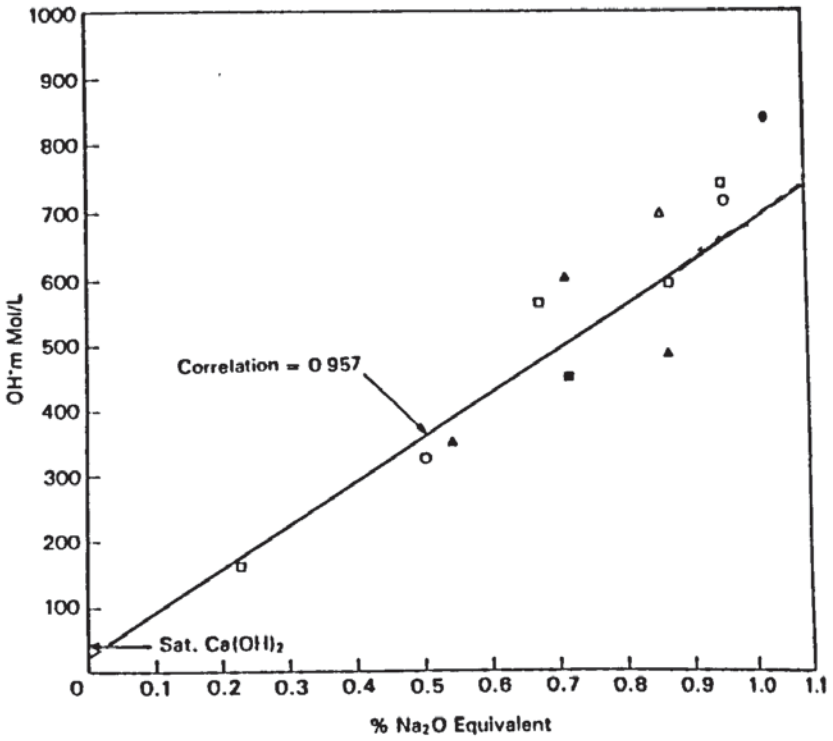

FIGURE 6.5 Hydroxyl ion concentrations and sodium oxide equivalents, in pore solutions from pastes (≯90 days old) at 0.5 water/cement ratio (after Nixon and Page (6.55))

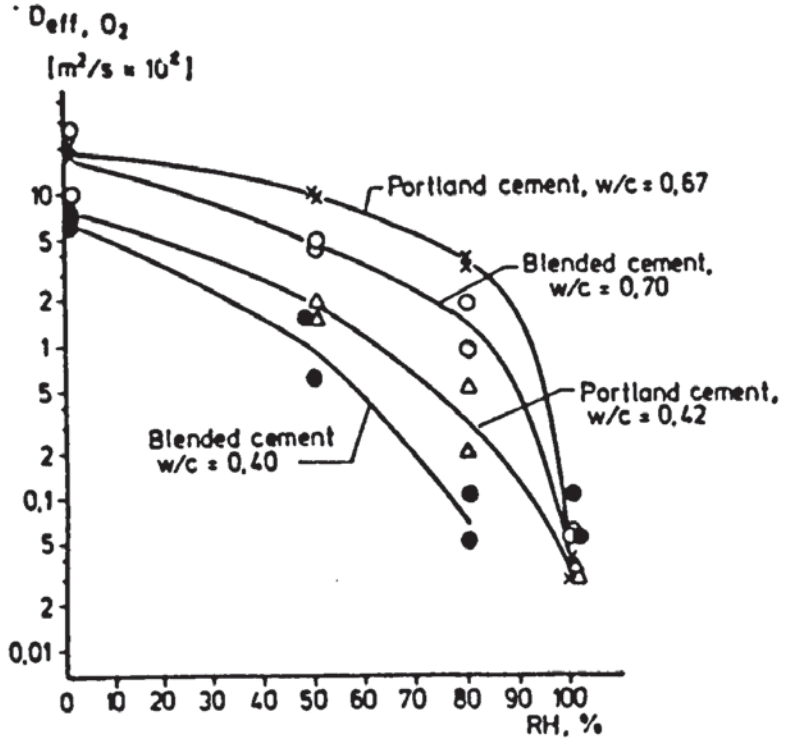

FIGURE 6.6 Variation in oxygen diffusion with humidity (after Tutti (6.44))

CHAPTER 7

CHLORIDE DIFFUSION THROUGH HARDENED MODIFIED CEMENT BASED SYSTEMS

7.1 INTRODUCTION

Chloride ions may be present within a structure due to contamination from sources such as sea water or de-icing salts (7.1, 7.2). Chloride may also be present during hydration in the form of a calcium chloride admixture, though the use of chloride containing admixtures is now discouraged (7.3). Chloride once present at the steel/concrete interface and capable of moving freely is likely to affect the passivity of embedded steel reinforcement (7.4).

In the case of chloride originating from an external source, the process by which ions reach the embedded reinforcement is one of diffusion. The Nernst-Einstein relationship shows that the mobility of an ionic species is related to its diffusivity :

$$D = ukT$$

where

D = diffusion coefficient

u = the mobility of the particle

k = Boltzmann's constant

T = temperature

Thus at a given temperature the rate of transport of a particular ionic species is directly proportional to the coefficient of diffusion (7.5).

By application of the laws developed by Fick it is possible to determine effective diffusivities of ions.

Fick's first law states the flux of a diffusing substance is proportional to the concentration gradient, the diffusion coefficient being the constant of proportionality in the relationship. Flux has units of mass over area by time. Concentration has units of mass over volume. Thus the diffusion coefficient has units of area over time, usually expressed in terms of square centimetres per second.

The diffusion of ions through various hardened cement paste, mortar and concrete systems have been studied (7.6-7.8). Data such as this incorporated into design specifications is likely to result in structures of enhanced durability. Mortar repair systems are formulated to restore serviceability and enhance durability. Their performance and properties can be evaluated in terms of adhesion, bond, shrinkage, permeability, mechanical strength, chemical resistance, etc (7.9). To date, these materials have not been studied systematically in terms of their ability to limit chloride diffusion. Clearly, however, for conditions involving chlorides, this is an important aspect of a modified mortar's performance. The work to be described in this chapter was therefore undertaken in order to determine effective chloride diffusion coefficients for characteristic modified mortars.

A range of pre batched, modified, repair mortars are commercially available for concrete repair. Owing to the sensitive commercial nature of the exact formulation for such materials, precise detail regarding the additives, dosages etc remain privy to each particular manufacturer. However, in order to limit chloride diffusion the following should be considered ; pore blocking, pore

lining and surfactant mechanisms. For the purposes of utilising one or more of these mechanisms, a range of additives are available. It is the objective of this chapter to investigate a range of generic type additives thought to work by one or more of the three means stated.

7.2 PREVIOUS WORK

In order to establish diffusion coefficients, two methodologies have been developed. Both techniques require long specimen exposure and monitoring periods.

The technique established by Collepardi et al (7.10, 7.11) involved preparing specimens within a vacuum in order to eliminate air bubbles and voids. Specimens were also prepared by conventional methods using vibration to achieve compaction. The end surfaces were exposed to temperatures of 10, 25 and 40 ^{o}C in a 3% calcium chloride solution. Specimens were removed periodically and cut into slices perpendicular to the axis of the cylinder, at known distances from the exposed surface. Diffusion coefficients were determined by using a solution of Fick's second law, as applied to non-steady state conditions for a semi-infinite solid.

An alternative methodology has been developed by several workers (7.6, 7.12-7.15) which has the advantage, over Collepardi's technique, of reducing specimen exposure and monitoring times thus providing a more rapid means of determining diffusion coefficients. The approach is based on Fick's first law of diffusion ;

$$J = -D \frac{dc}{dx}$$

where J = the amount of substance passing perpendicularly through a surface of unit area during unit time ie. the flux

D = the diffusion coefficient

dc/dx = the concentration gradient of the diffusant in the direction of diffusion

The essential feature of this approach being only a characteristic thin slice of specimen material is exposed to the diffusant. Work typical of this approach was carried out by Page et al (7.6). Specimen manufacture involved careful preparation of cement paste which was cast within cylindrical moulds and subjected to slow rotation about their horizontal axis in order to prevent segregation. As a measure of quality control ultra-sonic pulse velocity measurements were taken on specimens at early ages in order to identify and reject specimens containing voids. Discs approximately 3mm in thickness were cut from the central region of the cured specimen, a precision diamond saw was employed for this purpose. Prepared discs were sandwiched between the two portions of a glass cell, one portion containing a saturated calcium hydroxide solution, the other containing 1M sodium chloride saturated with calcium hydroxide. Small increases in concentration within the initially chloride-free cell compartment were measured and from them the slope of the rectilinear plot of chloride concentration against time was determined. Note : the small changes in concentration within either side of the cell were insignificant when compared to the overall difference in concentration between the two compartments. The concentration gradient being proportional to the flux, diffusion coefficients were then calculated from a solution of Fick's first law applied to quasi steady-state

diffusion.

This technique is not free from objections. Clearly the arrangement of a well prepared thin section of sample having one side exposed to a solution of high ionic concentration and the other side exposed to a solution of low ionic concentration is not likely to be found in practice. Atkinson and Nickerson (7.14) were critical of this arrangement involving concentrated and dilute solutions either side of the sample, as the conditions may give rise to an osmotic flow of liquid through the sample from the low concentration side to the high concentration side. Further comments were made by the above authors regarding the alternative definitions of the term "diffusion coefficient" that may be applied when considering diffusion in porous media. Diffusion will occur within the liquid phase constrained by the pore structure of the solid medium. The flux per unit cross-sectional area will refer to the area of pores rather than the overall unit area porous medium. Thus, the flux will be underestimated when compared to that flowing through the free liquid phase within the tortuous, irregular and constrained pore structure. As these effects are difficult to quantify, in most practical studies, investigators frequently quote the flux per unit area of medium as so called "effective diffusion coefficients".

Despite criticisms of the thin disc technique, the approach has been adopted by several workers. The merits of the technique include non-destructive nature, small specimen requirement, speed, simplicity and reproducibility.

Kondo, et al (7.12), calculated diffusion coefficients for chloride ion present in mixed solutions (lithium chloride, sodium chloride, potassium chloride, calcium chloride and magnesium

chloride) using hardened cement plates of various thickness. They found the cement plates behaved as electro-positive semi-permeable membranes and that chloride ion diffusion was greatly affected by co-existing cations ; this resulted in diffusion rates in the order of 10^{-7} to 10^{-8} cm^2 s^{-1} ($MgCl_2 > CaCl_2 > LiCl_2 > KCl > NaCl$). It was suggested that chloride diffusion rates of this order would accelerate corrosion of steel after five years, with steel embedded at 5cm. Takagi, et al (7.15) studied diffusion of sodium iodide in cements of various composition (blast furnace slag, sulphate resisting and fly ash) and found that iodide diffused faster than sodium. They suggested that this was due to the formation of a positively charged electrical double layer on the surfaces of the cement hydrates due to the adsorption of calcium ion. This layer would tend to attract anions and so facilitate speedier diffusion through micropores, whilst cations would tend to be repelled.

Page, et al (7.6), investigated chloride diffusion in hardened cement pastes of various compositions (pulverised fuel ash, blast furnace slag, sulphate resisting and OPC) and included variables of water/cement ratio and curing conditions. By diffusing chloride at several temperatures, they were able to demonstrate a linear relationship between the reciprocal of the absolute temperature and log of the effective diffusion coefficient, so enabling the calculation of activation energies for chloride ions at three water/cement ratios. The values obtained were in excess of those for chloride in normal electrolyte solutions which are typically in the region of 17.6 KJ/mole (7.16). They concluded that some form of surface interaction between diffusing ions and cement hydrates may be involved in this rate-limiting process.

Lambert, et al (7.17), studied the diffusion of chloride

through hardened pastes comprising pure cement minerals (alite and tricalcium aluminate) and found activation energies similar to that for OPC paste of the same water-solid ratio. They concluded the mechanism was similar in both cases and was related to diffusion through the C-S-H gel.

Goto and Roy (7.13) found that within the range investigated, water/cement ratio (0.30-0.40) had relatively small influence on the diffusion of chloride and sodium ions, which contrasts with the findings of Page et al (7.6). Furthermore, they suggested the hardened cement paste behaved as an electro-negative semi-permeable membrane which conflicts with the findings of Kondo et al (7.12).

Holden et al (7.18) reported diffusivities of chloride ions in various cements at fixed water/cement ratio and temperature, and constructed a rank order of the cements in terms of their ability to limit chloride in mobility.

In order to estimate induction times for chloride initiated corrosion of reinforcing steel, Byfors (7.19) determined diffusion coefficients for several cement based systems with additions of silica-fume and fly-ash working at four water/cement ratios. She concluded that service-life could be considerably extended, in terms of diffusion controlled chloride-initiated reinforcement corrosion, by additions of appropriate amounts of silica-fume or fly-ash.

A survey of the effects of blending components on fresh and hardened cements found that in addition to pore structure, diffusion of ions are influenced by the composition, structure and interfacial properties of the hydrates (7.20). Similarly in an extensive review concerning the durability and permeability of cementitious materials efforts were made to relate pore structure to

diffusion processes but in conclusion, it was suggested that further long-term field trials and laboratory investigations were needed (7.21).

Whilst a significant amount of work has been reported concerning diffusion in cement based materials, published work on modified cementitious materials, likely to be used for concrete repair purposes, is rather limited. It is for this reason that the present study was undertaken.

It is evident that the thin disc technique has been widely used for the study of ionic diffusion in cementitious materials. It is for reasons of simplicity and reliability that this technique has been adopted for this study involving chloride diffusion in modified cement based mortar systems.

7.3 EXPERIMENTAL

In order to prepare specimens of a homogeneous nature, and of a suitable size, a method involving casting individual discs of material was devised. This approach differs from that adopted by several workers (7.6, 7.7), whose method involved casting cylinders of material from which discs were subsequently cut. This approach was found unsatisfactory for mortars on two counts. First, the presence of large discrete air voids within the specimen and secondly, difficulty in cutting the mortar material on account of the hardness of the Leighton Buzzard aggregate used. Some success in reducing air voids was achieved by increasing vibration times. However, the problem of cutting the mortar containing these aggregates was not satisfactorily resolved. Using a conventional micro-slice cutting machine fitted with a sintered diamond blade

proved unsuccessful. Some success was achieved using an industrial high speed cutting wheel, however, the discs produced were dimensionally outside acceptable tolerances.

In view of these unsuccessful attempts to produce specimens by methods already established, a different approach to specimen manufacture was devised. This involved casting several discs simultaneously in a multi-disc mould. The multi-disc mould comprised a base plate of acrylic sheet, 6mm in thickness, a top plate to accommodate specimens, split several times in order to facilitate specimen removal. The top and base plates were held together by nut and bolt fixings. The assembly is shown in figure 7.1. In order to make the mould watertight whilst the specimen remained fluid, the top plate and base plate interface was sealed with paraffin wax.

The specimens were mixed according to the guidelines given in BS 4551 : 1980 (Methods for Testing Mortar, Screeds and Plasters). Compaction of the mix was achieved by light tamping two even layers followed by a short period of vibration. After an initial curing period of 48 hours, in a 100% relative humidity environment at $22 \pm 2^{o}C$, the specimens were demoulded, care being taken to remove any paraffin wax adhering to the edges. Specimens were further cured for a total of 60 ± 3 days in 100% relative humidity, at $22 \pm 2^{o}C$.

It was found that a narrow zone of segregation was formed at the specimen/base plate interface, whilst the top struck surface exhibited exposed aggregate surfaces. As specimens were cast at twice the final required thickness this surcharge of material was removed from either side of the disc by orbital grinding. Approximately 1.5mm of material was removed from either side of

each disc, each pass taking a cut of 0.1mm. In order to avoid overheating at the grinding head/specimen interface, the cutting wheel was fed with a supply of deionised water.

The selection of additives was on the basis that they were considered likely to affect chloride diffusion by pore blocking, pore lining or surfactant mechanisms. The influence of surfactant dosage level was also considered. Details of the specimens produced are given in table 7.1, whilst details of the additives used are given in Chapter 2 and the Appendices.

The surfactant systems were investigated on the premise that additions of a superplasticizer (surface active agent), whilst working at constant water/cement ratio, may be effective in limiting chloride diffusion by the formation of an anionic layer upon pore walls. This negative charge may tend to repulse diffusing ions of like charge. It was also thought possible that owing to the enhanced fluidity of superplasticized mixes, a refined pore structure may result and thus influence the rate of diffusion of chloride ions. To examine these possibilities three surfactants were used in mortars of constant water/cement ratio, and in addition to this, one surfactant was investigated at various dosage rates in cements of constant water/cement ratio.

The styrene-butadiene rubber and polyvinyl acetate modified mortar systems were investigated as it was considered that such systems may be effective in limiting chloride diffusion by a mechanism of pore blocking, either by the formation of a polymer film upon pore walls, or by the formation of discrete volumes of polymer within the pore structure. It was of interest to investigate the possible significance of these effects over a range of pore structures, and, consequently, two water/cement ratios were

used.

It was considered relevant to investigate two widely used penetrative surface coating treatments, one based on a silane and the other on methyl methacrylate. Unlike the previous systems described, these coatings can only be applied to a structure after hydration. If such treatments were to be effective in reducing chloride diffusion, then mechanisms involving pore lining and/or pore blocking would seem likely to be involved. The viscosity and relative molecular size of such coating materials are likely to be of importance; consequently coatings of low viscosity/small molecular size and higher viscosity/larger molecular size were compared.

The specimens containing the additives or penetrative coatings described above were then mounted in a glass diffusion cell of the type shown in figure 7.2. In order to provide a seal at the specimen/glass flange interface, an epoxy sealant putty was used, this material having first been examined for any possible leaching effects. The joints of the cell were tightly bound with P.T.F.E. tape and the assembly was further stabilised by holding cells together with elastic bands. The high concentration compartment of each cell was filled with 1M solution of sodium chloride saturated with calcium hydroxide and the low concentration compartment was filled with a known volume of saturated calcium hydroxide. The calcium hydroxide solution was used in order to minimise leaching from the cement mortar matrix. Each cell compartment was sealed with stoppers to avoid evaporation and prevent atmospheric carbon dioxide reacting with the solutions. Cells were supported in temperature controlled water baths and for every condition a set of five replicate discs were tested.

Once diffusion through the disc had become established, 100 microlitre aliquots of solution were withdrawn from the low concentration compartment and analysed for chloride ion by the spectophotometric technique described in Chapter 2; the withdrawn volume of solution was not replaced as the cumulative effect of removal was negligible.

To determine whether additives influenced porosity, discs from each set of specimens were subjected to mercury intrusion porosimetry (Chapter 2).

In order to obtain a measure of rheological and mechanical properties the flow of each fresh mortar was measured using a flow table, and twenty eight day compressive strengths of cubes were determined. Both methods are described in Chapter 2.

7.4 RESULTS AND DISCUSSION

When changes in chloride concentration measured in the low concentration compartment of each cell were plotted against time of diffusion linear relationships were obtained, an example of which is given in figure 7.3. After an initial period (t_o), diffusion became established across the thickness of the disc and the rate of increase in concentration became effectively constant for the duration of the experiment. If a condition of quasi-steady-state diffusion is assumed to be operating across the disc, then the flux and activity of the diffusing chloride ions are constant throughout the disc. The flux of the chloride ions (J in moles per square centimetres per second) entering the low compartment of the cell is related to Fick's first law and is given by

$$J = \frac{V}{A} \frac{dc_2}{dt} = \frac{D}{I} (C_1 - C_2)$$

where

V = volume of the low concentration side (cubic centimetres)

A = cross-sectional area of the disc exposed to the solution (square centimetres)

C_1 = chloride concentration of the high compartment of the cell (=1 mole/litre)

C_2 = chloride concentration of the low compartment of the cell (mole/litre)

t = time (seconds)

I = the thickness of the disc (centimetres)

D = diffusion coefficient (square centimetres per second)

This expression can be simplified knowing the slope (S) of the rectilinear plot C_2 vs. t, and the D value may be calculated :

$$D = \frac{SVI}{A\ (C_1 - C_2)}$$

The average D value from each set of specimens is given in table 7.2 whilst other relevant information for each of the 150 discs tested is given in Appendices. In all but a small number of cases, correlation coefficients of the rectilinear plots, of chloride concentration against time, were better than 0.95. At least five D values were used to determine an average for each particular set of specimens.

Mercury intrusion porosimetry (MIP) was carried out for each set of specimens, and the results are shown in the pore size distribution (psd) curves in figures 7.4 to 7.8. In all cases one MIP run was carried out in order to plot psd curves for material

previously used in the diffusion experiment. The specimen preparation involved drying the sample to constant weight by heating to 105 ^{o}C. It is possible that by heating sample material in this manner unwanted features were introduced to the materials' pore structure, hence distortions within the psd curves may have been introduced. If such effects are, in fact present, the influence may be more significant in those specimens containing organics. Previous workers have been critical of the mercury intrusion method and the direct oven dry technique. The effect of the mercury intrusion process upon pore structure has been investigated (7.22). It was reported that in certain instances direct oven drying may result in damage to relatively large, discontinuous, thin walled pores. Helium porosities for direct oven dried and propane treated specimens were compared (7.23), and it was shown that higher porosities were obtained for the former.

The mean diffusion coefficient obtained for the 0.4 water/cement ratio control mortar was $(2.98 \pm 0.88) \times 10^{-8}$ cm^2 s^{-1}. In all cases the range of values has been calculated for the 95% confidence limits. This result compares with the value of 2.60×10^{-8} cm^2 s^{-1} previously obtained for a cement paste of 0.4 water/cement ratio (7.6). The value obtained for the 0.6 water/cement ratio control mortar was $(4.18 \pm 1.52) \times 10^{-8}$ cm^2 s^{-1} which does not compare with that previously obtained, for 0.6 cement paste, of 12.35×10^{-8} (7.6). The value obtained compared more closely to 4.47×10^{-8} which was obtained for a cement paste of 0.5 water/cement ratio (7.6). The lack of comparability between a cement paste and cement mortar of similar water/cement ratio may be due to variations between the methods of specimen preparation used in this study and those used

previously.

Comparison of the MIP data (figure 7.4) shows that the 0.4 water/cement ratio mortar has a lower total porosity than that of the 0.6 water/cement ratio mortar. The maximum pore sizes of both 0.4 and 0.6 water/cement mortars are approximately 100μm diameter, and both mortars have a significant volume of pores greater than 0.1μm diameter. This contrasts with cement pastes of similar water/cement ratio which have few pores greater than approximately 0.1μm diameter. Pores of diameters greater than 0.1μm are present in slightly greater volume within the 0.4 water/cement ratio mortar when compared to the 0.6 water/cement ratio specimen.

The diffusion coefficients obtained for the control mortar specimens are broadly similar to those values obtained for cement paste specimens of similar water/cement ratio. There would not therefore appear to be any substantial evidence of any diffusion paths being introduced within the aggregate/cement hydrate interfacial regions. It seems likely that the introduction of aggregates would serve to increase the length and tortuosity of diffusion paths, by means of acting as discreet, numerous and relatively impervious "islands" within the cement matrix.

Diffusion coefficients obtained for the surfactant mortar systems were $(2.48 \pm 0.96) \times 10^{-8}$ cm^2 s^{-1} for the long molecular chain naphthalene sulphonate system $(3.18 \pm 0.75) \times 10^{-8}$ cm^2 s^{-1} for the short molecular chain naphthalene sulphonate and $(1.01 \pm 0.16) \times 10^{-7}$ cm^2 s^{-1} for the melamine formaldehyde condensate. In all cases the water/cement ratio was 0.6. Considering the influence of these surfactants upon the rheology of the fresh-mortar, inspection of the flow measurements (table 7.3) shows little difference between the naphthalene sulphonate systems.

The melamine system's flow was judged to be excessive, so rendering any comparisons with the naphthalene sulphonate systems invalid. It may, therefore, be considered that the melamine formaldehyde condensate was overdosed.

The MIP data (figure 7.5) shows very similar psd curves for both naphthalene sulphonate systems. This data compares closely with the control mortar of like water/cement ratio, although the diffusion coefficients for these two surfactant systems tend toward that obtained for the 0.4 water/cement ratio mortar. However, as already indicated, the assumed mercury/pore wall contact angle may not be valid for specimens of this type. This possibility, and also considering the criticism of drying process, may explain the conflicting MIP data and diffusion coefficients obtained for the melamine specimens; total porosity was lower than for the naphthalene sulphonates, but the diffusion coefficient was greater.

It would appear that surfactants investigated, at a 0.6 water/cement ratio, have not significantly influenced chloride diffusivity when compared to the control mortar specimens.

The influence of naphthalene sulphonate dosage upon chloride ion diffusion was studied using cement pastes. A control and three levels of dosage were used, the water/cement ratio remaining constant at 0.28. Had a mortar system been adopted, the likelihood existed of introducing unwanted artefacts, such as variable compaction in the control specimen and aggregate segregation for the high dosage specimen. Such difficulties may have masked any differences specifically attributable to the surfactant.

The diffusion coefficient obtained for the control specimen was $(2.54 \pm 0.17) \times 10^{-8}$ cm^2 s^{-1} which is similar to that

previously obtained for a cement paste of 0.4 water/cement ratio of 2.60×10^{-8} cm^2 s^{-1} (7.6). It is likely that the small variation can be attributed to the different methods of specimen preparation and differences in cement type. From table 7.2 it is evident that the addition of surfactant has reduced the diffusion coefficient and increasing dosage levels appear to further reduce the diffusivity. It can be seen from the MIP data (figure 7.6) that increasing surfactant levels correspond to an increase in the fineness of the micro-pore structure, coupled with a reduction in total porosity. The mechanism by which the pore structure was produced may be linked to higher rates of surfactant adsorption on to cement particles; hence their enhanced dispersion would tend to promote increasing levels of homogeneity in the hydrating cement system. It has been suggested that an increase in homogeneity within the microstructure of the cement hydrates gives rise to a higher strength when compared to a heterogeneous microstructure (7.24). Such a trend is not, however, reflected in the compressive strength obtained for the cement pastes investigated here. Table 7.3 shows the 28 day compressive strength reaching a maximum of $108.6N/mm^2$ for the lowest surfactant dosage, with 0.5% and 1.0% additions corresponding to $105.6N/mm^2$ and $99.9N/mm^2$ respectively, although these were still greater than the control pastes $95.7N/mm^2$. It has been reported that hydration is retarded as a result of polymer adsorption on cement particles (7.25). It may, therefore, be possible that at higher dosages no further improvement in dispersion was achieved, or possibly, any beneficial properties resulting from enhanced dispersion will be masked by stronger retardation at early ages. Such a theory would explain the slight reduction in the 28 day compressive strength found in specimens

containing over 0.25% additions of naphthalene sulphonate.

Polymer modified mortars were investigated at 0.4 and 0.6 water/cement ratio,with two additive types; using polyvinyl acetate (stabilised with polyvinyl alcohol), and styrene-butadiene rubber. These systems were expected to act by a pore blocking mechanism. For the styrene-butadiene rubber (SBR) system diffusion coefficients of $(1.48 \pm 0.05) \times 10^{-7}$ cm^2 s^{-1} and $(3.50 \pm 0.16) \times 10^{-7}$ cm^2 s^{-1} were recorded for 0.4 and 0.6 water/cement ratio specimens respectively, the dosage level being identical in both cases. The results for the polyvinyl acetate (PVA) systems were $(8.75 \pm 1.53) \times 10^{-8}$ cm^2 s^{-1} and $(7.64 \pm 0.94) \times 10^{-7}$ cm^2 s^{-1} for 0.4 and 0.6 water/cement ratio mortars respectively. Identical dosages were used for both sets of specimens. The factors representing change in diffusion coefficient are given in table 7.2 and in all instances, diffusion coefficients were greater than the control. The MIP data (figure 7.7) tends to substantiate these results. The psd curves are similar in type to those obtained for the control mortars, but the volumes of pores at any given radius are increased and suggest a more open pore structure. The MIP data suggests a reduction in the homogeneity of the hydrated matrix, which is also indicated by the reductions in 28 day compressive strengths. It is possible that the lower compressive strengths, particularly in the case of the 0.6 water/cement ratio polyvinyl acetate cubes may be due to polymer hindering the development of cement/aggregate interfacial bonds.

The surface coatings investigated had a beneficial effect in reducing chloride diffusion rates. The oligomeric alkoxy silane and polymeric methyl methacrylate treatments gave diffusion coefficients of $(1.46 \pm 0.48) \times 10^{-9}$ cm^2 s^{-1} and $(3.10 \pm 0.54) \times$

10^{-8} cm^2 s^{-1} respectively. In both instances the coatings were applied to mortars of 0.6 water/cement ratio. The MIP data (figure 7.8) suggested that these treatments reduce the volume of pores smaller in radius than approximately 0.1μm, particularly in the case of the oligomeric alkoxy silane - which was particularly effective in reducing chloride diffusion rates. The MIP data must be evaluated cautiously however as it is possible that these treatments involving a pore lining mechanism, may render the assumption of a constant mercury/cement hydrates pore wall contact angle invalid. This being the case, the greater total pore volume recorded for the oligomeric alkoxy silane, which conflicts with the observed trend in diffusion coefficient, may be explained.

The primary mechanism by which the silane system works is that of pore lining imparting water repellency. The methyl system is likely to have a greater propensity to block pores, rather than essentially pore lining. It is likely that the methyl treatment will be ineffective in intruding micro-pores. Silanes, having a superior penetration ability, would be more able to line pores over a greater range. The hydrophobic properties imparted by the silane will limit the number of diffusion paths available to chloride ions.

7.5 CONCLUSIONS

The chloride diffusion coefficients obtained for the 0.4 and 0.6 water/cement ratio control specimens, were similar to values obtained by previous workers for ordinary Portland cement paste systems of 0.4 and 0.5 water/cement ratio, respectively. It would appear that within a cement mortar system, the aggregate fraction

does not introduce significant diffusion paths at aggregate/cement interfacial regions.

The influence of different surfactants upon cement mortar systems, studied at constant water/cement ratio, revealed a slight reduction in diffusivity within those systems containing naphthalene sulphonates. The melamine formaldehyde condensate system gave a significant increase in diffusion coefficient when compared to the control mortar. This may have been associated with the excessive flow of the fresh material and thus possible segregation. A comparatively open pore structure would likely result from such effects.

When rates of surfactant addition were studied within an ordinary Portland cement paste, by the addition of naphthalene sulphonate, an increasing rate of addition was found to correspond to a diminishing diffusion coefficient. An increasing refinement in the micro-pore structure was suggested by the mercury intrusion porosimetry data. It was thought that the refinement in micro-pore structure was due to better dispersion of the cement during the mixing stage. Owing to the possible effect of the direct oven drying process, used for specimen preparation and uncertainty regarding the contact angle, the porosimetry data may be misleading. The reduction in 28 day compressive strength, found for the specimens containing higher dosages of naphthalene sulphonate, was attributed to retardation during the early stages of hydration. The diffusion coefficient for the control cement paste of 0.28 water/cement ratio was found to be similar to that obtained by previous workers for a 0.4 water/cement ratio cement paste. This variation in apparently similar systems was thought to be due to variations in the method of specimen preparation and possibly

influences of different cement types.

The systems thought to act by a pore blocking mechanism were found to be significantly less effective in limiting chloride diffusion when compared to the control mortars. The MIP data, which may not be entirely reliable, suggested these specimens were of comparatively open pore structure and of greater total porosity.

The two penetrative surface treatments increased the substrates' resistance to chloride diffusion and was most evident in the case of the oligomeric alkoxy silane treatment. This was attributed to the silane's ability to intrude a wider range of pores, including micro-pores, and impart hydrophobic properties.

From a practical point of view, there are several considerations. First, in cases of repair where no special flow characteristics are demanded of the repair material (high flow rates being required for soffits, etc), the arguments for plasticized and superplasticized concretes may not be particularly strong. On the basis of the effective diffusion coefficients, evaluating mortar in terms of the ability to limit chloride ingress, no significant advantage would be gained from the use of a modified mortar or concrete. However, in concrete repair, where placing the repair material is often difficult, the advantages of enhanced workability whilst not increasing the water/cement ratio are clear. Secondly, considering structures that are situated within environments where chloride ingress is likely, but no deterioration of the concrete has yet occurred, the benefits of applying a silane treatment would appear worthwhile. However, the long term stability of such treatments, within highly alkaline environments requires further investigation.

Specimen description	Additive dosage rate by weight of cement (%)	Aggregate cement ratio (c/a)
Control OPC mortars 0.4 and 0.6 W/C	-	1:3
Mortar 0.6 W/C, long chain naphthalene sulphonate	0.5	1:3
Mortar 0.6 W/C, short chain naphthalene sulphonate	0.5	1:3
Mortar 0.6 W/C, melamine formaldehyde condensate	0.8	1:3
Styrene butadiene rubber mortars 0.4 and 0.6 W/C	10.0 (active content)	1:3
Polyvinyl acetate mortars 0.4 and 0.6 W/C	3.0	1:3
Control OPC paste 0.28 W/C	-	-
Naphthalene sulphonate pastes	0.25, 0.5, 1.0	-
OPC mortar 0.6 W/C	Methyl methacrylate surface treatment approx. 0.02g/cm^2	1:3
OPC mortar 0.6 W/C	Alkoxy silane surface treatment approx 0.03g/cm^2	1:3

TABLE 7.1 Details of the specimens produced for diffusion studies

SPECIMEN DESCRIPTION	AVERAGE DIFFUSION COEFFICIENTS (D) $cm^2 s^{-1}$	FACTOR CHANGE IN D Vs CONTROL
Control OPC mortar 0.4 W/C	$(2.98 \pm 0.86) \times 10^{-8}$	1
Control OPC mortar 0.6 W/C	$(4.18 \pm 1.52) \times 10^{-8}$	1
Mortar 0.6 W/C, long chain naphthalene sulphonate	$(2.48 \pm 0.96) \times 10^{-8}$	0.59
Mortar 0.6 W/C, short chain naphthalene sulphonate	$(3.18 \pm 0.75) \times 10^{-8}$	0.76
Mortar 0.6 W/C, melamine formaldehyde condensate	$(1.01 \pm 0.16) \times 10^{-7}$	2.42
Mortar 0.6 W/C, styrene butadiene rubber	$(3.50 \pm 0.16) \times 10^{-7}$	8.37
Mortar 0.4 W/C, styrene butadiene rubber	$(1.48 \pm 0.05) \times 10^{-7}$	4.97
Mortar 0.6 W/C, polyvinyl acetate	$(7.64 \pm 0.94) \times 10^{-7}$	18·37
Mortar 0.4 W/C, polyvinyl acetate	$(8.75 \pm 1.53) \times 10^{-8}$	2.94
Mortar 0.6 W/C, alkoxy silane coating	$(1.46 \pm 0.48) \times 10^{-9}$	0.03
Mortar 0.6 W/C, methyl methacrylate coating	$(3.10 \pm 0.54) \times 10^{-8}$	0.74
Control OPC paste 0.28 W/C	$(2.54 \pm 0.17) \times 10^{-8}$	1
OPC paste 0.28 W/C, 0.25% naphthalene sulphonate	$(1.72 \pm 0.21) \times 10^{-8}$	0.68
OPC paste 0.28 W/C, 0.5% naphthalene sulphonate	$(1.44 \pm 0.26) \times 10^{-8}$	0.57
OPC paste 0.28 W/C, 1.0% naphthalene sulphonate	$(1.05 \pm 0.28) \times 10^{-8}$	0.41

TABLE 7.2 Average diffusion coefficients (D) mortar and cement paste systems

SPECIMEN DESCRIPTION	COMPRESSIVE STRENGTH (28 day) N/mm^2	FLOW INCREASE IN DIAMETER TO NEAREST 5%
Control OPC mortar 0.4 W/C	50.4	5
Control OPC mortar 0.6 W/C	35.0	70
Mortar 0.6 W/C, long chain naphthalene sulphonate	35.9	110
Mortar 0.6 W/C, short chain naphthalene sulphonate	29.6	140
Mortar 0.6 W/C, melamine formaldehyde condensate	39.4	>diameter of platten
Mortar 0.6 W/C, styrene butadiene rubber	23.5	>diameter of platten
Mortar 0.4 W/C, styrene butadiene rubber	35.9	105
Mortar 0.6 W/C, polyvinyl acetate	7.5	115
Mortar 0.4 W/C, polyvinyl acetate	36.7	30
Control OPC paste 0.28 W/C	95.7	NOT APPLICABLE
OPC paste 0.28 W/C, 0.25% naphthalene sulphonate	108.6	NOT APPLICABLE
OPC paste 0.28 W/C, 0.5% naphthalene sulphonate	105.6	NOT APPLICABLE
OPC paste 0.28 W/C, 1.0% naphthalene sulphonate	99.9	NOT APPLICABLE

TABLE 7.3 28 day compressive strengths and flow measurements for various mixes

FIGURE 7.1 The mould assembly used for casting diffusion specimens

FIGURE 7.2 The glass diffusion cell.

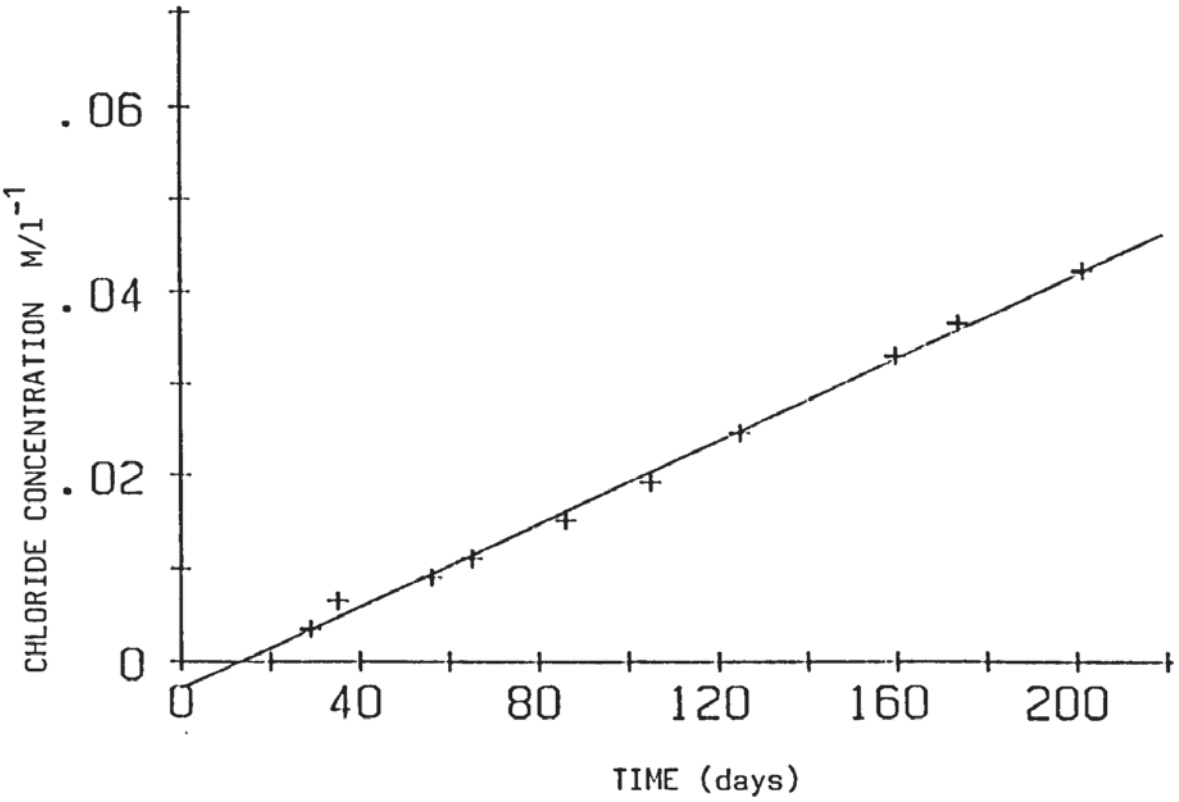

FIGURE 7.3 Increase in chloride concentration with time, measured in the low compartment of the diffusion cell

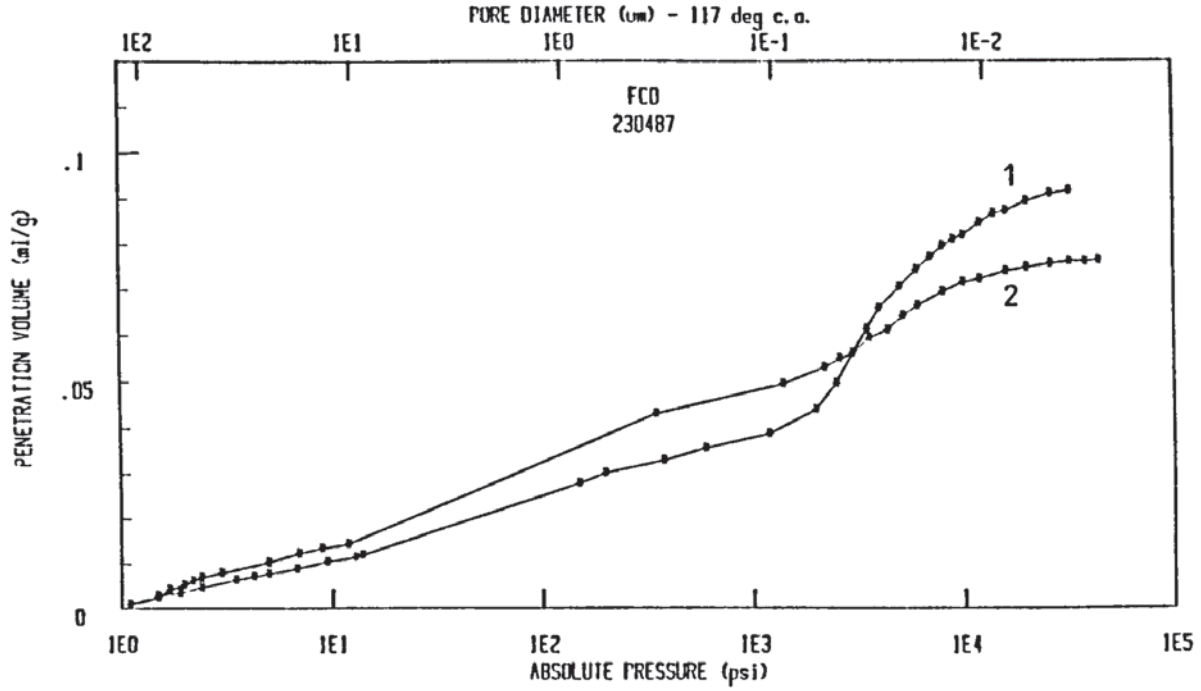

FIGURE 7.4 Pore size distributions for the following specimens; 1 = 0.6 W/C mortar, 2 = 0.4 W/C mortar

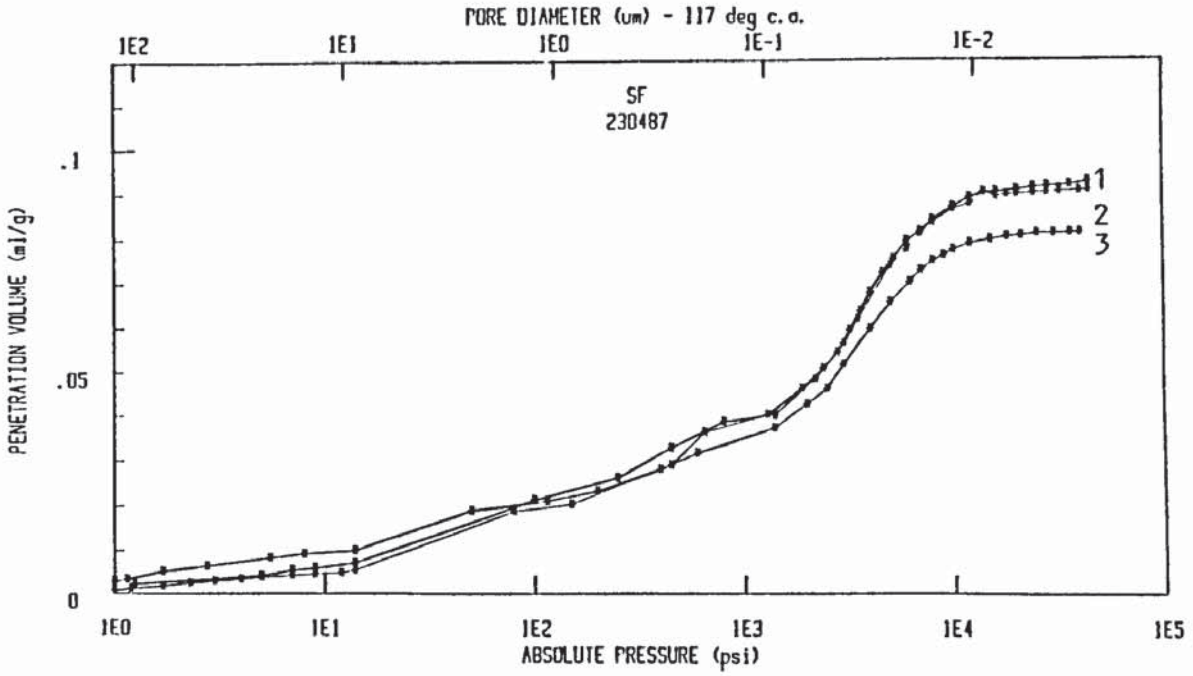

FIGURE 7.5 Pore size distributions for the following specimens; 1 = 0.6 W/C mortar with long chain naphthalene sulphonate, 2 = 0.6 W/C mortar with short chain naphthalene sulphonate, 3 = 0.6 W/C mortar with melamine formaldehyde condensate

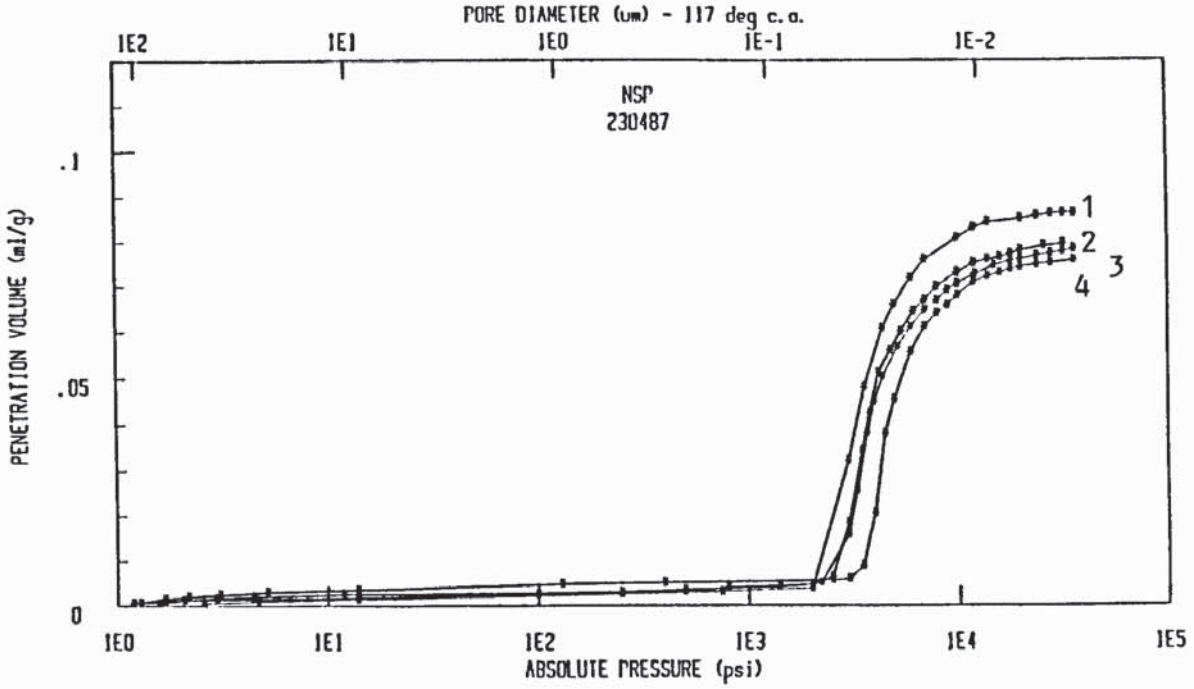

FIGURE 7.6 Pore size distributions for the following specimens; 1 = 0.28 W/C paste, 2 = 0.28 W/C paste with 0.25% naphthalene sulphonate, 3 = 0.28 W/C paste with 0.5% naphthalene sulphonate, 4 = 0.28 W/C paste with 1.0% naphthalene sulphonate

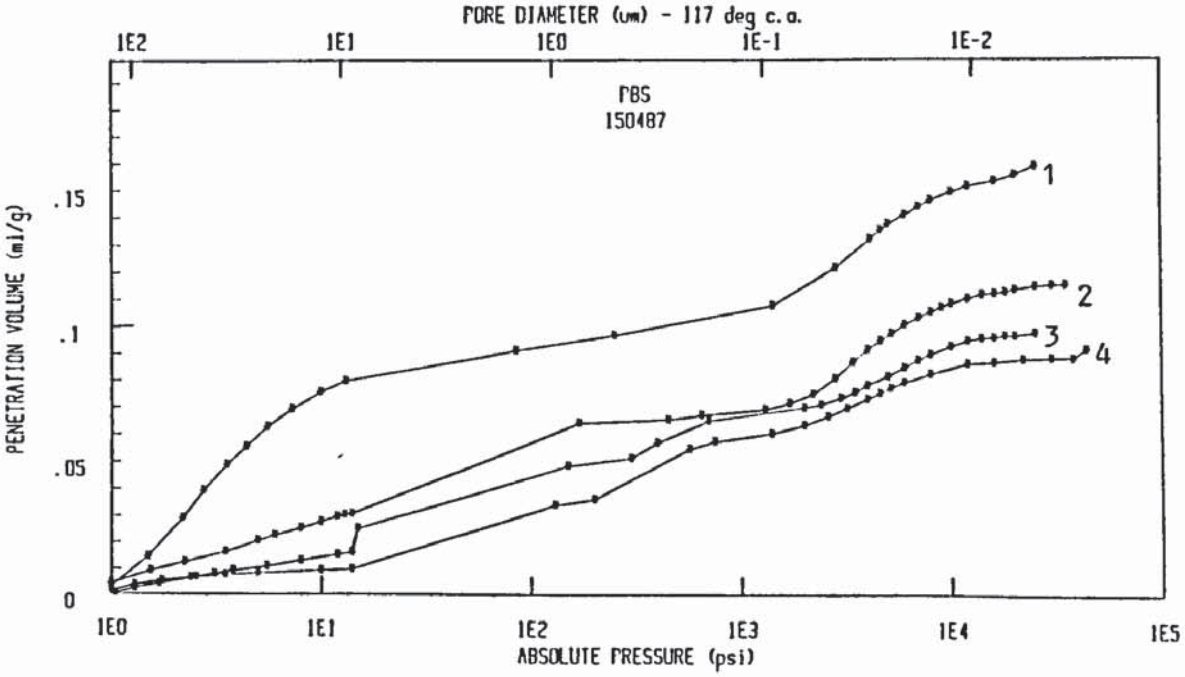

FIGURE 7.7 Pore size distributions for the following specimens; 1 = 0.6 water/cement ratio mortar with PVA, 2 = 0.6 water/cement ratio mortar with SBR, 3 = 0.4 water/cement ratio mortar with SBR, 4 = 0.4 water/cement ratio mortar with PVA

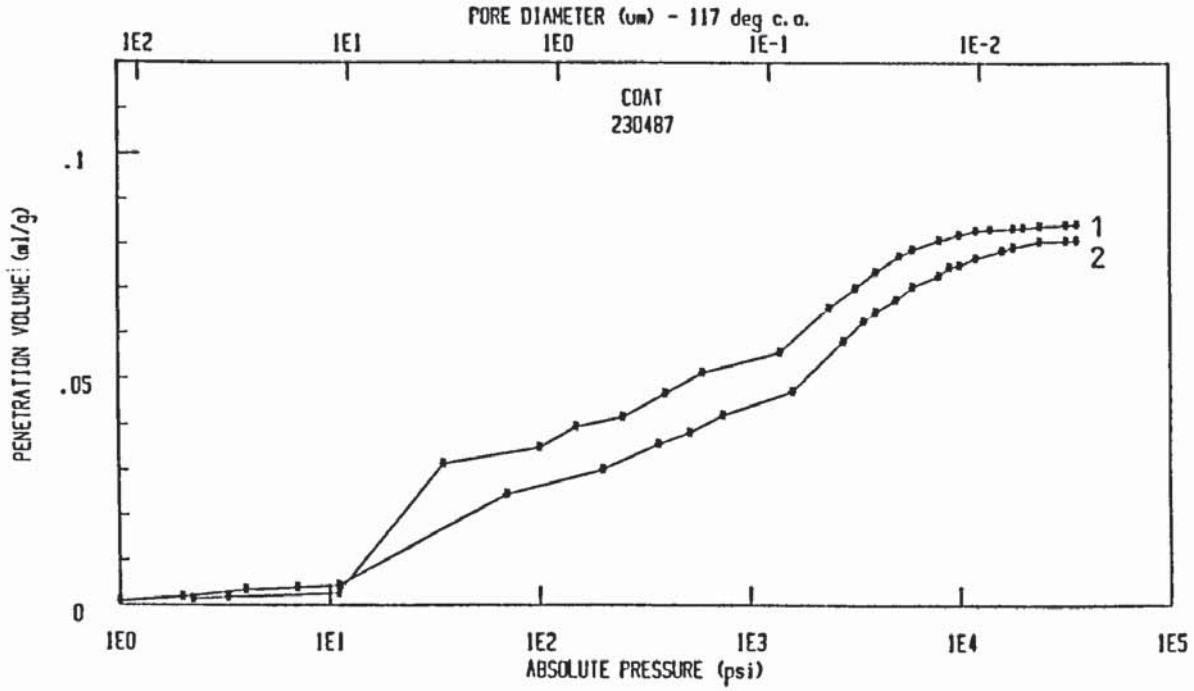

FIGURE 7.8 Pore size distributions for the following specimens; 1 = 0.6 W/C mortar coated with alkoxy silane, 2 = 0.6 W/C mortar coated with methyl methacrylate

CHAPTER 8

GENERAL CONCLUSIONS AND RECOMMENDATIONS FOR FURTHER WORK

8.1 GENERAL CONCLUSIONS

The study relates to steel reinforced concrete structures undergoing corrosion of embedded reinforcement, due to the presence of depassivating chloride anions. Investigations have been carried out specifically concerned with the rehabilitation of such structures and have sought to establish some of the factors involved in the loss, and restoration of, serviceability.

The presence of chloride ion at embedded reinforcement may arise due to a diffusion process, from an external source such as deicing salt, or from chloride introduced at the mixing stage. The presence of these contaminants in sufficient concentration, with adequate moisture and oxygen levels, is likely to result in the development of anodic and cathodic regions throughout the structure.

A methodology has been devised for the study, under laboratory conditions, of the processes involved in the pre, and post repair corrosion of steel embedded within a patch repaired element. The specimen developed for this purpose comprised seven hollow mild steel electrodes, which could be individually isolated. The assembled multi-segment electrode was cast within a mortar prism containing a cast-in chloride gradient. Macro-cell corrosion currents, $\dot{\iota}_{galv}$, flowing between various electrode combinations were monitored. It was found that anodic macro-cell activity, at the segment embedded within the 1% chloride region was suppressed due

to a partial cathodic protection effect, imparted by an adjacent strongly anodic electrode embedded within mortar containing 5% chloride.

The measurement of micro-cell corrosion, i_{corr}, that due to anodic and cathodic processes operating at a single segment, was determined by linear polarisation. Values of i_{corr} were found to increase with increasing chloride level. Values of i_{galv} and i_{corr} were used to derive a calculated weight loss, and when compared to the gravimetrically determined weight loss a reasonable agreement was found. The relative intensities of macro and micro-cell corrosion were compared, and i_{galv} was found to predominate at the higher chloride levels. Specimens were exposed to alternate wetting and drying cycles and the macro-cell intensity was found to be resistance controlled during the drying phase.

Having established the galvanic bar methodology as reliable, a range of reinforcement primers, representative of systems used in practice, were studied under conditions conducive to the activation of an incipient anode. For this purpose the well-characterised galvanic bar specimens were employed. The required condition for the primer study was created by removing the portion of the mortar containing the greatest chloride concentration, and then executing a patch/primer repair at the exposed segmental electrode. It was found that electrodes previously experiencing partial cathodic protection developed as highly active anodes. The intensity of the incipient macro-cell was strongly influenced by the nature of the priming system used at the adjacent patch repair. The system found to be most effective in limiting the intensity of the incipient macro-cell comprised an ordinary Portland cement slurry, applied directly to the electrode, the slurry and mortar substrate being

overcoated with an insulating epoxy. The effectiveness of the system was attributed to its ability to electrochemically isolate the repair region from the remainder of the electrodes.

Whilst the nature of a priming system has been shown to significantly influence the corrosion processes operating throughout the non-repaired regions of an element, the passivity of steel within the repair region itself will largely depend upon the nature of both primer and repair mortar. Most pre-batched concrete repair mortars contain a variety of additives, and a range of these were investigated to determine their resistances to chloride ion diffusion. Ordinary Portland cement mortars at 0.4 and 0.6 water/cement ratio were used as controls and diffusion coefficients of $(2.98 \pm 0.88) \times 10^{-8}$ cm^2 s^{-1} and $(4.18 \pm 1.52) \times 10^{-8}$ cm^2 s^{-1} were measured. Diffusion rates were slightly lower for those systems containing naphthalene sulphonates, whilst the addition of a melam ine formaldehyde condensate increased diffusivity. A mortar containing styrene butadiene rubber and another containing polyvinyl acetate, both thought to reduce permeability by a pore blocking mechanism, were found to be significantly less effective in limiting chloride diffusion. Constant workability based tests with superplasticizers and SBRs may produce more favourable results.

In order to study the influence of naphthalene sulphonate addition rates, a cement paste system was used. Mortars were found to be impracticable for this purpopse owing to segregation. Increasing dosage corresponded to diminishing diffusion rates, and this finding was tentatively attributed to a slight refinement within the micro-pore structure in those pastes containing the higher dosage.

Although not mix additives, two surface treatments were investigated, such materials frequently comprise a part of a

concrete repair package. An alkoxy silane applied to a 0.6 water/cement ratio mortar gave a significant reduction in chloride diffusion coefficient to $(1.46 \pm 0.48) \times 10^{-9}$ cm^2 s^{-1} .

Repairs involving the isolated patching of a structure are a widely used and well established site practice. Considering the difficulties associated with this type of repair it is reasonable to argue the case for an alternative repair strategy. One such possibility is cathodic protection. However, the technology is relatively new to the protection of steel in concrete and particular problems may be envisaged. Within the range of protection potentials likely to be used for steel embedded in concrete, the cathodic reaction involves the evolution of hydroxyl ion. This increase in alkali level may be of particular significance with regard to alkali-silica reactions. To investigate the possibility of measurable increases in alkali levels, a number of chloride containing mortar specimens were cathodically protected over the range of potentials -700mV to -1150mV (versus saturated calomel electrode) using an impressed current system. Pore solution expressions were obtained from mortar sampled within the vicinity of the reinforcement. An increase of approximately 50% in hydroxyl ion concentration was recorded for the cathodically protected specimens, and was found to exist over the complete range of potentials investigated. It is, therefore, not inconceivable that under certain conditions, the application of cathodic protection to a structure containing susceptible aggregates may induce an alkali-silica reaction.

The non-destructive investigation of corroding reinforced concrete structures is presently restricted to techniques unable to yield any direct measurement of corrosion rate within the

structure. Previous workers have suggested the measurement of electrochemical noise as a means of determining information more directly associated with corrosion rate. To investigate such possibilities, electrochemical potential noise was measured and when compared to macro and micro-cell corrosion data a generally good agreement was found. Best agreement was found for macro-cell corrosion currents where a clear distinction existed between anodes and cathodes. However, the experimental conditions found necessary, in order to achieve success with the technique, were far removed from the level of control attainable under site conditions. It was therefore thought unlikely that the technique would prove practicable for on-site monitoring purposes.

8.2 RECOMMENDATIONS FOR FURTHER WORK

The galvanic bar offers a range of possibilities for investigations involving metals embedded within cementitious materials. Already indicated is the possibility of developing a standard assessment methodology for repair systems. For such purposes a much simplified electrode design would be satisfactory.

The effectiveness of sacrificial zinc laden primers, used in patch repair, require further study. Of particular interest is the influence of residual chloride levels, near to regions containing zinc primed reinforcements and the effect of the alkali content of the repair mortar. In order to justify the use of zinc priming systems the question of current throwing power requires close examination. A suitable study may yield data facilitating the prediction of areas of a structure likely to benefit from a cathodic protection influence imparted by a zinc primer.

The investigation of large scale structural elements containing reinforcement, comprising galvanic bars, would provide a possible basis for the assessment of potential mapping, and resistivity techniques, in terms of their ability to predict macro-cell and micro-cell current distributions throughout a full-sized element. Closely allied to investigations of this type, is the evaluation of polarisation resistance techniques for on-site use. It may be possible to develop a model upon which the on-site measurement of polarisation resistance can be assessed, without a precise knowledge of the working electrode area under investigation.

The cathodic protection investigation provides a basis for more detailed studies of anion and cation migration induced as a result of cathodic protection. In order to investigate the possibilities of alkali-silica reactions, related to cathodic protection, a series of studies involving expansion measurements and petrographic thin section examinations would be of interest. Bar pull-out tests combined with micro-hardness studies provide a possible means for the investigation of interfacial bond softening around cathodically polarised electrodes. Work broadly of this nature is presently in progress at Aston.

More research is required in order to determine the effectiveness of silanes, and other surface treatments, under a wide range of experimental conditions. The variables requiring consideration include : long term stability, influence of substrate porosity, degree of carbonation, variation in substrate moisture content and influence of various application rates.

There would appear to be an increasing need for the development of a probe suitable for embedment, at the construction

stage, within new reinforced concrete structures to facilitate continuous remote monitoring (for instance via a MODEM link). It may be possible to develop such a device, based upon the galvanic bar principle, enabling monitoring of corrosion rate, corrosion potential, and resistivity.

REFERENCES

CHAPTER 1

1.1 Galileo Galilei.
"Discorsi e dimostrazioni matematiche, intorno a due ruoue scienze attentinti alla mecanica and movimenti locali"
Pub: In Leida, 1638.

1.2 Collins, P.
"Concrete the vision of a new architecture"
Pub: Faber & Faber, 1959, p60.

1.3 Stanley, C.C.
"Highlights in the history of concrete"
Pub: Cement and Concrete Association, 1979, pp 18-19

1.4 Anon.
"Concrete and steel supplement"
Builders Journal, June 1906, p1.

1.5 Leet, K.
"Reinforced concrete design"
Pub: Mcgraw Hill, 1982, p1.

1.6 Longuet, P., Burglen, L. and Zelwer, A.
"La phase liquid du ciment hydrate"
Materiaux de Construction et Travaux Publics, 676, 1973, pp 35-41.

1.7 Barneyback Jnr, R.S. and Diamond, S.
"Expression and analysis of pore fluids from hardened cement pastes and mortars"
Cement and Concrete Research, 11, 1981, pp 279-285.

1.8 Pourbaix, M.
"Atlas d'Equilibres Electrochimiques"
Pub: Pergamon Press, 1966.

1.9 Page, C.L.
"Mechanism of corrosion protection in reinforced concrete marine structures"
Nature, 258, 1975, pp 514-515.

1.10 Wig, R.J. and Ferguson, L.R.
"What is the trouble with concrete in sea water?"
Engineering News Record, 79, 1917, pp 532-535.

1.11 British Standard Code of Practice 114 : Part 2
"Structural use of reinforced concrete in buildings"
British Standards Institution, 1969.

1.12 British Standard Code of Practice 110 : Parts 1 & 2

"Structural use of concrete"
British Standards Institution, 1972.

1.13 British Standard 8110 : Part 1
"Structural use of concrete"
British Standards Institution, 1985.

1.14 Page, C.L. and Treadaway, K.W.J.
"Aspects of the electrochemistry of steel in concrete"
Nature, 297, 1982, pp 109-115.

1.15 Escalante, E and Ito, E.
"A bibliography on the corrosion and protection of steel in concrete"
National Bureau of Standards, NBS SP 550, August 1979.

1.16 Pullar-Strecker, P.
"Specifying and commissioning repair work"
Proc : 1st international conference on deterioration and repair of reinforced concrete in the Arabian Gulf, Vol 1, Bahrain, 1987, pp 1-14.

2.1 British Standard 12
"Ordinary and rapid hardening Portland cement"
British Standards Institution, 1978.

2.2 British Standard 4550 : Part 2
"Methods of testing cements. Chemical tests"
British Standards Institution, 1970.

2.3 British Standard 4551
"Methods of testing mortars, screeds and plasters"
British Standards Institution, 1980.

2.4 British Standard 1881 : Part 4 : Section 2
"Test for compressive strength of test cubes"
British Standards Institution, 1970.

2.5 British Standard 1610 : Section 2
"Methods for the load verification of testing machines"
British Standards Institution, 1964.

2.6 Diamond, S.
"Effects of microsilica (silica fume) on pore solution chemistry of cement pastes"
Journal of the American Ceramic Society, 66, 5, May 1983, pp 82-84.

2.7 Page, C.L. and Vennesland, Ø.
"Pore solution composition and chloride binding capacity of silica-fume cement pastes"
Materiaux et Constructions, 16, 91, 1983, pp 19-25.

2.8 Diamond, S.
"Effects of two Danish flyashes on alkali contents of pore solution of cement-flyash pastes"
Cement and Concrete Research, 11, 1981, pp 383-394.

2.9 Andrade, C and Page, C.L.
"Pore solution chemistry and corrosion in hydrated cement systems containing chloride salts : a study of cation specific effects"
British Corrosion Journal, 21, 1, 1986, pp 49-53.

2.10 Longuet, P., Burglen, L and Zelwer, A.
"La phase liquid du ciment hydrate"
Materiaux de Construction et Travaux Publics, 676, 1973, pp 35-41.

2.11 Vogel, A.I.
"A text-book of quantitative inorganic analysis"
Third edition. Pub: Longmans, 1961, pp 25-26.

2.12 Diamond, S.
"A critical comparison of mercury porosimetry and capillary condensation pore size distributions of Portand cement pastes"
Cement and Concrete Research, 1, 1971, pp 531-545.

2.13 Young, J.F.
"Capillary porosity in hydrated tricalcium silicate pastes"
Powder Technology, 9, 1974, pp 173-179.

2.14 Washburn, E.W.
"Porosity I. Purpose of investigation. II. Porosity and the mechanism of adsorption"
Journal of the American Ceramic Society, 4, 1921, pp 916-922.

2.15 Stern, M. and Geary, A.L.
"A theoretical analysis of the shape of polarisation curves"
Journal of the Electrochemical Society, 104, 1957, pp 56-63.

2.16 Stern, M.
"A method for determining corrosion rates for linear polarisation data"
Corrosion, 14, 9, 1958, pp 60-64.

2.17 Stern, M. and Weisert, E.D.
"Experimental observations on the relation between polarisation resistance and corrosion rate"
Proceedings of the American Society for Testing and Materials", 59, 1959, pp 1280-1291.

2.18 Andrade, C. and Gonzalez, J.A.
"Quantitative measurements of corrosion rate of reinforcing steels embedded in concrete using polarisation resistance measurements"
Werkstoffe und Korrosion, 29, 1978, pp 515-519.

2.19 Escalante, E., Ito, S. and Cohen, M.
"Measuring the rate of corrosion of steel in concrete"
Federal Highway Administration, National Bureau of Standards NBSIR 80-2012, March 1980.

2.20 Gonzalez, J.A., Molina, A., Escudero, M.L., and Andrade, C.
"Errors in the electrochemical evaluation of very small corrosion rates. Part 1 : Polarisation resistance method applied to corrosion of steel in concrete"
Corrosion Science, 25, 10, 1985, pp 917-930.

2.21. Page, C.L. and Lambert, P.
"Analytical and electrochemical investigations of reinforcement corrosion"
Transport Road Research Laboratory, Contract report number 30, Department of Transport, 1986.

2.22 Wenner, F.
"A method of measuring earth resistivity"
Bulletin of National Bureau of Standards, 12, 1915, pp 469-478.

2.23 Wilkins, N.J.M.
"Resistivity of concrete"
United Kingdom Atomic Energy Authority, Harwell report AERE - M3232, January, 1982.

CHAPTER 3

3.1 Dallaire, G.
"Halting deck deterioration on existing bridges"
Civil Engineering, American Society of Civil Engineers, October 1973, pp 80-86.

3.2 Stewart C.F.
"Considerations for repairing salt damaged bridge decks"
Journal of the American Concrete Institute, December 1975, pp 685-690.

3.3 Vrable, J.B.
"Cathodic protection for reinforcing steel in concrete"
Proc : Chloride corrosion of steel in concrete, American Society for Testing and Materials, ASTM STP 629, Eds : Tonini, D.E. and Dean, S.W., Chicago, June-July 1976, pp 124-149.

3.4 Henriksen, J.F.
"The corrosion and protection of steel in saturated $Ca(OH)_2$ contaminated with NaCl"
Corrosion Science, 20, 1980, pp 1241-1249.

3.5 Hausman, D.A.
"Criteria for cathodic protection of steel in concrete structures"
Materials Protection, October 1969, pp 23-25.

3.6 Hausman, D.A.
"Steel corrosion in concrete - How does it occur?"
Materials Protection, November 1967, pp 19-23.

3.7 Leckie, H.P. and Uhlig, H.H.
"Environmental factors affecting the critical potential of pitting in 18-8 stainless steel"
Journal of the American Electrochemical Society, 113, 12, 1966, pp 1262-1267.

3.8 Gouda, V.K.
"Corrosion and corrosion inhibition of reinforcing steel. 1. Immersed in alkaline solutions"
British Corrosion Journal, 5, 9, 1970, pp 198-203.

3.9 Barneyback Jnr., R.S. and Diamond, S.
"Expression and analysis of pore fluids from hardened cement pastes and mortars"
Cement and Concrete Research, 11, 1981, pp 279-285.

3.10 Roberts, M.H.
"Effect of calcium chloride on the durability of pre-tensioned wire in pre-stressed concrete"
Magazine of Concrete Research, 14, 1962, pp 143-154.

3.11 Richartz, W.
"Die bindung von chlorid be : der zementerhartung"
Zement-Kalk-Gips, 22, 10, 169, pp 447-456.

3.12 Monfore, G.E. and Verbeck, G.J.
"Corrosion of pre-stressed wire in concrete"
Journal of the American Concrete Institute, 57, 5, 1960, pp 491-516.

3.13 Ramachandran, V.S.
"Possible state of chlorides in the hydration of tricalcium silicate in the presence of calcium chloride"
Materieux et Constructions, 19, 4, 1971, pp 3-12.

3.14 Lambert, P., Page, C.L. and Short, N.R.
"Pore solution chemistry of the hydrated system tricalcium silicate/sodium chloride/water"
Cement and Concrete Research, 15, 1985, pp 675-680.

3.15 Page, C.L., Short, N.R. and EL Tarras, A.
"Diffusion of chloride ions in hardened cement pastes"
Cement and Concrete Research, 11, 1981, pp 395-406.

3.16 Collepardi, M., Marcialis, A. and Turriziani, R.
"Penetration of chloride ions into cement pastes and concretes"
Journal of the American Ceramic Society, 55, 10, October 1972, pp 534-535.

3.17 Page, C.L. and Lambert, P.
"Kinetics of oxygen diffusion in hardened cement pastes"
Journal of Materials Science, 22, 1987, pp 942-946.

3.18 Rajagopalan, K.S., Rengaswamy, N.S. and Muralidharan, V.S.
"Role of oxygen diffusion in the corrosion of steel reinforcements embedded in cement concrete"
Indian Journal of Technology, 11, January 1973, pp 34-37.

3.19 Page, C.L.
"Mechanism of corrosion protection of reinforced concrete marine structures"
Nature, 258, December 1975, pp 514-515.

3.20 Page, C.L. and Treadaway, K.W.J.
"Aspects of the electrochemistry of steel in concrete"
Nature, 297, 5862, May 1982, pp 109-115.

3.21 Page, C.L. and Lambert, P.
"Analytical and electrochemical investigations of reinforcement corrosion"
Transport Road Research Laboratory, Contract research report Number 30, Department of Transport, 1986.

3.22 Feliu, S., Gonzalez, J.A.. Andrade, C. and Feliu, V.
"On - site determination of polarization resistance in a reinforced concrete beam"
Proc : Corrosion 87, National Association of Corrosion Engineers, San Fransisco, April 1987, paper number 145.

3.23 Escalante, E., Whitenton, E. and Qui, F.
"Measuring the rate of corrosion of reinforcing steel in concrete"

United States Federal Highway Administration, National Bureau of Standards NBSIR 86-3456, October 1986.

3.24 Beeby, A.W.
"Corrosion of reinforcing steel in concrete and its relation to cracking"
The Structural Engineer, 56A, 3, March 1978, pp 77-81.

3.25 Vennesland, Ø. and Gjorv, O.E.
"Effect of cracks on steel corrosion in submerged concrete sea structures"
Proc : Corrosion 81, National Association of Corrosion Engineers, Toronto, April 1981, paper number 50.

3.26 Gjorv, O.E.
"Concrete in the oceans"
Marine Science Communications, 1, 1, 1975, pp 51-74.

3.27 Rehm, G. and Moll, H.
"Versuche zum stadium des einflusses der rizzbreite auf die rostbildung und der Bewehrung von stahlbetonbauteilen"
Deutcher Ausschuss für Stahlbeton, Heft 169. 1964, pp 3-22.

3.28 Tuutti, K.
"Corrosion of steel in concrete"
Swedish Cement and Concrete Institute, report number fo 4.82, 1982.

CHAPTER 4

4.1 Building Research Establishment Digest 263 : Part 1
"The durability of steel concrete : Part 1 Mechanism of protection and corrosion"
Pub: Her Majesty's Stationary Office, July 1982.

4.2 Arup, H.H.
"Surveys of reinforced concrete structures"
Proc: U.K. Corrosion 86 7th International corrosion event of the Institute of Corrosion Science and Technology, Birmingham, November 1986, pp 7-15.

4.3 Building Research Establishment Digest 263 : Part 3
"The durability of steel in concrete : Part 3 The repair of reinforced concrete"
Pub: Her Majesty's Stationary Office, September, 1982.

4.4 Keer, J.G.
"Behaviour or concrete members repaired by resin injection"
Proc: Cement and Concrete Association Research Seminar, Slough, June/July 1986, pp 163-167.

4.5 McCurrich, L.H., Keeley, C., Cheriton, L.W. and Turner, K.J.
"Mortar repair systems - Corrosion protection for damaged reinforced concrete"
Corrosion of Reinforcement in Concrete Construction.
Ed: Crane, A.P., Pub: Ellis Horwood, 1983, pp 235-253.

4.6 Bijen, J.M. and van der Widen, N.G.B.
"Alternatives for repair of chloride contaminated structures"
Proc: 1st International conference of deterioration and repair of reinforced concrete in the Arabian Gulf, Vol 1, Bahrain, 1987, pp 449-468.

4.7 Kukacka, L.E.
"The use of polymer materials for bridge deck applications"
Proc: Chloride corrosion of steel in concrete, American Society of Testing and Materials, Eds: Tonini, D.E. and Dean, S.W., Chicago, June-July 1976, pp 100-109.

4.8 Kilareski, W.P.
"Corrosion induced deterioration of reinforced concrete - An overview"
Materials Performance, march 1980, pp 48-50.

4.9 Slater, J.E., Lankard, D.R., and Moreland, P.J.
"Electrochemical removal of chlorides from concrete bridge decks"
Materials Performance, November, 1976, pp 21-26.

4.10 Statfull, R.F.
"Cathodic protection of a bridge deck : Preliminary investigation"
Materials Performance, April 1974, pp 24-25.

4.11 Kay, E.A. and Regan, J.
"Acceptance and compliance testing of patch repair materials"
Proc: 1st International conference on deterioration and repair of reinforced concrete in the Arabian Gulf, Vol 1, Bahrain, 1987, pp 235-248.

4.12 Page, C.L. and Treadaway, K.W.J.
"Aspects of the electrochemistry of steel in concrete"
Nature, 297, 5862, May 1982, pp 109-115.

4.13 O'Brien, T.P.
"Concrete deterioration and repair"
Proc: Institute of Civil Engineers, Part 1, 68, 1980, pp 399-408.

4.14 Pullar-Strecker, P.
"Specifying and commissioning repair work"
Proc: 1st International conference on deterioration and repair of reinforced concrete in the Arabian Gulf, Vol 1, Bahrain, 1987, pp 1-14.

4.15 Treadaway, K.W.J.
"Testing the properties of materials for concrete repair - A review"
Proc: 1st International conference on deterioration and repair of reinforced concrete in the Arabian Gulf, Vol 1, Bahrain, 1987, pp 49-78.

4.16 McCurrich, L.H., Lambe, R.W. and Jackson, J.B.
"A systematic approach to reducing chloride penetration"
Proc: 1st International conference on deterioration and repair in the Arabian Gulf, Vol 1, Bahrain, 1987, pp 553-554.

4.17 Hamenstein, P. and Taylor, M.
"Polymers used to upgrade the quality of concrete repair materials"
Proc: 1st International conference on deterioration and repair of concrete in the Arabian Gulf, Vol 1, Bahrain, 1987, pp 15-48.

4.18 McCurrich, L.H., Cheriton, L.W. and Little, D.R.
"Repair systems for preventing further corrosion in damaged reinforced concrete"
Proc: 1st International conference on the deterioration and repair of reinforced concrete in the Arabian Gulf, Vol 1, Bahrain, 1985, pp 151-168.

4.19 John, D.G., Coote, A.T., Treadaway, K.W.J. and Dawson, J.L.
"The repair of concrete - a laboratory and exposure site investigation"
Corrosion of Reinforcement in Concrete Construction.
Ed: Crane, A.P., Pub: Ellis Horwood, 1983, pp 263-286.

4.20 McKenzie, S.G., Treadaway, K.W.J. and Coote, A.T.
"Repairs to reinforced concrete in marine structures: assessment of a method for studying and evaluating repair systems"
Marine Concrete, Pub: Concrete Society, 1986, pp 333-348.

4.21 Chamberlain, J.
"Cell reversal of the zinc/iron system in sodium bicarbonate and sodium nitrate solutions"
Surface Technology, 25, 1985, pp 229-257.

4.22 Chatalov, A. Ya.
"Effect du pH sur la comportement electrochimique des metaux et leur restistance a la corrosion"
Duklad. Akad. Nauk. S.S.S.R. 86, 1952, pp 775-7.

4.23 Nixon, P. and Page, C.L.
"Pore solution chemistry and alkali aggregate reaction"
Concrete Durability, American Concrete Institute, SP-100 Volume 2, Detroit, 1987, pp 1833-1862.

4.24 Sergi, G., Short, N.R. and Page, C.L.
"Corrosion of galvanised and galvannealed steel in solutions of pH 9.0 to 14.0"
Corrosion, 41, 11, 1985, pp 618-624.

4.25 Macias, A. and Andrade, C.
"Corrosion of galvanised steel reinforcements in alkaline solutions"
"Part 1 : Electrochemical results"
British Corrosion Journal, 22, 2, 1987, pp 113-118.

4.26 Macias, A. and Andrade, C.
"Corrosion of galvanised steel reinforcements in alkaline solutions"
"Part 2 : SEM study and identification of corrosion products"
British Corrosion Journal, 22, 2, 1987, pp 119-124.

CHAPTER 5

5.1 Arup, H.H.
"Surveys of reinforced concrete structures"
Proc: U.K. Corrosion 86, 7th International corrosion event of the Institute of Corrosion and Science and Technology, Birmingham, November 1986, pp 7-15.

5.2 Roberts, M.H.
"Carbonation of concrete made with dense natural aggregates"
Building Research Establishment information paper 1P6/81, 1981.

5.3 Building Research Establishment
"Simplified method for the detection and determination of chloride in hardened concrete"
Building Research Establishment information sheet 15 12/77, 1977.

5.4 Building Research Establishment
"Determination of chloride and cement content in hardened Portland cement concrete"
Building Research Establishment information sheet 15 13/77, 1977.

5.5 American Society for Testing and Materials
"Standard test method for half-cell potentials of reinforcing steel in concrete"
American Society for Testing and Materials C876-80, 1980.

5.6 Page, C.L. and Treadaway, K.W.J.
"Aspects of the electrochemistry of steel in concrete"
Nature, 297, 5862, May 1982, pp 109-115.

5.7 Page, C.L.
"Problems in service life prediction of building and construction materials"
North Atlantic Treaty Organisation, AS1 series E, number 95, Ed: Masters, L.W., Pub: Martins Nijhoff, 1985, pp 59-74.

5.8 Andrade, C. and Gonzalez, J.A.
"Quantitative measurements of corrosion rate of reinforcing steels embedded in concrete using polarisation resistance measurements"
Werkstoffe und Korrosion, 29, 1978, pp 515-519.

5.9 Gonzalez, J.A., Molina, A., Escudero, M.L. and Andrade, C.
"Errors in the electrochemical evaluation of very small corrosion rates. part 1: Polarisation resistance method applied to corrosion of steel in concrete"
Corrosion Science, 25, 10, 1985, pp 917-930.

5.10 Escalante, E., Ito, S. and Cohen, M.
"Measuring the rate of corrosion of reinforcing steel in concrete"

Federal Highway Administration, National Bureau of Standards NBSIR 80-2012, March 1980.

5.11 Escalante, E., Cohen, M. and Kahn, A.H.
"Measuring the rate of corrosion of reinforcing steel in concrete"
Federal Highway Administration, National Bureau of Standards, NBSIR 84- 2853. April 1984.

5.12 Dawson, J.L.
"Corrosion monitoring of steel in concrete"
Corrosion of Reinforcement in Concrete Construction, Ed: Crane, A.P., Pub: Ellis Horwood, 1983, pp 175-191.

5.13 Vassie, P.R.W.
"Evaluation of techniques for investigating the corrosion of steel in concrete"
Transport Road Research laboratory, supplementary report number 397, 1978.

5.14 Van Daveer, J.R.
"Techniques for evaluating reinforced concrete bridge decks"
Journal of the American Concrete Institute, December 1975, pp 697-704.

5.15 Stratfull, R.F.
"Half-cell potentials and the corrosion of steel in concrete"
State of California, Department of Public Works, Division of Highways Materials and Research Department, Research Paper CA-HY-MR-5166-7-72-T2, Interim report PB 218-70, November 1972.

5.16 Arup, H.H. and Gronvold, F.O.
"Localisation of corroding reinforcement by electrochemical potential surveys"
RILEM Quality control of concrete structures, Vol 1, June 1979, pp 251-258.

5.17 Wilkins, N.J.M. and Lawrence, P.F.
"The corrosion of steel reinforcements in concrete immersed in seawater"
Corrosion of Reinforcement in Concrete Construction, Ed: Crane, A.P., Pub: Ellis Horwood, 1983, pp 119-142.

5.18 Stern, M. and Geary, A.L.
"1. A theoretical analysis of the shape of polarisation curves"
Journal of the Electrochemical Society, 104, 1, January 1957, pp 56-63.

5.19 Ecalante, E., Cohen, M. and Kahn, A.H.
"Measuring in the rate of corrosion of reinforcing steel in concrete"
FHWA, NBSIR 84-2853, April 1984.

5.20 Escalante, E., Whitenton, E. and Qui, F.
"Measuring the rate of corrosion of reinforcing steel in concrete"
United States Federal Highway Administration, National Bureau of Standards NBSIR 86-3456, October 1986.

5.21 Page, C.L. and Lambert, P.
"Analytical and electrochemical investigations of reinforcement corrosion"
Transport Road Research Laboratory, Contract report number 30, Department of Transport, 1986.

5.22 Macias, A. and Andrade, C.
"Corrosion of galvanised steel reinforcements in alkaline solutions"
British Corrosion Journal, 22, 2, 1987, pp 113-118.

5.23 Haldky, K., Callow, L.M. and Dawson, J.L.
"Corrosion rates from impedence measurements : An introduction"
British Corrosion Journal, 15, 1, 1980, pp 20-25.

5.24 John, D.G., Searson, P.C. and Dawson, J.L.
"Use of ac impedence technique in studies on steel in concrete in immersed conditions"
British Corrosion journal, 16, 2, 1981. pp 102-106.

5.25 John, D.G., Coote, A.T., Treadaway, K.W.J. and Dawson, J.L.
"The repair of concrete - A laboratory and exposure site investigation"
Corrosion of Reinforcement in Concrete Construction, Ed: Crane, A.P., Pub: Ellis Horwood, 1983, pp 263-286.

5.26 Houge, F.N. and Hoppenbrouwers, A.M.H.
"1/f Noise in continuous thin gold films"
Physica, 45, 1969, pp 386-392.

5.27 Kiser, K.M.
"1/f Noise in thin films of semiconductors"
Journal of the Electrochemical Society, 111, 5, 1964, pp 556-560.

5.28 Barker, G.C.
"Noise connected with electrode processes"
Journal of Electroanalytical Chemistry and Interfacial Electrochemistry, 21, 1969, 127-136.

5.29 Fleischann, M. and Oldfield, J.W.
"Generation-recombination noise in weak electrolytes"
Journal of Electroanalytical Chemistry and Interfacial Electrochemistry, 27, 1970, pp 207-218.

5.30 Blanc, G., Epelboin, I., Gabrielli, C. and Keddam, M.
"Electrochemical noise generated by anodic dissolution or diffusion processes"
Journal of Electroanalytical Chemistry, 75, 1977, pp 97-124.

5.31 Blanc, G., Gabrielli, C. and Keddam, M.
"Measurement of electrochemical noise by a cross correlation method"
Electrochimica Acta, 20, 1975, pp 687-689.

5.32 Haldky, K. and Dawson, J.L.
"The measurement of localised corrosion using electrochemical noise"
Corrosion Science, 21, 4, 1981, pp 317-322.

5.33 Bertocci, U. and Yang-Xiang, Y.
"An examination of current fluctuations during pit initiation in Fe-Cr alloys"
Journal of the Electrochemical Society : 5, May 1984, pp 1011-1017.

5.34 Simoes, A.M.P. and Ferreira, M.G.S.
"Crevice corrosion studies on stainless steel using electrochemical noise measurements"
British Corrosion Journal, 22. 1, 1987, pp 21-25.

CHAPTER 6

6.1 Uhlig, H.H. and Winston Revie, H.
"Corrosion and control"
3rd edition, Pub : John Wiley and Sons, 1985, p217.

6.2 Davy, H.
"Additional experiments and observations on the application of electrical combinations to the preservation of the copper sheeting of ships"
Philosophical Transactions of the Royal Society, 114, 1825, pp 242-246.

6.3 Lynes, W.
"Some historical developments relating to corrosion"
Journal of the Electrochemical Society, 98, 3C, 1951.

6.4 Escalante, E.
National Bureau of Standards, Final report number NBS-MN-158, 1977.

6.5 Reinhart, F.
United States Naval Civil Engineering Laboratories, Project AF 2102, 1975.

6.6 Mears, R.B. and Brown, R.H.
"A theory of cathodic protection"
Transactions of the Electrochemical Society, 74, 1938, pp 519-531.

6.7 Hoar, T.P.
"The electrochemistry of protective metallic coatings"
Journal of the Electrodepositors' Technical Society, 14, 13, 1938, pp 33-46.

6.8 Stern, M. and Geary, A.L.
"I.Electrochemical polarization. A theoretical analysis of the shape of polarization curves"
Journal of the Electrochemical Society, 104, 1, 1957, pp 56-63.

6.9 Jones, D.A.
"The application of electrode kinetics to the theory and practice of cathodic protection"
Corrosion Science, 11, 1971, pp 439-451.

6.10 Glasstone, S.
"Introduction to electrochemistry"
Pub : Van Nonstrand, 1942, p 447.

6.11 Barneyback, R.S. Jr. and Diamond, S.
"Expression and analysis of pore fluids from hardened cement pastes and mortars"
Cement and Concrete Research, 11, 1979, pp 279-285.

6.12 Dent Glasser, L.S.

"Osmotic pressure and the swelling of gels"
Cement and Concrete Research, 9, 1979, pp 515-517.

6.13 Dent Glasser, L.S. and Katauka, N.
"The chemistry of alkali-aggregate reactions"
Proc : 5th International Conference on : Alkali-aggregate reaction in concrete, Cape Town, March-April, 1981.

6.14 Schwerdtfeger, W.J. and McDorman, O.N.
"Potential and current requirements for cathodic protection of steel in soil"
National Bureau of Standards Journal of Research 47, 2, 1951, pp 104-112.

6.15 Schwerdtfeger, W.J.
"Polarization measurements as related to corrosion of underground steel piling"
Journal of Research, National Bureau of Standards, 75, 2, April-June 1971, pp 107-121.

6.16 Peterson, M.H.
"Principles and criteria for cathodic protection of steel in sea water"
Corrosion, 15, 1959, pp 51-55.

6.17 Kuhn, R.J.
"Cathodic protection of underground pipelines from soil corrosion"
Proceedings of the American Petrol Institute, 141, section 4, 1933.

6.18 Kilareski, W.P.
"Corrosion induced deterioration of reinforced concrete"
Materials Performance, March 1980, pp 48-50.

6.19 National Association of Corrosion Engineers
"Deicing salts, their use and effects"
Materials Performance, April 1975, pp 9-13.

6.20 Fromm, H.
"Cathodic protection of rebar in concrete bridge decks"
Materials Performance, 16, 11, 1977, pp 21-26.

6.21 Manning, D.G. and Schell, H.C.
"Cathodic protection of bridges"
Ontario ministry of transportation and communication, Report Report number ME-86-05, 1986.

6.22 Stratfull, R.F.
"Progress report on inhibiting the corrosion of steel in a concrete bridge"
Corrosion, 15, 1959, pp 331t-334t.

6.23 Jackson, D.R.
"Cathodic protection for reinforced concrete bridge decks"
Federal Highway Administration, Report number FHWA-DP-34-2

6.24 Stratfull, R.F.
"Criteria for the protection of bridge decks"
Corrosion of reinforcement in concrete construction,
Crane, A.P. Pub : Ellis Horwood, 1983, pp 287-332.

6.25 Brown, R.P. and Kessler, R.J.
"A new concept in cathodic protection of steel in concrete - The use of conductive materials"
National Association of Corrosion Engineers, Corrosion 83, Anaheim, 1983, paper number 179.

6.26 Brown, R.P. and Powers, R.G.
"Update on the use of conductive materials for cathodic protection of steel in concrete"
National Association of Corrosion Engineers, Corrosion 85, Boston 1985, Paper number 264.

6.27 Scott, G.N.
"Corrosion protective properties of Portland cement concrete"
Journal of the American Water Works Association, 57, 8, 1965, pp 1038-1052.

6.28 Hausmann, D.A.
"Criteria for cathodic protection of steel in concrete structures"
Materials Protection, October 1969, pp 23-25.

6.29 Vrable, J.B. and Wilde, B.E.
"Electrical potential requirements for cathodic protection of steel in simulated concrete environments"
Corrosion, 36, 1980, pp 18-23.

6.30 Pourbaix, M.
"Applications of electrochemistry in corrosion science and practice"
Corrosion Science, 14, pp 25-82, 1974.

6.31 Schutt, W.R.
"Practical experiences with bridge deck cathodic protection"
National Association of Corrosion Engineers, Corrosion 78, Houston, 1978, paper number 74.

6.32 Heuzé, B.
Proc. 5th International congress on metallic corrosion, Tokyo, 1972, p598.

6.33 Vrable, J.B.
"Cathodic protection for reinforcing steel in concrete"
American Society for Testing and Materials, ASTM STP 629, Philadelphia, 1977, pp 124-149.

6.34 Shaw, J.A.
"Understanding the corrosion resistance of concrete pipe"
Civil Engineering, American Society of Civil Engineers, 1965, pp 39-43.

6.35 Gjörv, O.E. and Vennesland, Ø.

"Cathodic protection of steel in offshore concrete platforms"
National Association of Corrosion Engineers, Corrosion 79, Atlanta, 1979, paper number 139.

6.36 Heuzé, B.
"Cathodic protection of steel in prestressed concrete"
Materials Protection, 1965, pp 57-62.

6.37 Lock, C.E., Dehghanian, C. and Gibbs, L.
"Effect of impressed current on bond strength between steel rebar and concrete"
National Association of Corrosion Engineers, Corrosion 83, Anaheim, 1983, paper number 178.

6.38 Longuet, P., Burglen, L. and Zelwar, A.
"La phase liquide du ciment hydrate"
Revue des Materiaux de Constructions et des Travaux Publics, Ciments of Betons, 676, 1973, pp 35-41.

6.39 Diamond, S. and Lopez-Flores, F.
"Fate of calcium chloride dissolved in concrete mix water"
Journal of the American Ceramic Society, 64, 1981, pp 162-164.

6.40 Page, C.L. and Vennesland, Ø.
"Pore solution composition and chloride binding capacity of silica-fume cement pastes"
Materiaux et Constructions, 16, 91, 1983, pp 19-25.

6.41 Andrade, C. and Page, C.L.
"Pore solution chemistry and corrosion in hydrated cement systems containing chloride salts : A study of specific effects"
British Corrosion Journal, 20, 4, 1985, pp 49-53.

6.42 Page, C.L. and Lambert, P.
"Analytical and electrochemical investigations of reinforcement corrosion"
Transport and Road Research Laboratory, Contract report number 30, Department of Transport, 1986.

6.43 Wyatt, B.S. and Irvine, D.J.
"Cathodic protection of reinforced concrete"
Institute of Corrosion Science and Technology, UK Corrosion 86, Birmingham, 1986, pp 17-38.

6.44 Tutti, K.
"Corrosion of steel in concrete"
Swedish Cement and Concrete Research Institute, report number F04 : 82, Stockholm, 1982.

6.45 Gjorv, O.E., Vennesland, Ø. and EL-Busaidy, A.H.S.
"Electrical resistivity of concrete in the oceans"
Offshore technology conference, Houston, 1977, pp 581-588.

6.46 Lawrence, C.D.
"Diffusion of oxygen through saturated concrete"

5th seminar on cement and concrete science, Oxford University, 1984.

6.47 Page, C.L. and Lambert, P.
"Kinetics of oxygen diffusion in hardened cement pastes"
Journal of Materials Science, 22, 1987, pp 942-946.

6.48 Palmer, D.
"Alkali-aggregate reactions, recent occurrences in the British Isles"
Proceedings 4th International conference on the effect of alkalis in cement and concrete, Purdue University, 1978, pp 285-296.

6.49 Moore, A.E.
"Effect of electric current on alkali-silica reaction"
Proceedings 4th International conference on the effect of alkalis in cement and concrete, Purdue University, 1978, pp 69-72.

6.50 Page, C.L., Al Khalif, M.N. and Ritchie, A.G.B.
"Steel/mortar interfaces : Mechanical characteristics and electrocapillarity"
Cement and Concrete Research, 8, 1978, pp 481-490.

6.51 Mussinelli, G., Tettamanti, M. and Pedeferri, P.
"The effect of current density on anode behaviour and on concrete in the anode region"
Proc : 1st International conference on deterioration and repair of reinforced concrete in the Arabian Gulf, Vol. 1, Bahrain, September 1987, pp 99-120.

6.52 Hover, K.C. and Natesaiyer, K.
"Effect of cathodic protection currents on alkali-aggregate reaction in concrete"
Summary of work presented at the international conference on alkali-aggregate reaction in concrete, Ottawa, August 1986.

6.53 National Association of Corrosion Engineers.
"Proposed NACE standard recommended practice for cathodic protection of reinforcing steel in concrete structures"
Unpublished draft of NACE technical practices committee T-3K-E, October 1986.

6.54 Page, C.L.
"Cathodic protection of reinforced concrete structures above ground"
Personal communication on the meeting of NACE/Institute of Corrosion Science and Technology joint venture task group E4-9, September 1987, (unpublished).

6.55 Nixon, P. and Page, C.L.
"Pore solution chemistry and alkali aggregate reaction"
Concrete Durability : AC1 Special Publication SP100, Vol. 2 1987, pp 1833-1862.

7.1 Gjorv, O.E. and Vennesland, Ø.
"Diffusion of chloride ions from seawater into concrete"
Cement and Concrete Research, 9, 1979, pp 229-238.

7.2 Ost, B. and Monfore, G.E.
"Penetration of chloride into concrete"
Journal of the Portland Cement Association, Research and Development Laboratory, 8, 1966, pp 46-52.

7.3 British Standard Code of Practive 110 : Part 1
"Structural use of concrete"
British Standards Institution, 1972 (amended May 1977).

7.4 Page, C.L.
"The corrosion of reinforcing steel in concrete;its causes and and control"
Bulletin of the Institute of Corrosion Science and Technology, 77, 1979, pp 2-7.

7.5 Jost, W.
"Diffusion in solids, liquids, gases"
Pub : Academic Press, 1960, p 139.

7.6 Page, C.L., Short, N.R. and EL Tarras, A.
"Diffusion of chloride ions in hardened cement pastes"
Cement and Concrete Research, 11, 1981, pp 395-406.

7.7 Sorenson, B. and Maahn, E.
"Penetration rate of chloride in marine concrete structures"
Nordic Concrete Research, 1, December 1982, pp 24.1-24.18.

7.8 Efes, Y.
"Effect of cements with varying content of granulated blast furnace slag on chloride diffusion in concrete"
Betonwerk and Fertigteil - Technik, Heft, 4, 1980, pp 224-228.

7.9 McCurrick, L.H., Keeley, C., Cheriton, L.W. and Turner, K.J.
"Mortar repair systems-corrosion protection for damaged reinforced concrete"
Corrosion of Reinforcement in Concrete Construction, Ed : Crane, A.P., Pub : Ellis Horwood, 1983, pp 235-253.

7.10 Collepardi, M., Marcialis, A and Turriziani, R.
"Penetration of chloride ions into cement pastes and concretes"
Journal of the American Ceramic Society, 55, 10, October 1972, pp 534-535.

7.11 Collepardi, M., Marcialis, A. and Turriziani, R.
"Kinetics of penetration of chloride ions into concrete"
It Cimento, 4, 1970, pp 157-163.

7.12 Kondo, R., Satake, M. and Ushiyama, H.

"Diffusion of various ions in hardened Portland cement"
Review of the 28th general meeting, The Cement Association of Japan, 1974, pp 41-43.

7.13 Goto, S. and Roy, D.M.
"Diffusion of ions through hardened cement pastes"
Cement and Concrete Research, 11, 1981, pp 751-757.

7.14 Atkinson, A. and Nickerson, A.K.
"The diffusion of ions through water-saturated cement"
Journal of Materials Science, 19, 1984, pp 3068-3078.

7.15 Takagi, T.,Goto, S. and Daimon, M.
"Diffusion of I^- ion through hardened cement paste"
Review of the 38th general meeting, The Cement Association of Japan, 14, 1984, pp 72-75.

7.16 Parsons, R.
"Handbook of electrochemical constants"
Pub : Butterworth, 1959, p79.

7.17 Lambert, P., Page, C.L. and Short, N.R.
"Diffusion of chloride ions in hardened cement pastes containing pure cement minerals"
Proc : The Chemistry of Chemically Related Properties of Cement, Ed : F.P. Glasser, British Ceramic Society, 35, Oxford, September 1984, pp 267-276.

7.18 Holden, W.R., Page, C.L. and Short, N.R.
"The influence of chlorides and sulphates on durability of reinforcement in concrete"
Corrosion of Reinforcement in Concrete Construction, Ed : Crane, A.P., Pub : Ellis Horwood, 1983, pp 143-150.

7.19 Byfor, K.
"Influence of silica fume and fly-ash on chloride diffusion and pH values in cement pastes"
Cement and Concrete Research, 17, 1987, pp 115-130.

7.20 Uchikawa, H.
"Effect of blending components on hydration and structure formation"
Proc : 8th International Congress on Chemistry of Cements, Rio de Janeiro, 1986, pp 250-280.

7.21 Feldman, R.F.
"Pore structure, permeability and diffusivity related to durability"
Proc : 8th International Congress on Chemistry of Cements, Rio de Janeiro, 1986, pp 336-356.

7.22 Feldman, R.F.
"Pore structure damage in blended cements caused by mercury intrusion"
Journal of the American Ceramic Society, 62, 1, 1984, pp 30-33.

7.23 Marsh, B.K. and Day, R.L.

"Some difficulties in the assessment of pore structure of high performance blended cement pastes"
Proc : Materials Research Symposium, "Very high strength cement-based materials", 42, 1, 1985, pp 113-122.

7.24 Verbeck, G.
"Cement hydration reactions at early ages"
Research Department Bulletin of the Portland Cement Association, Stokie, U.S.A., p 189.

7.25 Collepardi, M., Corrali, M. and Valente, M.
"Influence of polymerization of sulfonated naphthalene condensate and its interaction with cement"
American Concrete Institute, Developments in the use of Superplasticizers, AC1 SP 68, 1981, pp 485-498.

APPENDIX 1

Details of certain mix additives and surface treatments used in the production of diffusion specimens described in Chapter 7.

Additives.

Naphthalene sulphonate; relatively long molecular chain length (>10) relatively high molecular weight, low sulphate content.

Naphthalene sulphonate; relatively short molecular chain length (<10), relatively low molecular weight, low sulphate content.

Melamine formaldehyde condensate; no further detail available.

Styrene butadiene rubber; copolymer typically 25% styrene and 75% butadiene, in a water emulsion containing approximately 50% solids.

Polyvinyl acetate; copolymer stabilised with polyvinyl alcohol.

Surface treatments.

Alkoxy silane; oligomerous, small molecular size (approximately 10 Å).

Methyl methacrylate; polymeric acrylic.

APPENDIX 2

Details of reinforcement and mortar primers used in Chapter 4.

Ordinary Portland cement slurry;
Mix of OPC (Ketton) and deionized water, a water/cement ratio of 3.0 was used in order to achieve a brushable consistency.

Acrylic bonding agent; an emulsion based on an approximately 50% acrylic dispersion.

Zinc rich epoxy primer; a single component epoxy resin containing a high zinc loading, approximately 30% by volume(ZINC PLUS RESIN)

Insulating epoxy; high build, two part material based on epoxy resins and fine fillers.

APPENDIX 3

Details of the proprietary repair mortar used in Chapter 4.

Description; a pre-blended polymer modified repair compound containing graded aggregates, lightweight fillers and various additives. The material was mixed with deionized water at the optimum water/powder ratio of 0.175.

Typical properties :

1 day compressive strength	= 6-8 N/mm^2
28 day compressive strength	= 20-25 N/mm^2
Coefficient of chloride diffusion	= 1.1×10^{-9} cm^2 s^{-1}
Coefficient of thermal expansion	= $(7\text{-}10) \times 10^{-6}/^{o}C$

APPENDIX 4

Twenty eight day compressive strength determination used for the specimens in Chapter 7.

Example of calculation :

Maximum load sustained;

Cube 1 = 987 KN

Cube 2 = 960 KN

Cube 3 = 923 KN

average maximum load = 957 KN

Cross-sectional area through which load was applied = 10 000 mm^2

$$= \frac{957\ 000\ N}{10\ 000\ mm^2}$$

$$= 95.7\ N/mm^2$$

APPENDIX 5

Example of the calculation of hydroxyl ion concentration

Volume of pore solution for analysis = 0.1 ml aliquot.

Volume of 10mM nitric acid dispensed = 8.13 ml

Hydroxyl ion concentration = (8.13 x 0.01 x 10)M

OH^- = 0.813 M

On the pH scale = $14 + \log_{10} (OH^-)$

$= 14 + \log_{10} 0.813$

$= 14 + (-0.09)$

pH = 13.91

APPENDIX 6

Applied pressure (psi)	Penetration counter * indication	Pore diameter (μm)	Volume of pores of indicated diameter and larger (cm^3/g) x 10^{-2}
1	12	124	0.18
14	48	8	0.71
100	143	1.2	2.11
250	175	0.5	2.58
800	259	0.155	3.82
1800	293	0.069	4.32
4200	453	0.029	6.68
8000	563	0.015	8.31
18000	605	0.009	8.93
24000	608	0.005	8.97
32000	610	0.004	9.00
40000	611	0.003	9.01
44000	612	0.0028	9.03

Example of the calculation of pore size distribution from porosimetry data for OPC mortar, 0.6 water/cement ratio containing short chain naphthalene sulphonate additive. Note: for the purposes of this example the number of data points calculated here has been reduced to approx. a third of those recorded and plotted in Chapter 7. A contact angle of 117° was assumed for all specimens

* corrected for blank run

APPENDIX 7

Traces of macro-cell galvanic current against time, for specimens in wet and dry conditions. Three traces per graph are shown, each trace represents the galvanic current measured between the following segment combinations (% chloride ion by weight of cement).

Trace 1 = 5.0% vs 1.0% + 0.0%

Trace 2 = 1.0% vs 0.1% + 0.0%

Trace 3 = 0.1% vs 0.0%

APPENDIX 7.1 = wet

APPENDIX 7.2 = dry

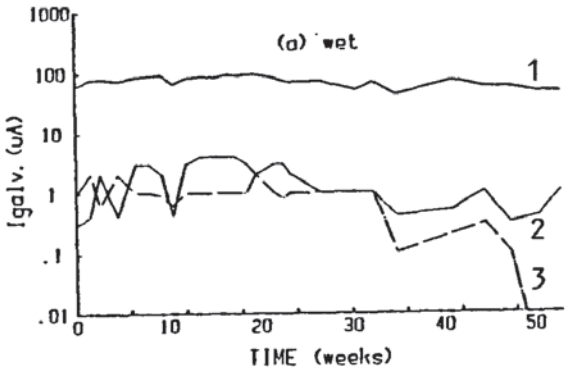
(a) wet
1
2
3
Igalv. (uA)
1000
100
10
1
.1
.01
0
10
20
30
40
50
TIME (weeks)

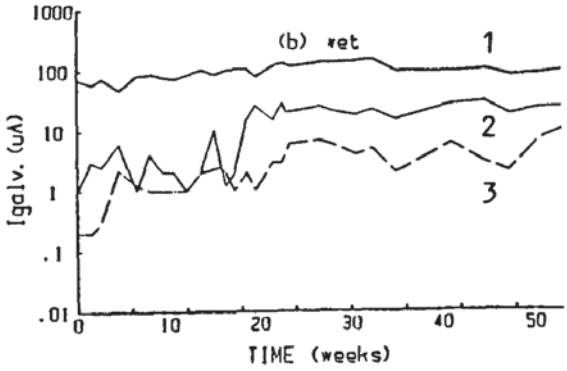
(b) wet
1
2
3
Igalv. (uA)
1000
100
10
1
.1
.01
0
10
20
30
40
50
TIME (weeks)

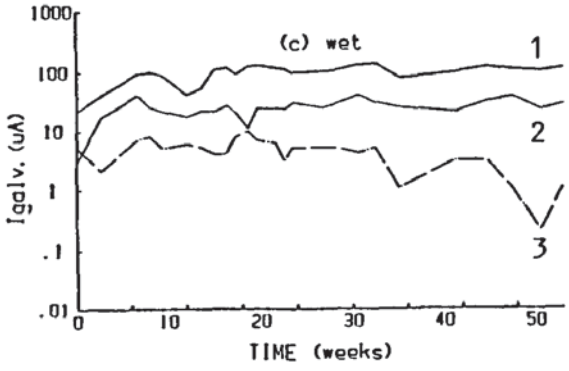
(c) wet
1
2
3
Igalv. (uA)
1000
100
10
1
.1
.01
0
10
20
30
40
50
TIME (weeks)

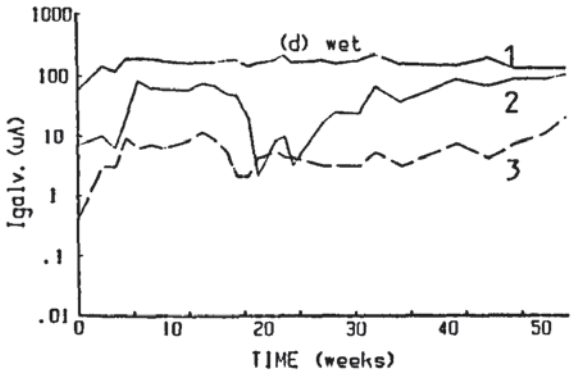
(d) wet
1
2
3
Igalv. (uA)
1000
100
10
1
.1
.01
0
10
20
30
40
50
TIME (weeks)

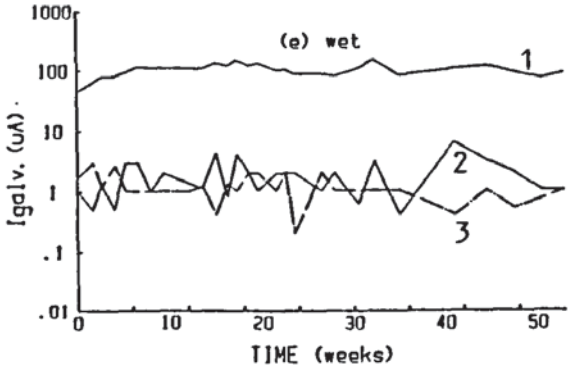
(e) wet
1
2
3
Igalv. (uA)
1000
100
10
1
.1
.01
0
10
20
30
40
50
TIME (weeks)

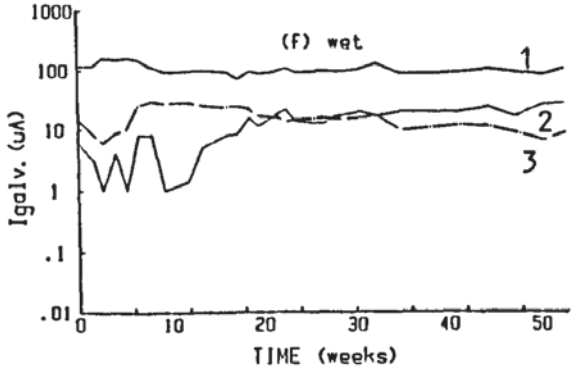
(f) wet
1
2
3
Igalv. (uA)
1000
100
10
1
.1
.01
0
10
20
30
40
50
TIME (weeks)

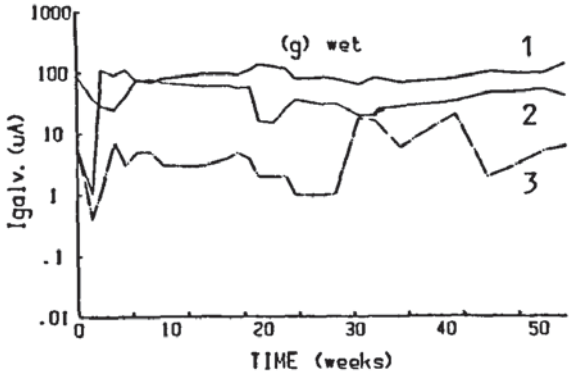
(g) wet
1
2
3
Igalv. (uA)
1000
100
10
1
.1
.01
0
10
20
30
40
50
TIME (weeks)

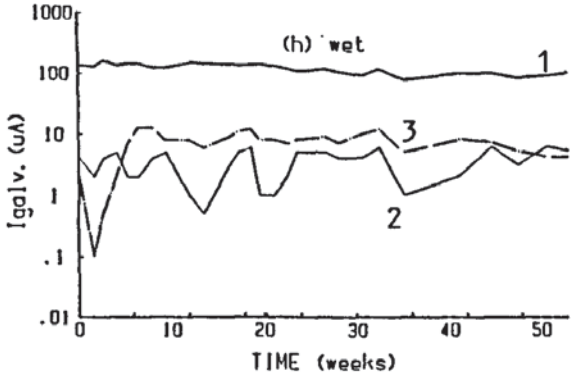
(h) wet
1
2
3
Igalv. (uA)
1000
100
10
1
.1
.01
0
10
20
30
40
50
TIME (weeks)

APPENDIX 7.1

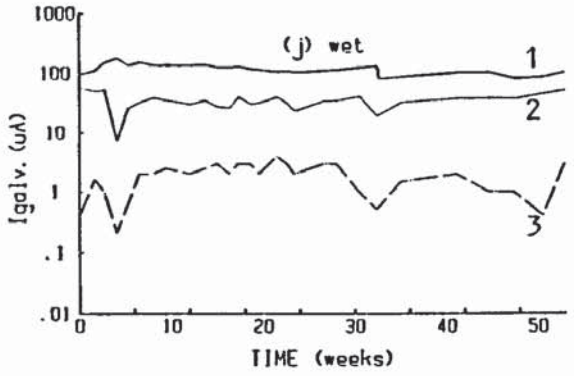

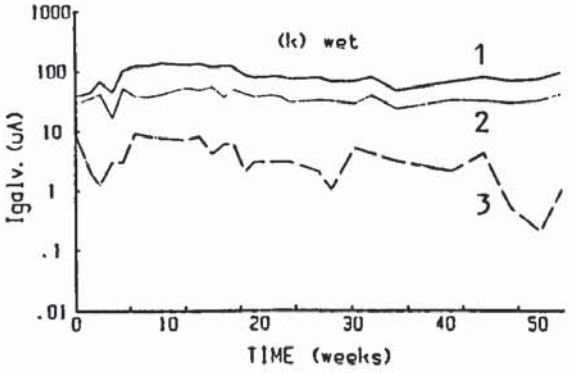

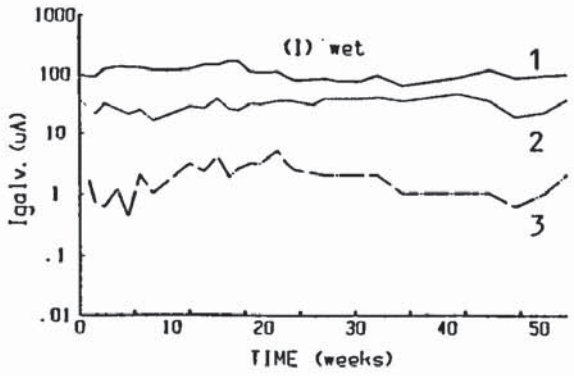

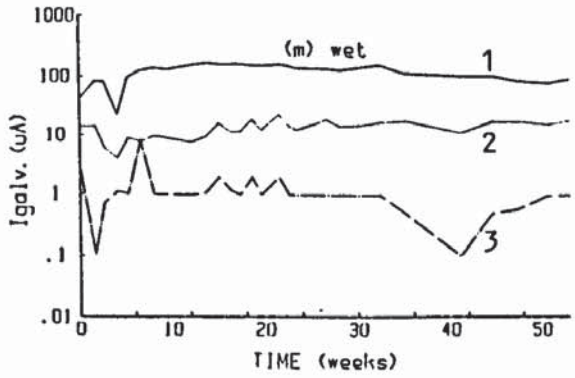

APPENDIX 7.1 (continued)

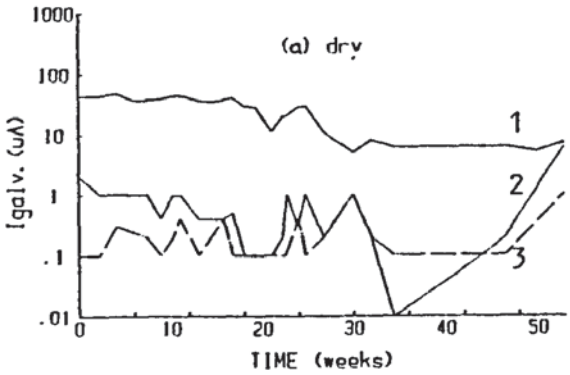
(a) dry
Igalv. (uA)
1000
100
10
1
.1
.01
0
10
20
30
40
50
TIME (weeks)
1
2
3

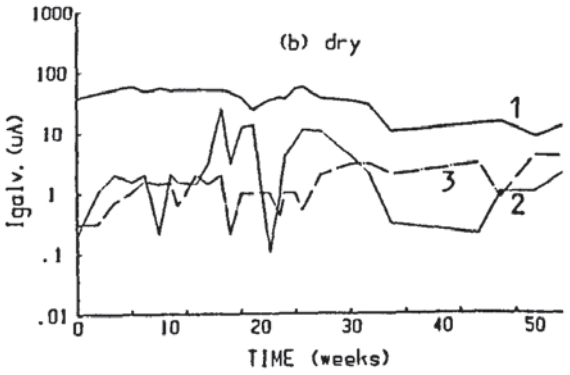
(b) dry
Igalv. (uA)
1000
100
10
1
.1
.01
0
10
20
30
40
50
TIME (weeks)
1
2
3

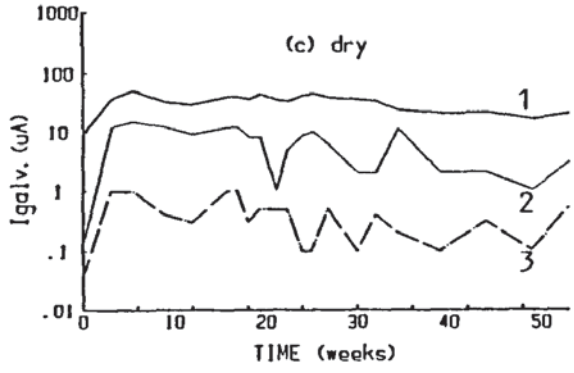
(c) dry
Igalv. (uA)
1000
100
10
1
.1
.01
0
10
20
30
40
50
TIME (weeks)
1
2
3

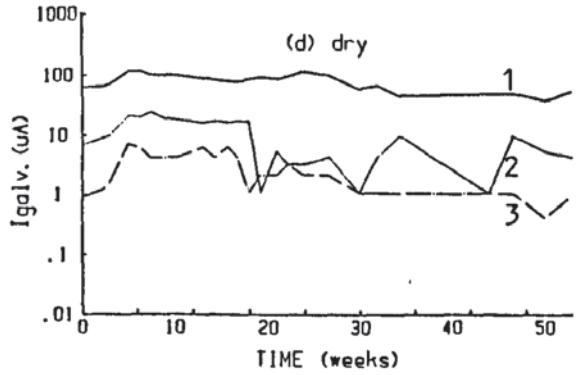
(d) dry
Igalv. (uA)
1000
100
10
1
.1
.01
0
10
20
30
40
50
TIME (weeks)
1
2
3

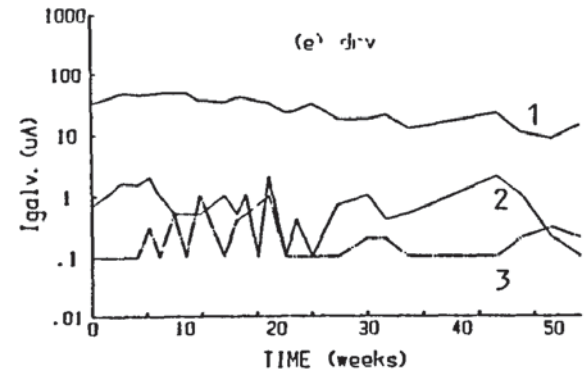
(e) dry
Igalv. (uA)
1000
100
10
1
.1
.01
0
10
20
30
40
50
TIME (weeks)
1
2
3

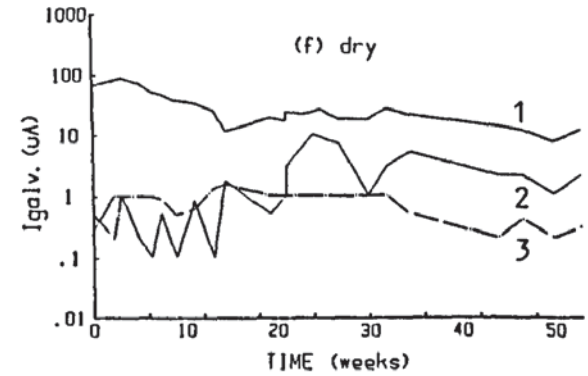
(f) dry
Igalv. (uA)
1000
100
10
1
.1
.01
0
10
20
30
40
50
TIME (weeks)
1
2
3

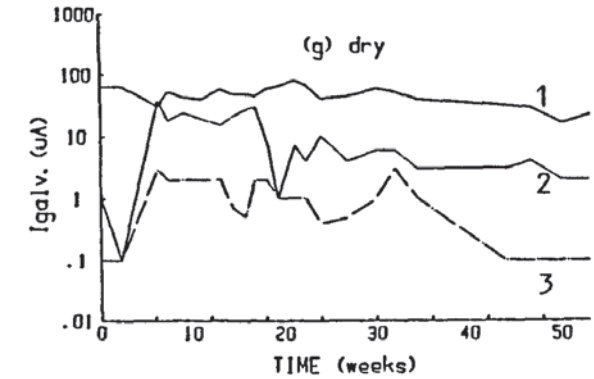
(g) dry
Igalv. (uA)
1000
100
10
1
.1
.01
0
10
20
30
40
50
TIME (weeks)
1
2
3

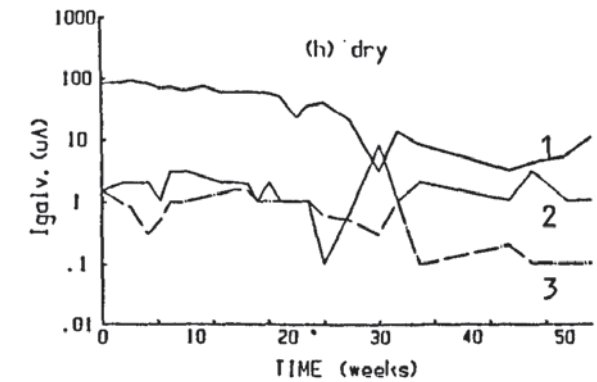
(h) dry
Igalv. (uA)
1000
100
10
1
.1
.01
0
10
20
30
40
50
TIME (weeks)
1
2
3

APPENDIX 7.2

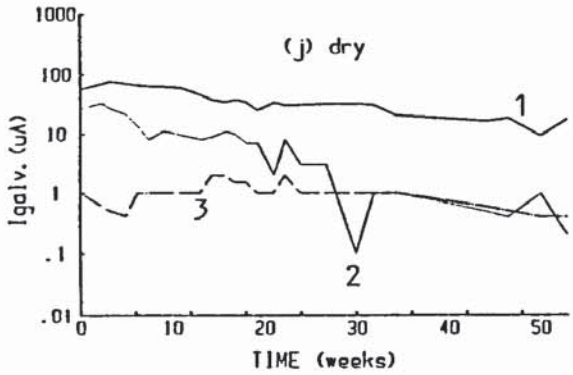

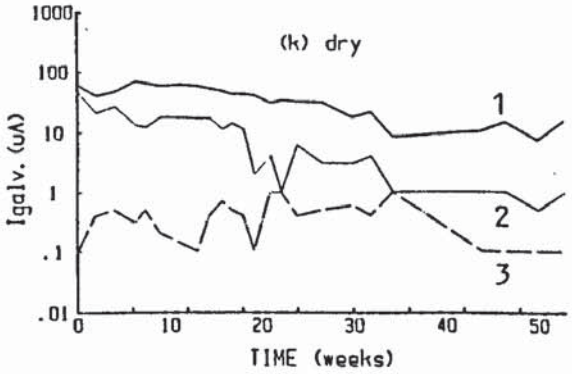

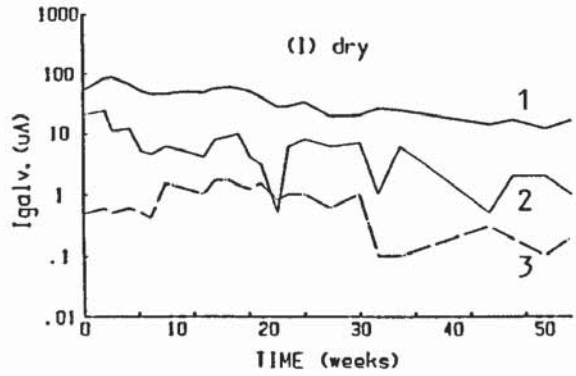

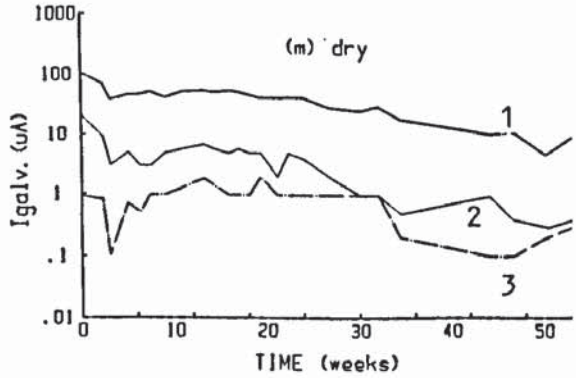

APPENDIX 7.2 (continued)

APPENDIX 8

Traces of galvanic current (cathodic) for specimens in wet and dry condition. The galvanic current was measured between the following combination of segments (% chloride ion by weight of cement).

1% vs 5.0% + 0.1% + 0.0%

APPENDIX 8.1 = wet

APPENDIX 8.2 = dry

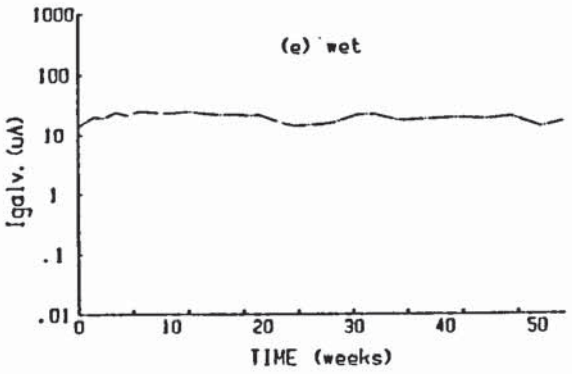
(e) wet
Igalv. (uA)
1000
100
10
1
.1
.01
0
10
20
30
40
50
TIME (weeks)

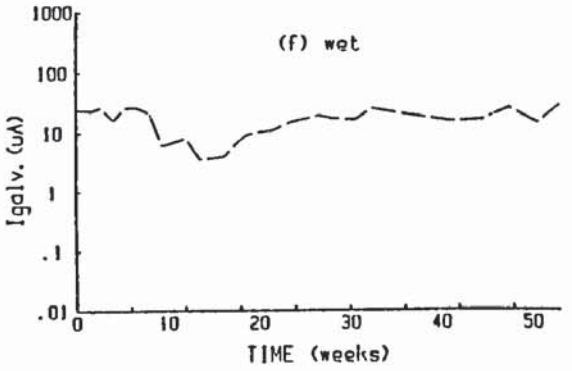
(f) wet
Igalv. (uA)
1000
100
10
1
.1
.01
0
10
20
30
40
50
TIME (weeks)

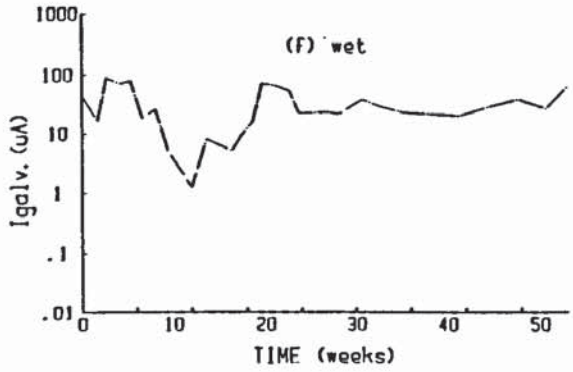
(f) wet
Igalv. (uA)
1000
100
10
1
.1
.01
0
10
20
30
40
50
TIME (weeks)

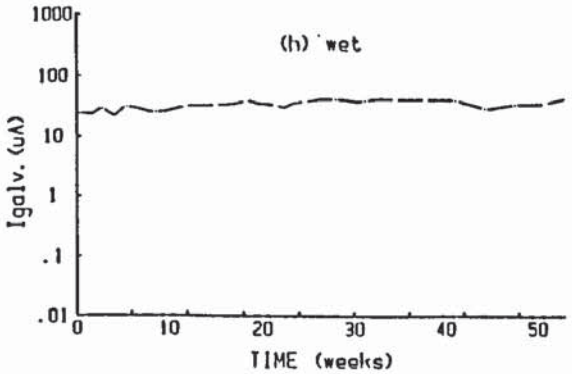
(h) wet
Igalv. (uA)
1000
100
10
1
.1
.01
0
10
20
30
40
50
TIME (weeks)

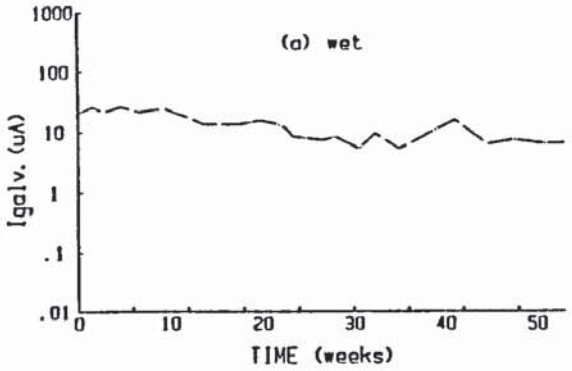
(a) wet
Igalv. (uA)
1000
100
10
1
.1
.01
0
10
20
30
40
50
TIME (weeks)

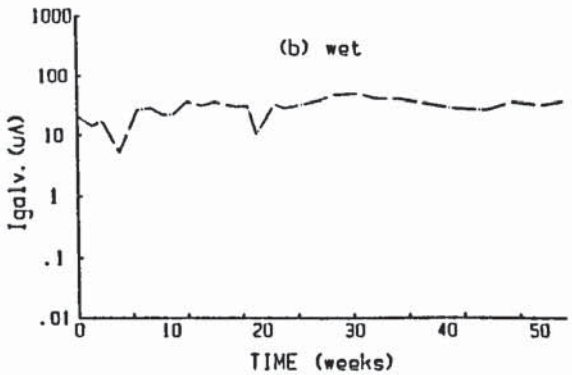
(b) wet
Igalv. (uA)
1000
100
10
1
.1
.01
0
10
20
30
40
50
TIME (weeks)

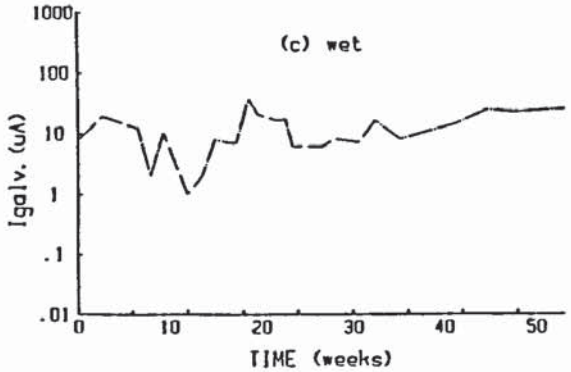
(c) wet
Igalv. (uA)
1000
100
10
1
.1
.01
0
10
20
30
40
50
TIME (weeks)

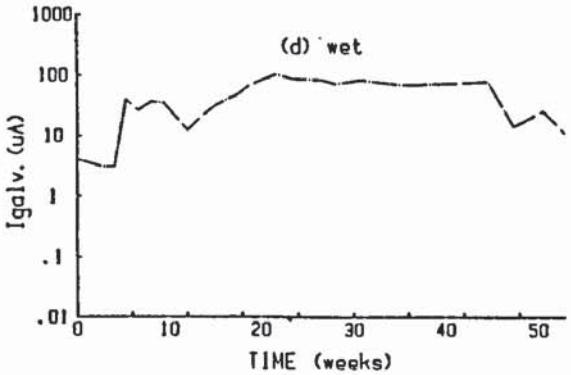
(d) wet
Igalv. (uA)
1000
100
10
1
.1
.01
0
10
20
30
40
50
TIME (weeks)

APPENDIX 8.1

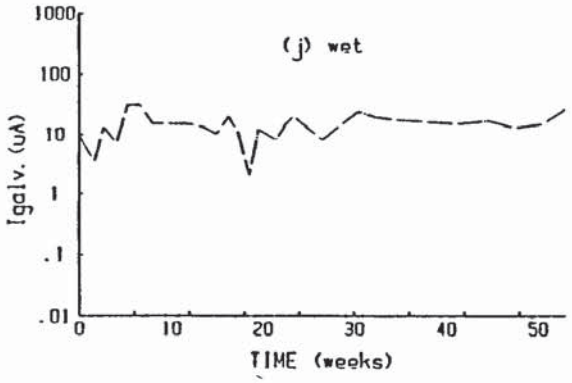

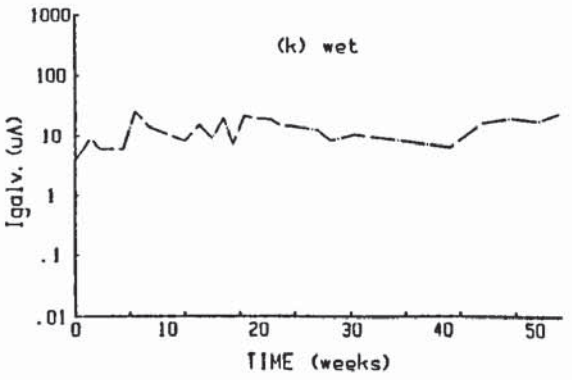

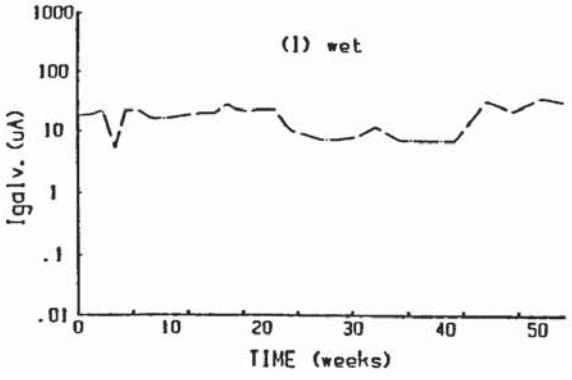

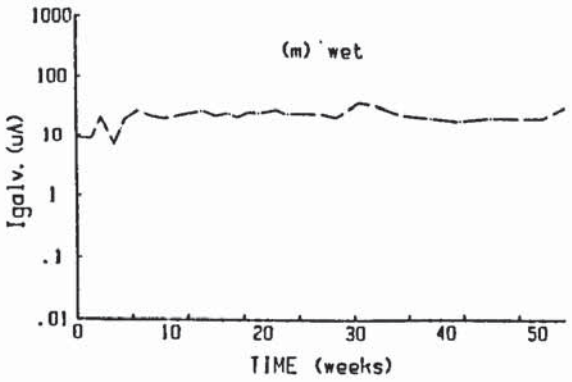

APPENDIX 8.1 (continued)

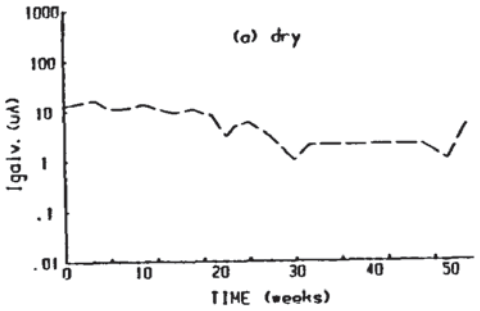
(a) dry
Igalv. (uA)
1000
100
10
1
.1
.01
0
10
20
30
40
50
TIME (weeks)

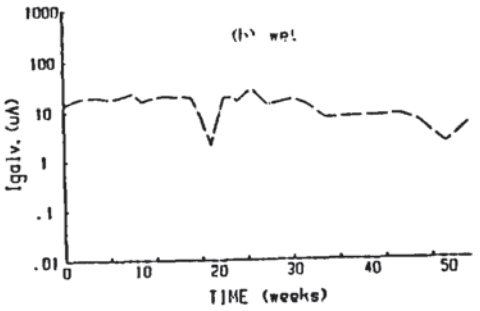
(b) wet
Igalv. (uA)
1000
100
10
1
.1
.01
0
10
20
30
40
50
TIME (weeks)

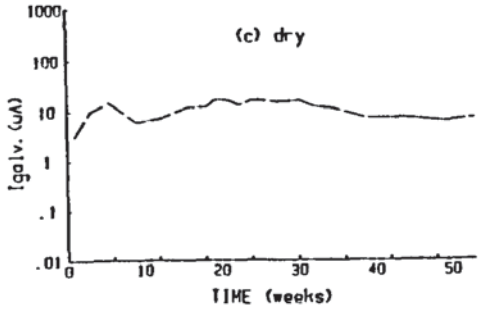
(c) dry
Igalv. (uA)
1000
100
10
1
.1
.01
0
10
20
30
40
50
TIME (weeks)

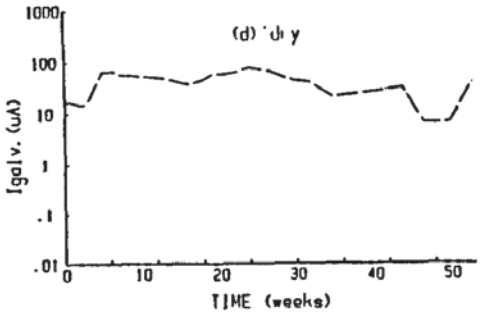
(d) dry
Igalv. (uA)
1000
100
10
1
.1
.01
0
10
20
30
40
50
TIME (weeks)

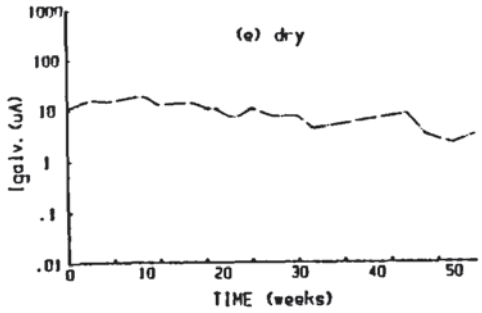
(e) dry
Igalv. (uA)
1000
100
10
1
.1
.01
0
10
20
30
40
50
TIME (weeks)

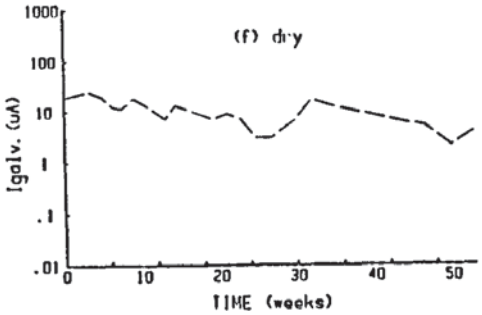
(f) dry
Igalv. (uA)
1000
100
10
1
.1
.01
0
10
20
30
40
50
TIME (weeks)

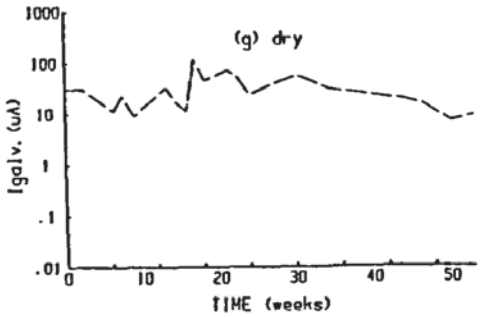
(g) dry
Igalv. (uA)
1000
100
10
1
.1
.01
0
10
20
30
40
50
TIME (weeks)

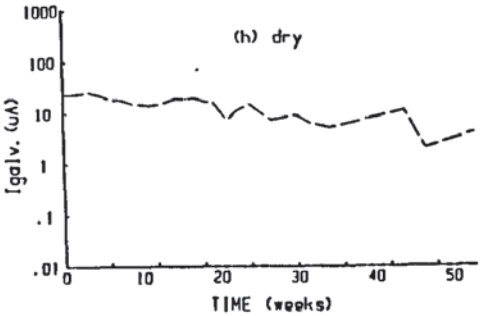
(h) dry
Igalv. (uA)
1000
100
10
1
.1
.01
0
10
20
30
40
50
TIME (weeks)

APPENDIX 8.2

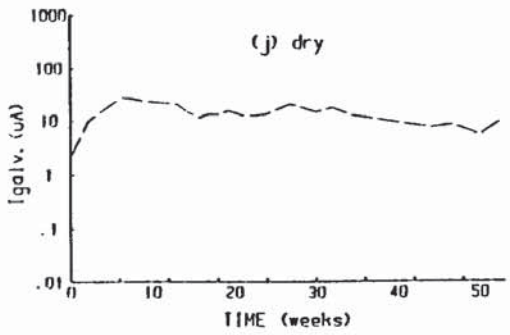

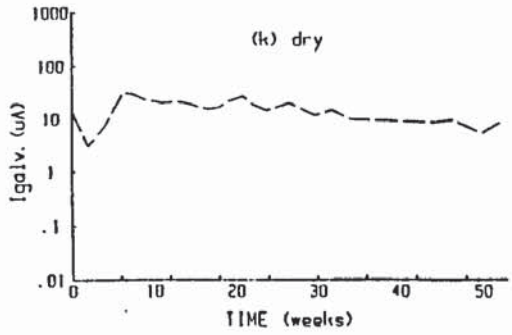

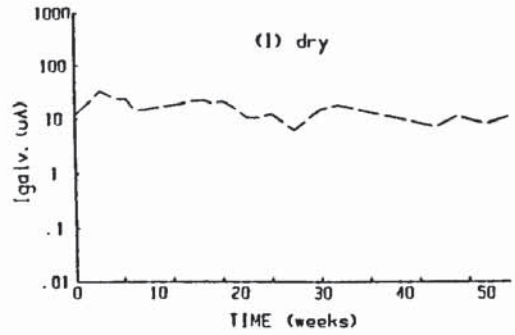

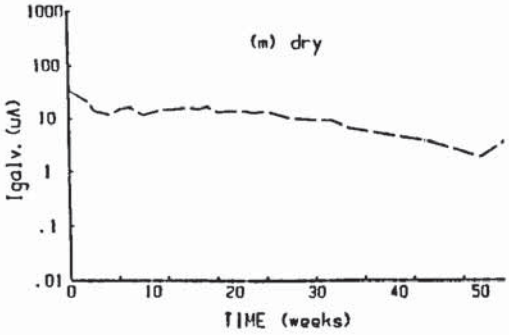

APPENDIX 8.2 (continued)

APPENDIX 9

Traces of corrosion potential against time for segments in wet and dry conditions, embedded in mortar containing the following chloride concentrations (% chloride ion by weight of cement).

APPENDIX 9.1 = 5.0% wet

APPENDIX 9.2 = 5.0% dry

APPENDIX 9.3 = 1.0% wet

APPENDIX 9.4 = 1.0% dry

APPENDIX 9.5 = 0.1% wet

APPENDIX 9.6 = 0.1% dry

APPENDIX 9.7 = 0.0% wet

APPENDIX 9.8 = 0.0% dry

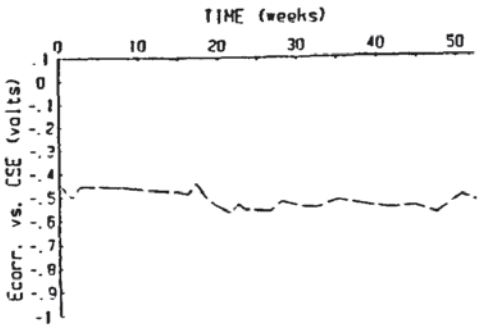

5% (a) wet

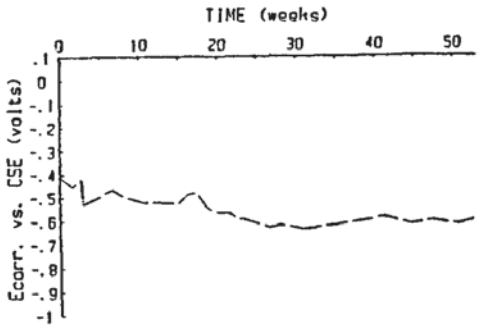

5% (b) wet

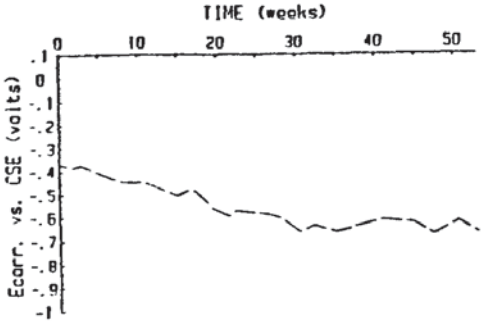

5% (c) wet

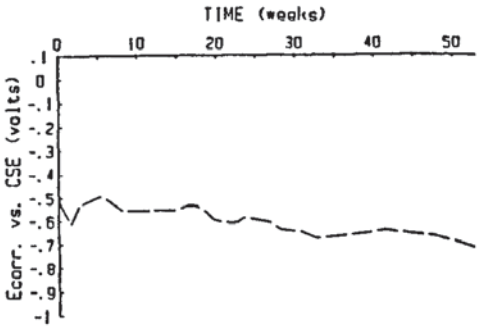

5% (d) wet

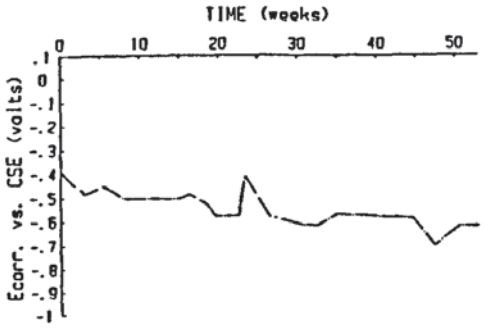

5% (e) wet

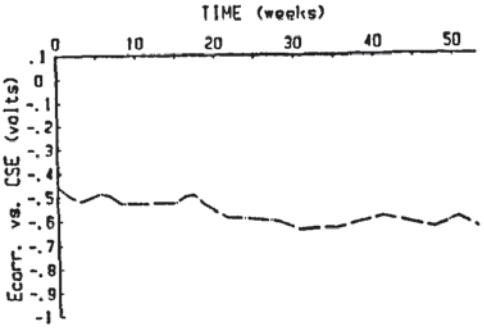

5% (f) wet

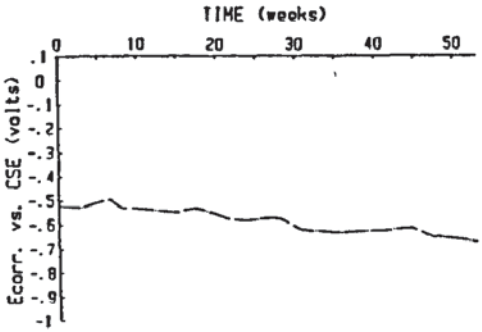

5% (g) wet

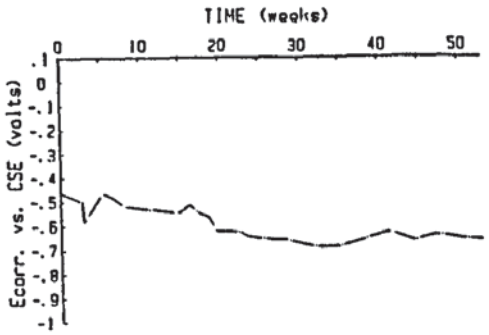

5% (h) wet

APPENDIX 9.1

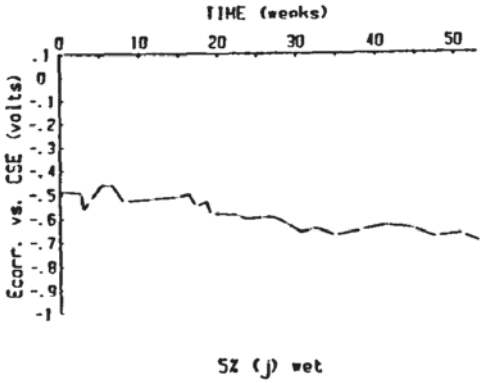

5% (j) wet

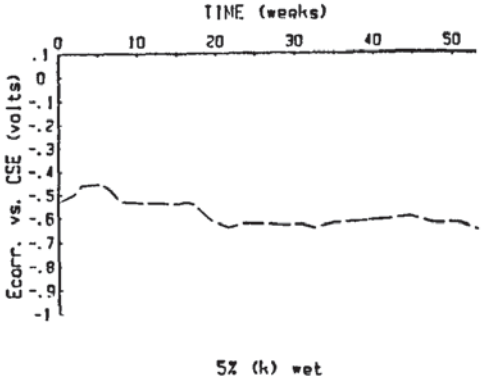

5% (k) wet

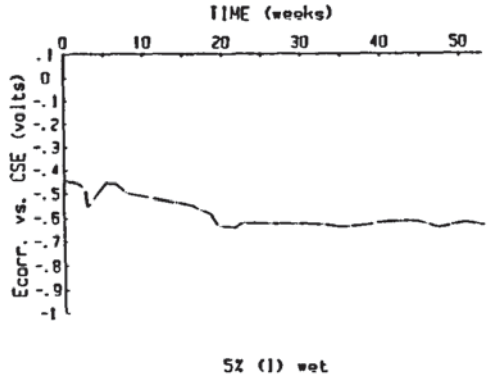

5% (l) wet

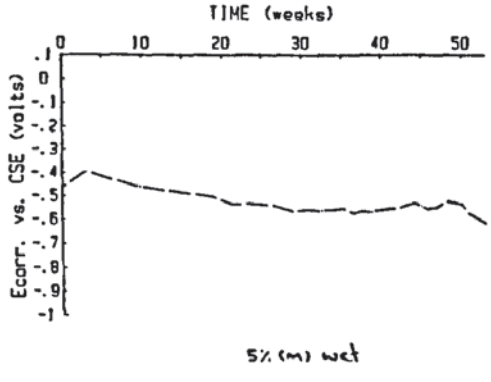

5% (m) wet

APPENDIX 9.1 (continued)

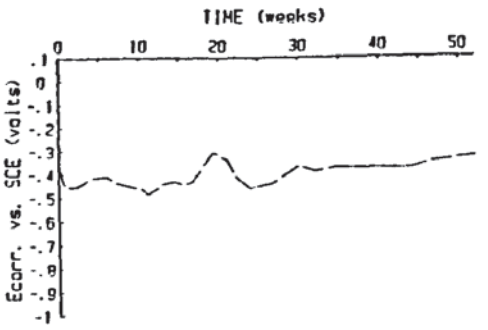

5% (a) dry

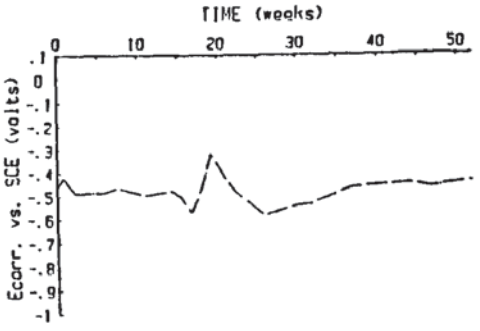

5% (b) dry

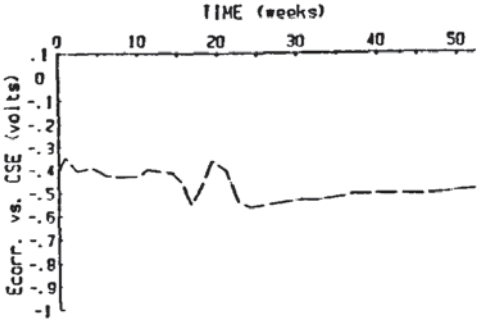

5% (c) dry

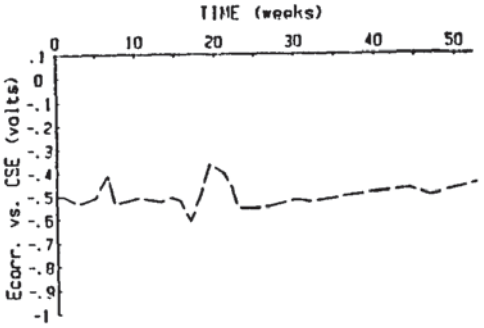

5% (d) dry

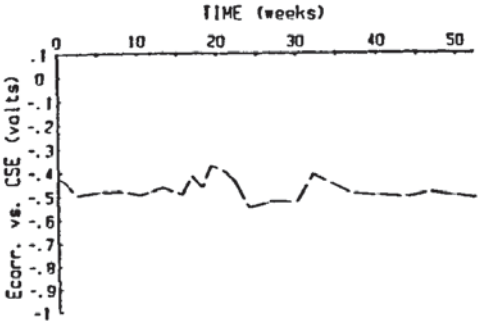

5% (e) dry

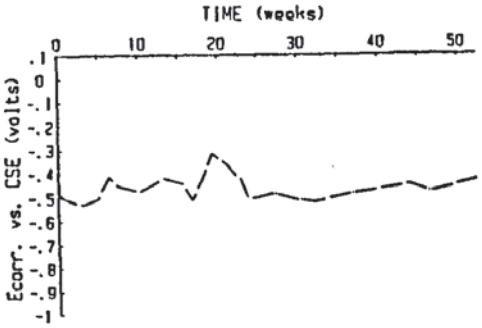

5% (f) dry

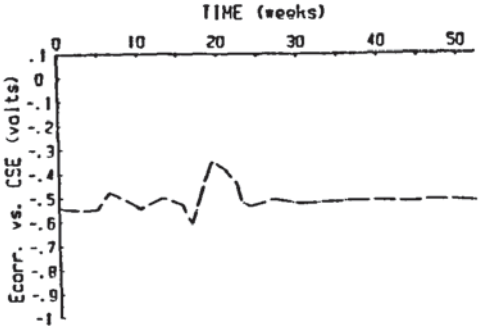

5% (g) dry

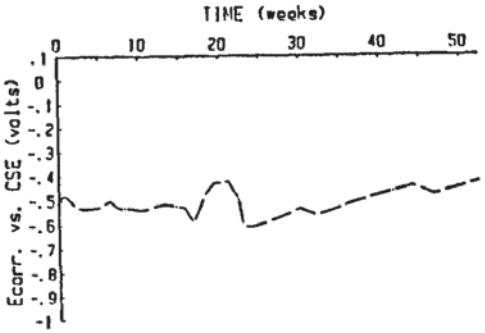

5% (h) dry

APPENDIX 9.2

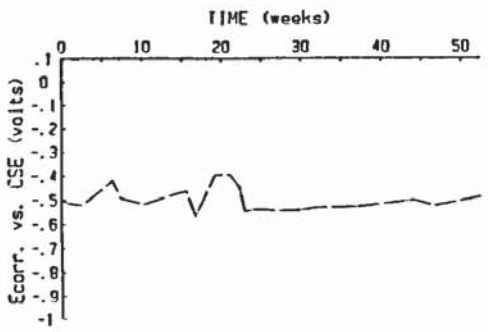

5% (j) dry

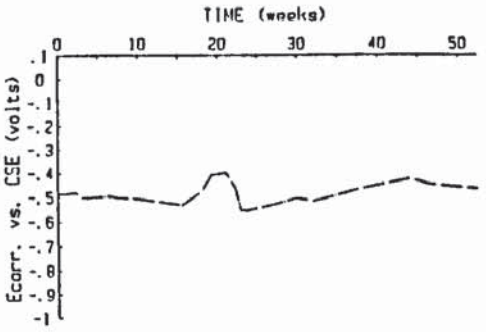

5% (k) dry

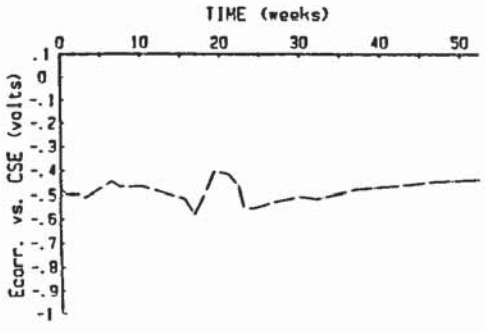

5% (l) dry

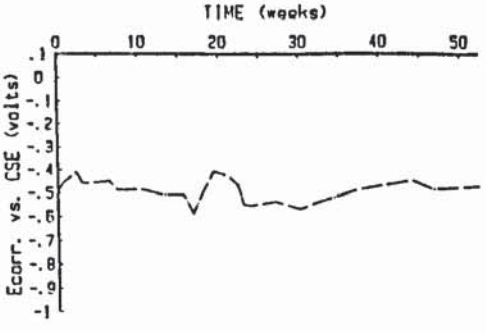

5% (m) dry

APPENDIX 9.2 (continued)

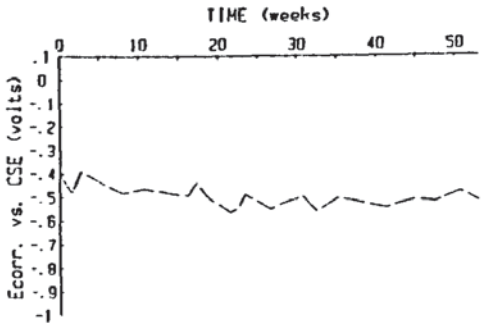

1% (a) wet

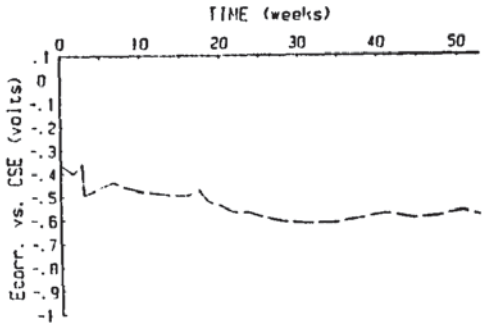

1% (b) wet

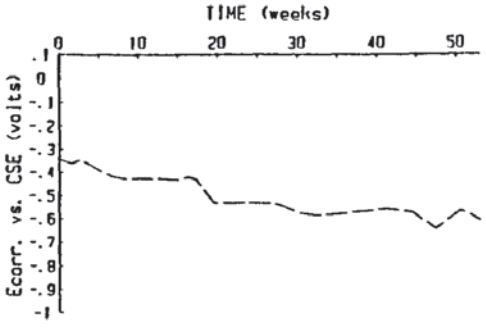

1% (c) wet

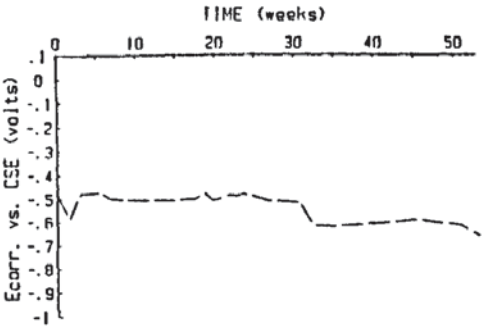

1% (d) wet

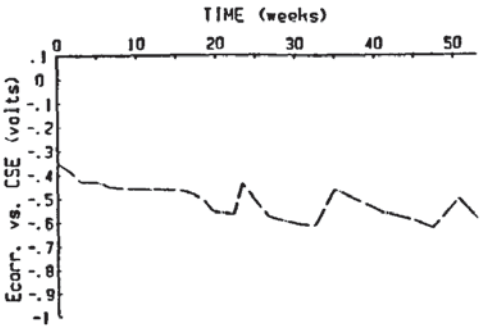

1% (e) wet

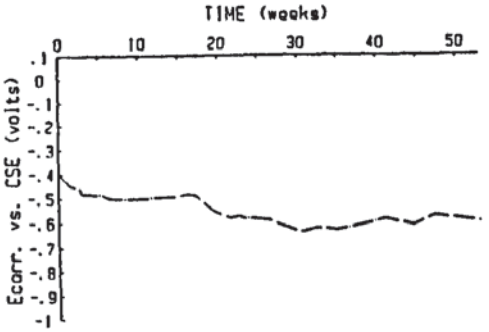

1% (f) wet

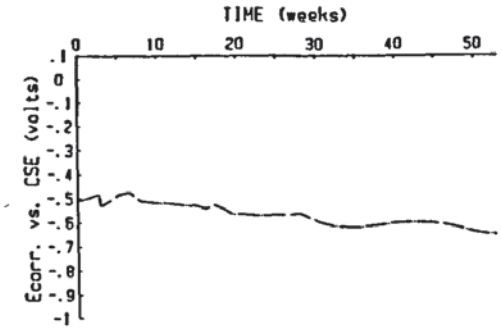

1% (g) wet

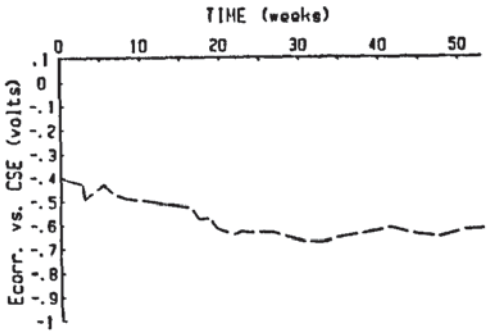

1% (h) wet

APPENDIX 9.3

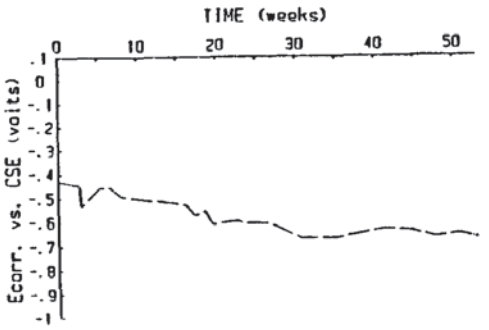

1% (j) wet

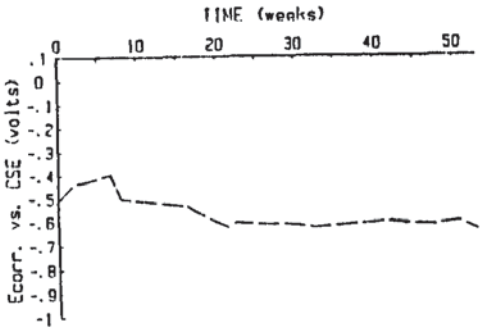

1% (k) wet

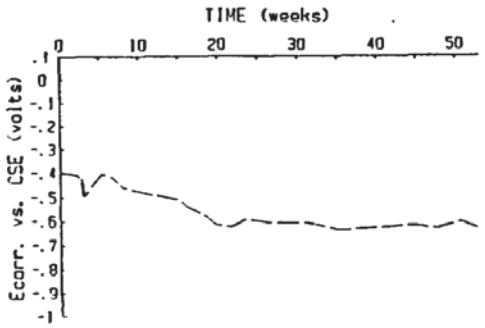

1% (l) wet

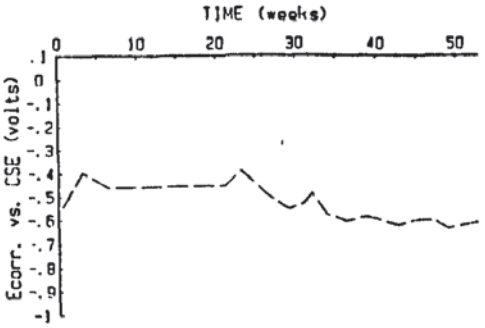

1% (m) wet

APPENDIX 9.3 (continued)

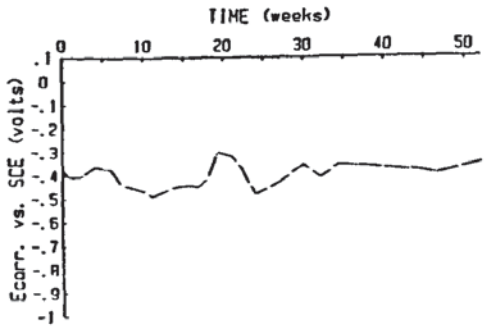

1% (a) dry

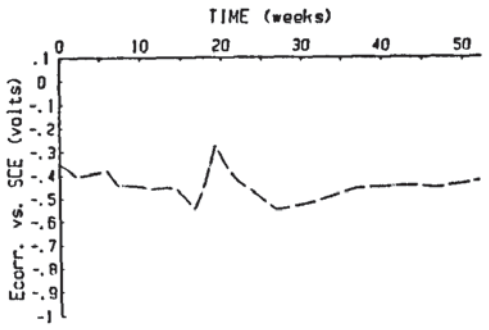

1% (b) dry

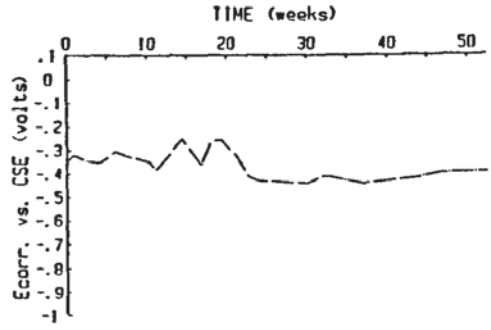

1% (c) dry

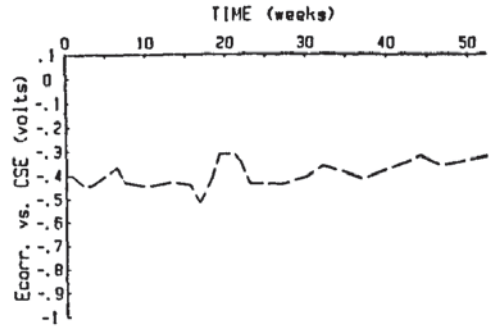

1% (d) dry

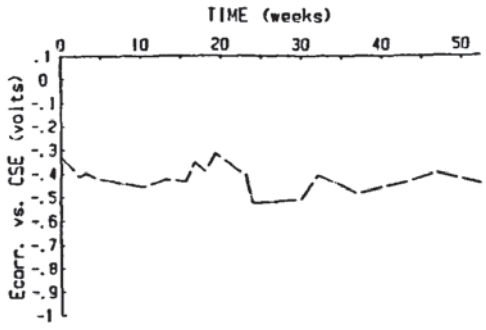

1% (e) dry

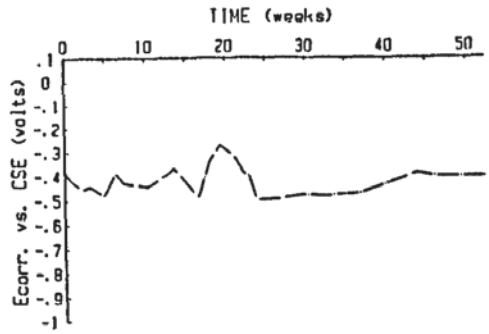

1% (f) dry

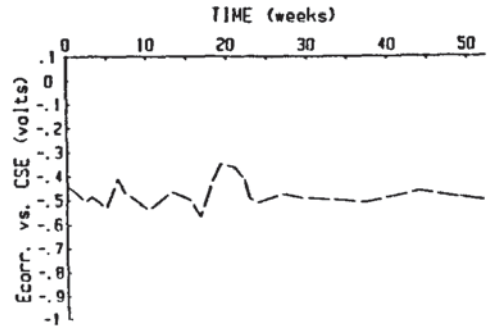

1% (g) dry

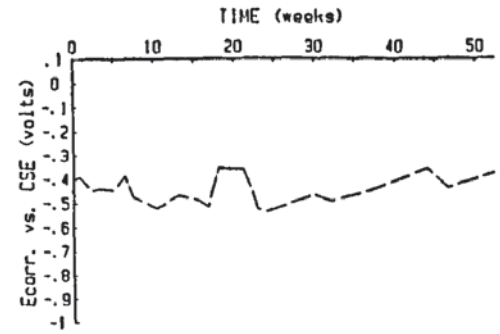

1% (h) dry

APPENDIX 9.4

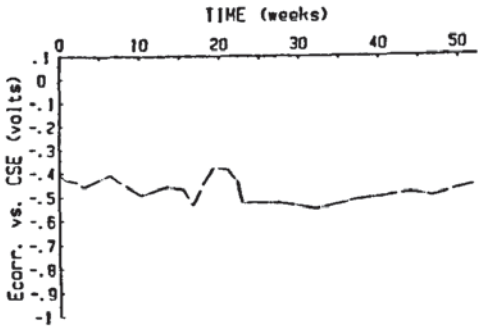

1% (j) dry

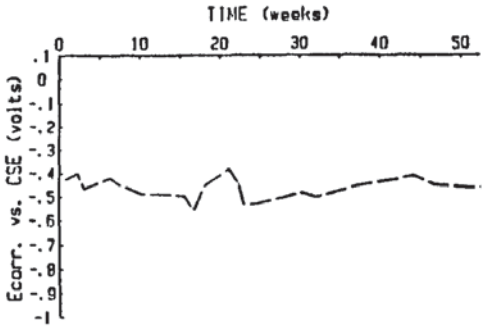

1% (k) dry

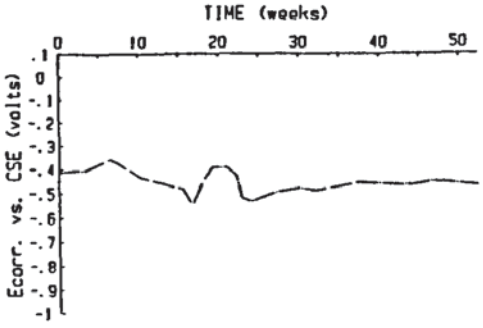

1% (l) dry

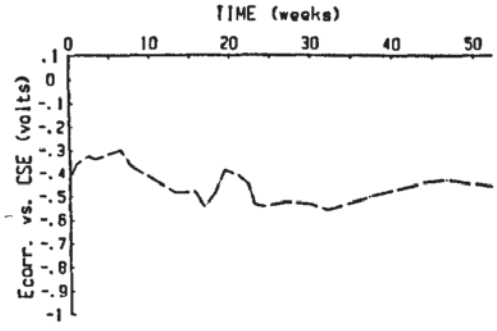

1% (m) dry

APPENDIX 9.4 (continued)

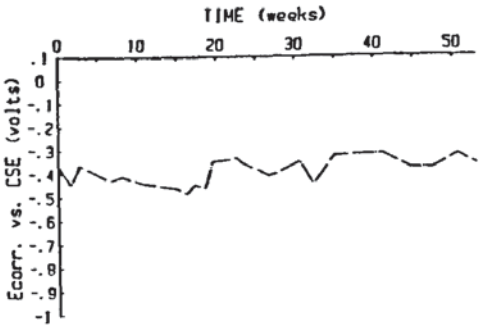

0.1% (a) wet

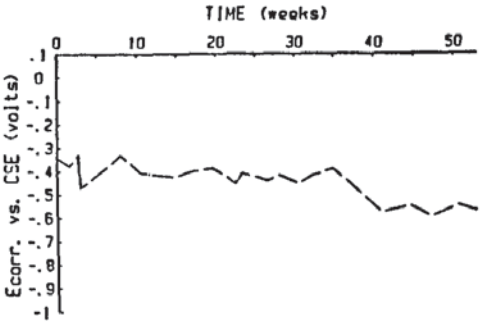

0.1% (b) wet

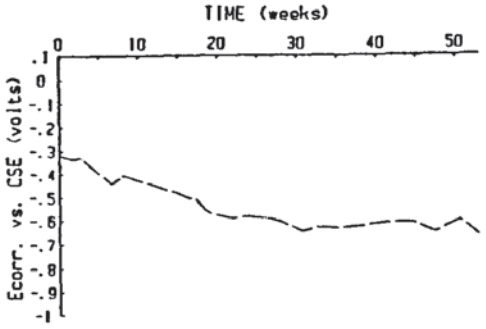

0.1% (c) wet

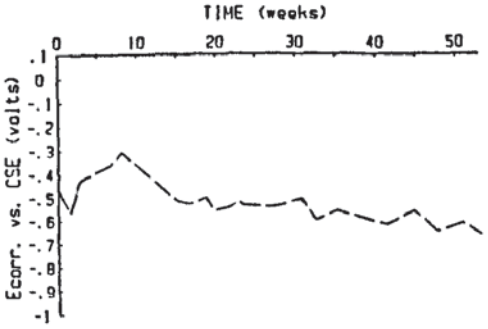

0.1% (d) wet

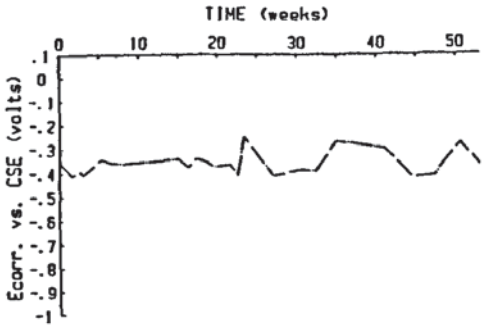

0.1% (e) wet

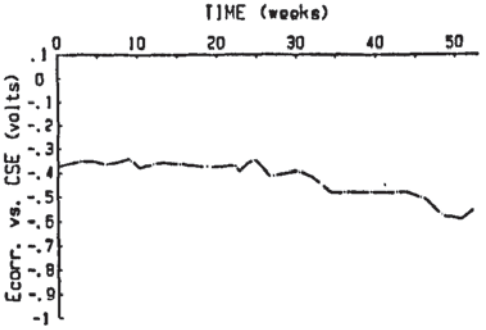

0.1% f wet

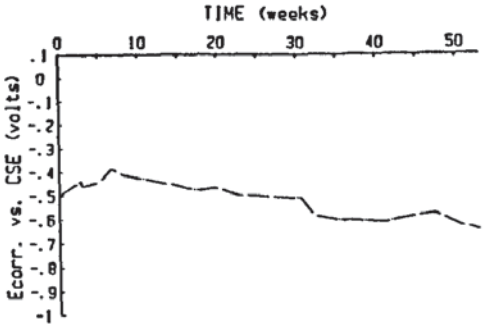

0.1% (g) wet

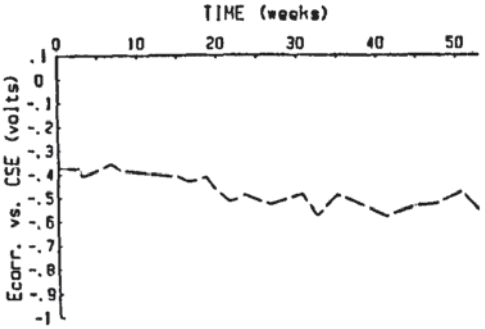

0.1% (h) wet

APPENDIX 9.5

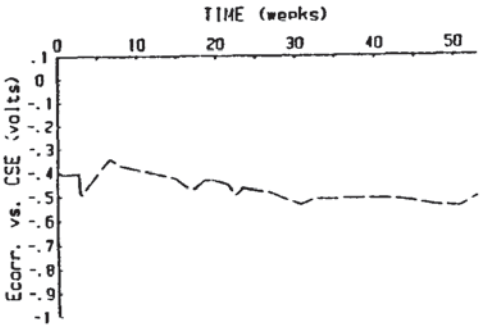

0.1% (j) wet

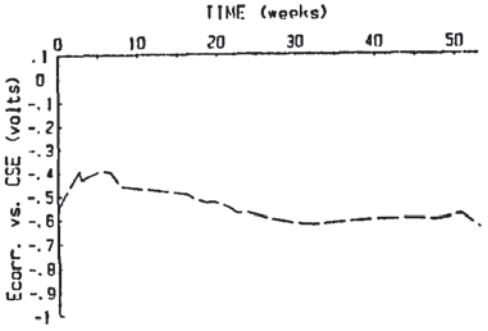

0.1% (k) wet

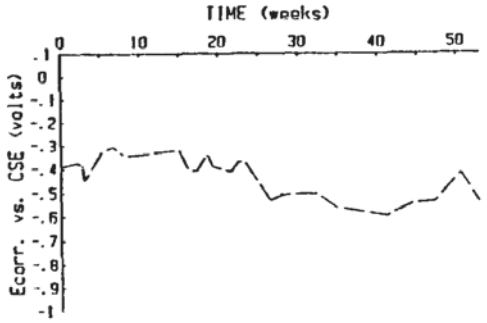

0.1% (l) wet

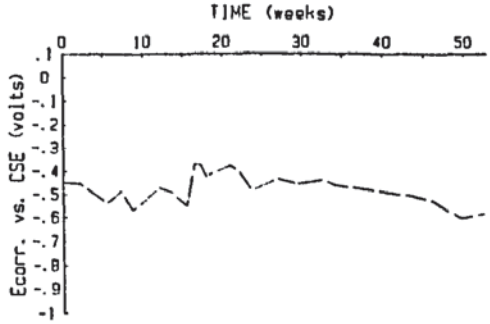

0.1 (m) wet

APPENDIX 9.5 (continued)

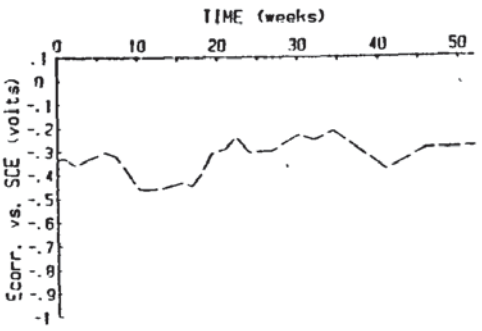

0.1% (a) dry

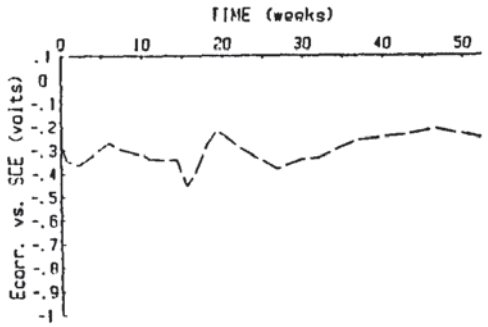

0.1% (b) dry

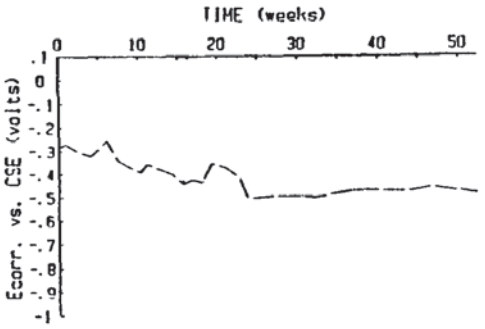

0.1%(c) dry

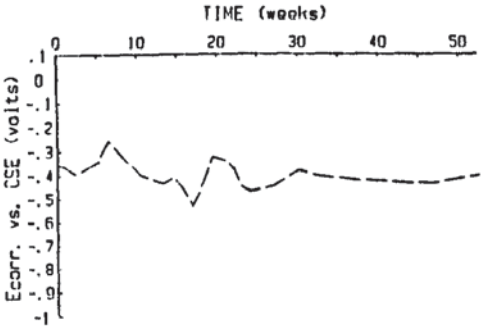

0.1% (d) dry

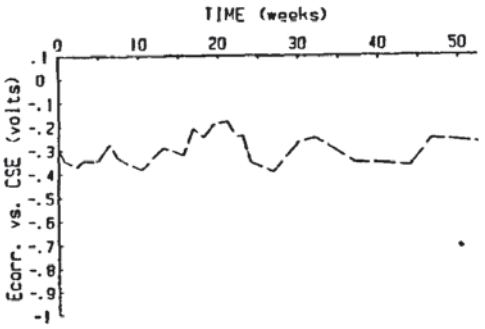

0.1% (e) dry

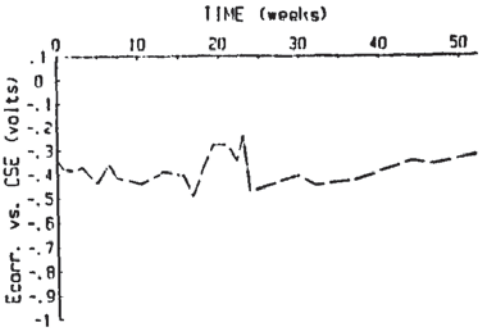

0.1% (f) dry

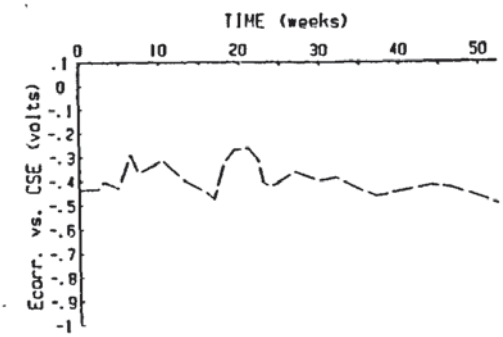

0.1% (g) dry

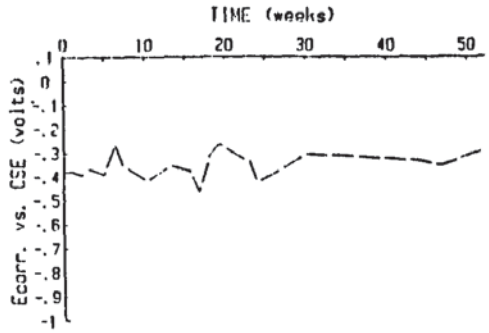

0.1% (h) dry

APPENDIX 9.6

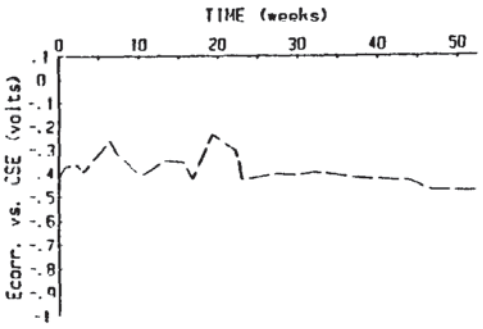

0.1% (j) dry

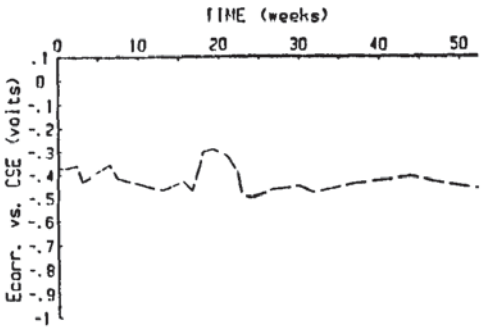

0.1% (k) dry

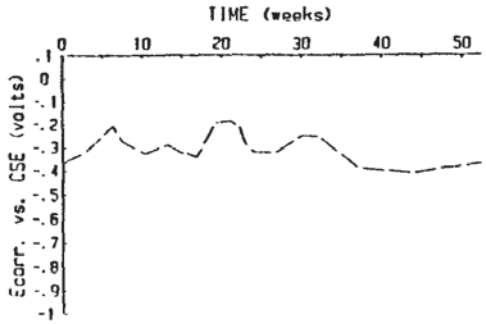

0.1% (l) dry

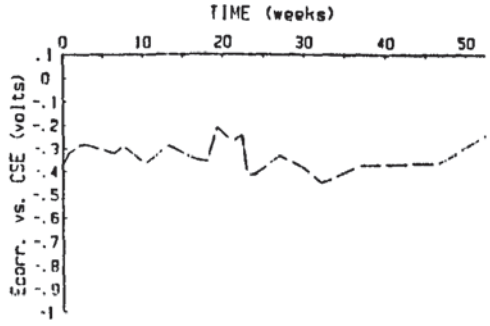

0.1% (m) dry

APPENDIX 9.6 (continued)

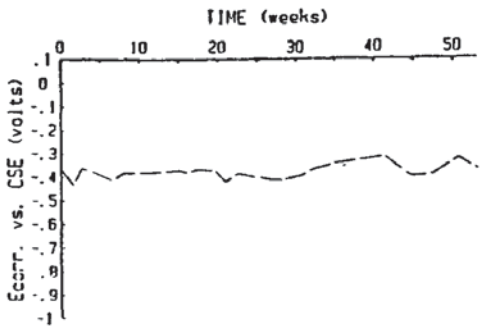

O/a (a) wet

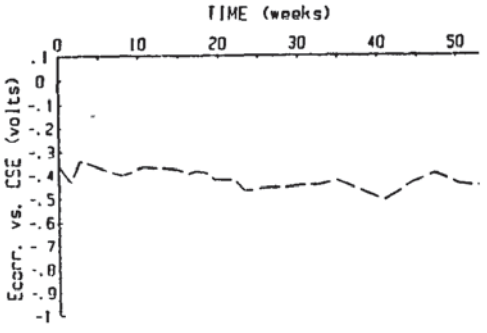

O/b (a) wet

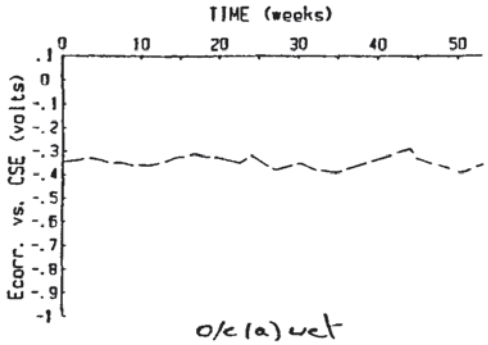

O/c (a) wet

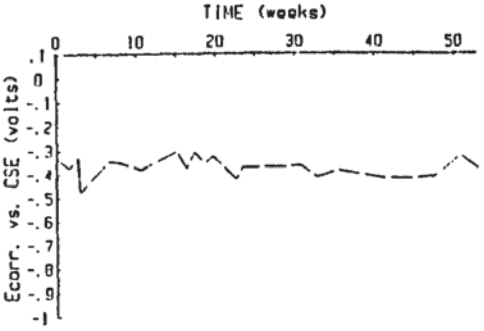

O/a (b) wet

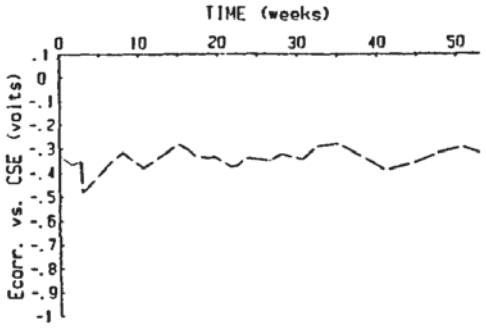

O/b (b) wet

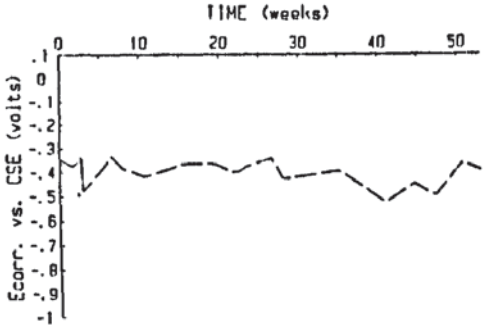

O/c (b) wet

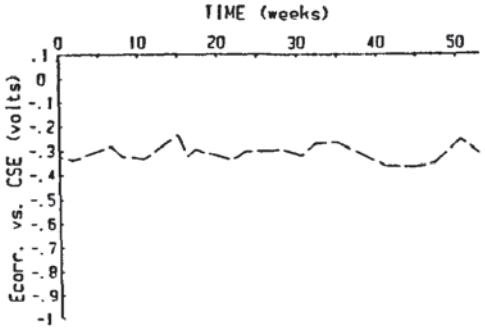

O/a (c) wet

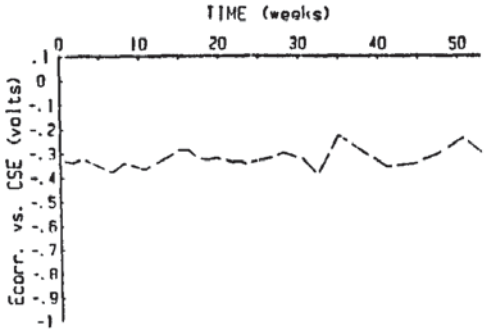

O/b (c) wet

APPENDIX 9.7

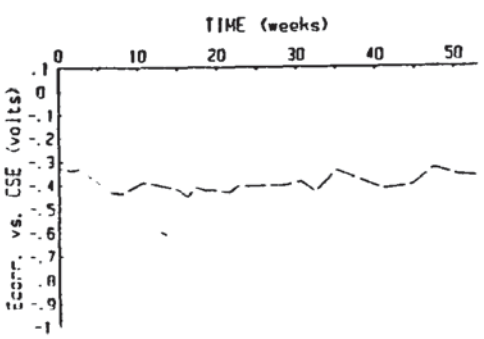

O/c (c) wet

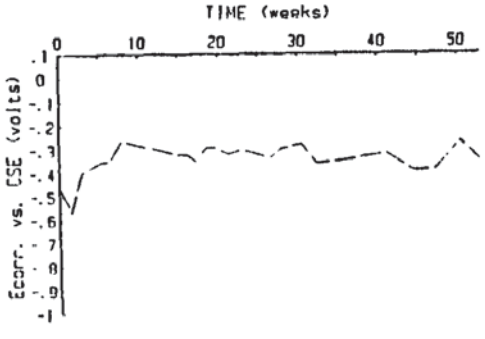

O/a (d) wet

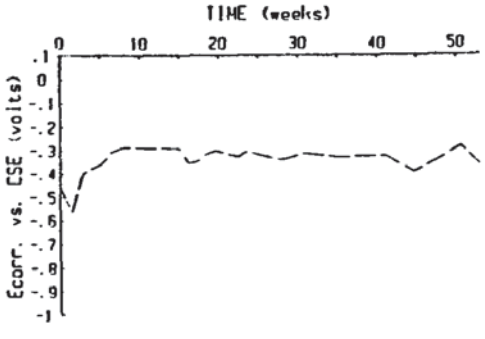

O/b (d) wet

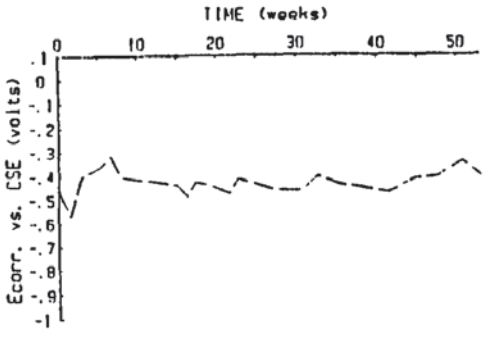

O/c (d) wet

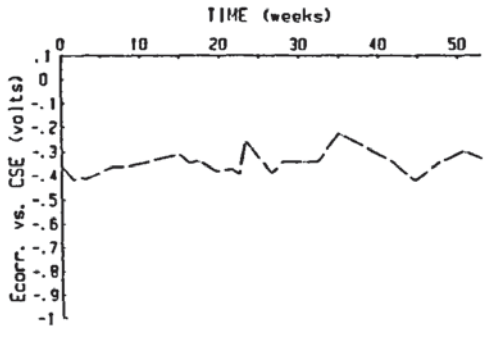

O/a (e) wet

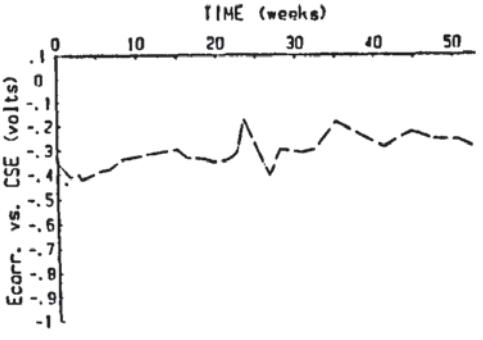

O/b (e) wet

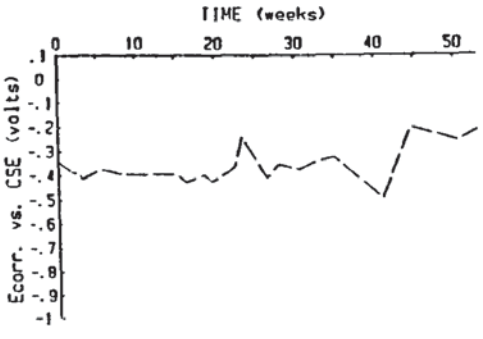

O/c (e) wet

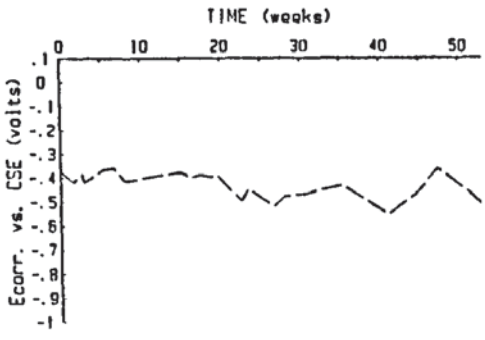

O/a (f) wet

APPENDIX 9.7 (continued)

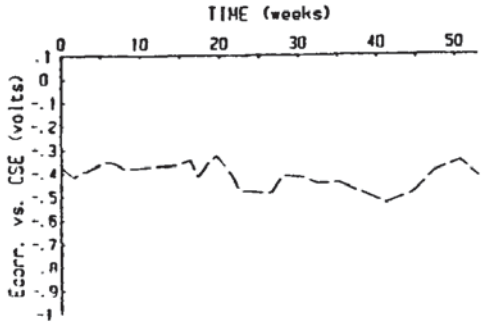

O/b (f) wet

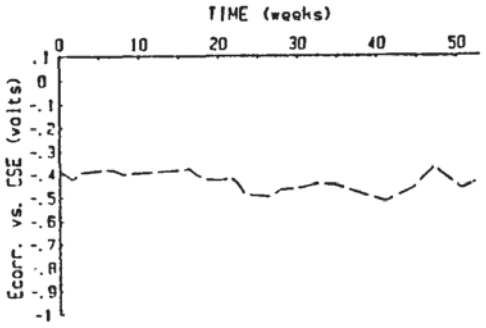

O/c (f) wet

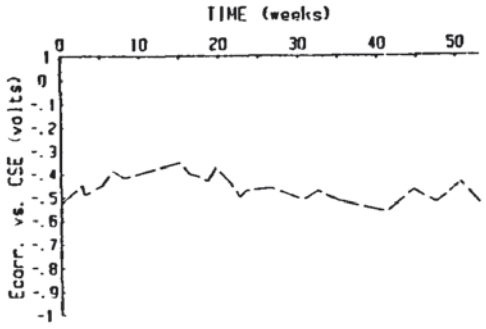

O/a (g) wet

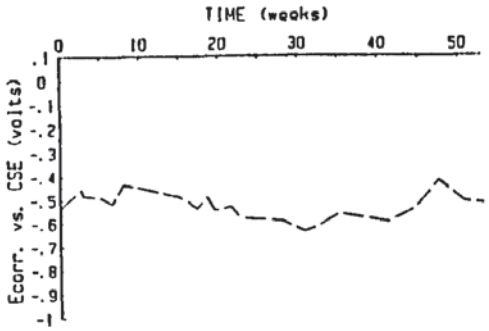

O/b (g) wet

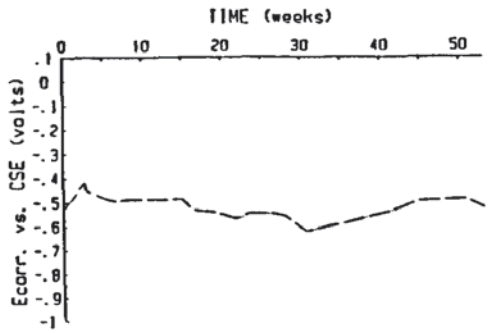

O/c (g) wet

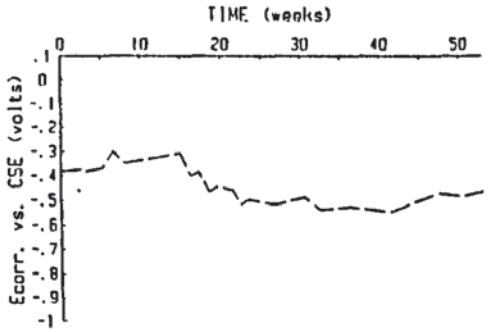

O/a (h) wet

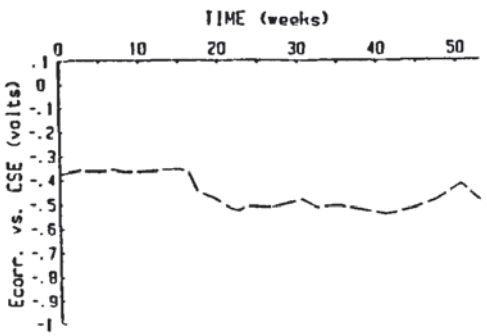

O/b (h) wet

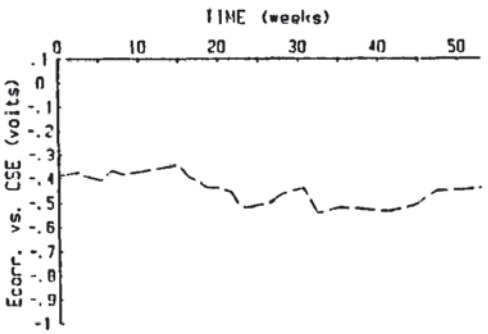

O/c (h) wet

APPENDIX 9.7 (continued)

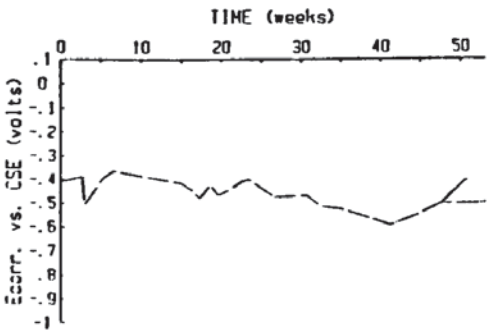

O/a (j) wet

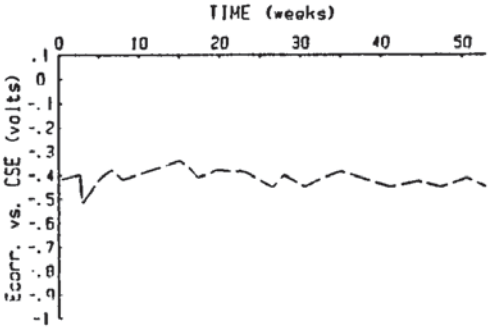

O/b (j) wet

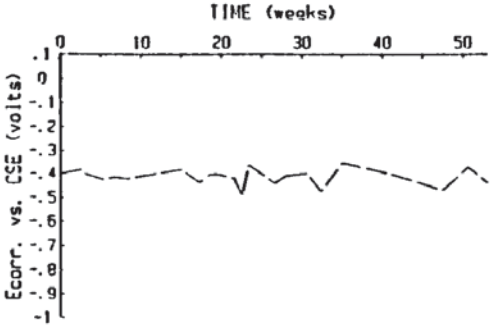

O/c (j) wet

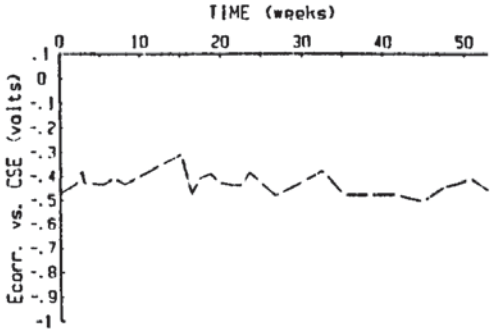

O/a (k) wet

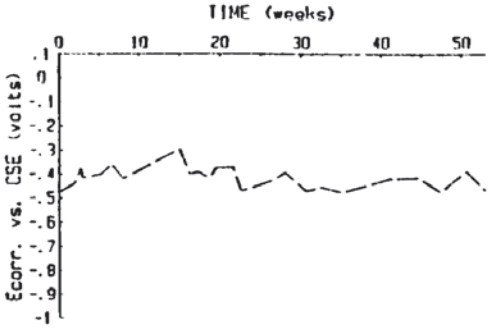

O/c (k) wet

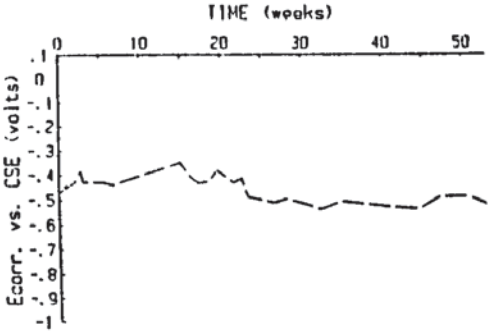

O/b (k) wet

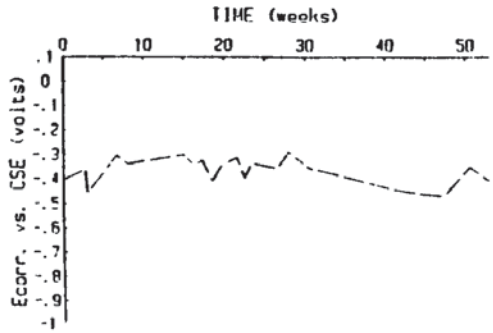

O/b (l) wet

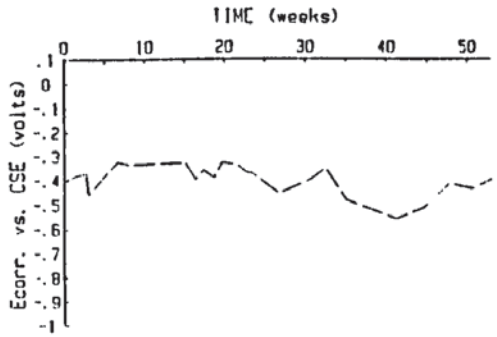

O/a (l) wet

APPENDIX 9.7 (continued)

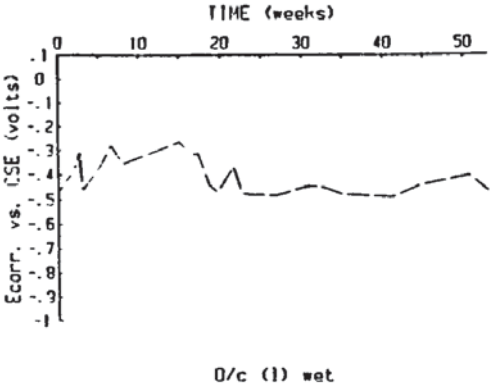

O/c (1) wet

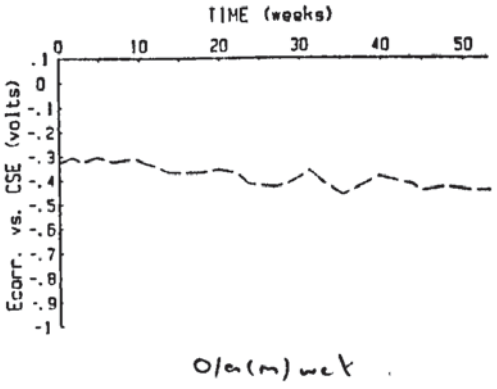

O/a(m) wet

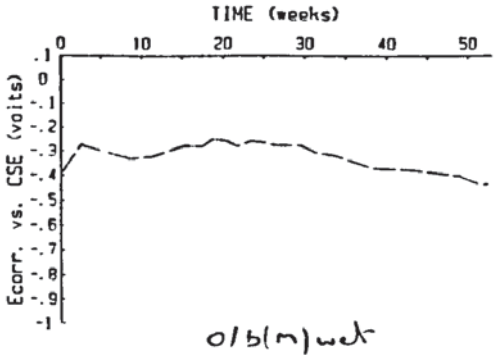

O/b(m) wet

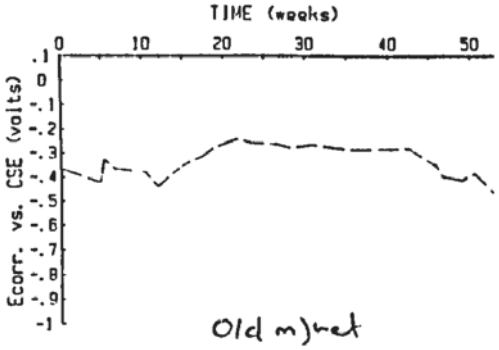

O/d m) wet

APPENDIX 9.7 (continued)

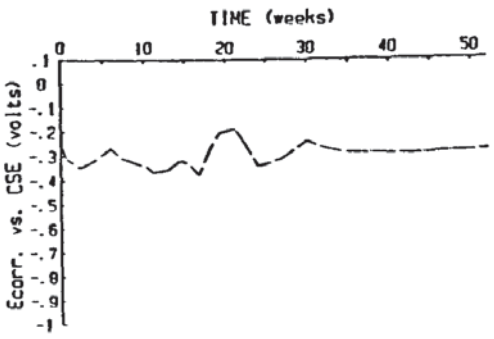

O/a (a) dry

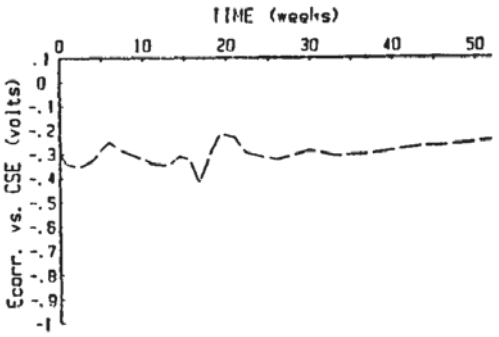

O/b (a) dry

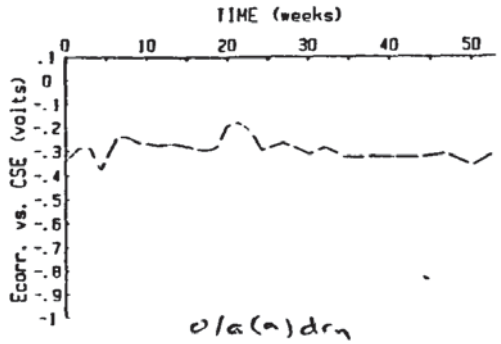

O/a (a) dry

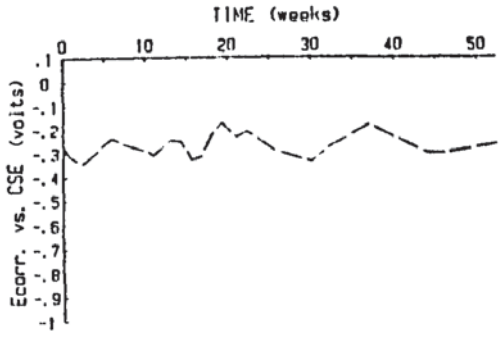

O/a (b) dry

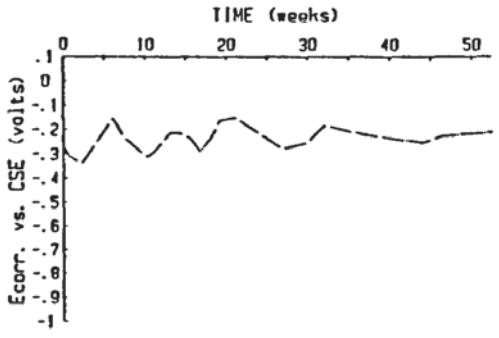

O/b (b) dry

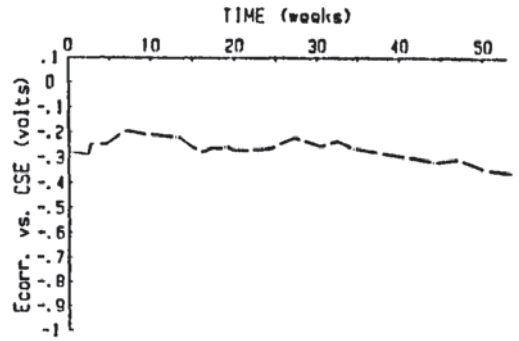

O/c (b) dry

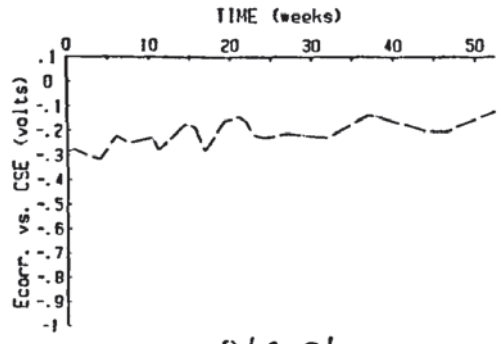

O/a dry

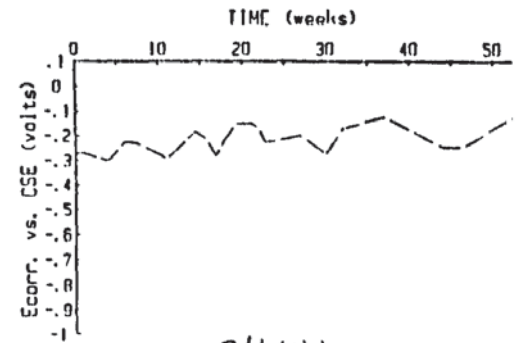

O/b (c) dry

APPENDIX 9.8

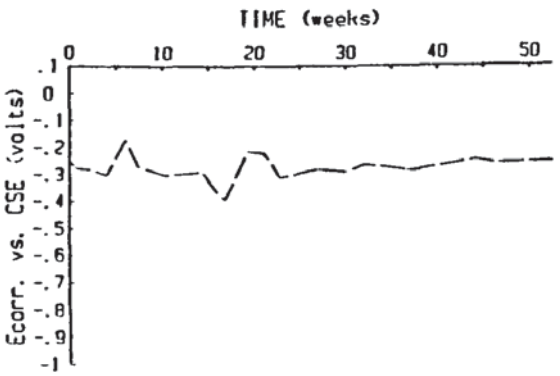

O/c (c) dry

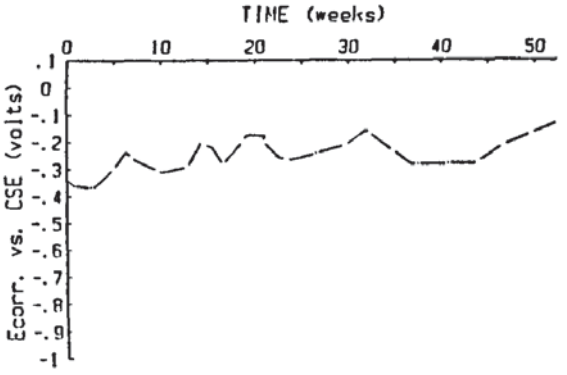

O/a (d) dry

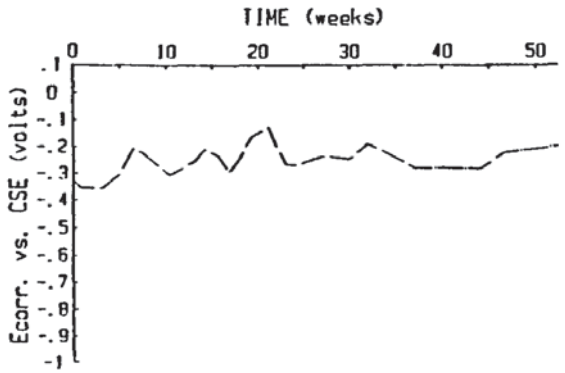

O/b (a) dry

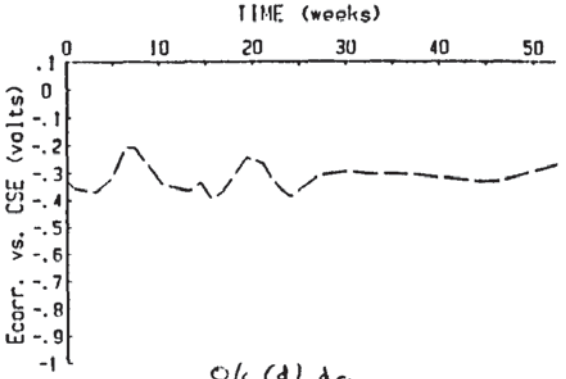

O/c (d) dry

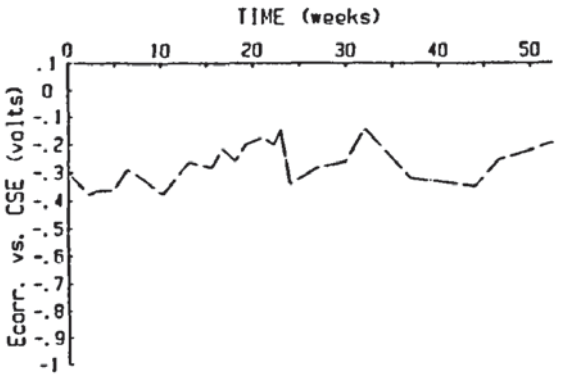

O/a (e) dry

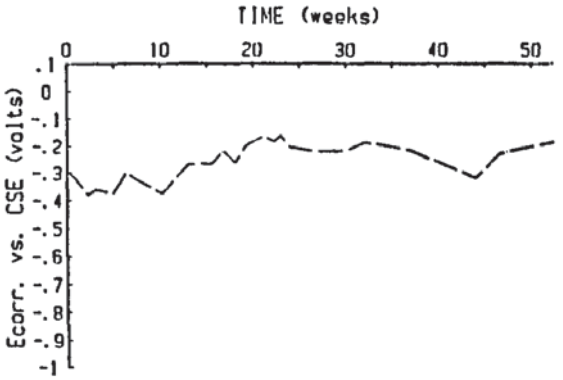

O/b (e) dry

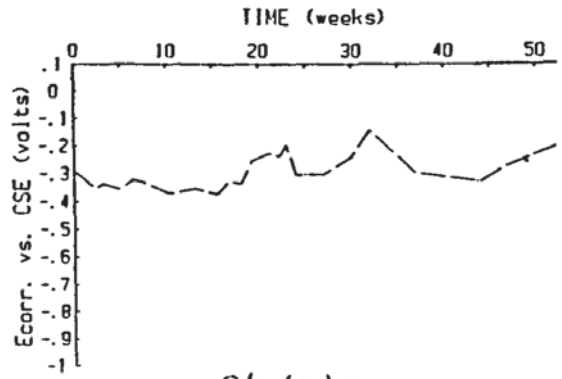

O/c (e) dry

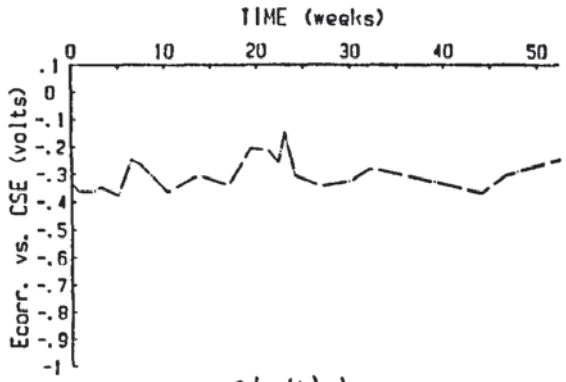

O/a (f) dry

APPENDIX 9.8 (continued)

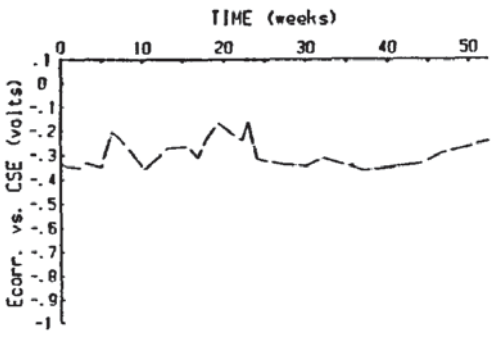

O/b (f)

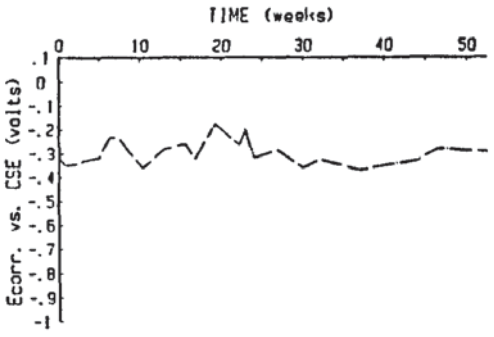

O/c (f) dry

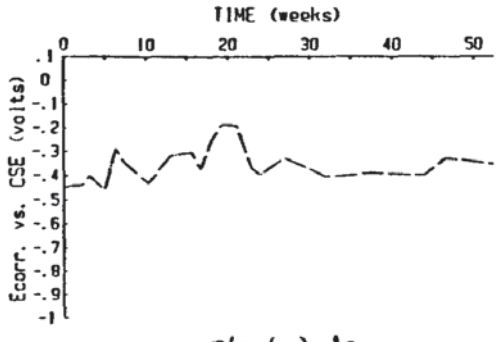

O/a (g) dry

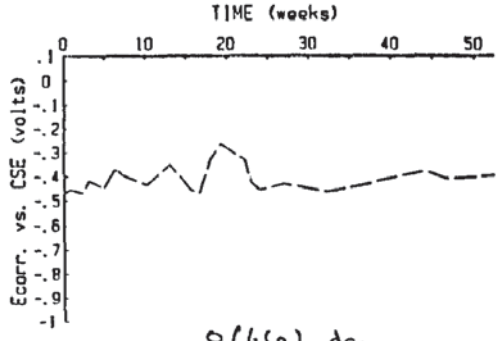

O/b (g) dry

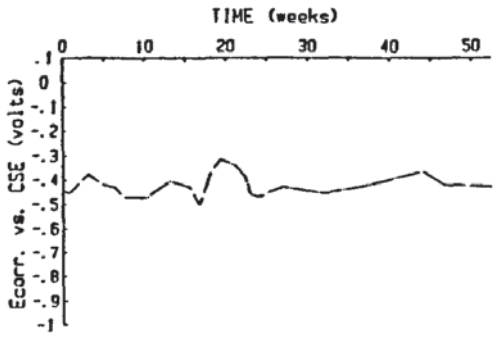

O/c (g) dry

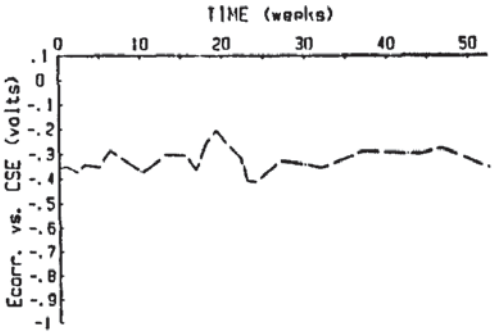

O/a (h) dry

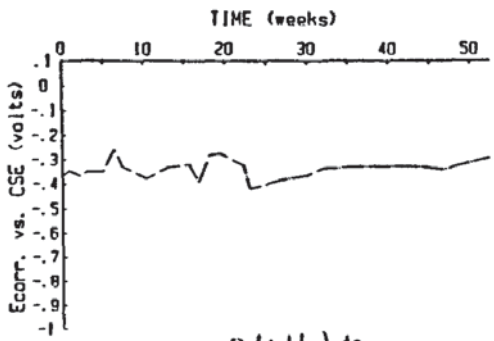

O/b (h) dry

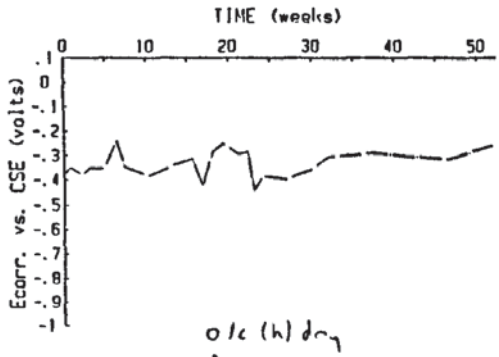

O/c (h) dry

APPENDIX 9.8 (continued)

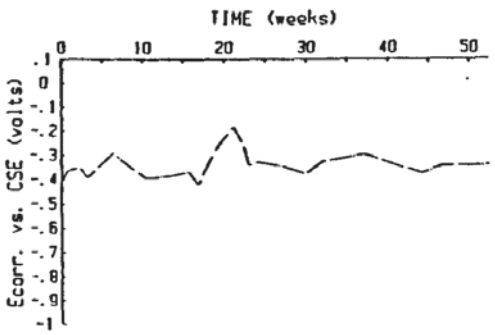

O/a (j) dry

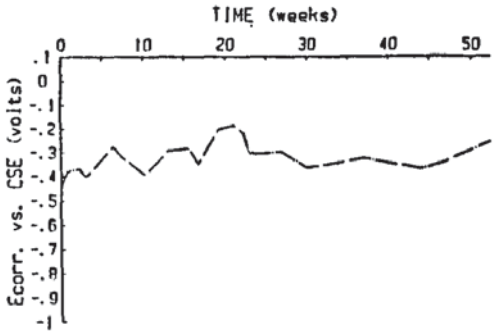

O/b (j) dry

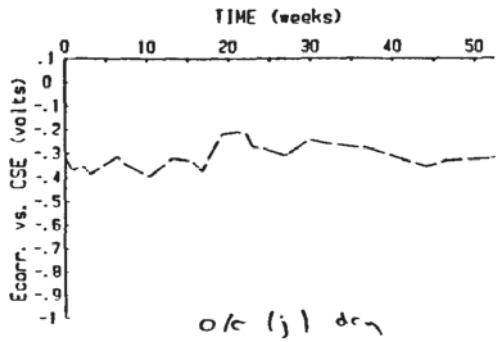

O/c (j) dry

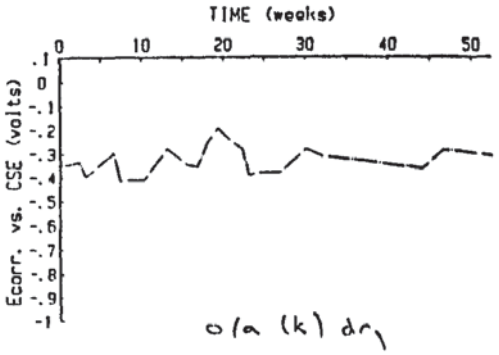

O/a (k) dry

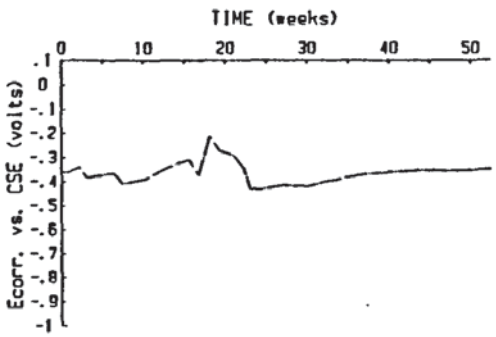

O/b (k) dry

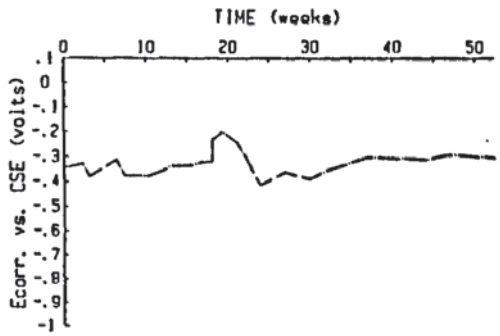

O/c (k) dry

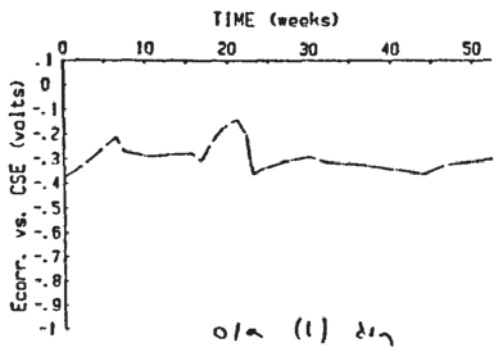

O/a (l) dry

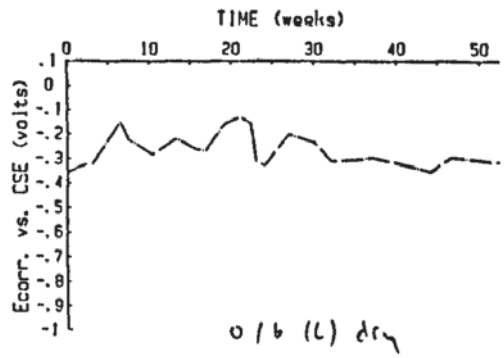

O/b (l) dry

APPENDIX 9.8 (continued)

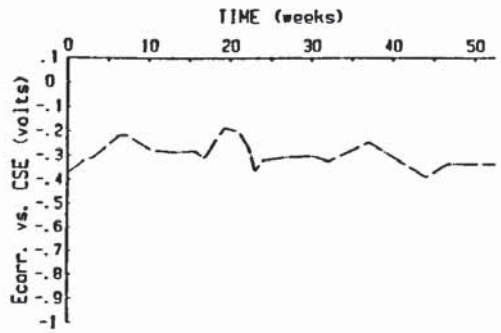

O/c (1) dry

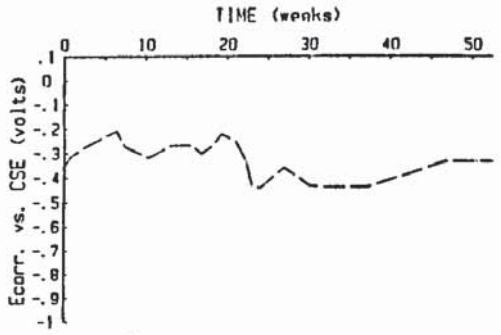

O/a (m) dry

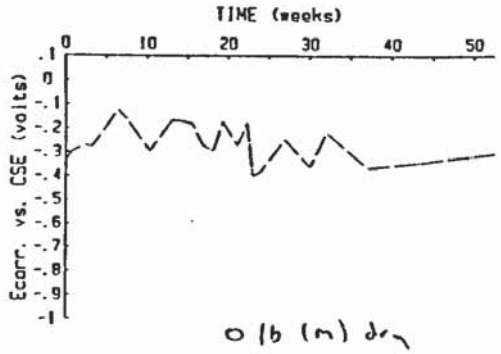

O/b (m) dry

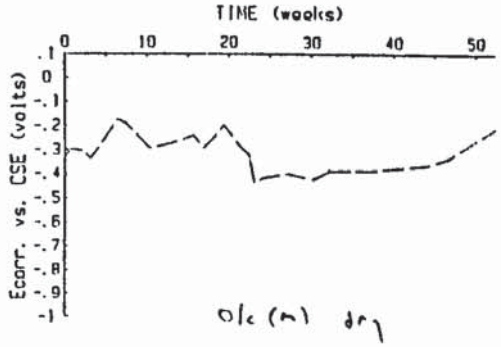

O/c (m) dry

APPENDIX 9.8 (continued)

APPENDIX 10

Details of the grout, described in Chapter 4, used to seal cracks.

The material consisted of all liquid two pack epoxy resin.

Properties.

Compressive strength at 20°C (7day)	= 70 N/mm^2
Tensile strength at 20°C (7 day)	= 27 N/mm^2
Flexural strength at 20°C (7 day)	= 55 N/mm^2
Viscosity at 25°C	= 2 poise
at 10°C	8 poise

APPENDIX 11

Example of calculated and actual weight loss previously obtained (after Escalante (3.23)

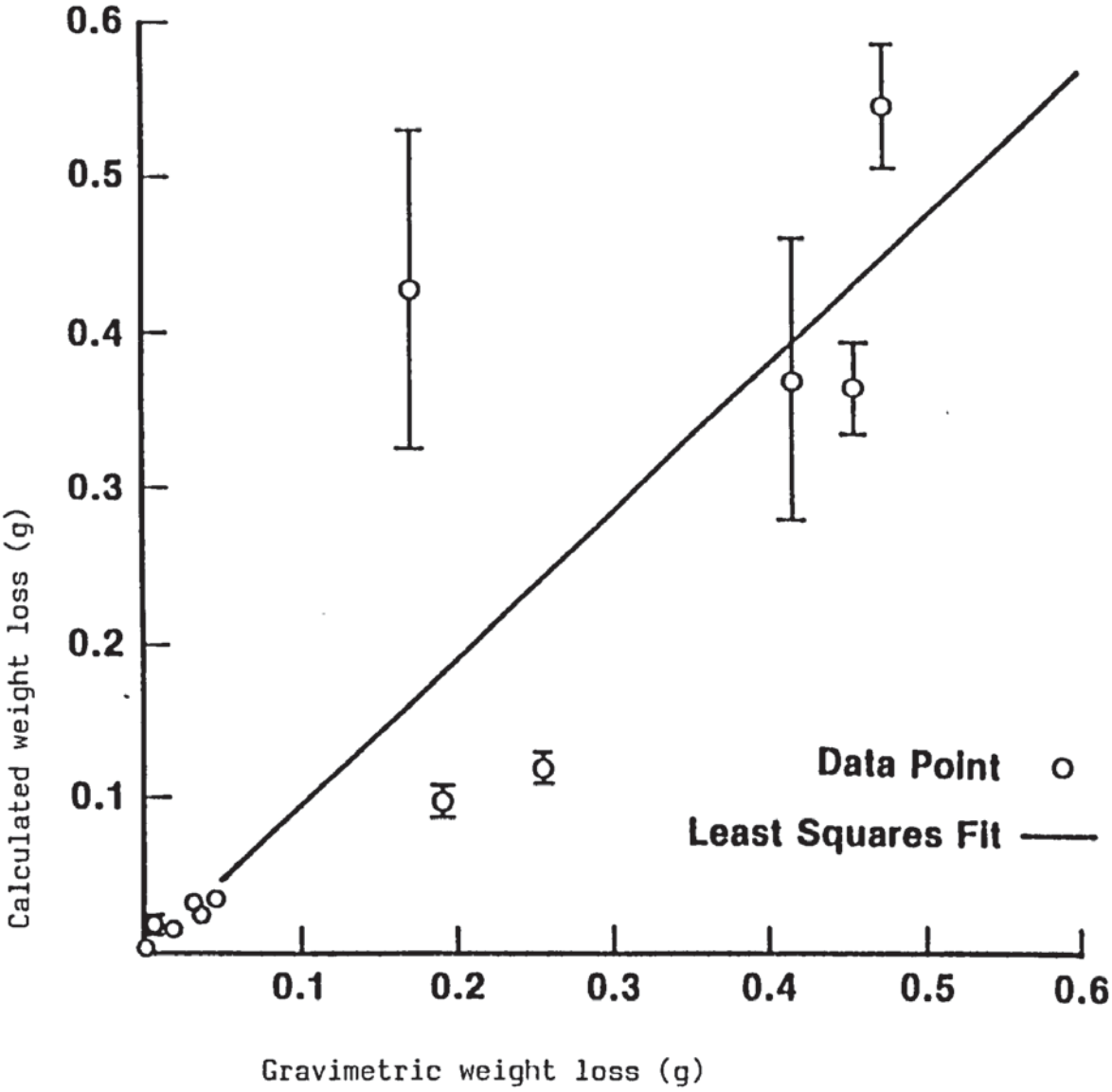

APPENDIX 12

Details of the diffusion specimens described in Chapter 7.

TIME (seconds)	CHLORIDE CONCENTRATION (M/l)				
	DISC a	DISC b	DISC c	DISC d	DISC e
172800	0.0050	0.0060	0.0075	0.0035	0.0045
1123200	0.0175	0.0090	0.0110	0.0140	0.0950
1728000	0.0235	0.0105	0.0120	0.0200	0.0120
2246400	0.0300	0.0145	0.0165	0.0270	0.0165
3110400 (36 days)	0.0385	0.0190	0.0210	0.0340	0.0210
VOLUME OF CELL (mls)	83.5	78.0	81.0	80.0	86.0
THICKNESS OF DISC (cms)	0.446	0.492	0.523	0.463	0.419
SURFACE AREA (cms^2)	10.179	9.079	9.621	9.079	9.079
GRADIENT ($\times 10^{-9}$)	11.40	4.43	5.26	10.38	5.62
CORRELATION	0.996	0.959	0.956	0.995	0.990
D-VALUE ($\times 10^{-8}$)	4.17	1.87	2.36	4.24	2.29

AVERAGE D-VALUE $(2.98 \pm 0.88) \times 10^{-8}\ cm^2\ s^{-1}$

CONTROL ORDINARY PORTLAND CEMENT MORTAR, 0.4 WATER/CEMENT RATIO, CHLORIDE ION DIFFUSION RESULTS ($25^{\circ}C$).

APPENDIX 12

TIME (seconds)	CHLORIDE CONCENTRATION (M/l)				
	DISC a	DISC b	DISC c	DISC d	DISC e
518 400	0.0130	0.0110	0.0050	0.0135	0.0070
1 123 200	0.0205	0.0170	0.0090	0.0255	0.0115
1 814 400	0.0260	0.0240	0.0130	0.0340	0.0140
2 332 800	0.0335	0.0310	0.0150	0.0500	0.0175
2 764 800	0.0385	0.0350	0.0160	0.0550	0.0235
VOLUME OF CELL (mls)	81.0	81.0	82.0	81.0	86.0
THICKNESS OF DISC (cms)	0.491	0.497	0.499	0.466	0.516
SURFACE AREA (cms^2)	9.079	10.179	11.946	10.179	10.179
GRADIENT ($\times 10^{-9}$)	11.35	10.68	4.90	18.47	7.35
CORRELATION	0.993	0.997	0.962	0.982	0.952
D-VALUE ($\times 10^{-8}$)	4.97	4.22	1.68	6.85	3.20

AVERAGE D-VALUE (4.18 ± 1.52) $\times 10^{-8}$ cm^2 s^{-1}

CONTROL ORDINARY PORTLAND CEMENT MORTAR, 0.6 WATER/CEMENT RATIO, CHLORIDE ION DIFFUSION RESULTS ($25^{\circ}C$).

APPENDIX 12 (continued)

TIME (seconds)	CHLORIDE CONCENTRATION (M/l)				
	DISC a	DISC b	DISC c	DISC d	DISC e
518 400	0.0100	0.0100	0.0100	0.0100	0.0150
1 641 600	0.0200	0.0185	0.0200	0.0165	0.0170
2 073 600	0.0250	0.0205	0.0210	0.0185	0.0190
2 592 000	0.0260	0.0255	0.0255	0.0235	0.0225
3 196 800	0.0305	0.0300	0.0312	0.0270	0.0265
VOLUME OF CELL (mls)	79.0	75.0	77.0	74.5	80.0
THICKNESS OF DISC (cms)	0.447	0.467	0.444	0.435	0.446
SURFACE AREA (cms^2)	9.621	7.068	7.548	7.548	9.621
GRADIENT ($\times 10^{-9}$)	2.37	7.43	7.74	6.35	4.29
CORRELATION	0.970	0.995	0.987	0.989	0.909
D-VALUE ($\times 10^{-8}$)	0.869	3.679	3.506	2.758	1.592

AVERAGE D-VALUE (2.48 ± 0.96) $\times 10^{-8}$ cm^2 s^{-1}

NAPTHALENE SULPHONATE (LONG CHAIN) MORTAR, 0.6 WATER/CEMENT RATIO, CHLORIDE ION DIFFUSION RESULTS ($25^{o}C$).

APPENDIX 12 (continued)

TIME (seconds)	CHLORIDE CONCENTRATION (M/l)				
	DISC a	DISC b	DISC c	DISC d	DISC e
345 600	0.0120	0.0105	0.0170	0.0090	0.0110
1814 400	0.0210	0.0230	0.0385	0.0150	0.0185
2 246 400	0.0255	0.0295	0.0440	0.0185	0.0225
2 764 800	0.0315	0.0355	0.0475	0.0225	0.0295
3 369 600	0.0375	0.0405	0.0575	0.0275	0.0325
VOLUME OF CELL (mls)	82.0	82.5	81.5	84.0	78.0
THICKNESS OF DISC (cms)	0.418	0.416	0.409	0.412	0.410
SURFACE AREA (cms^2)	10.179	10.179	9.621	9.079	9.079
GRADIENT ($\times 10^{-9}$)	8.43	9.92	13.78	6.12	7.47
CORRELATION	0.975	0.991	0.991	0.965	0.962
D-VALUE ($\times 10^{-8}$)	2.84	3.35	4.77	2.33	2.63

AVERAGE D-VALUE $(3.18 \pm 0.75) \times 10^{-8}\ cm^2\ s^{-1}$

NAPTHALENE SULPHONATE (SHORT CHAIN) MORTAR, 0.6 WATER/CEMENT RATIO, CHLORIDE ION DIFFUSION RESULTS ($25^{\circ}C$).

APPENDIX 12 (continued)

TIME (seconds)	CHLORIDE CONCENTRATION (M/l)				
	DISC a	DISC b	DISC c	DISC d	DISC e
259 200	0.0195	0.0190	0.0160	0.0195	0.0185
345 600	0.0235	0.0215	0.0192	0.0200	0.0235
432 000	0.0292	0.0265	0.0235	0.0310	0.0280
518 400	0.0355	0.0310	0.0265	0.0365	0.0312
604 800	0.0370	0.0320	0.0320	0.4050	0.0390
VOLUME OF CELL (mls)	76.0	72.4	80.0	80.6	80.2
THICKNESS OF DISC (cms)	0.213	0.217	0.232	0.218	0.212
SURFACE AREA (cms^2)	7.548	7.068	9.079	9.621	9.621
GRADIENT ($x10^{-9}$)	53.97	40.90	51.39	67.39	40.17
CORRELATION	0.974	0.966	0.987	0.944	0.981
D-VALUE ($x10^{-8}$)	11.57	9.09	10.50	12.31	7.09

AVERAGE D-VALUE $(1.01 \pm 0.16) \times 10^{-7}$ cm^2 s^{-1}

MELAMINE MORTAR, 0.6 WATER/CEMENT RATIO, CHLORIDE ION DIFFUSION RESULTS ($25^{\circ}C$).

APPENDIX 12 (continued)

TIME (seconds)	CHLORIDE CONCENTRATION (M/l)				
	DISC a	DISC b	DISC c	DISC d	DISC e
578 88	0.0070	0.0075	0.0050	0.0090	0.0060
82 944	0.0100	0.0110	0.0100	0.0120	0.0140
144 288	0.0150	0.0170	0.0120	0.0170	0.0170
247 968	0.0205	0.0245	0.0225	0.0225	0.0220
< 3 days					
VOLUME OF CELL (mls)	72.2	80.2	73.4	71.2	75.0
THICKNESS OF DISC (cms)	0.190	0.219	0.211	0.231	0.206
SURFACE AREA (cms^2)	7.068	9.621	9.621	7.548	8.553
GRADIENT ($x10^{-9}$)	72.16	89.41	81.02	71.02	84.17
CORRELATION	0.966	0.986	0.961	0.976	0.987
D-VALUE ($x10^{-8}$)	14.00	16.32	13.04	15.48	15.20

AVERAGE D-VALUE $(1.48 \pm 0.05) \times 10^{-7}$ cm^2 s^{-1}

STYRENE BUTADIENE RUBBER MORTAR, 0.4 WATER/CEMENT RATIO, CHLORIDE ION DIFFUSION RESULTS ($25^{\circ}C$).

APPENDIX 12 (continued)

TIME (seconds)	CHLORIDE CONCENTRATION (M/l)				
	DISC a	DISC b	DISC c	DISC d	DISC e
57 888	0.0010	0.0010	0.0020	0.0010	0.0010
144 288	0.0015	0.0015	0.0065	0.0020	0.0020
230 688	0.0125	0.0130	0.0205	0.0110	0.0160
317 088	0.0340	0.0380	0.0465	0.0355	0.0430
VOLUME OF CELL (mls)	76.2	79.8	75.0	76.4	77.2
THICKNESS OF DISC (cms)	0.271	0.305	0.275	0.318	0.271
SURFACE AREA (cms^2)	9.079	9.079	9.079	9.621	9.079
GRADIENT ($x10^{-9}$)	127.4	140.7	169.9	129.5	161.3
CORRELATION	0.846	0.833	0.904	0.818	0.853
D-VALUE ($x10^{-8}$)	28.98	37.72	38.60	32.70	37.17

AVERAGE D-VALUE $(3.50 \pm 0.16) \times 10^{-7}\ cm^2\ s^{-1}$

STYRENE BUTADIENE RUBBER MORTAR, 0.6 WATER/CEMENT RATIO, CHLORIDE ION DIFFUSION RESULTS ($25^{\circ}C$).

APPENDIX 12 (continued)

TIME (seconds)	CHLORIDE CONCENTRATION (M/l)				
	DISC a	DISC b	DISC c	DISC d	DISC e
75 168	0.0015	0.0025	0.0025	0.0055	0.0015
158 112	0.0040	0.0045	0.0040	0.0095	0.0040
244 512	0.0060	0.0065	0.0060	0.0650	0.0055
330 912	0.0110	0.0130	0.0100	0.0205	0.0110
418 176	0.0135	0.0155	0.0115	0.0225	0.0125
VOLUME OF CELL (mls)	72.4	73.2	75.4	75.0	73.8
THICKNESS OF DISC (cms)	0.275	0.250	0.239	0.251	0.267
SURFACE AREA (cms^2)	7.068	9.621	8.042	9.079	7.548
GRADIENT ($x10^{-9}$)	36.28	40.00	27.40	53.00	33.78
CORRELATION	0.979	0.953	0.973	0.977	0.954
D-VALUE ($x10^{-8}$)	10.22	7.61	6.14	10.99	8.82

AVERAGE D-VALUE $(8.75 \pm 1.53) \times 10^{-8}$ cm^2 s^{-1}

POLYVINYL ACETATE MORTAR, 0.4 WATER/CEMENT RATIO, CHLORIDE ION DIFFUSION RESULTS ($25^{\circ}C$).

APPENDIX 12 (continued)

TIME (seconds)	CHLORIDE CONCENTRATION (M/l)				
	DISC a	DISC b	DISC c	DISC d	DISC e
93 312	0.0190	0.0085	0.0145	0.0050	0.0210
158 112	0.0275	0.0197	0.0290	0.0140	0.0330
227 232	0.0535	0.0382	0.0450	0.0285	0.0530
269 568	0.0590	0.0415	0.0560	0.0330	0.0570
VOLUME OF CELL (mls)	75.0	80.6	77.8	76.2	77.6
THICKNESS OF DISC (cms)	0.403	0.449	0.455	0.425	0.480
SURFACE AREA (cms^2)	8.553	9.621	9.621	8.553	9.079
GRADIENT ($\times 10^{-9}$)	237.5	190.8	220.3	151.3	204.2
CORRELATION	0.976	0.992	0.985	0.993	0.997
D-VALUE ($\times 10^{-8}$)	83.93	71.77	85.16	57.29	83.78

AVERAGE D-VALUE $(7.64 \pm 0.94) \times 10^{-7}$ cm^2 s^{-1}

POLYVINYL ACETATE MORTAR, 0.6 WATER/CEMENT RATIO, CHLORIDE ION DIFFUSION RESULTS ($25^{o}C$).

APPENDIX 12 (continued)

TIME (seconds)	CHLORIDE CONCENTRATION (M/l)				
	DISC a	DISC b	DISC c	DISC d	DISC e
2 592 000	0.0005	0.0010	0.0005	0.0010	0.0010
3 542 400	0.0010	0.0015	0.0010	0.0015	0.0015
5 443 200	0.0015	0.0020	0.0015	0.0020	0.0020
9 590 400	0.0050	0.0055	0.0025	0.0035	0.0035
VOLUME OF CELL (mls)	78.0	77.6	81.4	75.1	82.6
THICKNESS OF DISC (cms)	0.392	0.400	0.357	0.387	0.392
SURFACE AREA (cms^2)	9.621	9.080	9.621	9.080	10.179
GRADIENT ($\times 10^{-9}$)	0.64	0.65	0.27	0.35	0.36
CORRELATION	0.961	0.961	0.982	0.995	0.995
D-VALUE ($\times 10^{-8}$)	0.20	0.22	0.08	0.11	0.11

AVERAGE D-VALUE $(1.46 \pm 0.48) \times 10^{-9}$ cm^2 s^{-1}

ALKOXY SILANE COATED MORTAR, 0.6 WATER/CEMENT RATIO, CHLORIDE ION DIFFUSION RESULTS ($25^{\circ}C$).

APPENDIX 12 (continued)

TIME (seconds)	CHLORIDE CONCENTRATION (M/l)				
	DISC a	DISC b	DISC c	DISC d	DISC e
345 600	0.0015	0.0010	0.0010	0.0020	0.0015
1 468 800	0.0155	0.0105	0.0021	0.0165	0.0075
2 160 000	0.0200	0.0170	0.0075	0.0300	0.0255
2 592 000	0.0220	0.0190	0.0090	0.0320	0.285
2 937 600	0.0250	0.0230	0.0115	0.0352	0.0318
VOLUME OF CELL (mls)	79.8	76.7	81.5	85.1	78.2
THICKNESS OF DISC (cms)	0.405	0.384	0.375	0.391	0.376
SURFACE AREA (cms^2)	9.348	10.179	10.179	9.080	9.621
GRADIENT ($x10^{-9}$)	9.20	8.33	4.15	13.03	12.78
CORRELATION	0.988	0.993	0.903	0.965	0.929
D-VALUE ($x10^{-8}$)	3.18	2.41	1.24	4.78	3.91

AVERAGE D-VALUE $(3.10 \pm 0.54) \times 10^{-8}\ cm^2\ s^{-1}$

METHYL METHACRYLATE COATED MORTAR, 0.6 WATER/CEMENT RATIO, CHLORIDE ION DIFFUSION RESULTS ($25^{\circ}C$).

APPENDIX 12 (continued)

TIME (seconds)	CHLORIDE CONCENTRATION (M/l)				
	DISC a	DISC b	DISC c	DISC d	DISC e
345 600	0.0050	0.0020	0.0020	0.0020	0.0020
1 209 600	0.0200	0.0110	0.0110	0.0135	0.0130
1 555 200	0.0240	0.0138	0.0139	0.0175	0.0160
2 160 000	0.0330	0.0190	0.0165	0.0228	0.0223
2 678 400	0.0370	0.0235	0.0227	0.0285	0.0275
VOLUME OF CELL (mls)	79.0	74.0	75.8	81.8	80.2
THICKNESS OF DISC (cms)	0.219	0.300	0.270	0.257	0.282
SURFACE AREA (cms^2)	9.079	7.069	7.069	10.179	9.079
GRADIENT ($\times 10^{-9}$)	13.84	9.06	8.42	11.14	10.80
CORRELATION	0.985	0.997	0.979	0.993	0.996
D-VALUE ($\times 10^{-8}$)	2.65	2.84	2.44	2.29	2.49

AVERAGE D-VALUE $(2.54 \pm 0.17) \times 10^{-8}$ cm^2 s^{-1}

CONTROL CEMENT PASTE, 0.28 WATER/CEMENT RATIO, CHLORIDE ION RESULTS, ($25^{\circ}C$).

APPENDIX 12 (continued)

TIME (seconds)	CHLORIDE CONCENTRATION (M/l)				
	DISC a	DISC b	DISC c	DISC d	DISC e
345 600	0.0030	0.0010	0.0010	0.0010	0.0010
1 209 600	0.0090	0.0050	0.0170	0.0055	0.0070
1 555 200	0.0120	0.0070	0.0205	0.0065	0.0100
2 160 000	0.0150	0.0100	0.0240	0.0100	0.0130
3 110 400	0.0225	0.0145	0.0305	0.0160	0.0175
VOLUME OF CELL (mls)	81.4	82.8	80.6	75.0	79.4
THICKNESS OF DISC (cms)	0.299	0.305	0.271	0.295	0.277
SURFACE AREA (cms^2)	9.621	10.179	8.553	7.548	8.814
GRADIENT ($\times 10^{-9}$)	6.93	4.88	10.09	5.36	5.96
CORRELATION	0.996	0.999	0.910	0.992	0.985
D-VALUE ($\times 10^{-8}$)	1.75	1.21	2.58	1.57	1.49

AVERAGE D-VALUE $(1.72 \pm 0.21) \times 10^{-8}\ cm^2\ s^{-1}$

NAPTHALENE SULPHONATE (0.25%) CEMENT PASTE, 0.28 WATER/CEMENT RATIO, CHLORIDE ION RESULTS ($25^{\circ}C$).

APPENDIX 12 (continued)

TIME (seconds)	CHLORIDE CONCENTRATION (M/l)				
	DISC a	DISC b	DISC c	DISC d	DISC e
345 600	0.0010	0.0010	0.0010	0.0020	0.0010
1 209 600	0.0040	0.0035	0.0025	0.0025	0.0190
2 160 000	0.008	0.0075	0.0060	0.0060	0.0235
3 110 400	0.0140	0.0120	0.0105	0.0115	0.0305
3 628 800	0.0165	0.0135	0.0130	0.0135	0.0370
VOLUME OF CELL (mls)	76.0	72.2	82.4	81.2	76.0
THICKNESS OF DISC (cms)	0.302	0.278	0.301	0.299	0.236
SURFACE AREA (cms^2)	7.068	7.068	8.814	10.179	6.605
GRADIENT ($\times 10^{-9}$)	4.77	3.96	3.68	3.95	9.30
CORRELATION	0.998	0.994	0.973	0.960	0.921
D-VALUE ($\times 10^{-8}$)	1.55	1.13	1.03	0.94	2.52

AVERAGE D-VALUE $(1.44 \pm 0.26) \times 10^{-8}\ cm^2\ s^{-1}$

NAPTHALENE SULPHONATE (0.5%) CEMENT PASTE, 0.28 WATER/CEMENT RATIO, CHLORIDE ION RESULTS ($25^{o}C$).

APPENDIX 12 (continued)

TIME (seconds)	CHLORIDE CONCENTRATION (M/l)				
	DISC a	DISC b	DISC c	DISC d	DISC e
345 600	0.0110	0.0010	0.0010	0.0010	0.0010
1 209 600	0.0020	0.0020	0.0110	0.0035	0.0035
2 160 000	0.0055	0.0050	0.0240	0.0080	0.0070
3 110 400	0.0100	0.0095	0.0335	0.0120	0.0120
3 628 800	0.0150	0.0110	0.0340	0.0125	0.0130
VOLUME OF CELL (mls)	81.6	82.4	81.0	80.4	77.0
THICKNESS OF DISC (cms)	0.257	0.256	0.257	0.232	0.236
SURFACE AREA (cms^2)	9.621	9.079	9.621	10.752	10.752
GRADIENT ($\times 10^{-9}$)	4.17	3.22	10.60	3.65	3.85
CORRELATION	0.925	0.964	0.976	0.976	0.988
D-VALUE ($\times 10^{-8}$)	0.91	0.75	2.29	0.63	0.65

AVERAGE D-VALUE $(1.05 \pm 0.28) \times 10^{-8}$ cm^2 s^{-1}

NAPTHALENE SULPHONATE (1.0%) CEMENT PASTE, 0.28 WATER/CEMENT RATIO, CHLORIDE ION DIFFUSION RESULTS ($25^{o}C$).

APPENDIX 12 (continued)

PUBLISHED WORK